

N O T I C E

THIS DOCUMENT HAS BEEN REPRODUCED FROM
MICROFICHE. ALTHOUGH IT IS RECOGNIZED THAT
CERTAIN PORTIONS ARE ILLEGIBLE, IT IS BEING RELEASED
IN THE INTEREST OF MAKING AVAILABLE AS MUCH
INFORMATION AS POSSIBLE

E82-10260

NASA-CR-167517

MICROWAVE SOIL MOISTURE MEASUREMENTS AND ANALYSIS

*"Made available under NASA sponsorship
in the interest of early and wide dis-
semination of Earth Resources Survey
Program information and without liability
for any use made thereof."*

By

Principal Investigator
R. W. Newton
Co-Investigators
T. A. Huwell
J. L. Nieber
C. H. M. van Bavel

FINAL REPORT
May 1980

**ORIGINAL CONTENTS
COLOR ILLUSTRATIONS**

Supported by:
National Aeronautics and Space Administration
Goddard Space Flight Center
Greenbelt, Maryland 20771
Grant No. NAS 9-13904



**TEXAS A&M UNIVERSITY
REMOTE SENSING CENTER
COLLEGE STATION, TEXAS**



(E82-10260) MICROWAVE SOIL MOISTURE
MEASUREMENTS AND ANALYSIS Final Report
(Texas A&M Univ.) 398 p HC A17/MF A01

N82-24538

CSCCL 03M

Unclass

G3/43 00260

MICROWAVE SOIL MOISTURE MEASUREMENTS AND ANALYSIS

By

Principal Investigator

R. W. Newton

Co-Investigators

T. A. Howell

J. L. Nieber

C. H. M. van Bavel

FINAL REPORT

May 1980

Supported by:

National Aeronautics and Space Administration

Goddard Space Flight Center

Greenbelt, Maryland 20771

Grant No. NAS 9-13904

**MICROWAVE SOIL MOISTURE MEASUREMENTS
AND ANALYSIS**

Principal Investigator:

R. W. Newton

Co-Investigators:

**Terry Howell
John Nieber
C. H. M. Van Bavel**

**Remote Sensing Center
Texas A&M University
College Station, Texas 77843**

Supported by:

**National Aeronautics and Space Administration
Johnson Space Center
Houston, Texas**

Contract NAS 9-13904

May 1980

TABLE OF CONTENTS

	Page
INTRODUCTION.	1
OVERVIEW	2
Controlled Ground Experiments.	4
Aircraft Experiments	6
Electrical Properties of Soil Water Mixtures	7
Theoretical Models	8
Soil Water Profile Models.	8
SUMMARY OF SIGNIFICANT ACHIEVEMENTS	9
Electrical Properties of Soils	10
Experimental Measurement Programs.	11
Measurement Interpretation	12
Development of Soil Moisture Algorithm	13
SUMMARY OF DOCUMENTATION	14
UNREPORTED RESULTS	14
1978 Colby Experiment	23
Development and Tests of Soil Moisture Algorithms	37
Sensitivity Tests.	38
Summary of Previously Reported Efforts.	38
The Effect of Spatial Variability of Soil- Water Properties.	42
Summary of Model Tests with Field Notes.	71
Model Input: Choice of Daily vs. 30 Minute Weather Data	71
Comparison of Measured and Simulated Results	72
References	85

Table of Contents (Continued)

	Page
Controlled Field Experiment Test Site	86
Summary.	86
Introduction	87
Field Site Description.	87
Data System.	88
Data Acquisition Problems.	98
Data Files	98
Quality of Data.	99
Data Summary100
Soil Physical Properties100
Projected Research113
References114
Attachment A115
B119
C125
 APPENDIX A: Ground Data Report: 1978 Colby MSAS Experiment	
 APPENDIX B: A Numerical Method to Compute Soil Water Content and Temperature Profiles Under a Bare Surface	
 APPENDIX C: Improved Water and Nutrient Management Through High-Frequency Irrigation	

LIST OF FIGURES

Figure Page

1978 Colby Experiment

1	L-Band Measurement of Antenna Temperature vs. Incident Angle for Field 13.	27
2	C-Band Measurement of Antenna Temperature vs. Incident Angle for Field 13.	28
3	X-band Measurement of Antenna Temperature vs. Incident Angle for Field 13.	29
4	L-Band Antenna Temperature Measurement vs. 0-2 cm Soil Moisture for Horizontal Polarization and 20° Incidence.	30
5	L-Band Antenna Temperature Measurement vs. 0-5 cm Soil Moisture for Horizontal Polarization and 20° Incidence.	31
6	C-Band Antenna Temperature Measurement vs. 0-2 cm Soil Moisture for Horizontal Polarization and 20° Incidence.	32
7	C-Band Antenna Temperature Measurement vs. 0-5 cm Soil Moisture for Horizontal Polarization and 20° Incidence.	33
8	X-Band Antenna Temperature Measurement vs. 0-2 cm Soil Moisture for Horizontal Polarization and 20° Incidence.	34
9	X-Band Antenna Temperature Measurement vs. 0-5 cm Soil Moisture for Horizontal Polarization and 20° Incidence.	36

Development and Tests of Soil Moisture Algorithms

1	Input data used in sensitivity test of bare soil water balance model. The saturated conductivity is varied by the factors shown, in reference to the best data fit for Norwood silty clay loam. The graph displays the resulting conductivity vs. water content relations . . .	40
---	---	----

List of Figures (Continued)

Figure	Page
2	Sensitivity of the calculated daily evaporation rate to relative errors in the measured input value of the saturated hydraulic conductivity, over a scale from 16 to 1/16. Results should be compared to those shown at triangles for scale 1. Overestimation up to a factor of 4 gives appreciable error but underestimation by a like factor does not. 41
3	Daily drainage rate as affected by assumed error in the saturated conductivity as measured for Norwood silty clay loam. Rain of 50 mm on the 10th day. The effect on drainage after the first 5 days is not large. 43
4	Water content of the 0-150 mm surface layer as influenced by assumed error in the saturated conductivity as measured for Norwood silty clay loam. Rain of 50 mm on the 10th day 44
5	Initial volumetric water content (m^3/m^3) as a function of depth (m) below the soil surface at midnight. 47
6	Initial soil temperature ($^{\circ}C$) as a function of depth (m) below the soil surface at midnight. 48
7	Unsaturated hydraulic conductivity as a function of water content for horizon I and scale. The symbol (+) is for scale 1.619 (Δ) is for 1.000, and (0) is for 0.381 50
8	Unsaturated hydraulic conductivity as a function of water content for horizon II and scale. The symbol (+) is for scale 1.619 (Δ) is for 1.000, and (0) is for 0.381 51
9	Relationship between the \log_{10} of pressure potential and volumetric water content for horizon I and scale. The symbol (∇) is for scale 1.619, (Δ) is for scale 1.000, and (0) is fo 0.381 53
10	Relationship between the \log_{10} of pressure potential and volumetric water content for horizon II and scale. The symbol (+) is for scale 1.619, (Δ) is for scale 1.000, and (0) is for 0.381 54
11	Daily evaporation (mm) as a function of time (days) and scaling factor. The symbol (+) is for scale 1.619, (Δ) is for 1.000 and (0) is for 0.381 55

List of Figures (Continued)

Figure	Page
12	Daily drainage (mm) as a function of time (days) and scaling factor. The symbol (+) is for scale 1.619, (Δ) is for 1.000 and (0) is for 0.381 56
13	Total water (mm) as a function of time (days) and scaling factor. The symbol (+) is for scale 1.619, (Δ) is for 1.000 and (0) is for 0.381 57
14	Total water (mm) in the top 0.25 m of the soil profile as a function of time (days) and scaling factor. The symbol (+) is for scale 1.619, (Δ) is for 1.000 and (0) is for 0.381. 58
15	Volumetric water content (m^3/m^3) of the soil surface at 4:00 p. m. as a function of time (days) and scaling factor. The symbol (+) is for scale 1.619, (Δ) is for 1.000 and (0) is for 0.381 59
16	Surface temperature ($^{\circ}C$) at 4:00 p.m. as a function of time (days) and scaling factor. The symbol (+) is for scale 1.619, (Δ) is for 1.000 and (0) is for 0.381. . . . 60
17	Soil temperature ($^{\circ}C$) at a depth of 4.0 cm at 4:00 p.m. as a function of time (days) and scaling factor. The symbol (+) is for scale 1.619, (Δ) is for 1.000 and (0) is for 0.381. 62
18	Soil temperature ($^{\circ}C$) at a depth of 17.5 cm at 4:00 p.m. as a function of time (days) and scaling factor. The symbol (+) is for scale 1.619, (Δ) is for 1.000 and (0) is for 0.381. 63
19	Volumetric water content (m^3/m^3) of the soil surface at 4:00 p.m. (day 8) as a function of scaling ratio 65
20	Volumetric water content (m^3/m^3) of the soil surface at 4:00 p.m. (day 11) as a function of scaling ratio 66
21	Surface temperature ($^{\circ}C$) at 4:00 p.m. as a function of scaling ratio (day 8) 67
22	Surface temperature ($^{\circ}C$) at 4:00 p.m. as a function of scaling ratio (day 11). 68
23	Total water (mm) in the top 0.30 m of the soil profile as a function of scaling ratio (day 8). 69
24	Total water (mm) in the top 0.30 m of the soil profile as a function of scaling ratio (day 11) 70

List of Figures (Continued)

Figure	Page	
25	Volumetric water content (m^3/m^3) as a function of depth (m) and frequency of weather input data for Julian day 93, at 4:00 p.m. The symbol (O) is for daily weather input data, (Δ) is for daily and windspeed as a function of time, and (+) is for 30 minute data.74
26	Volumetric water content (m^3/m^3) as a function of depth (m) and frequency of weather input data for Julian day 126, at 4:00 p.m. The symbol (O) is for daily weather input data, (Δ) is for daily and windspeed as a function of time, and (+) is for 30 minute data.75
27	Soil temperature ($^{\circ}C$) as a function of depth (m) and frequency of weather input data for Julian day 93, at 4:00 p.m. The symbol (O) is for daily weather input data, (Δ) is for daily and windspeed as a function of time, and (+) is for 30-minute data.76
27	Soil temperature ($^{\circ}C$) as a function of depth (m) and frequency of weather input data for Julian day 126, at 4:00 p.m. The symbol (O) is for daily weather input data, (Δ) is for daily and windspeed as a function of time, and (+) is for 30-minute data.77

Controlled Field Experiment Test Site

1	Photographic Illustration of the Fallow Plot at the Texas A&M University Farm.89
	Photographic Illustration of the Vegetated Plots at the Texas A&M University Farm.89
3	Plan View of the Experimental Site Illustrating the Location of the Experimental Plots and the Data Acquisition Systems.90
4	Photographic Illustration of the Weather Station Tower at the Texas A&M University Farm92
5	Photographic Illustration of the Recording Raingage and U.S.W.B. Standard Raingage at the Texas A&M University Farm92
6	Photographic Illustration of the U.S.W.B. Class A Evaporation Pan.93

List of Figure (Continued)

Figure	Page
7 Photographic Illustration of the CR5 Data Acquisition System.	93
8 Illustration of the Tensiometer-Manometer Arrangement . .	95
9 Photographic Illustration of the Field Installation of a Tensiometer-Manometer Bank.	96
10 Calibration Curve for Neutron Soil Moisture Probe. (From Humphreys, 1979.)	97
11 Water Retentivity Determined in the Laboratory, 0-15 cm Soil Depth. (From Humphreys, 1979.)	104
12 Water Retentivity Determined in the Laboratory, 15-55 cm Soil Depth. (From Humphreys, 1979.)	105
13 Water Retentivity Determined in the Laboratory, 55-90 cm Soil Depth. (From Humphreys, 1979.)	106
14 Relationship between hydraulic conductivity and water content determined from field measurements for 10-30 cm soil depth. (From Humphreys, 1979.)	107
15 Relationship between hydraulic conductivity and water content determined from field measurements for 40-80 cm soil depth. (From Humphreys, 1979.)	108
16 Relationship between hydraulic conductivity and water content determined from field measurements for 90-120 cm soil depth. (From Humphreys, 1979.)	109
17 Relationship between hydraulic conductivity and water content determined from field measurements for 140-160 cm soil depth. (From Humphreys, 1979.)	110
18 Relationship between hydraulic conductivity and water content determined from field measurements for 170-180 cm soil depth. (From Humphreys, 1979.)	111

LIST OF TABLES

Table	Page
<u>Summary of Documentation</u>	
1	Contracting Summary.15
2	Summary of Contract NAS 9-13904 Documentation.16
<u>1978 Colby Experiment</u>	
1	MSAS Support of Colby Experiment26
<u>Development and Tests of Soil Moisture Algorithms</u>	
1	The scaling factor α (ratio of microscopic dimension of soil to its mean) and the corresponding values of the saturated hydraulic conductivities (K) for both soil horizons, as obtained with equation (1)49
2	The scaling factor α (ratio of microscopic dimension of soil to its mean) used to generate curves as those shown in Figures 9 and 10. The same values of α were used for both horizons using equation (2).52
3	Daily meteorological data used to evaluate the frequency of weather input data used with CONSERVB73
4	Weather input data used for the simulation of the heat and water balance of Norwood silt loam soil over a period of 33 days. The data was recorded at the Agronomy Farm of Texas A&M University between April 16 and May 18, 197978
5	Initial water content and temperature profiles as a function of depth used in the simulation79
6	Calculated and measured values of water content and matric potential for several days of the 33-day simulation period.81

List of Tables (continued)

Table	Page
<u>Controlled Field Experiment Test Site</u>	
1	Field Measurement of Bulk Density.101
2	Texture Profile of Field Site.103
3	Saturated Hydraulic Conductivities Determined* in the Field with the Double-Tube Method112

MICROWAVE SOIL MOISTURE MEASUREMENTS AND ANALYSIS

Contract NAS 9-13904

Principal Investigator: R. W. Newton

INTRODUCTION

The Remote Sensing Center of Texas A&M University (TAMU) was funded by the NASA/Johnson Space Center (JSC) during the period from February 11, 1974 to March 31, 1980 to perform research toward developing a technique for measuring soil moisture using remote sensing procedures. Considerable effort has been devoted to this project at TAMU resulting in numerous technical reports, verbal presentations and publications. An overview of the project will be provided with a list of documentation that describes the details of the research supported by the contract. No attempt will be made in this report to document the details of the project effort. However, this report does contain documentation of an effort during the last year of the contract to develop a model that simulates the distribution of water content and of temperature in bare soil, a description of the field experimental set up designed to acquire the data to test this model and documentation of the Microwave Signature Acquisition System (MSAS) field measurements acquired in Colby, Kansas during the summer of 1978. This information is contained in this report since it has not been reported to JSC in a formal written document prior to this date, although it has been presented in the Supporting Research and Technology Quarterly Progress Reviews.

OVERVIEW

From 1969 to 1974 under the leadership of Dr. J. W. Rouse, Jr., the Remote Sensing Center at Texas A&M University devoted considerable effort to demonstrating the capability of microwave remote sensing systems to measure soil moisture. Much of this work was done in conjunction with Dr. T. Schmugge of the NASA Goddard Space Flight Center and Dr. B. J. Blanchard at that time from the Agricultural Research Service of the USDA in Chickasha, Oklahoma. These preliminary efforts were instrumental in supporting the establishment of a NASA funded program to become known as the Joint Soil Moisture Experiment. This program was instituted in 1974 resulting in the contract summarized in this document. In addition to TAMU, the Goddard Space Flight Center, Agricultural Research Service of the USDA, the University of Kansas, the University of Arkansas, and the Environmental Research Institute of Michigan (ERIM) also became the initial participants in the program.

Dr. J. W. Rouse, Jr. was the initial principal investigator on the contract held by TAMU. In 1977, Dr. Rouse left TAMU for employment elsewhere. At that time, Dr. R. W. Newton was named principal investigator of the contract and remained so until its completion in 1980. From the period 1974 until 1976 the program was known as the Joint Soil Moisture Experiment and had as program managers at the Johnson Space Center Mr. Kirk Mason, Dr. Bill Lenore, and Dr. Owen Garriot. In 1976, the program was placed under the Large Area Crop Inventory Experiment (LACIE) within the supporting research activity area headed by Dr. Jon Erickson. At this time, the program became known as the Agricultural Soil Moisture Experiment. The name change

was an effort to reflect a change in the program direction. Prior to becoming known as the Agricultural Soil Moisture Experiment, the objectives of the Joint Soil Moisture Experiment were to develop techniques of remotely measuring soil moisture information of application to agriculture, hydrology, and climate. However, under the LACIE program the objective of the soil moisture work being funded from the NASA Johnson Space Center was to report the application of agriculture. The objective of the program supported by the Goddard Space Flight Center, however, continued to support agriculture, hydrology, and climate. In 1980, a decision was made at the NASA headquarters level to fund the soil moisture research effort from the NASA Goddard Space Flight Center. It was due to this decision that the contract reporting in this document was drawn to a close. However, the research supported by the contract basically continues from NASA grant NAG5-31 supported by the NASA Goddard Space Flight Center. The overall program in which that grant falls is the Plan of Research for Integrated Soil Moisture Studies (PRISMS). The purpose of this program is to be an integrated plan of research for NASA in which techniques for remotely measuring soil moisture information would be developed. These techniques are not to be developed exclusively for any applications in agriculture, hydrology, weather and climate.

The ultimate objective of the support to TAMU was to demonstrate the capability to remotely estimate a soil moisture parameter. The approach taken by TAMU was to develop a thorough understanding of the interaction phenomena between the microwave energy and the soil moisture parameters of interest. This required the development of an understanding of the electrical properties of soil moisture mixtures

at microwave frequencies. In addition, it required the development of theoretical models that would accurately stimulate the thermal microwave emission and microwave backscatter from soil volumes. In order to validate the theoretical models, controlled ground based experiments were implemented for a variety of soil conditions. These controlled experimental measurements were used to validate the models which could then be utilized to predict the behavior of microwave signals for a variety of scene conditions. Algorithms, developed with the assistance of these theoretical models for estimating soil moisture microwave measurements were tested for applicability to real scene situations using aircraft experimental measurements.

In implementing the approach described in the above paragraph, controlled ground base experiments and extensive aircraft experiments were implemented during the same time frame. In addition, laboratory investigations into the dependence of the permittivity of soil at microwave frequencies on the percentage water content were implemented. These efforts are summarized below.

Controlled Ground Experiments

Prior to the initiation of this contract, a controlled ground experiment was held at TAMU in 1973 in conjunction with NASA/JSC and Lockheed Electronics Company. The truck mounted passive microwave radiometer system operating at 1.4 GHz and 10.7 GHz was utilized in the experiment. The purpose of the experiment was to acquire experimental measurements over bare soil as a function of soil moisture content and vegetative cover consisting of oats and sorghum. In 1974 a cooperative measurements program was undertaken at TAMU in conjunction with the University of Kansas, Lockheed Electronics Company, and

NASA/JSC. The purpose of this experiment was to acquire simultaneous active and passive microwave measurements over bare and vegetated soil. There were a total of 10 fields involved in the experiment. Three fields were bare, one smooth, one medium rough, and one very rough. Two additional sets of three fields each prepared to the same surface roughness conditions were planted with a high density of sorghum. Another field was row tilled and planted with sorghum such that measurements could be acquired perpendicular and parallel to the row directions.

In 1975 another controlled ground based experiment was held at TAMU. Only the passive microwave radiometer system operating at 1.4 GHz and 10.7 GHz was utilized in that experiment. The purpose of the experiment was to acquire measurements to identify the effect of row directions. Two fields were utilized in the experiment. One was bare, the other was vegetated with cotton. The surface was row tilled and measurements were acquired parallel to the row direction, 30° off parallel, 45° off parallel, 60° off parallel and perpendicular to the row direction.

During the period from 1976 to 1977 the microwave signature acquisition system was modified to add a third frequency, C band at 5.0 GHz. In the summer of 1978, the MSAS was taken to Colby, Kansas in order to acquire ground measurements during the "Colby Aircraft Experiment". Only a minimum number of measurements were acquired during that experiment due to hardware difficulties which arose during the measurement process with the digital tape drive. These measurements are described in this document.

Aircraft Experiments

Very extensive aircraft experiments were held in Phoenix, Arizona in 1974 jointly by TAMU, University of Kansas, NASA Johnson Space Center, Environmental Research Institute of Michigan, and the Agricultural Research Service of the USDA. During that experiment, MFMR, and PMIS measurements were acquired. In addition, L and X-band synthetic aperture radar imagery were obtained with the ERIM system. Little results were obtained from the ERIM measurements due to inconsistencies in the imagery. However, a considerable amount of passive microwave MFMR and PMIS data were acquired and proved to be very valuable. A repeat of that aircraft experiment was held in Phoenix, Arizona in 1975 in order to acquire additional measurements under more moist field conditions. No radar scatterometer data were acquired in Phoenix in 1975. The combination of the Phoenix 1974 and 1975 aircraft experiment did produce a data set with soil moisture varying from very dry to very wet.

In 1976 to 1977 aircraft experiments were conducted at the LACIE test site in Garden City, Kansas. Again, only passive microwave data were acquired in those experiments. In 1977, a functional check flight prior to the Garden City experiment was held in Lawrence, Kansas. Radar scatterometer data were acquired at this site. These data were used to compare the University of Kansas truck mounted radar measurements to the aircraft radar scatterometer measurements.

In 1978, an aircraft experiment was held at the LACIE test site in Colby, Kansas. During this experiment, both active and passive microwave data were acquired. Passive microwave data were acquired with the MFMR and PMIS. Radar measurements were acquired with the 0.4

GHz, 1.6 GHz, 4.75 GHz, and 13.3 GHz radar scatterometers. During this aircraft experiment, a sequence of 6 flights, approximately three days apart were conducted in order to acquire aircraft information that could be used to demonstrate the capability of measuring soil moisture changes over time. During this experiment the University of Kansas brought their truck mounted radar system to the test site and TAMU brought the MSAS system to the test site. As noted previously, only minimal measurements were acquired with the TAMU MSAS system. The data acquired in these aircraft experiments has demonstrated that the capability does exist to measure soil moisture with microwave sensors over actual agricultural fields.

Electrical Properties of Soil Water Mixtures

In support of the theoretical modeling and analyses of the aircraft and ground based experiments, a series of laboratory measurements of the permittivity of soil were made as a function of soil moisture for soils acquired from the TAMU ground based test site as well as the aircraft test sites. A waveguide technique was used at 1.5 GHz and 10.0 GHz for making these measurements. The measurements at 1.5 GHz demonstrated the dependence of permittivity on soil texture and formed the basis for our understanding of the dependence of permittivity on soil moisture. In an attempt to make permittivity measurements of highly saline soils, two additional techniques were devised to make permittivity measurements at 10 GHz. Each technique involved using a swept frequency system to radiate the soil sample. The permittivity was computed from the reflection coefficient and/or transmission coefficient measured across the frequency band. In one technique a plexi-glass sample holder was devised that interfaced to

an open ended waveguide. This technique did not prove very satisfactory due to the resonant effect of the sample holder. In the other technique, standard gain horns were used to radiate soil held in an open frame plexi-glass sample holder. Permittivities of saline soil as a function of moisture were actually measured using this technique. However, for dry soil condition the computed permittivity was less than one. This discrepancy could never be resolved although the shape of the permittivity versus moisture curves were as expected.

Theoretical Models

Several theoretical models were investigated during the contract. A plan layered stratified radiative transfer model first published by Burke and Paris (NASA Technical Memorandum TMX-58166, NASA/JSC, August 1975) was used most extensively throughout the endeavor. This model is an incoherent model, but proved to be very satisfactory provided that the soil moisture and soil temperature profiles were handled properly near the air soil boundary. Significant effort was put into the development of a surface roughness model that could be used in conjunction with the Burke Paris radiative transfer model. A surface roughness model was based on a Kirkhoff Huggen's approach and proved to demonstrate the surface roughness characteristics found in the experimental ground base passive microwave measurement satisfactorily.

Soil Water Profile Models

A deterministic model for predicting a soil moisture profile as well as the soil temperature profile was developed during the later phases of the program. Extensive field measurements of mineralogical conditions as well as soil moisture and soil measured potential as a

function of depth were acquired in order to validate the model. The model was validated on a limited set of field measurements and numerous tests were run using the model to demonstrate the sensitivity of the model to various input parameters. This model will be the basis for which an overall algorithm utilizing microwave measurements as an input to a root zone soil moisture prediction algorithm will be based.

SUMMARY OF SIGNIFICANT ACHIEVEMENTS

This project has been extremely successful from the standpoint that it has been responsible for bringing the state of knowledge concerning thermal microwave emission and microwave backscatter from natural scenes (especially bare soil scenes) from a state of infancy to sophistication. At the time the project started there was little knowledge concerning the electrical characteristics of soils in the microwave frequency range or of the behavior of microwave systems to scene parameters such as surface roughness, vegetation cover, soil texture, soil water content, and soil temperature, that vary naturally in agricultural and hydrologic scenes. At the conclusion of the project the scientific understanding of the effect of each of these parameters is known to the extent that they can be predicted within a reasonable degree of accuracy. The current research effort that will be carried on from this point center around not if you can measure soil moisture, but how you integrate the soil moisture information available from microwave sensors into a procedure for predicting soil moisture at root zone depths for the purpose of assisting in predicting the effect of moisture on the yield of agriculture crops prior to harvest. The significant achievements of this program are far reaching, but are briefly summarized in the following paragraphs.

Electrical Properties of Soils

The basic phenomena upon which microwave remote sensing of soil moisture is based, is the variation of the electrical properties, or permittivity, of soil as a function of soil moisture. Prior to this program there was little understanding of the interaction between the electromagnetic energy and the soil water mixture. As a result of this program, we now understand how the permittivity of soil water mixtures vary as a function of percentage soil moisture at different microwave frequencies, and we understand why this behavior occurs. Specifically, it is understood that the bonding of the soil water molecule to the soil particles plays a major role in the permittivity characteristics of the soil water mixture. The amount of water molecules that can be firmly bonded electrostatically to soil particles is largely dependent upon the surface area of the particle and somewhat dependent upon the mineralogy of the particle. As a result, permittivity of soil water mixtures is affected to a great degree by the soil texture especially at frequencies within the L-band region. In addition, any ions contained within the soil water mixture can affect the permittivity. As a result, saline soils can have a significantly different permittivity, at a particular microwave frequency, than non-saline soils.

It was also demonstrated that the permittivity of soil water mixtures is related to the volumetric water content rather than the gravimetric water content since the permittivity is determined to a large extent by the number of active water molecules present within a volume. This meant that microwave measurements should be interpreted with respect to soil moisture measured on a volumetric basis rather

than a gravimetric basis. If microwave measurements are interpreted based on a gravimetric basis, then the soil density must also be taken into account.

Experimental Measurement Programs

Both ground based and airborne experimental measurement programs were devised during the course of this project to determine the effects of scene parameters such as surface roughness, soil texture, vegetation cover, soil water and soil temperature dynamics, and areal distribution of soil moisture. Passive microwave ground based experiments were implemented at 1.4 GHz and 10.7 GHz that demonstrate conclusively the dependence of microwave emission on soil moisture. The effect of a uniform surface roughness on this soil moisture dependence was shown to cause a decrease in the sensitivity of the thermal microwave emission to soil moisture. However, it was also demonstrated that polarization information within the measurement could be used to estimate the surface roughness conditions over which the measurements were made, thereby providing a means for correcting the measurements for surface roughness effects.

It was also demonstrated that row tilled surface roughness can be considered a two scale roughness. The row undulations can be considered a large scale periodic roughness while the small surface deviations riding on top of row undulations can be considered a small scale surface roughness. When viewing the scene parallel to the rows, the small scale surface roughness has nearly the same effect as if the row construction were not there. However, when viewing the field perpendicular to the rows, the large scale row undulations have the effect of tilting the small scale roughness with respect to the viewing angle.

This has a significant effect when viewing a small field with a ground base system. However, aircraft measurements covering a much larger portion of a field have not been demonstrated to have as large of an adverse effect.

During this program an extensive controlled ground based measurements program was implemented during which simultaneously active and passive microwave measurements were acquired in conjunction with detailed ground truth. This is the only data set known to be in existence that contains simultaneously acquired ground-based and passive microwave measurements. As a result, this data set is of fundamental value to investigations into the relationships between active and passive measurements of soil moisture.

During this research program joint aircraft experiments were held at various locations in which tremendous amounts of active and passive microwave measurements were acquired over actual agricultural terrain. These data demonstrate the capability of using microwave sensors for estimating soil moisture in actual field situations.

Measurement Interpretation

Significant achievements were realized in the interpretation of active and passive microwave signals for soil moisture information. Considerable research was performed utilizing theoretical models in conjunction with experimental microwave measurements in order to develop an understanding of the relationships between the soil moisture and soil temperature profiles with depth, and the thermal passive microwave energy ultimately emitted by the soil volume. In addition, theoretical models were used to develop a thorough understanding of the effect of surface roughness on the relationship between thermal

microwave emission and soil moisture. Theoretical models were also used to describe the effects of vegetation on the thermal microwave emission from soil volumes. However, adequate experimental measurements of soil with vegetation cover were not available to completely validate these models.

Significant achievements in the interpretation of microwave signals with respect to soil moisture are: 1) the identification of the soil depths from which detectable thermal microwave emission originates (as a function of the degree of soil saturation and microwave frequency); 2) distinguishing between the effects of the soil moisture profile and the soil temperature profile on the thermal microwave emission from soil volumes; and 3) identifying the sensitivity reduction of thermal microwave emission to soil moisture due to surface roughness and identifying the technique for utilizing polarization information to take surface roughness into consideration in an algorithm for estimating soil moisture from thermal microwave emission.

Development of Soil Moisture Algorithm

A deterministic model for simulating the flow of water in a soil volume was developed. The rationale for developing such a model was to identify a technique which would utilize microwave measurements as well as ancillary information to predict soil moisture at depths to the root zone of typical agricultural crops. The model is ideal for utilization with passive microwave measurements since it also predicts the soil temperature profile with depth. Experimental measurements of meteorological inputs as well as soil characteristics, soil moisture and soil temperature were obtained in order to verify the model. In addition, sensitivity analyses were run to determine the accuracy to

which the parameters of the model must be known in order for the model to provide accurate results.

SUMMARY OF DOCUMENTATION

During the project period, Texas A&M University generated a significant number of reports documenting the research effort. This documentation took the form of progress reports generated for the NASA Johnson Space Center, technical reports and technical memorandum published by the Remote Sensing Center and documents published either in symposium proceedings or refereed journals. The contract progress reports initially were provided in written form up through 1977. At that time the project became part of the supporting research effort of LACIE and progress reports took the form of verbal presentations in the Supporting Research and Technology quarterly progress reviews. Table 1 provides a listing of the Contract Statement of Work Exhibits along with contracting periods and dollar amounts. Table 2 provides a listing of the documentation associated with this contract.

UNREPORTED RESULTS

There are several efforts performed during the pre-contract period that have as yet been officially unreported to the NASA Johnson Space Center in written form. However, the result of all of these efforts have been reported in oral presentation material to NASA technical representatives.

TABLE 1
CONTRACTING SUMMARY

<u>Date</u>	<u>Contract Exhibit</u>	<u>Modification Number</u>	<u>Incremental Award</u>	<u>Total Award</u>
2/11/74-1/31/75	A	initial contract	\$36,650	
	B	1S	4,180	
2/1/75-1/31/76	C	2S	39,000	\$81,830
9/15/75-1/31/76	D	3S	7,000	88,330
2/1/76-3/31/76	time extension	4S	-0-	
4/1/76-3/31/77	E	5S	98,900	187,730
1/18/77-3/31/77	F	6S	25,780	213,510
4/1/77-4/30/77	time extension	7S	-0-	
5/1/77-5/31/77	time extension	8S	-0-	
6/1/77-4/30/78	G	9S	91,700	305,210
5/1/78-6/30/78	time extension	10S	-0-	
7/1/78-8/30/78	time extension	11S	-0-	
8/31/78-2/28/79	H,I	12S	94,616	399,826
3/1/79-3/31/79	time extension	13S	-0-	
4/1/79-11/30/79	J	14S	99,270	499,096
12/1/79-2/29/80	time extension	15S	-0-	
12/1/79-2/29/80	K	16S	39,000	538,096
3/1/80-3/31/80	time extension	17S	-0-	

TABLE 2

SUMMARY OF CONTRACT NAS 9-13904 DOCUMENTATION

Progress Reports

1. Progress Report 3058-1, February-April 1974
2. Progress Report 3058-2, May-July 1974
3. Progress Report 3058-3, August-October, 1974
4. Progress Report 3058-4, November 1974-January 1975
5. Progress Report 3058-5, February-April 1975
6. Progress Report 3058-6, May-July 1975
7. Progress Report 3058-7, August-October 1975
8. Progress Report 3058-8, November 1975-March 1976
9. Progress Report 3058-9, April 1976-July 1977
10. Supporting Research and Technology (SR&T) Quarterly Progress Review, NASA/JSC, September 12-16, 1977.
11. SR&T Quarterly Progress Review, NASA/JSC, December 5-8, 1977
12. SR&T Quarterly Progress Review, NASA/JSC, March 16-17, 1978
13. SR&T Quarterly Progress Review, NASA/JSC, June 12-15, 1978
14. SR&T Quarterly Progress Review, NASA/JSC, September 11-14, 1978
15. SR&T Quarterly Progress Review, NASA/JSC, December 1, 1978
16. SR&T Quarterly Progress Review, NASA/JSC, March 6-9, 1979
17. SR&T Quarterly Progress Review, NASA/JSC, June 4-8, 1979
18. SR&T Quarterly Progress Review, NASA/JSC, September 10-13, 1979

Formal Planning and Organizational Meetings

1. Joint Soil Moisture Experiment Review, NASA/JSC, May 9-10, 1975
2. Joint Soil Moisture Experiment Review, NASA/JSC, October 30-31, 1975
3. Soil Moisture Planning Meeting: Experiment Operations For 1978, NASA/JSC, October 27-28, 1977.
4. Agriculture Soil Moisture Experiment: NASA/HQ Steering Committee Preparation, NASA/JSC, October 4-5, 1978.
5. Agricultural Soil Moisture: Investigators Meeting, NASA/JSC, March 8, 1979.

Published Papers and Presentations

1. Newton, R. W., "Characteristics of Microwave Emission of Significance to Satellite Remote Sensing of Soil Water," Satellite Hydrology, American Water Resources Association, TPS 81-1, 1981.
2. Schmutge, T. J., A. Chang, R. W. Newton and B. J. Choudhury, "Effect of Surface Roughness on the Microwave Emission from Soils," Journal of Geophysical Research, Vol. 84, No. C9, September 1979 (Also NASA Technical Memorandum 79606, Goddard Space Flight Center).

Table 2. Continued

3. Newton, R. W. and J. W. Rouse, Jr., "Microwave Radiometer Measurements of Soil Moisture," IEEE Transactions on Antennas and Propagation, Vol. AP-28, No. 5, September 1980.
4. Wang, J. R., R. W. Newton, J. W. Rouse, Jr., "Passive Microwave Remote Sensing of Soil Moisture," IEEE Transactions on Geoscience and Remote Sensing, Vol. GE-18, No. 4, October 1980 (Also NASA Technical Memorandum 80311, Goddard Space Flight Center).
5. Blanchard, A. J. and J. W. Rouse, Jr., "Depolarization of Electromagnetic Waves Scattered from an Inhomogeneous Half Space Bounded by a Rough Surface," Radio Science, Vol. 15, No. 4, July, August 1980.
6. Newton, R. W., J. W. Rouse, Jr., S. L. Lee, and J. R. Paris, "On the Feasibility of Remote Monitoring of Soil Moisture with Microwave Sensors," Proceedings of the Ninth International Symposium on Remote Sensing, University of Michigan, Ann Arbor, Michigan, April 15-19, 1974.
7. Newton, R. W., J. W. Rouse, Jr., and W. R. McClellan, "Dielectric Properties of Soil at X- and L-Band Frequencies," International Union of Radio Science (URSI)--Annual Meeting, University of Colorado, Boulder, Colorado, October 20-23, 1975.
8. Newton, R. W. and J. W. Rouse, "Interpretation of Passive Microwave Data for Soil Moisture Information," Proc. of the Colloquium on Water in Planetary Regoliths, Dartmouth College, Hanover, New Hampshire, October 5-7, 1976.
9. Newton, R. W., "Significant Passive Microwave Results of the NASA Joint Soil Moisture Experiment," NASA Office of Applications Annual Microwave Program Review, January 1977.
10. Rouse, J. W., Jr. and R. W. Newton, "Predictions of Future Use of Active Microwave Systems for All Weather Sensing of the Earth," Satellite Applications to Marine Technology, American Institute of Aeronautics and Astronautics (AIAA), New Orleans, November 15-17, 1977.
11. Newton, R. W., "Advances in Passive Microwave Techniques of Remotely Estimating Soil Water Content," Proc. of the Microwave Remote Sensing Symposium, Remote Sensing Center, Texas A&M University (for NASA/JSC, Houston), Texas, December 6-7, 1977.
12. Blanchard, A. J. and J. W. Rouse, Jr., "Measurements of the Depolarization of Microwave Backscatter from Rough Surface," National Radio Science Meeting, University of Colorado, Boulder Colorado, January 9-13, 1978.

Table 2. Continued

13. Newton, R. W., "Characteristics of Microwave Emission of Significance to Satellite Remote Sensing of Soil Water," Fifth Annual Pecora Symposium, Satellite Hydrology, American Water Resources Association, Sioux Falls, South Dakota, June 11-15, 1979.
14. Wang, J. R., R. W. Newton and J. W. Rouse, Jr., "Passive Microwave Sensing of Soil Moisture: The Effect of Tilled Row Structure," American Geophysical Union, Washington, D. C., June 11, 1979.
15. Blanchard, A. J., "Realistic Earth/Land Radar Models," Invited Presentation, Radar Geology Workshop. Snowmass, Colorado, July 16-21, 1979.
16. Blanchard, A. J., "Depolarization Effects in Radar Backscatter from Vegetation Layers," National Radio Science Meeting, Boulder, Colorado, November 5-8, 1979.

Significant Reports Published by the Remote Sensing Center

1. RSC-104, "Realistic Earth/Land Radar Models," A. J. Blanchard, July, 1979.
2. RSC-100, "Characteristics of Microwave Emission," R. W. Newton, 1979.
3. RSC-94, "A Dual Polarized X-band Pulse Radar for Ground Based Electromagnetic Scattering Experiment," A. W. White, May 1978.
4. RSC-93, "A Partial Examination into Factors Affecting Radiometric Measurements at UHF Frequencies," J. P. Claassen and H. Singh, July, 1978.
5. RSC-90, "Design Evaluation of a Ground-Based Radiometer System," W. R. McClellan, May 1977.
6. RSC-84, "Thermal Microwave Emission from an Inhomogeneous Half-Space," C. M. Hansen, May 1977.
7. RSC-83, "Volumetric Effects in the Depolarization of Electromagnetic Waves Scattered from Rough Surfaces," A. J. Blanchard, May 1977.
8. RSC-61, "Microwave Remote Sensing and its Application to Soil Moisture Detection," R. W. Newton, January 1977.
9. RSC-72, "Passive Microwave Data Report: Joint Soil Moisture Experiment at Texas A&M University," July 13-July 25, 1975, R. W. Newton, April 1976.

Table 2. Continued

10. RSC-71, "Ground Data Report: Joint Soil Moisture Experiment at Texas A&M University," E. A. Tesch and R. W. Newton, January 1976.
11. RSC-70, "Ground Truth Report: 1975 Phoenix Microwave Experiment," B. J. Blanchard, November 1975.
12. RSC-65, "Passive Microwave Data Report: Joint Soil Moisture Experiment at Texas A&M University," June 26-July 21, 1974, R. W. Newton, January 1975.
13. RSC-61, "Ground Truth Report of a Joint Soil Moisture Experiment," S. L. Lee and R. W. Newton, October 1974.
14. RSC-58, "Permittivity Measurements of Soils at L-band," R. W. Newton and W. R. McClellan III, June 1975.
15. RSC-56, "Dual Frequency Microwave Radiometer Measurements of Soil Moisture for Bare and Vegetated Rough Surfaces," S. L. Lee, August 1974.
16. RSC-44, "Microwave Emission and Scattering from Vegetated Terrain," T. G. Sibley, August 1973.
17. RSC-43, "Remote Monitoring of Soil Moisture Using Airborne Microwave Radiometers," C. L. Kroll, August 1973.
18. RSC-37, "On the Performance of Infrared Sensors in Earth Observations," L. F. Johnson, August 1972.
19. RSC-32, "Microwave Radiometer Measurements of Soil Moisture," B. R. Jean, C. L. Knoll, J. A. Richerson, J. W. Rouse, Jr., T. G. Sibley, and M. L. Wiebe, October 1972.
20. RSC-30, "Selected Applications of Microwave Radiometric Techniques," B. R. Jean, August 1971.
21. RSC-27, "An Experimental Evaluation of a Theoretical Model of the Microwave Emission of a Natural Surface," J. A. Richerson, August 1971.
22. RSC-25, "Experimental Microwave Measurements of Controlled Surfaces," B. R. Jean, J. A. Richerson, and J. W. Rouse, Jr., May 1971.
23. RSC-23, "Laboratory Measurement of the Complex Dielectric Constant of Soils," M. L. Wiebe, June 1971.
24. RSC-22, "Survey of Remote Sensing Applications to Hydrology with a Selected Bibliography," S. W. Sers, October 1971.

Table 2. Continued.

Significant Reports Published by the Remote Sensing Center

25. RSC-12, "Wavelength Dependence of Backscatter from Rough Surfaces," J. W. Rouse, Jr., August 1970.
26. RSC-10, "Discussion of a Model of the Apparent Temperature of Natural Surfaces in the Microwave Range," J. A. Richerson, May 1970.
27. RSC-03, "Passive Microwave Sensing of the Earth's Environment: A Bibliography with Abstracts," J. A. Richerson, September 1969.

Technical Memoranda Published by the Remote Sensing Center

1. RSC-166, "Realistic Earth/Land Radar Models," A. J. Blanchard, January 1980.
2. RSC-165, "Calibrating a Gamma Probe for Soil Moisture Measurement," S. T. Hodapp, January 1980.
3. RSC-164, "Gamma Probe Measurement of Bulk Density and Soil Moisture," S. T. Hodapp, August 3, 1979.
4. RSC-162, "GRAF/PEN-TI980A Interface," D. Simpson and M. Weichold, April 1978.
5. RSC-157, "Digital Thermometer," T. York and M. Walls, April 1978.
6. RSC-156, "An L-Band Microwave Amplifier," R. Black and J. Mejorada, Not in file.
7. RSC-155, "Design of an X-Y Plotter Interface for a Digital Computer," M. H. Weichold, April 1978.
8. RSC-151, "The Microprocessor Subsystem of the Microwave Signature Acquisition System," R. Stroud, April 1978.
9. RSC-134, "Error in the Determination of the Subsurface Backscattered Field as Determined by Rouse," A. J. Blanchard, September 1976.
10. RSC-130, "The Design and Specification of a Short Pulse Scatterometer," J. P. Claassen, March 1976.
11. RSC-124, "Equations of Geometric and Aircraft Parameter Dynamics in PMIS Data," A. J. Blanchard and B. J. Blanchard, December 1975.
12. RSC-120, "A Partial Analysis of the ERIM Radar Imagery", A. J. Blanchard, June 1975.

Table 2. Continued

13. RSC-106, "An X-Band Radar for Ground Based Scattering Experiments," B. R. Jean, January 24, 1975.
14. RSC-98, "Investigations of the Problem of Reflections from Soil Samples," P. Babai, October 1974.
15. RSC-96, "Computation of the Brightness Temperature of a Vertically Structured Medium," P. Babai, May 1974.
16. RSC-95, "Measurement of Complex Dielectric Constant of Soil Types in X-Band," P. Babai, June 1974.
17. RSC-92, "Newton's Method of Root Extraction as Applied to the Computer," C. McMillan, May 1974.
18. RSC-91, "On the Feasibility of Remote Monitoring of Soil Moisture with Microwave Sensors," R. W. Newton, S. L. Lee, J. W. Rouse, Jr., and J. F. Paris, April 1974.
19. RSC-84, "Soil Skin Depth Determination," S. L. Lee, October 1973.
20. RSC-73, "On Radio Science Techniques for Remote Sensing," John W. Rouse, Jr., June 1973.
21. RSC-68, "On the Measuring of Soil Moisture by Microwave Radiometric Techniques," C. L. Kroll, T. G. Sibley, and J. W. Rouse, Jr., April 1973.
22. RSC-61, "Prediction of Apparent Temperatures of Several Agricultural Test Sites," T. Sibley, October 1972.
23. RSC-52, "On the Effect of Moisture Variations on Radar Backscatter from Rough Soil Surfaces," J. W. Rouse, Jr., July 1972.
24. RSC-51, "Discussion of a Simplified Procedure for Measuring Dielectric Constant of Soil as a Function of Moisture Content," T. G. Sibley, July 1972.
25. RSC-46, "Weslaco Ground Truth Survey in Support of NASA/GSFC CV-990 Aircraft," C. L. Kroll, June 1972.
26. RSC-45, "Complex Dielectric Constant Measurements for Selected Soil Types," C. L. Kroll and T. G. Sibley, May 1972.
27. RSC-41, "The Effect of the Subsurface on the Depolarization of Rough Surface Backscatter," J. W. Rouse, Jr., September 1971.
28. RSC-36, "Re-evaluation of the Correlation of Measured Apparent Temperature to Soil Moisture Content," T. G. Sibley, December 1971.

Table 2. Continued

29. RSC-34, "A New Philosophy of Microwave Remote Sensing," J. W. Rouse, Jr., October 1971.
30. RSC-33, "Development of the Reflection Coefficient of a Layered Dielectric," J. A. Richerson, September 1971.
31. RSC-32, "Estimation of Surface Roughness Characteristics," J. A. Richerson, September 1971.
32. RSC-30, "Microwave Characteristics of Soil Surfaces," B. R. Jean, J. A. Richerson, J. W. Rouse, Jr., and M. L. Wiebe, September 1971.
33. RSC-23, "Development of the Reflection Coefficient of a Layered Dielectric," J. A. Richerson, May 1971.
34. RSC-22, "Various Techniques of Dielectric Constant Measurement as Applied to the Relative Dielectric Constant of Sand as a Function of Moisture Content," M. L. Wiebe, May 1971.
35. RSC-21, "Comparison of Peake's Microwave Emission Model to Experimental Measurements," J. A. Richerson, April 1971.
36. RSC-15, "The Size-Filtering Effect Inherent in the Slope-Facet Model of Radar Backscatter from the Sea," J. W. Rouse, Jr., August 1970.
37. RSC-06, "Comments on Microwave Radiometry as a Remote Sensor for the Geosciences," B. R. Jean, May 1970.
38. RSC-04, "Comments on Microwave Sensing of Soil Moisture," B. R. Jean, April 1970.

1978 Colby Experiment

The experiment held at the Colby test site in 1978 was to be a coordinated exercise involving the NASA Earth Resources aircraft, the University of Kansas truck mounted radar systems and the Texas A&M University truck mounted microwave radiometers, the Microwave Signature Acquisitions System (MSAS). The approach was to acquire ground-based microwave measurements at selected fields simultaneously with the aircraft overflights. The ground-based measurements were to be used as calibration points for the aircraft measurements. Only limited simultaneous aircraft and ground-based radar measurements had been made in the past, and no simultaneous aircraft and ground-based passive microwave measurements had ever been made. Considerable results were being derived from the ground based experimental program and a need existed to be able to utilize these results in aircraft measurements. However, it was unknown as to how well aircraft and ground-based sensors correlated with one another. This objective was met for the most part using the active systems, however, not for the passive systems. The following paragraphs document the effort that was made to acquire data with the MSAS simultaneously with the aircraft overflights.

Texas A&M personnel departed College Station, Texas on July 8, 1978 for Colby, Kansas driving the MSAS. The Texas A&M University team arrived at Colby, Kansas on July 10, 1978. Texas A&M maintained a crew of five individuals at Colby at all times. This required ferrying people to and from the Colby test site every two weeks. An apartment was rented in Colby, Kansas at the same location as the apartment rented by the University of Kansas personnel. Texas A&M

University personnel remained at the Colby, Kansas test site until July 30, 1978.

Unfortunately, data were not acquired from the MSAS throughout the entire period of the Colby aircraft experiment. After arriving at the Colby test site, the MSAS developed intermittent magnetic tape transport controller malfunctions. In the early stages the malfunctions were intermittent such that data could be acquired. However, data sets had to be retaken immediately after any malfunction since no data would have been placed on the magnetic tape. As long as this malfunction occurred only periodically, this inconvenience was accepted. However, by July 14 the malfunction occurred so often as to make progress in obtaining MSAS data virtually nil. As a result, repair efforts were initiated on July 14, 1978. These repair efforts were performed mainly during the night such that data could be acquired during the daytime, as possible. Due to the increasing frequency that the malfunction occurred, the last good set of MSAS data were acquired on July 22, 1978.

Intensive repair efforts were initiated on July 23, 1978. Field operations had to be terminated in order to initiate the intensive repair effort. On July 25, 1978 several bad transistors were discovered in the magnetic tape transfer reel servo control. Suitable replacement transistors were located on the opposite end of Kansas. A special flight was made to purchase these transistors. After replacing the transistors the tape transport operation was verified, however, malfunctions continued to occur. At that time a decision was made to send the Roim transport controller boards back to the manufacturer for the repair. Immediately thereafter, the Texas A&M University team departed Colby, Kansas on July 30, 1978.

During the stay at the Colby, Kansas test site, 11 field data acquisitions were obtained. Table 1 lists the date of these acquisitions, the field numbers on which they were obtained and the percent gravimetric moisture in the 0-5 cm layer. Measurements were acquired on five separate fields, two of these fields contained wheat stubble, one was bare, one contained corn, and one contain cut alfalfa. The majority of the measurements were acquired on Fields 11 and 13 which contained wheat stubble. Luckily, significant rainfall occurred between July 18 and July 20 producing a significant moisture change in the fields that were measured between these two dates. Appendix A contains the Ground Data report for the 1978 Colby, MSAS measurements.

MSAS measurements acquired at Colby, Kansas are presented in Figures 1 through 8. It should be noted that the data presented in these figures are not calibrated in the absolute sense. Due to the difficulties with the MSAS hardware at Colby, Kansas, it was not possible to acquire measurements over water or other standard reference targets for absolute calibration purposes. As a result, in reducing the raw measurements, previous calibrations were utilized. In comparing these measurements to previously acquired data or data acquired from other sensors, it should be noted that these measurements could be offset somewhat. However, these measurements are consistent relative to one another. Figures 1, 2, and 3 contain radiometric antenna temperature as a function of incident angle for L-band, C-band, and X-band respectively, for Field 13. These figures demonstrate the angular response for both horizontal and vertical polarization. Note that the measurement at nadir contains self emission from the system. Measurement at nadir can normally be taken as the average of the measurement at 20°.

Table 1

MSAS SUPPORT OF COLBY EXPERIMENT

Schedule

Departed TAMU - July 8
 Arrived Colby - July 10
 Departed Colby - July 30

Data Acquired

<u>Field</u>	<u>Date</u>	<u>% Moisture (0-5 cm)</u>
11 - Stubble	7/12	3.8
30 - Stubble	7/13	7.9
13 - Bare	7/15	3.4
24 - Corn	7/16	15.7
18 - Cut Alfalfa	7/17	4.9
11	7/18	4.5
13	7/18	3.1
11	7/20	27.5
13	7/20	24.3
11	7/22	22.9
13	7/22	22.2

L-Band Field 13 (July 22, 1978)

△ - Vertical
○ - Horizontal

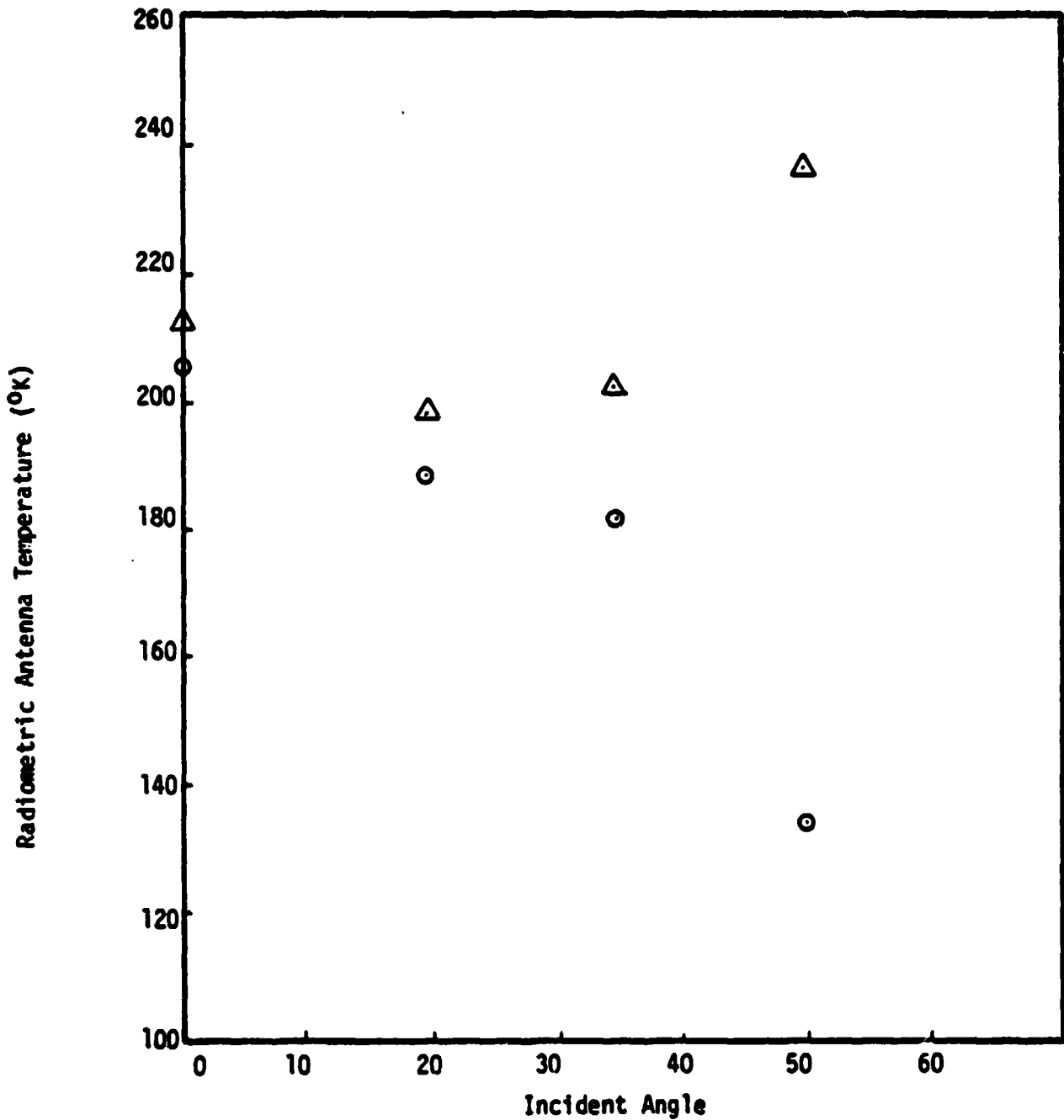


Figure 1. L-Band Measurement of Antenna Temperature vs. Incident Angle for Field 13.

C-Band Field 13 (July 13, 1978)

△ -Vertical

○ -Horizontal

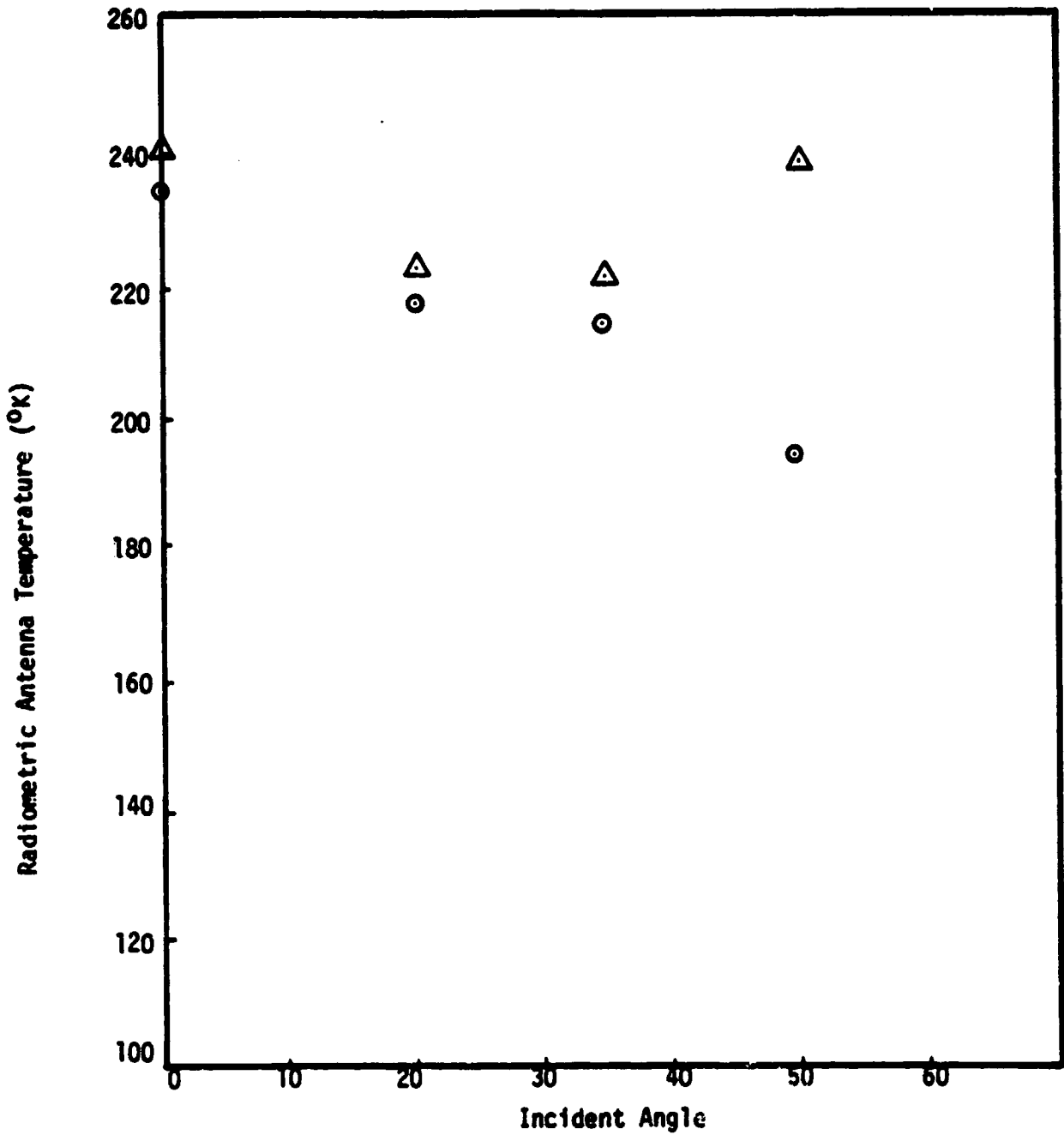


Figure 2. C-Band Measurement of Antenna Temperature vs. Incident Angle for Field 13

X-Band Field 13 (July 22, 1978)

△ -Vertical
○ -Horizontal

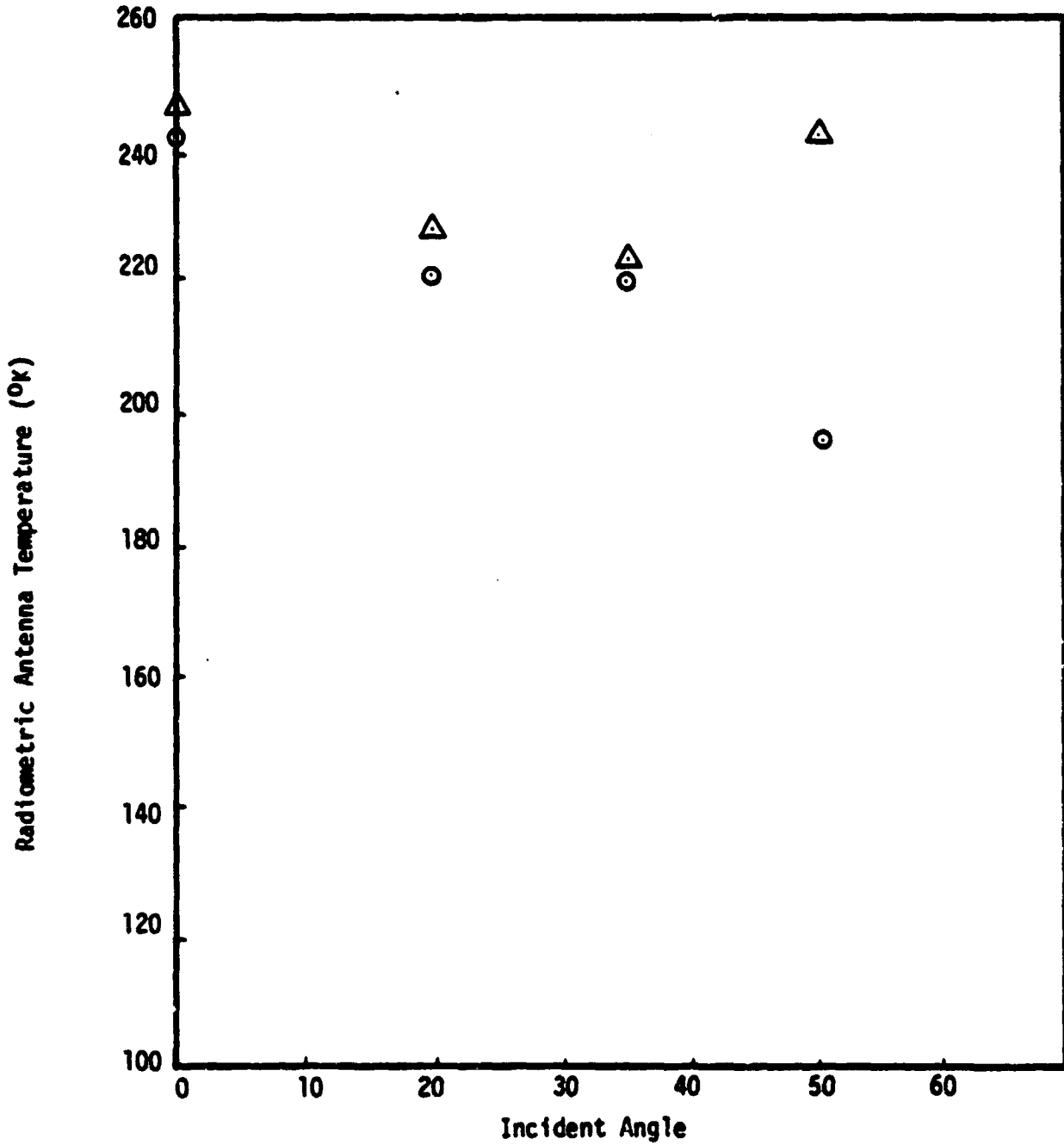


Figure 3. X-Band Measurement of Antenna Temperature vs. Incident Angle for Field 13.

L-Band
Horizontal Polarization
20° Incident Angle

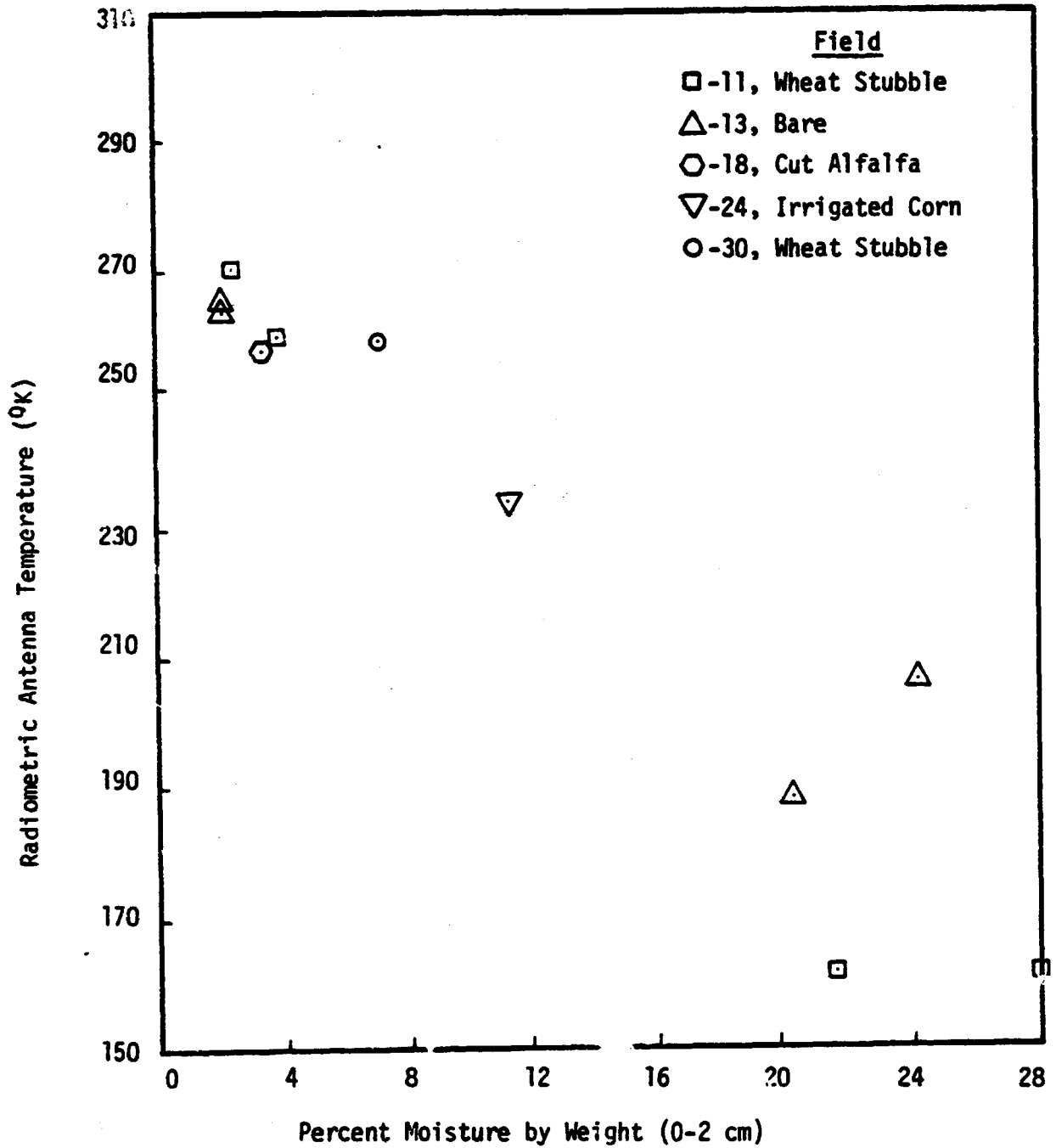


Figure 4. L-Band Antenna Temperature Measurement vs. 0-2 cm Soil Moisture for horizontal polarization and 20° incidence.

L-Band
Horizontal Polarization
20° Incidence Angle

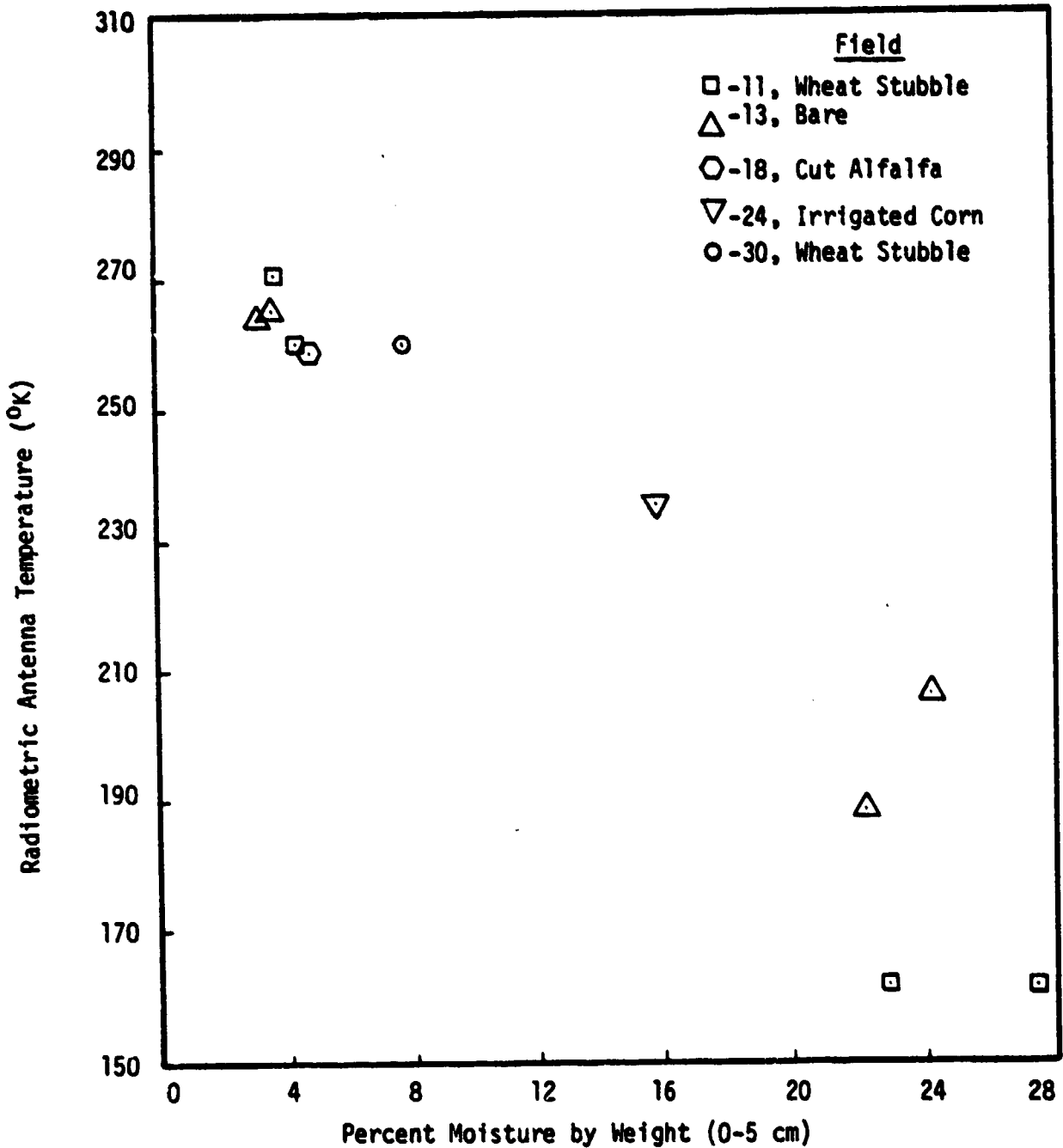


Figure 5. L-Band Antenna Temperature Measurement vs. 0-5 cm Soil Moisture for horizontal polarization and 20° incidence.

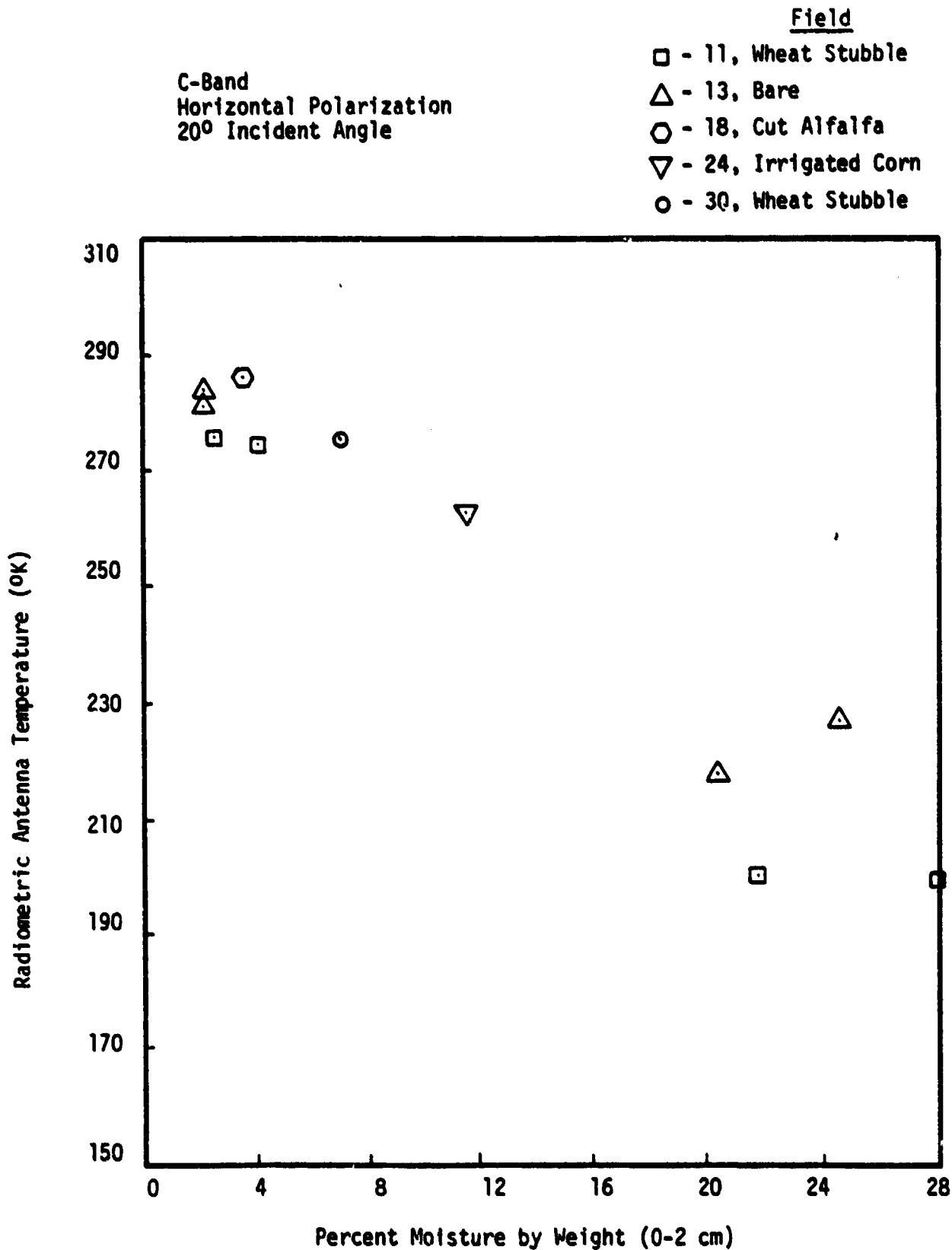


Figure 6. C-Band Antenna Temperature Measurement vs. 0-2 cm Soil Moisture for horizontal polarization and 20° incidence.

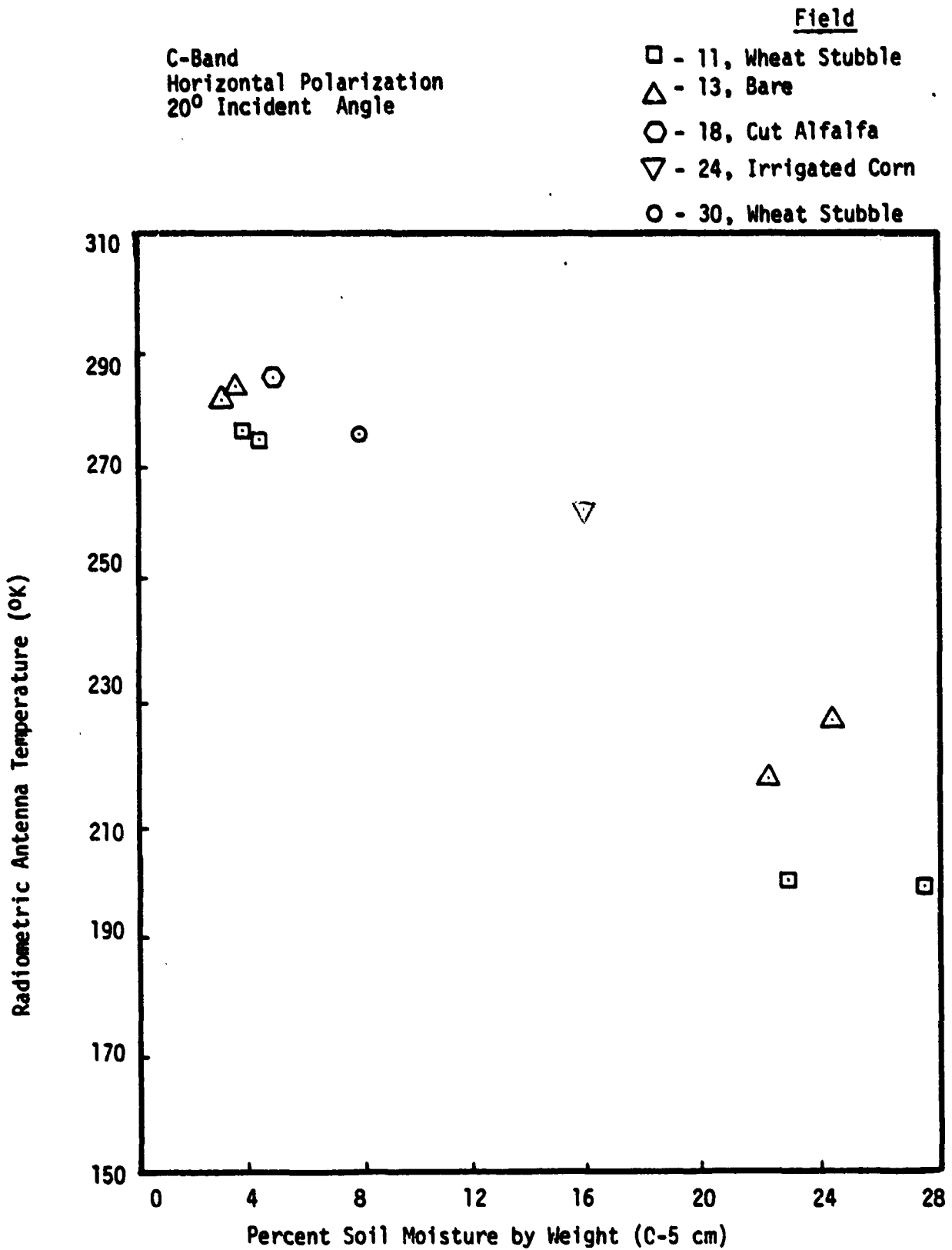


Figure 7. C-Band Antenna Temperature Measurement vs. 0-5 cm Soil Moisture for horizontal polarization and 20° incidence.

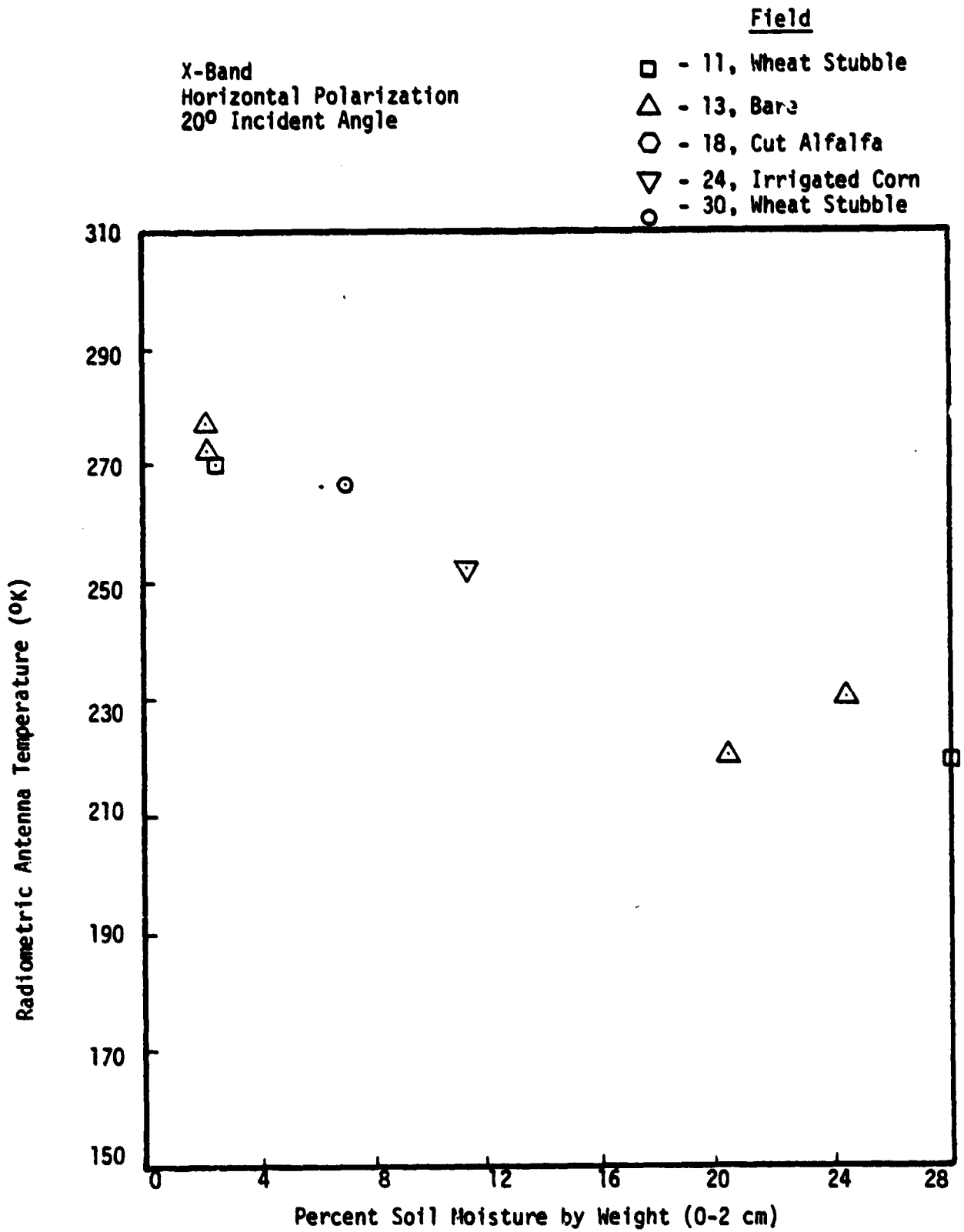


Figure 8. X-Band Antenna Temperature Measurement vs. 0-2 cm Soil Moisture for horizontal polarization and 20° incidence.

Figures 4 through 9 contain radiometric antenna temperature measured at L-band, C-band, and X-band for both the 0-2 cm average moisture and the 0-5 cm average moisture measured on a gravimetric basis. These data demonstrate a good response to soil moisture as expected. The X-band measurements show a slightly decreased sensitivity to moisture which is most likely due to surface roughness effects.

Unfortunately, only one measurement of cut alfalfa and one measurement of irrigated corn were obtained. This was not enough to demonstrate the effect of vegetation. It should also be pointed out that the irrigated corn was in the process of being irrigated at the time of the measurement. Gravimetric soil samples were taken on the ridges of the furrows between corn plants. As a result, the average gravimetric soil moisture content in the 0-5 cm layer of 15.7 percent is misleading. This is due to the fact that the ridges were reasonably dry while the furrows contained water. Therefore, Field 24 was unusual in the sense that the corn was mature corn with a height of well over 6 feet but with water running in the troughs between the corn plants. Care should be exercised in utilizing the measurement on this field in analysis. The measurements on Field 24 were taken parallel to the row direction of the corn.

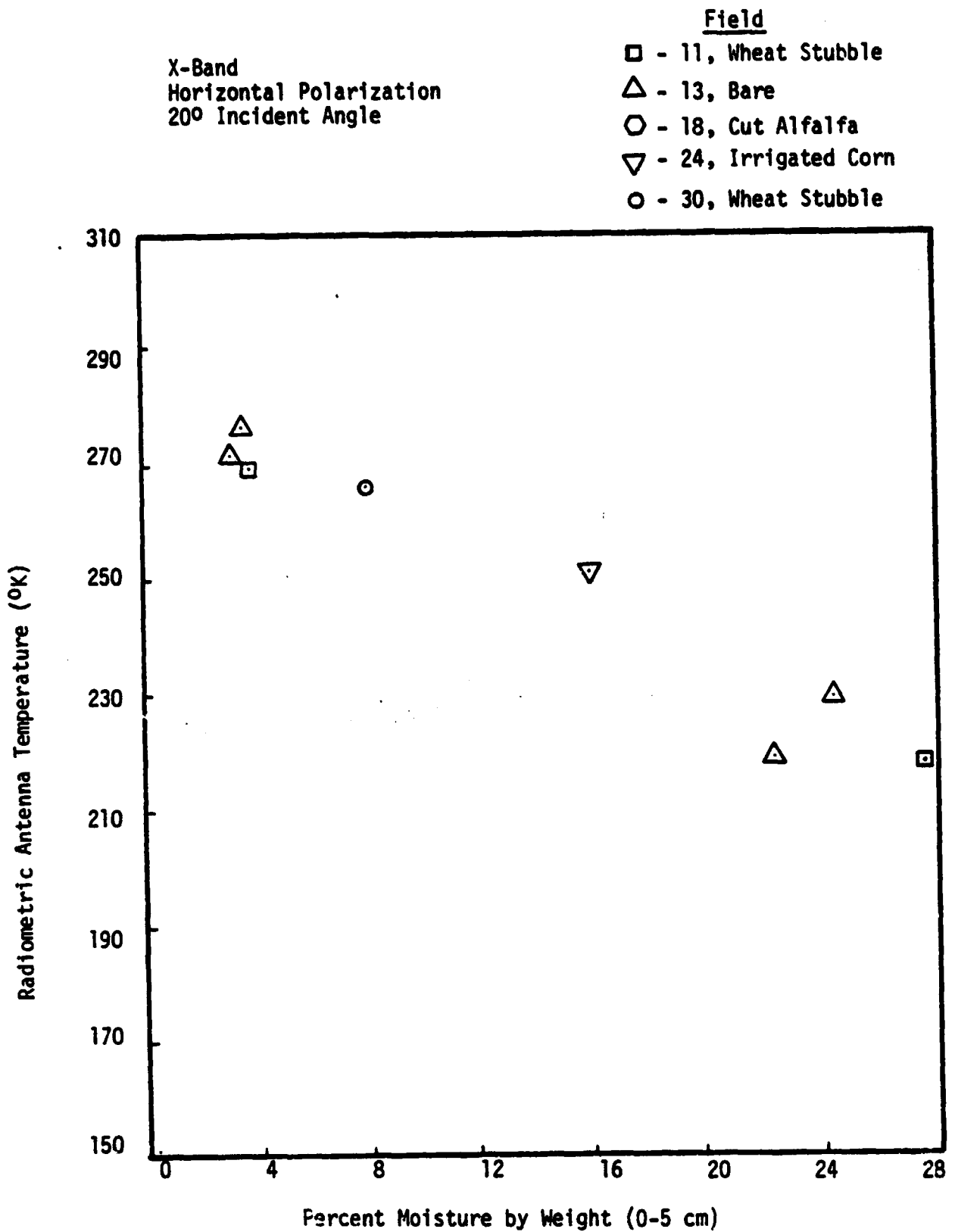


Figure 9. X-Band Antenna Temperature Measurement vs. 0-5 sm Soil Moisture for horizontal polarization and 20° incidence.

Development and Tests of Soil Moisture Algorithms

In August 1978, work was started to develop a model to calculate from measured soil properties and routine weather data, including precipitation, the distribution of water content and of temperature in a bare soil profile, starting with a set of known initial conditions. The model was to be mechanistic and, therefore, would also predict evaporation rates, drainage rates and soil moisture potentials, as well as surface temperatures, surface albedo and emittance.

The purpose of such a model is (1) to bridge the ground data sets in field tests of the feasibility of microwave detection of soil moisture, (2) to estimate soil moisture profiles in instances where only meteorological data are available, (3) to form a complementary theory to that of passive microwave emission by soil, (4) to enable rational calculations of subsurface moisture from microwave data, and (5) to form the basis for similar models for vegetated land.

The progress made through November 1979, at the end of the contract period, consists of the completion of a model and its documentation (see Appendix B), prepared in July 1979. This model has been tested and improved, in a numerical sense, for stability and efficiency. Also, it was shown that half-hourly weather data do not give much more information, for the purposes at hand, than daily weather data on solar radiation, air temperature and humidity, windspeed and rainfall.

A number of sensitivity tests were made to explore the effect of errors and of spatial variation, as anticipated in the measurement of the hydraulic properties of the soil profile in a real situation. The results are given as Appendix C. On the whole, they demonstrate that the soil medium can be "scaled" over a fair range without affecting

the predicted values of interest too severely. The explanation is in the deterministic nature of the model, in that it adheres to the principles of conservation of mass and energy.

Preliminary results of the soil moisture observation site at the Agronomy farm were used to test the model against field data. These tests are continuing and nonconclusive at this point. They are reported in the following text.

We believe that, at this time, a reasonably sound foundation exists for the analysis and design of field tests of microwave soil moisture detection, obtained at a modest investment of time and resources. Further tests are planned, refinements are likely in order, and improved accuracy of the needed field data is indicated.

Sensitivity Tests

Summary of Previously Reported Efforts

The model was first tested in regard to its sensitivity to errors in the input data of the soil hydraulic characteristics, i.e. saturated hydraulic conductivity and the relationship between the volumetric water content and pressure potential. Even if a field test site were entirely uniform, the measurement itself could be in error for a number of reasons, hence, the need for sensitivity tests.

The hydraulic characteristics of the Norwood silt loam were varied by a factor of 1/16, 1/4, 4.0, and 16.0, that is to say, the saturated hydraulic conductivity or, separately, the pressure potential at a given water content was allowed to range as indicated.

In order to evaluate the variation produced by the introduction of the above mentioned factors, separate simulation runs were done for a period of 15 days, to a total of fifteen in each of two categories.

In general, each simulation started with a saturated soil profile, weather input data were kept constant from day to day, and a rainfall of 50.0 mm was assumed on day 10. Specifically, the following simulation runs were done:

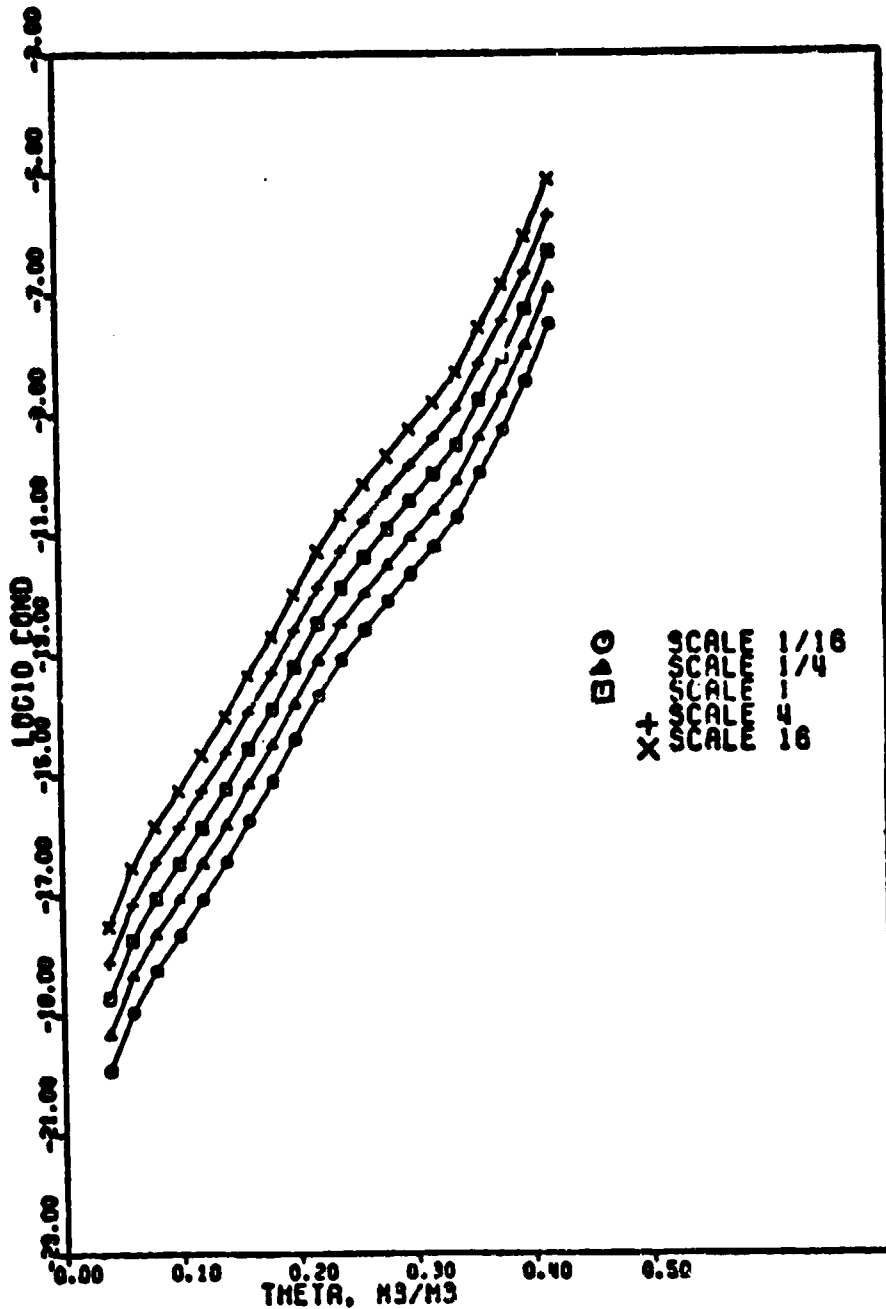
1. the saturated hydraulic conductivity of both horizons were varied simultaneously,
2. the saturated hydraulic conductivity of the top horizon was varied,
3. the saturated hydraulic conductivity of the bottom horizon was varied,
4. the soil moisture retention curve of both horizons varied simultaneously,
5. the soil moisture retention curve of the top horizon was varied, and
6. the soil moisture retention curve of the bottom horizon was varied.

An example of the effect of errors in the measurement of the saturated hydraulic conductivity of both horizons of the soil is presented. The interpretation of the results obtained is not straightforward because of the fact that, in reality, conductivity and retention cannot vary independently. Nevertheless, the measurement errors are potentially independent.

Figure 1 shows the variation induced in the input data as the result of errors in the measurement of the saturated hydraulic conductivity. From Figure 2 we conclude that the evaporation rate is not greatly affected if the saturated hydraulic conductivity is found within a factor of 4 of its true value. Drainage rate, as shown in

TAMU - RSC

DEPT. OF S4C

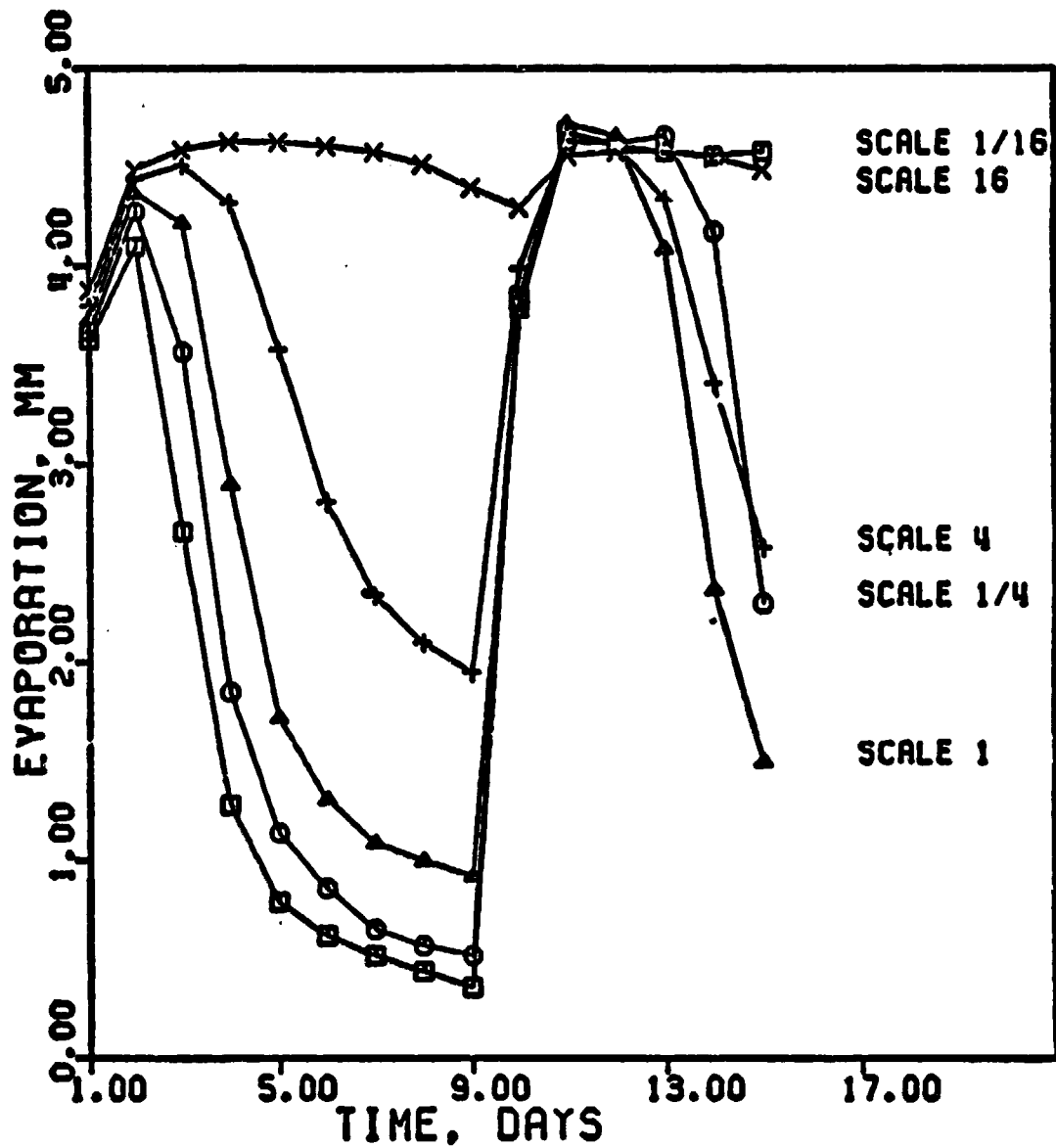


HYDRAULIC CONDUCTIVITY (M/S) VS. WATER CONTENT

Figure 1. Input data used in sensitivity test of bare soil water balance model. The saturated conductivity is varied by the factors shown, in reference to the best data fit for Norwood silty clay loam. The graph displays the resulting conductivity vs. water content relations.

TAMU - RSC

DEPT. OF S&C



DAILY EVAPORATION VS. TIME

Figure 2. Sensitivity of the calculated daily evaporation rate to relative errors in the measured input value of the saturated hydraulic conductivity, over a scale from 16 to 1/16. Results should be compared to those shown as triangles for scale 1. Overestimation up to a factor of 4 gives appreciable error but underestimation by a like factor does not.

Figure 3 is similarly affected. Of particular interest is the water content of the superficial (0-150 mm) layer. Its magnitude varies by less than 10% if the hydraulic conductivity is found within 4 and 1/4 of its true value.

Similar data, not reported here, but detailed in earlier quarterly reports, suggests that the measurement technique itself is perhaps not the greatest source of discrepancy between calculated and measured water reserves, soil temperatures and soil water potentials. An order-of-magnitude estimate of the permanent soil properties appears a reasonable first step toward rational and useful interpretation of weather data and/or of magnitude signals.

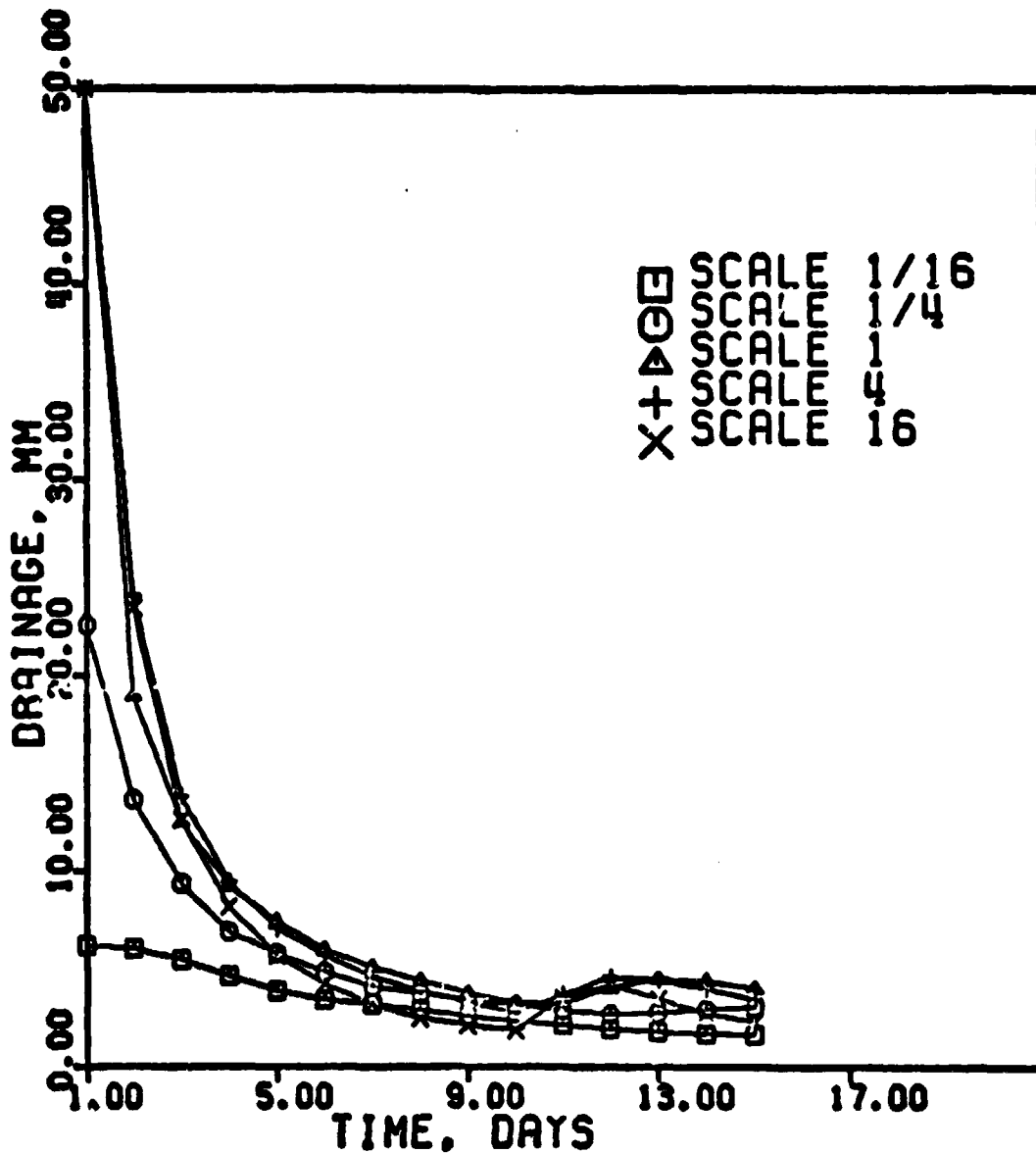
An entirely different matter is the implication of the enormous site-to-site variation of the soil properties in even the most homogeneously appearing fields and test plots. This matter is analyzed, with our model as a vehicle for interpretation, in the next section.

The Effect of Spatial Variability of Soil-Water Properties

Background - Nielsen et al. (1973) investigated the spatial variability of hydraulic conductivity, soil water content, texture, bulk density and soil moisture retention curves in a 150 ha field. Data were reported for 20 sites within the area. They concluded that variations in water content with depth and horizontal distance throughout the field were normally distributed, while values of the hydraulic conductivity were log-normally distributed. Peck et al. (1977) turned the proposition around; that is, they investigated the applicability of extrapolating soil hydraulic properties as obtained from a few sites to a larger area within the field. To do so, they combined statistics with scaling theory.

TAMU - RSC

DEPT. OF S&C

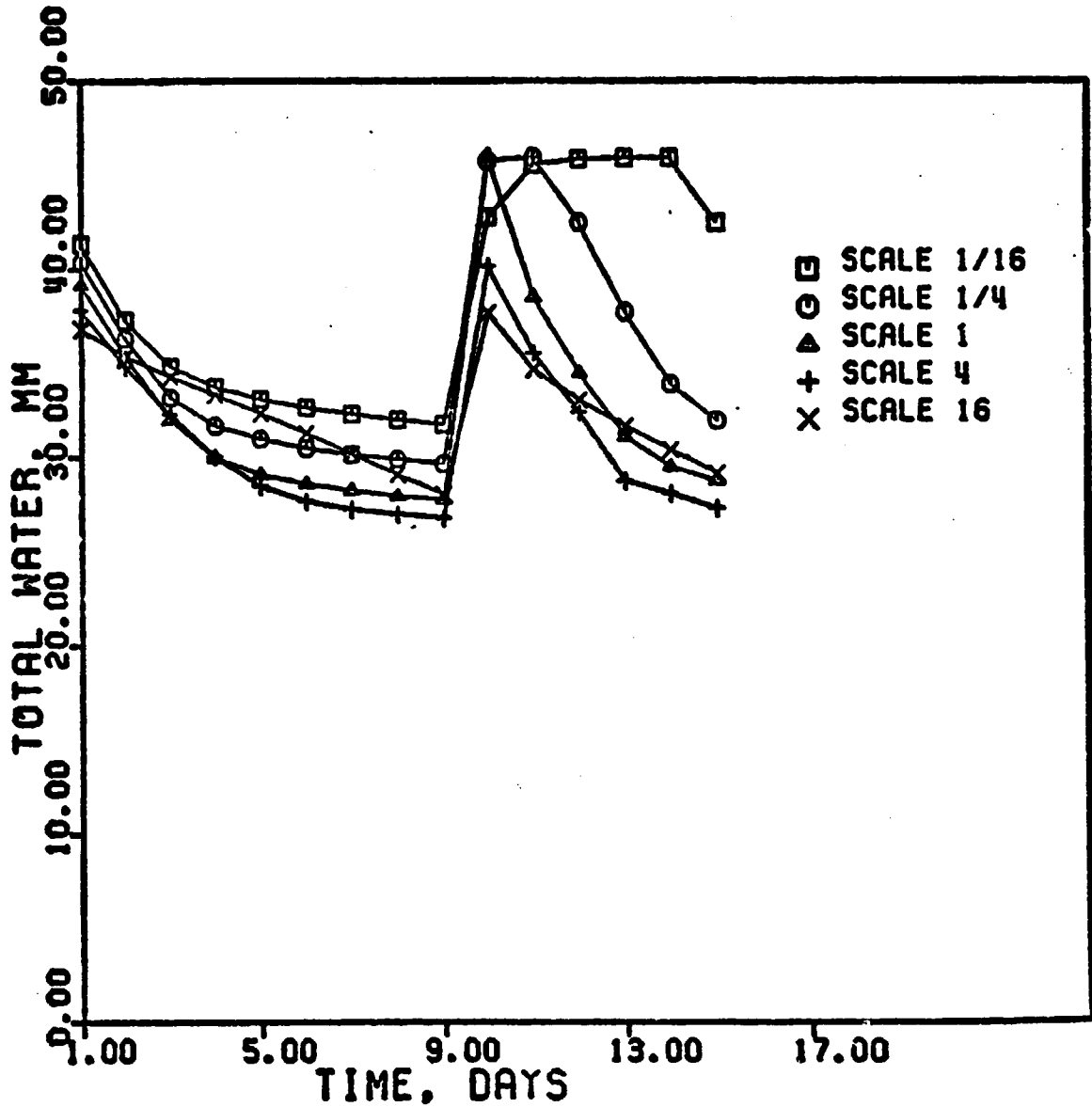


DAILY DRAINAGE VS. TIME

Figure 3. Daily drainage rate as affected by assumed error in the saturated conductivity as measured for Norwood silty clay loam. Rain of 50 mm on the 10th day. The effect on drainage after the first 5 days is not large.

TAMU - RSC

DEPT. OF S&C



TOTAL WATER VS. TIME

Figure 4. Water content of the 0-150 mm surface layer as influenced by assumed error in the saturated conductivity as measured for Norwood silty clay loam. Rain of 50 mm on the 10th day.

Scaling theory is based on consideration of the microscopic dimensions of a pore, a particle, an aggregate or some average of these parameters for a particular soil sample. It is derived from scaling theory that, at given water contents, the pressure potential is related to an average pressure potential by

$$\lambda_r \psi_r = \bar{\lambda} \psi_m \quad (1)$$

where λ_r is the scaling factor, $\bar{\lambda}$ is the average scaling factor, ψ_r is the reference pressure potential, and ψ_m is the average pressure potential. Likewise for the hydraulic conductivity,

$$K_r / \lambda_r^2 = K_m / \bar{\lambda}^2 \quad (2)$$

where K_r is the reference hydraulic conductivity and K_m is the average hydraulic conductivity. In this analysis, it is implied that water transmission and water retention are jointly affected by the scaling factor, which then becomes the parameter that varies from site to site and of which the effect upon water profile balance need to be known.

Peck et al. (1977) defined a ratio $\alpha = \lambda_r / \bar{\lambda}$, and assumed that it was normally distributed with a mean of 1 and a coefficient of variation of 0.25. We have adopted their method for a sensitivity analysis, using our data for the average saturated hydraulic conductivities and soil moisture retention curves for Norwood silt loam. We have also assumed in our calculations a normal distribution and a coefficient of variation of 0.25, as suggested by Peck et al.

Simulation - To evaluate the effect of variability in the scale ratio, α , the saturated hydraulic conductivity and soil moisture retention relation were varied in separate 15-day simulations. The environmental conditions were kept constant from day to day, and a

rainfall of 50.0 mm was simulated on day 10. The assumed initial soil water content and temperature profile of the soil system are given in Figure 5 and 6, respectively. They represent a well-watered bare Norwood soil after several days of clear weather in early spring.

Independent simulation runs were done for each scaling ratio. Table 1 summarizes the values of α and the corresponding values for the saturated hydraulic conductivities. The resulting unsaturated hydraulic conductivity was calculated by the method of Jackson (1972), and is represented in Figure 7 for horizon I, and in Figure 8 for horizon II. Table 2 summarizes the values of α used to obtain the pressure potential values, and Figure 9 shows the resulting soil moisture retention curve for horizon I and Figure 10 for horizon II. In the figures only the two extreme values, as well as the base value are represented.

For a given simulation, that is, for a given value of the scaling ratio, both the saturated hydraulic conductivity and the soil moisture retention relation of both horizons were scaled simultaneously, in an attempt to simulate what can be expected if the scaling theory is valid, both qualitatively and quantitatively.

Results - The results of the simulation runs for the average hydraulic properties and the two extreme values of the scaling factor are presented in Figures 11 through 16.

Discussion - Figure 11 shows that a 20% to 30% variability in evaporation rates is entailed by the full range of scaling during a drying period, but none during and immediately after a wetting event. The corresponding variation in drainage rate is greater and, in fact, overwhelming during the early stages of drainage, as shown in Figure

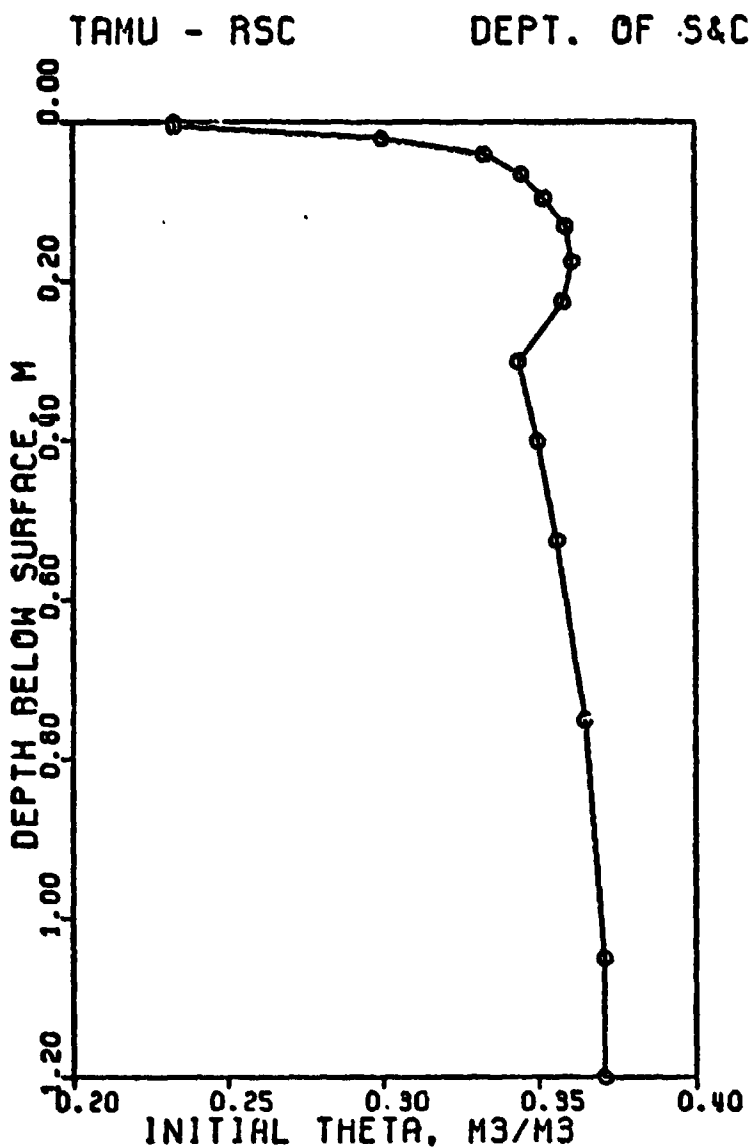


Figure 5. Initial volumetric water content (m^3/m^3) as a function of depth (m) below the soil surface at midnight.

TAMU - RSC

DEPT. OF S&C

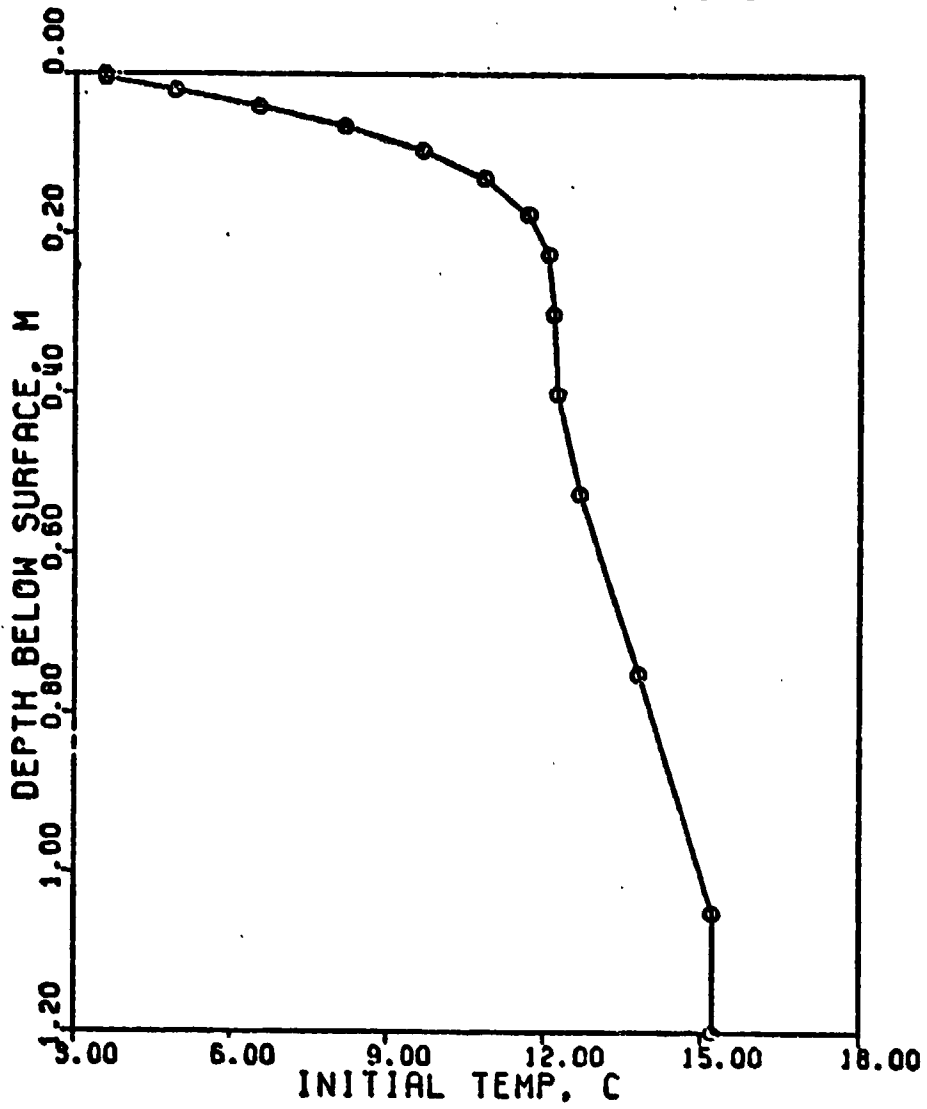


Figure 6. Initial soil temperature ($^{\circ}\text{C}$) as a function of depth (m) below the soil surface at midnight.

Table 1. The scaling factor α (ratio of microscopic dimension of soil to its mean) and the corresponding values of the saturated hydraulic conductivities (K) for both soil horizons, as obtained with equation (1).

α	α^2	K(horizon I) m/s	K(horizon II) m/s
0.381	0.145	7.258×10^{-8}	8.710×10^{-7}
0.559	0.312	1.562×10^{-7}	1.875×10^{-6}
0.735	0.540	2.701×10^{-7}	3.241×10^{-6}
0.911	0.830	4.150×10^{-7}	4.980×10^{-6}
1.000	1.000	5.000×10^{-7}	6.000×10^{-6}
1.089	1.186	5.930×10^{-7}	7.116×10^{-6}
1.265	1.000	8.001×10^{-7}	9.601×10^{-6}
1.441	2.076	1.038×10^{-6}	1.246×10^{-5}
1.619	2.621	1.311×10^{-6}	1.573×10^{-5}

TAMU - RSC

DEPT. OF S&C

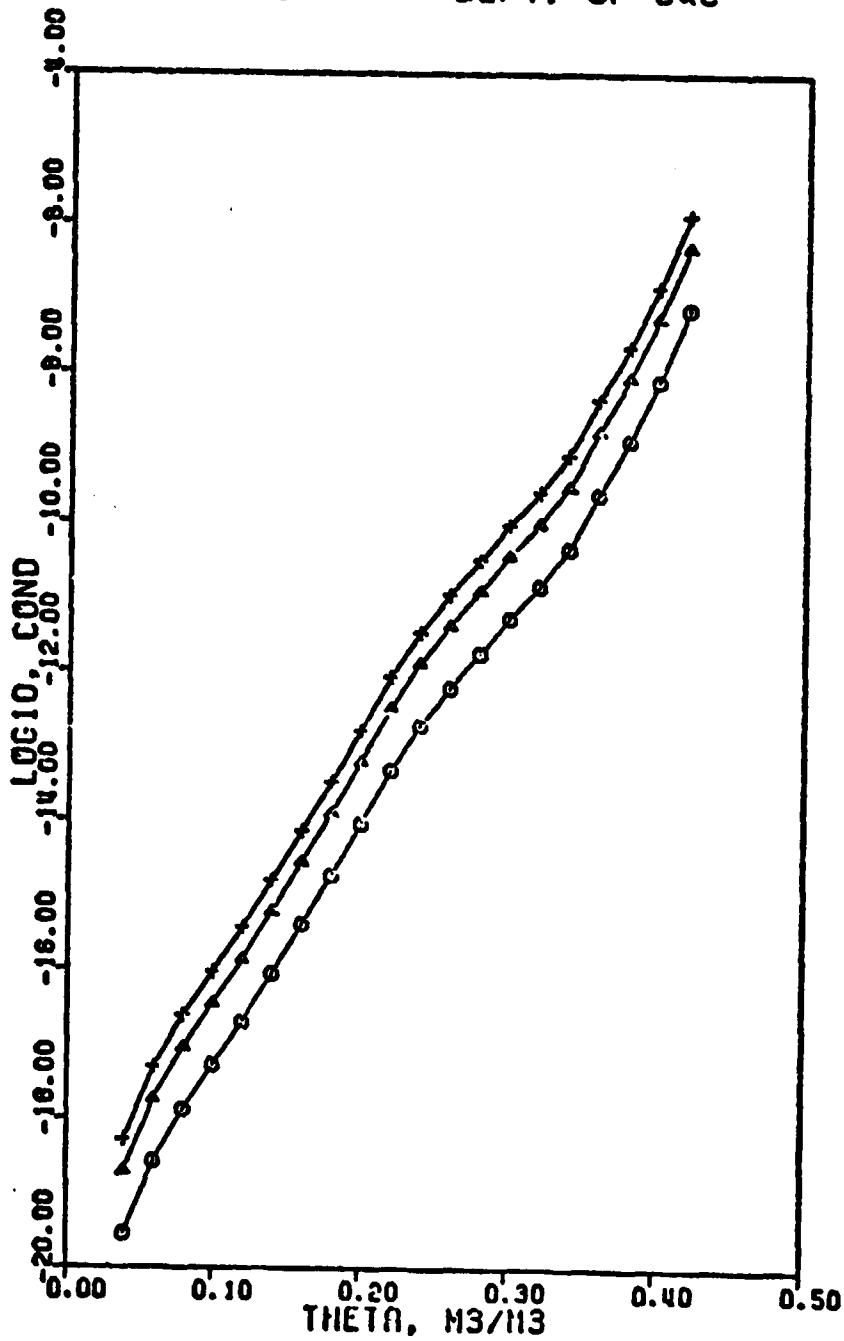


Figure 7. Unsaturated hydraulic conductivity as a function of water content for horizon I and scale. The symbol (+) is for scale 1.619 (Δ) is for 1.000, and (O) is for 0.381.

ORIGINAL PAGE IS
OF POOR QUALITY

TAMU - RSC

DEPT. OF S&C

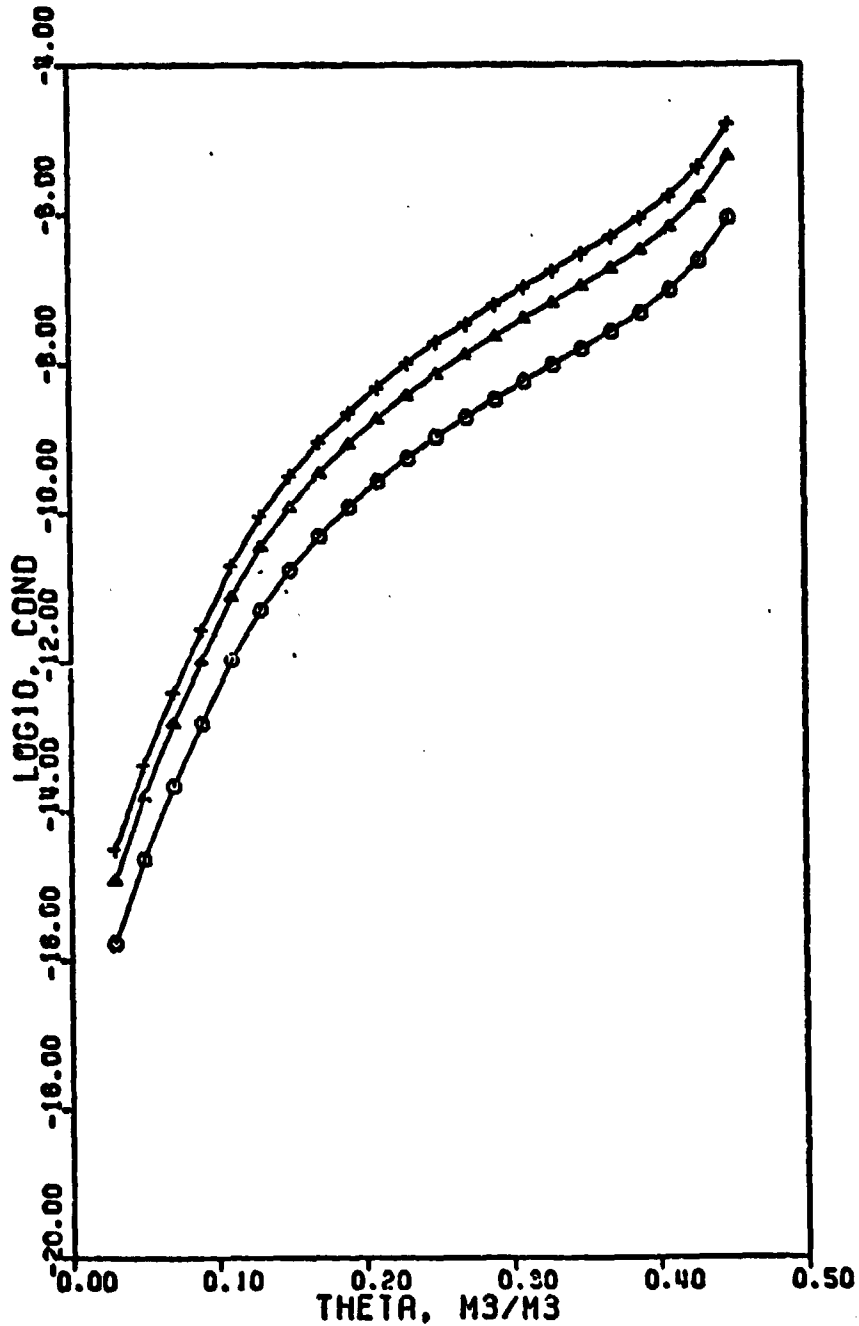


Figure 8. Unsaturated hydraulic conductivity as a function of water content for horizon II and scale. The symbol (+) is for scale 1.619, (Δ) is for 1.000 and (O) is for 0.381.

Table.2. The scaling factor α (ratio of microscopic dimension of soil to its mean) used to generate curves as those shown in Figures 9 and 10. The same values of α were used for both horizons using equation (2).

α	$1/\alpha$
0.381	2.625
0.559	1.789
0.735	1.361
0.911	1.098
1.000	1.000
1.089	0.918
1.265	0.791
1.441	0.694
1.619	0.618

TAMU - RSC

DEPT. OF S&C

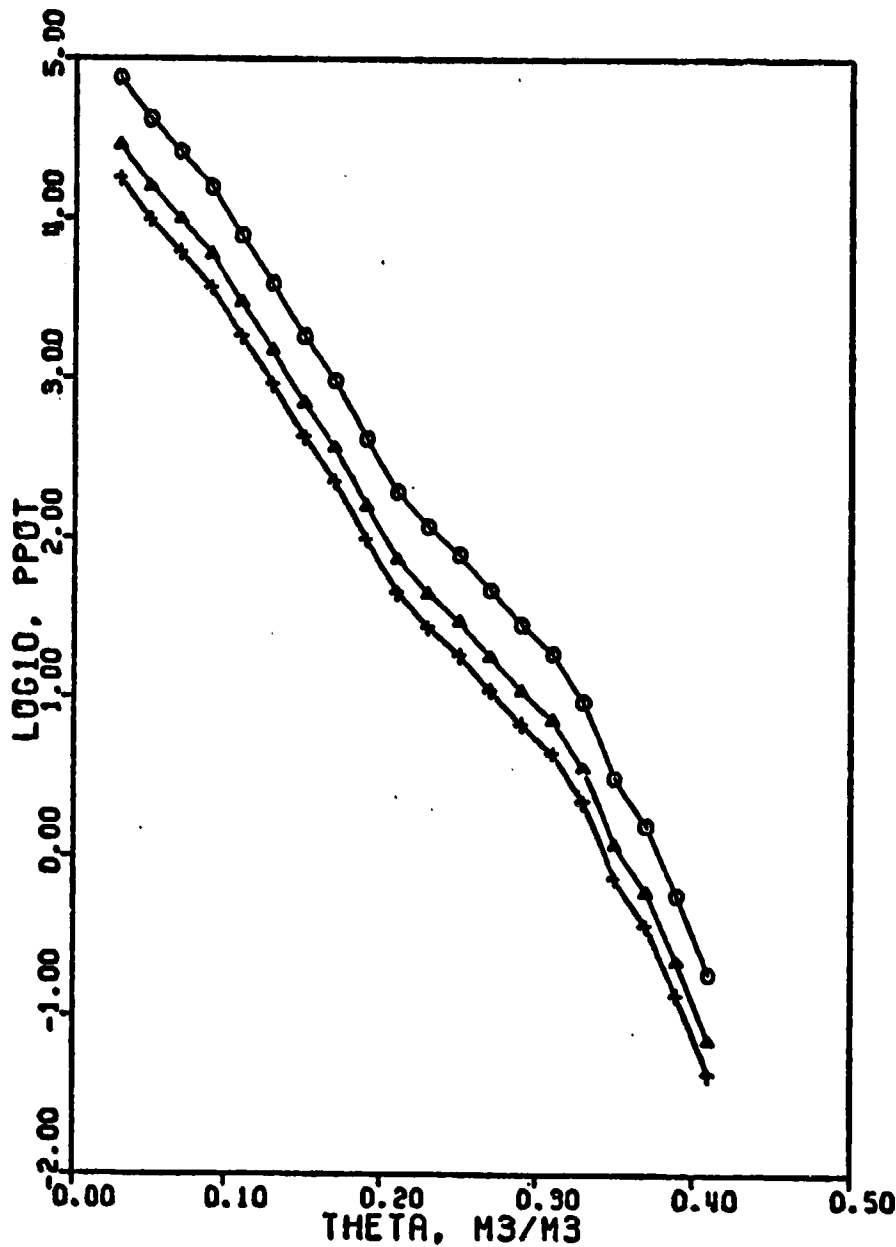


Figure 9. Relationship between the \log_{10} of pressure potential and volumetric water content for horizon I and scale. The symbol (+) is for scale 1.619, (Δ) is for scale 1.000, and (O) is for 0.381.

TAMU - RSC

DEPT. OF S&C

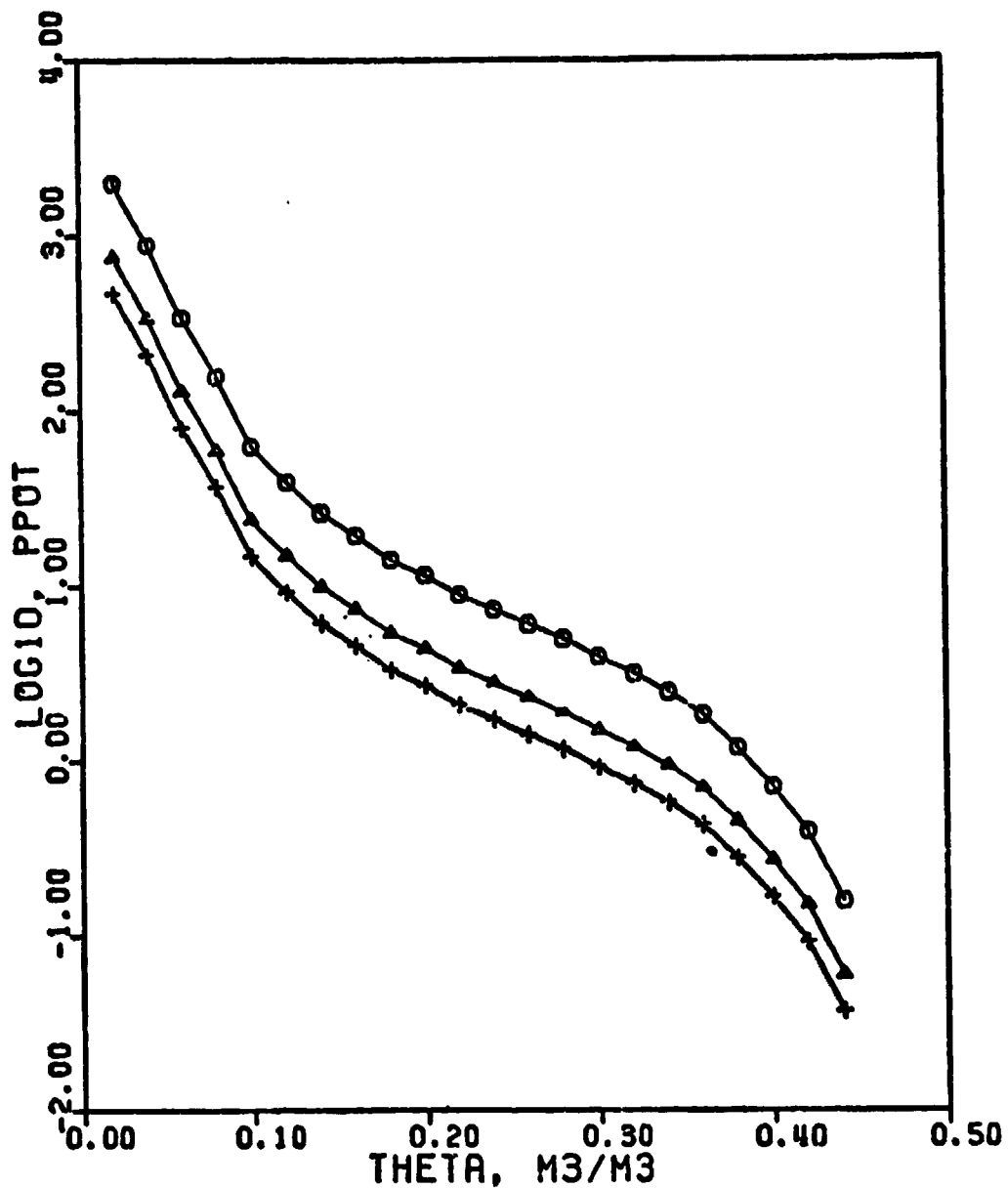


Figure 10. Relationship between the \log_{10} of pressure potential and volumetric water content for horizon II and scale. The symbol (+) is for scale 1.019, (Δ) is for scale 1.000 and (O) is for 0.381.

TAMU - RSC

DEPT. OF S&C

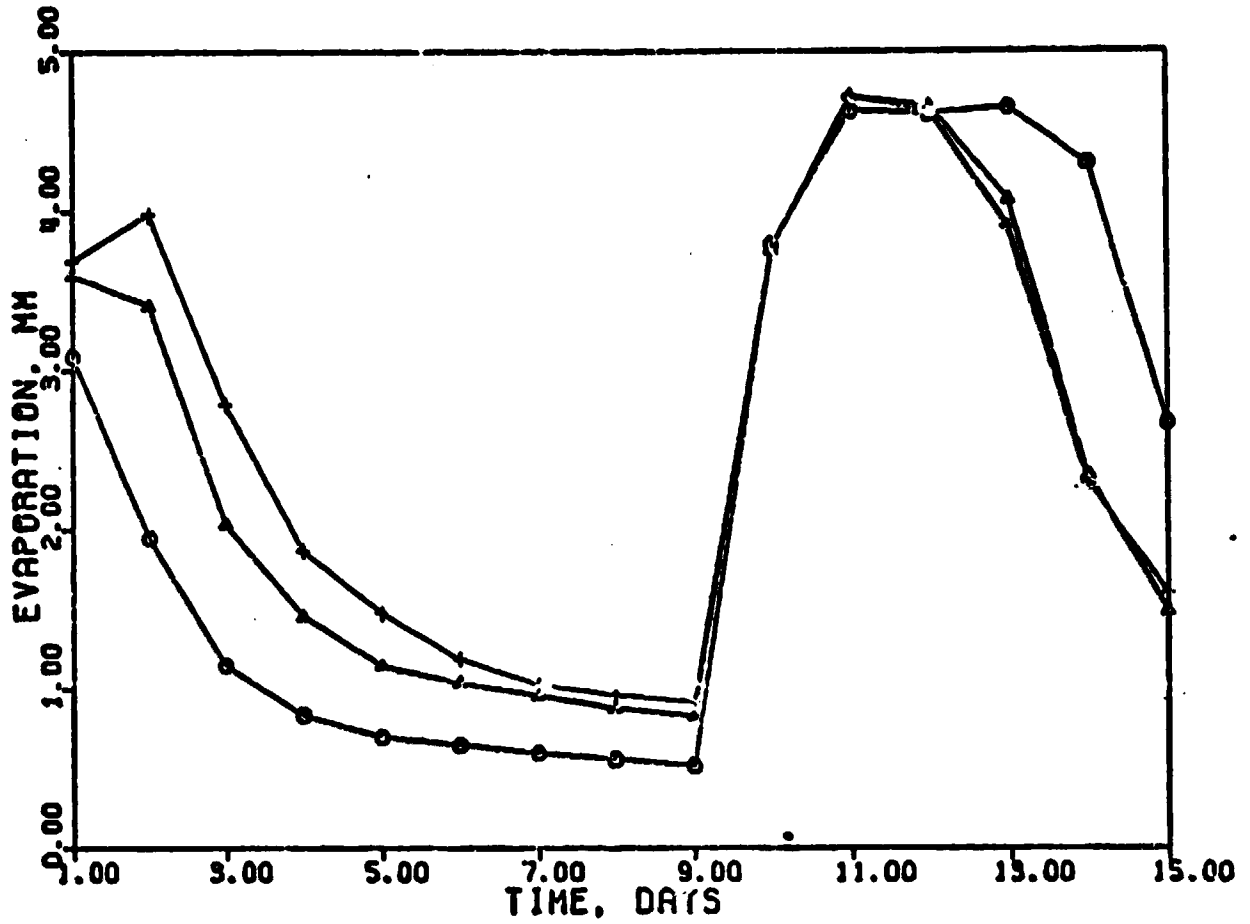


Figure 11. Daily evaporation (mm) as a function of time (days) and scaling factor. The symbol (+) is for scale 1.619, (Δ) is for 1.000 and (O) is for 0.381.

ORIGINAL PAGE IS
OF POOR QUALITY.

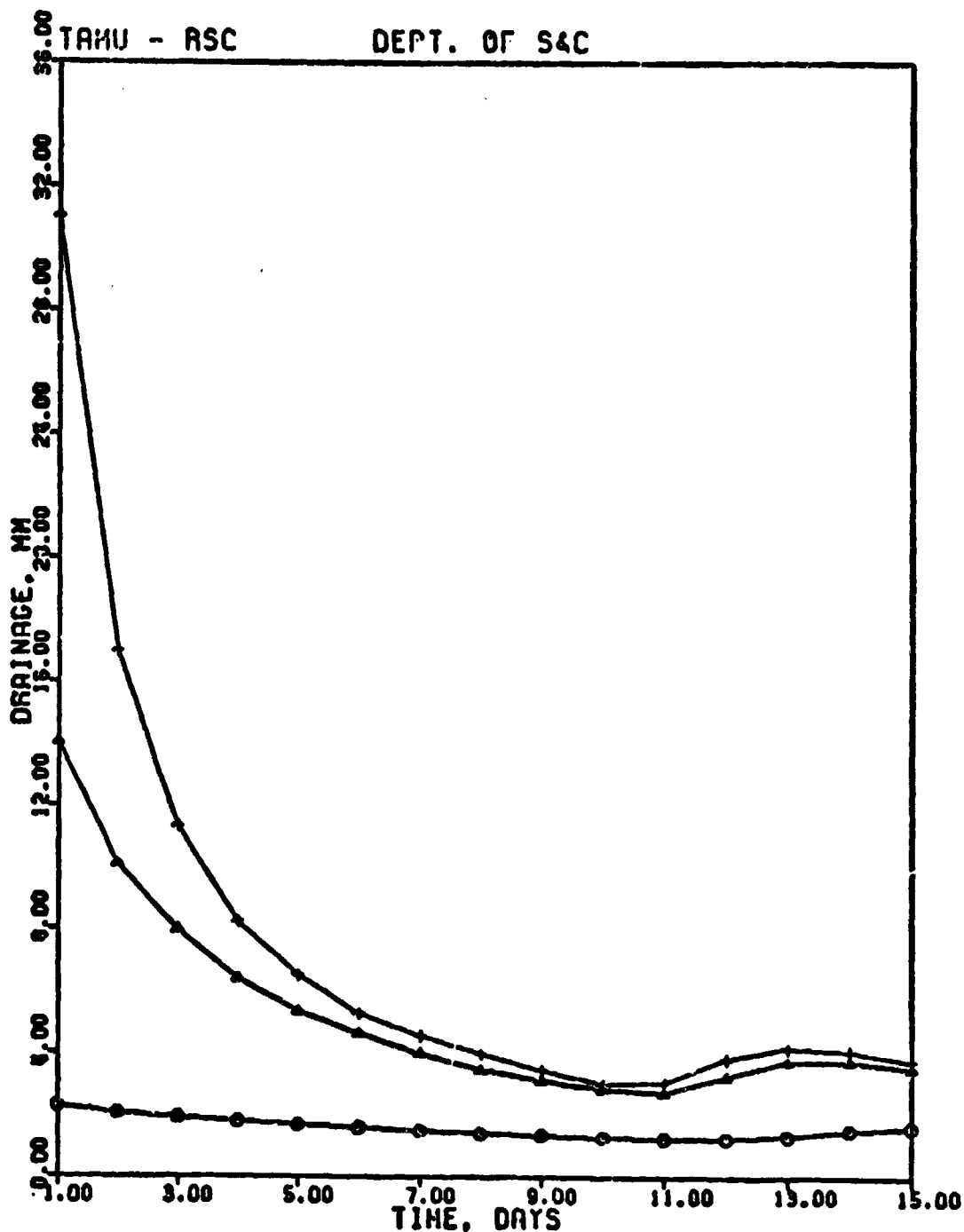


Figure 12. Daily drainage (mm) as a function of time (days) and scaling factor. The symbol (+) is for scale 1.619, (Δ) is for 1.000 and (O) is for 0.381.

ORIGINAL PAGE IS
OF POOR QUALITY

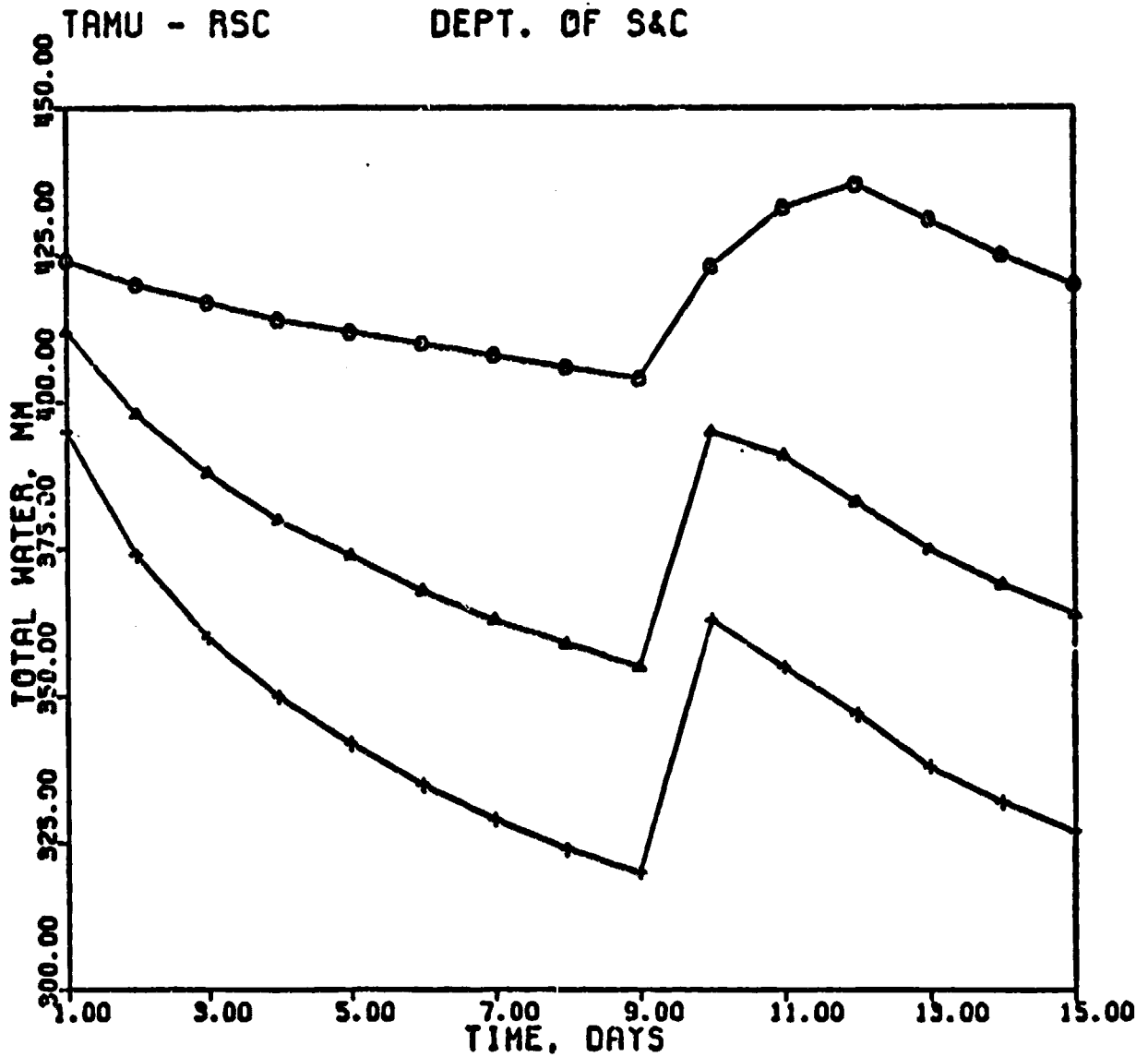


Figure 13. Total water (mm) as a function of time (days) and scaling factor. The symbol (+) is for scale 1.619, (Δ) is for 1.000 and (O) is for 0.381.

ORIGINAL PAGE IS
OF POOR QUALITY

TAMU - RSC

DEPT. OF S&C

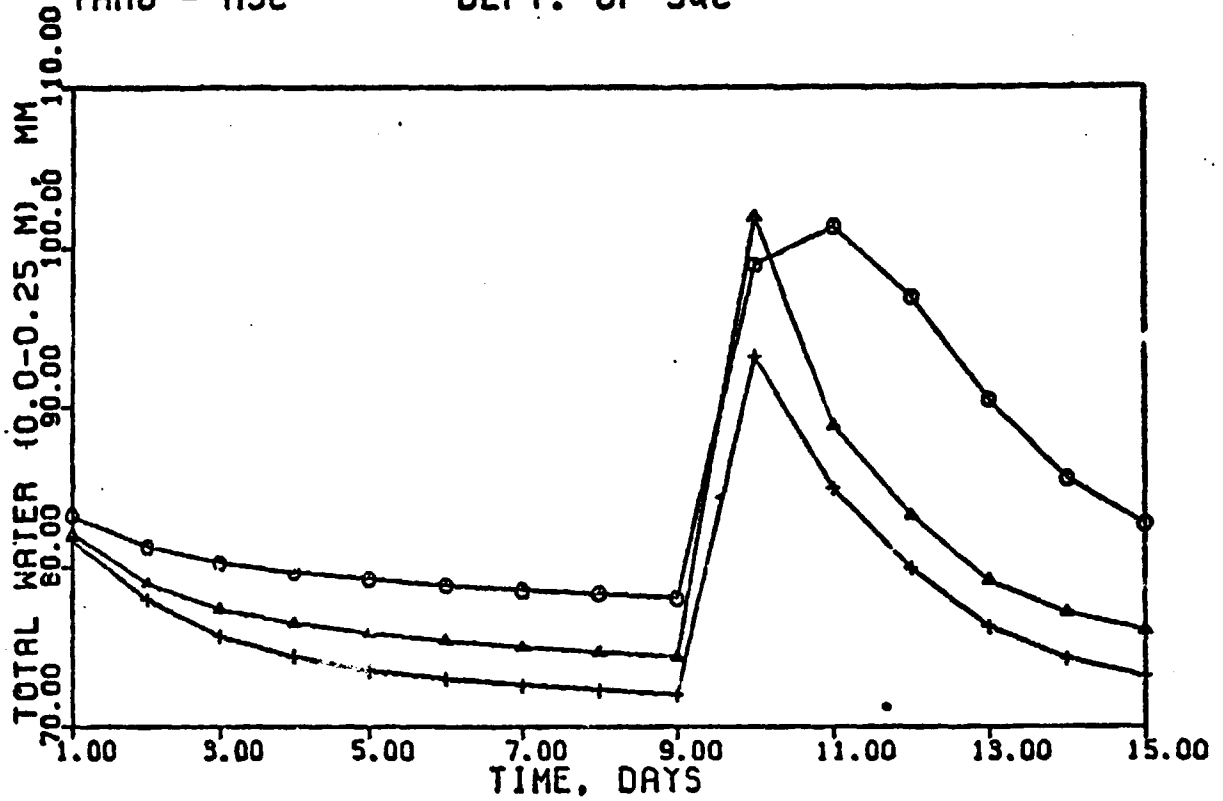


Figure 14. Total water (mm) in the top 0.25 m of the soil profile as a function of time (days) and scaling factor. The symbol (+) is for scale 1.619, (Δ) is for 1.000 and (O) is for 0.381.

ORIGINAL PAGE IS
OF POOR QUALITY

TAMU - RSC

DEPT. OF S&C

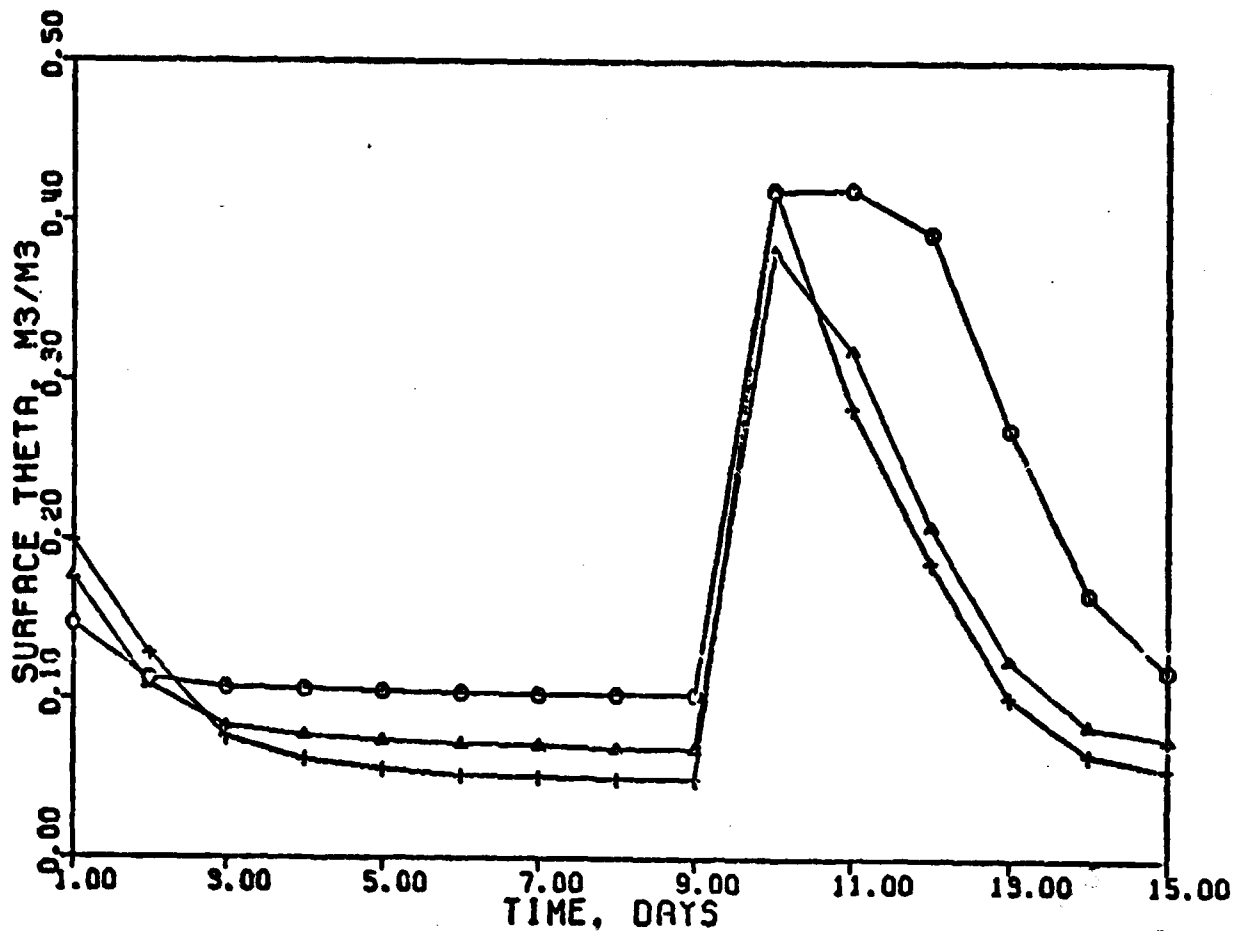


Figure 15. Volumetric water content (m^3/m^3) of the soil surface at 4:00 p. m. as a function of time (days) and scaling factor. The symbol (+) is for scale 1.619, (Δ) is for 1.000 and (O) is for 0.381.

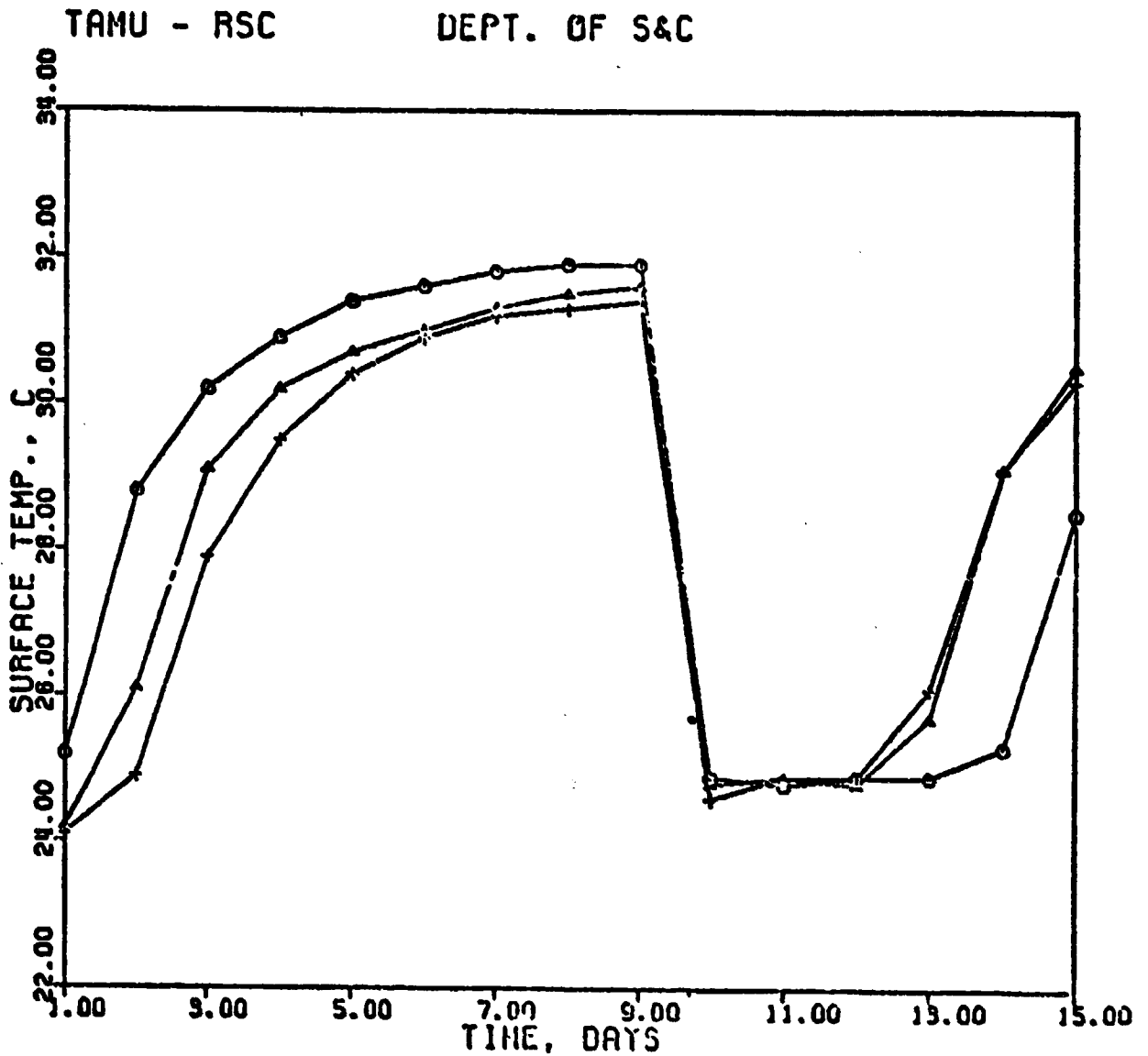


Figure 16. Surface temperature ($^{\circ}\text{C}$) at 4:00 p.m. as a function of time (days) and scaling factor. The symbol (+) is for scale 1.619, (Δ) is for 1.000 and (O) is for 0.381.

12. The entire range of scaling modifies the total amount of water in the profile by about 20% on either side of the "normal", as may be seen in Figure 13, whereas the surface water content is affected much less, except immediately following a rainfall event for the down-scale situation. This response is depicted in Figure 15. Again, the principal quantity of interest, the water content of the surface 0.25 m, is affected much less than either of the previous elements. Over the total range of scaling the excursion is 5-10% from the normal value.

The effect of scaling on soil temperatures is minor, except at the very surface, as may be seen in Figures 15, 16, 17, and 18. Even so, it cannot be ignored, which is a matter of interest in the interpretation of bare-soil thermal scans.

To properly evaluate the results obtained by applying a scaling ratio to the "normal" hydraulic properties of the Norwood silt loam soil, we must restate the implications of the scaling method used. In our application, the average scaling factor ($\bar{\lambda}$) is taken as the mean value of the microscopic length (λ_r) in the soil area considered. We have assumed that the ratio of the standard deviation of λ_r to $\bar{\lambda}$, that is, the coefficient of variation to be 0.25. By relating the values of the scaling ratio ($\alpha = \lambda_r/\bar{\lambda}$) to a normal frequency distribution with mean 1, we cover a range that represent 99.6% of the total area of the soil. The physical interpretation of the scaling ratio, α , is that, over the range 0.381 - 1.196, the ratios represent soils of increasing dimension, e.g. particle size, or pore size. Therefore, the use of the chosen values of α produces corresponding variations of the simulated water balance over the soil area, when introduced in our model.

ORIGINAL PAGE IS
OF POOR QUALITY

TAMU - RSC

DEPT. OF S&C

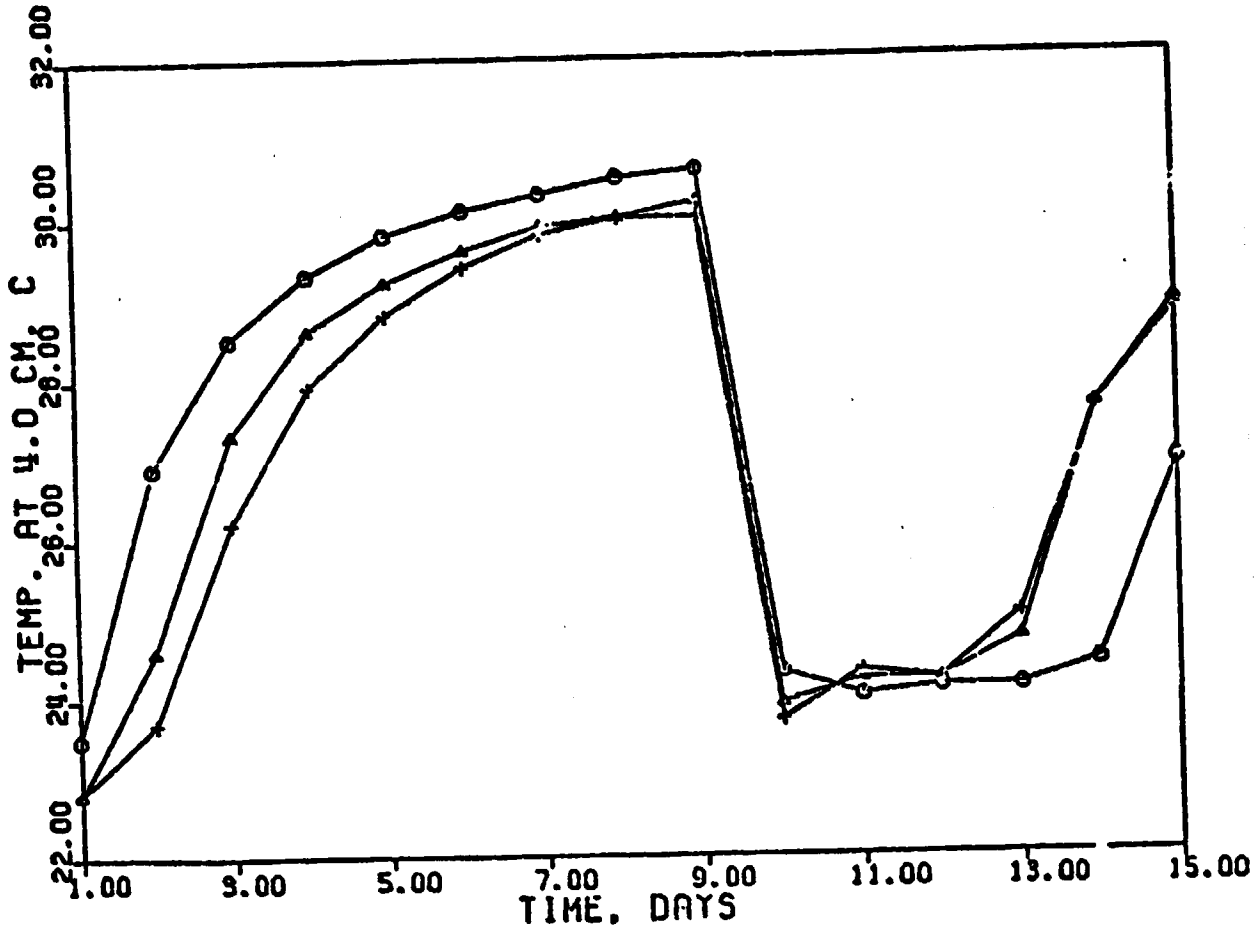


Figure 17. Soil Temperature ($^{\circ}\text{C}$) at a depth of 4.0 cm at 4:00 p.m. as a function of time (days) and scaling factor. The symbol (+) is for scale 1.619, (Δ) is for 1.000 and (O) is for 0.381.

ORIGINAL PAGE IS
OF POOR QUALITY

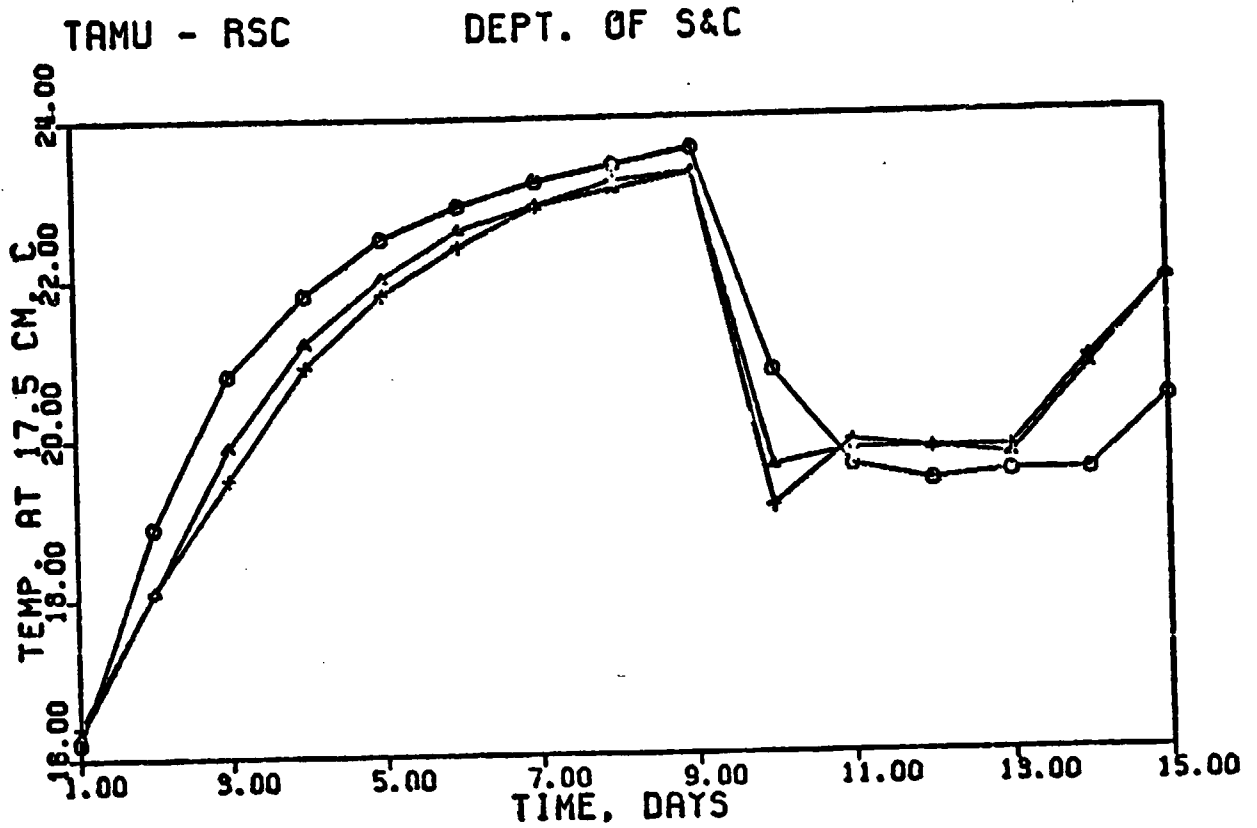


Figure 18. Soil temperature ($^{\circ}\text{C}$) at a depth of 17.5 cm at 4:00 p.m. as a function of time (days) and scaling factor. The symbol (+) is for scale 1.619, (Δ) is for 1.000 and (O) is for 0.381.

From the preceding illustrations (11 through 18), the 99% "confidence domain" with regard to specific hydrologic variables over time can be qualitatively judged. A more precise evaluation can be obtained by plotting the scaling ratio α itself against the value of important parameters for a specific time. For the time moment we have chosen 4 p.m. on a day in the end of the drying period and, in addition, on a day following a 50 mm rain.

The water content and temperature of the soil surface on these two days, as a function of the scaling ratio, is illustrated in Figures 19 through 22. The water content of the top 0.30 m of the soil profile for the two days is illustrated in Figures 23 and 24. These results have a common characteristic, that is, as the scaling ratio increases the water content decreases. When the soil profile is relatively dry (Figure 19), the water content of the soil surface varies between 0.05 and 0.10, with a value of 0.07 for the mean hydraulic properties of the soil. However, when the soil is moist (Figure 20), the surface water content varies between 0.28 and 0.42, with a value of 0.31 for the mean hydraulic properties of the soil. These results suggest that the influence of the space variability over an area increases as the water content increases. This effect is also apparent when the water contents of the top 0.30 m of the soil profile for the two days are compared (Figures 23 and 24). The effect of the scaling ratio over surface temperature for a dry and wet profile (Figures 22 and 23) is significant only if the temperature can be measured with an accuracy of 0.2°C.

It appears that the use of a 99% + "confidence domain" is a very stringent criterion. From Figures 19 through 24, we can easily judge

TAMU - RSC

DEPT. OF S&C

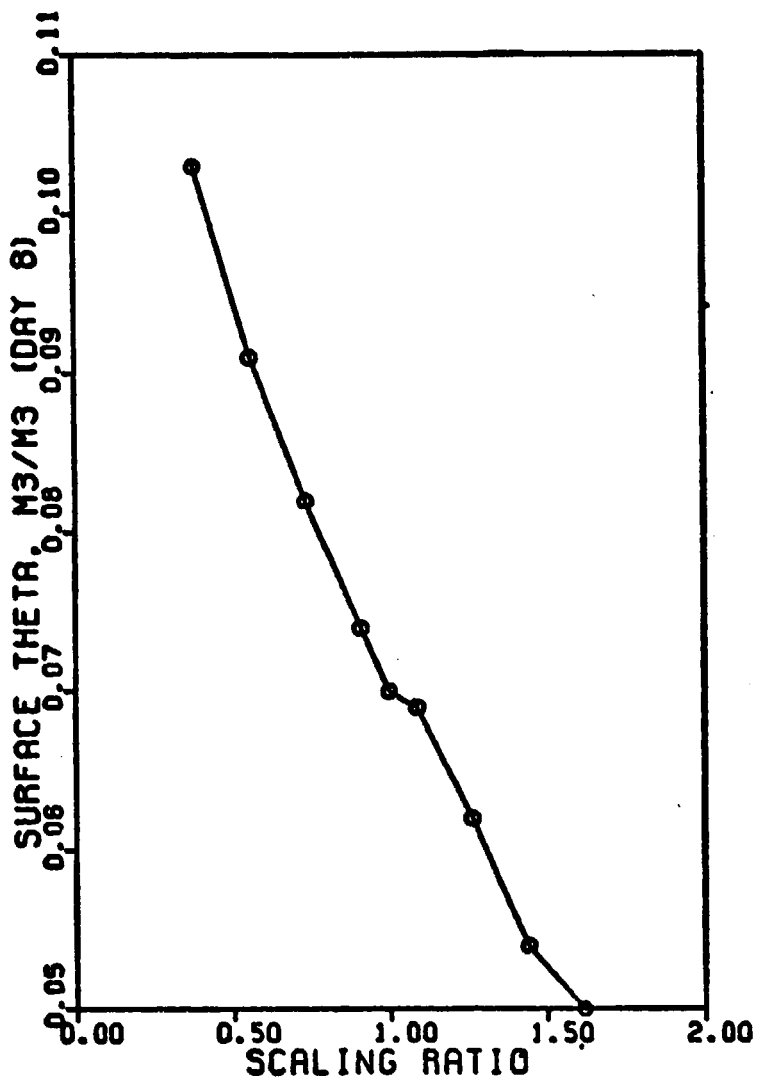


Figure 19. Volumetric water content (m^3/m^3) of the soil surface at 4:00 p.m. (day 8) as a function of scaling ratio.

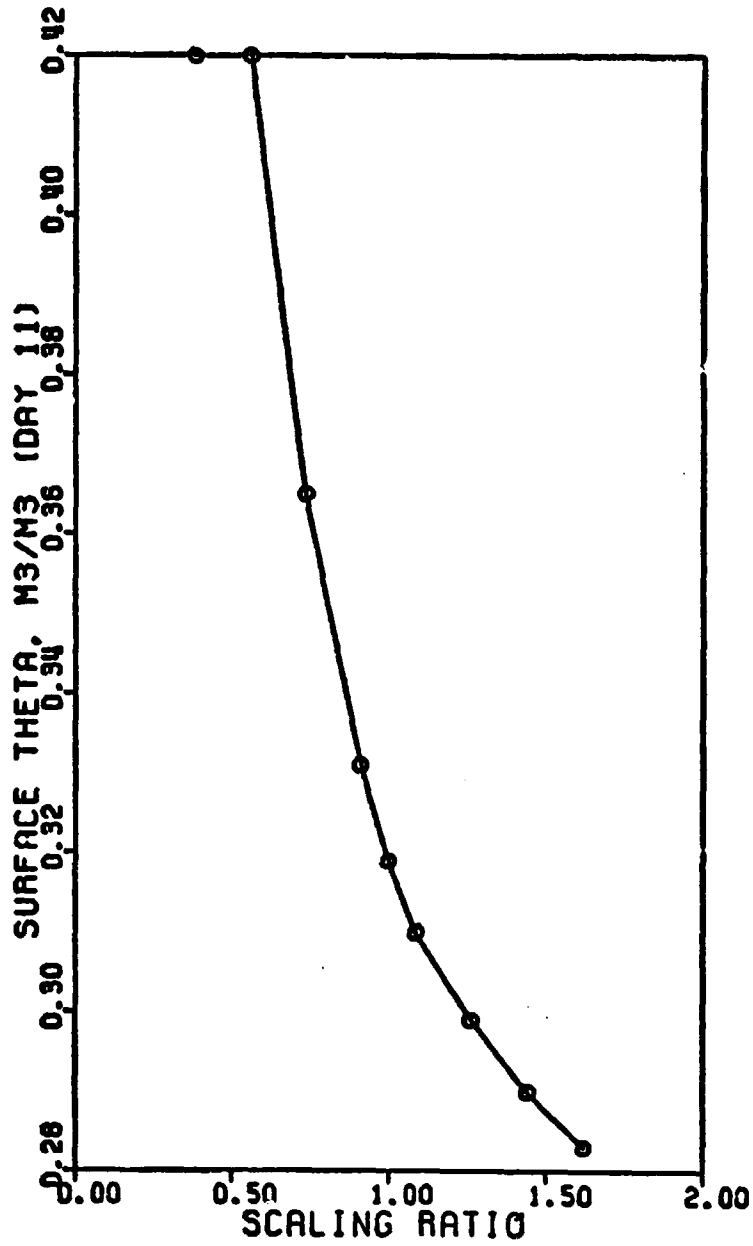


Figure 20 Volumetric water content (m^3/m^3) of the soil surface at 4:00 p.m. (day 11) as a function of scaling ratio.

ORIGINAL PAGE IS
OF POOR QUALITY

ORIGINAL PAGE IS
OF POOR QUALITY

TAMU - RSC

DEPT. OF S&C

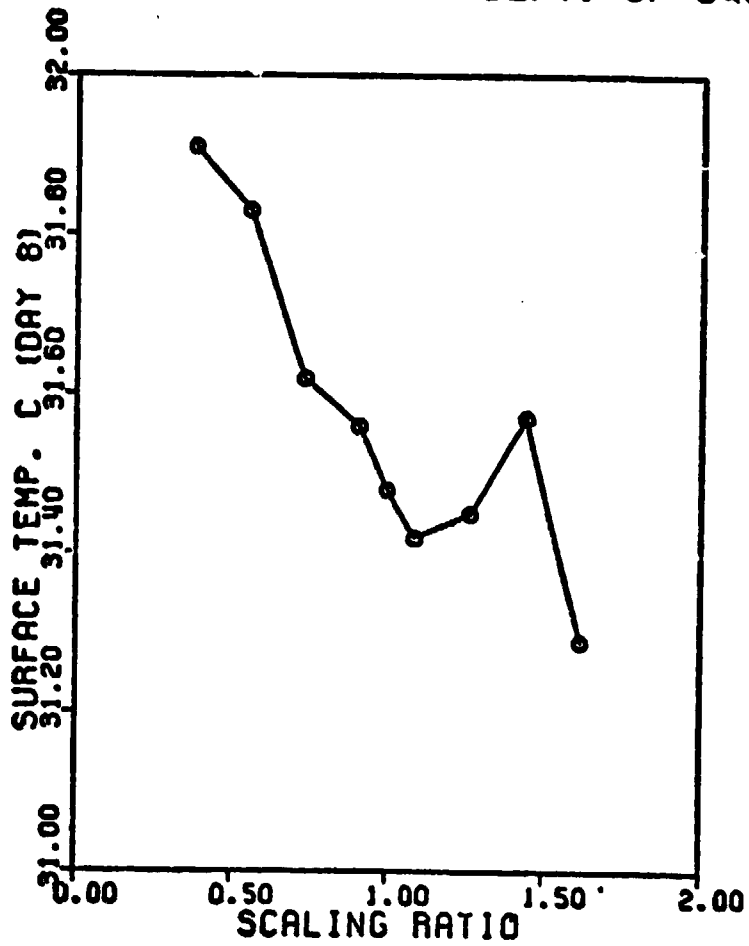


Figure 21 Surface temperature ($^{\circ}\text{C}$) at 4:00 p.m. as a function of scaling ratio (day 8).

TAMU - RSC

DEPT. OF S&C

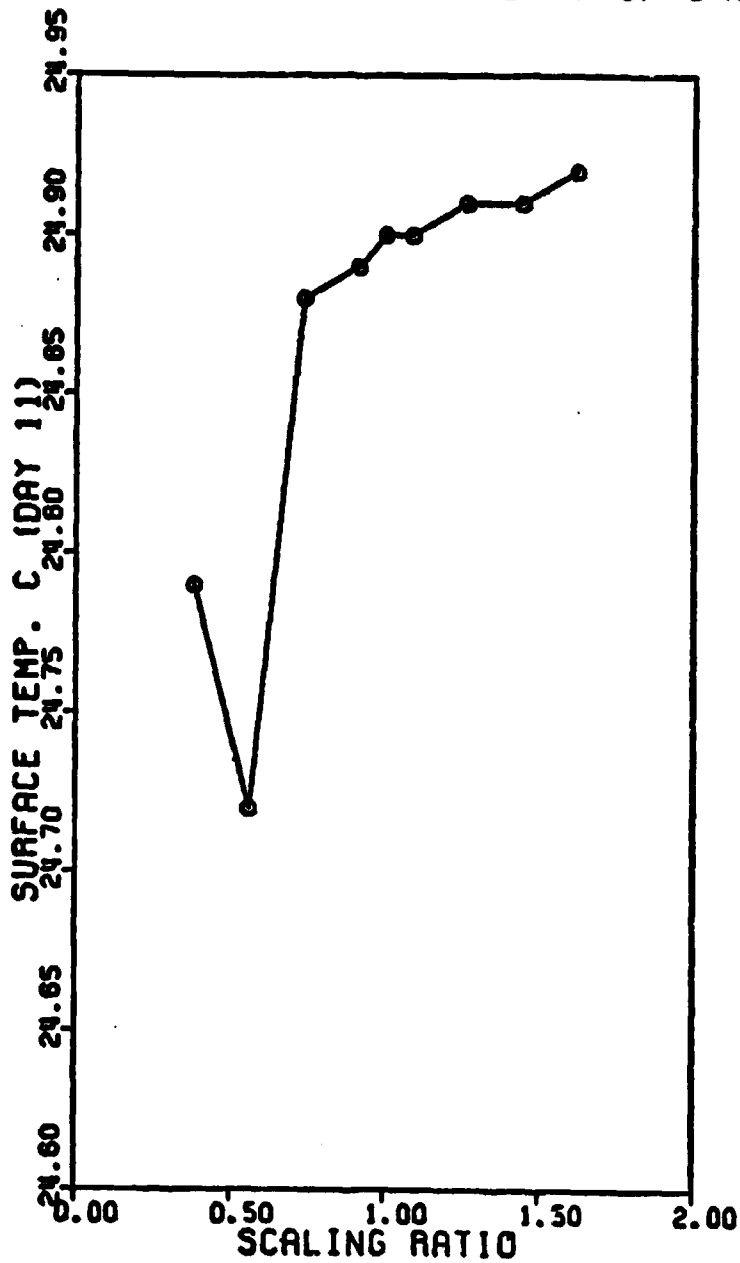


Figure 22. Surface temperature ($^{\circ}\text{C}$) at 4:00 p.m. as a function of scaling ratio (day 11).

TAMU - RSC

DEPT. OF S&C

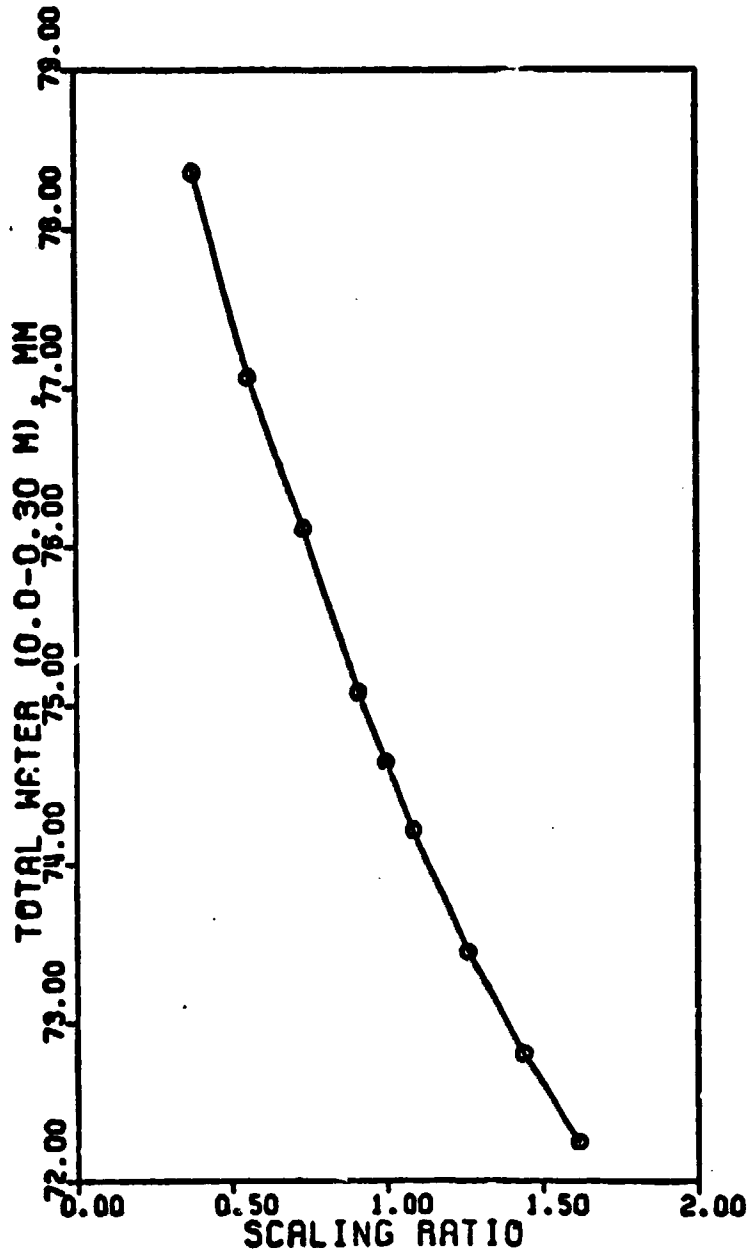


Figure 23. Total water (mm) in the top 0.30 m of the soil profile as a function of scaling ratio (day 8).

ORIGINAL PAGE IS
OF POOR QUALITY

TAMU - RSC

DEPT. OF S&C

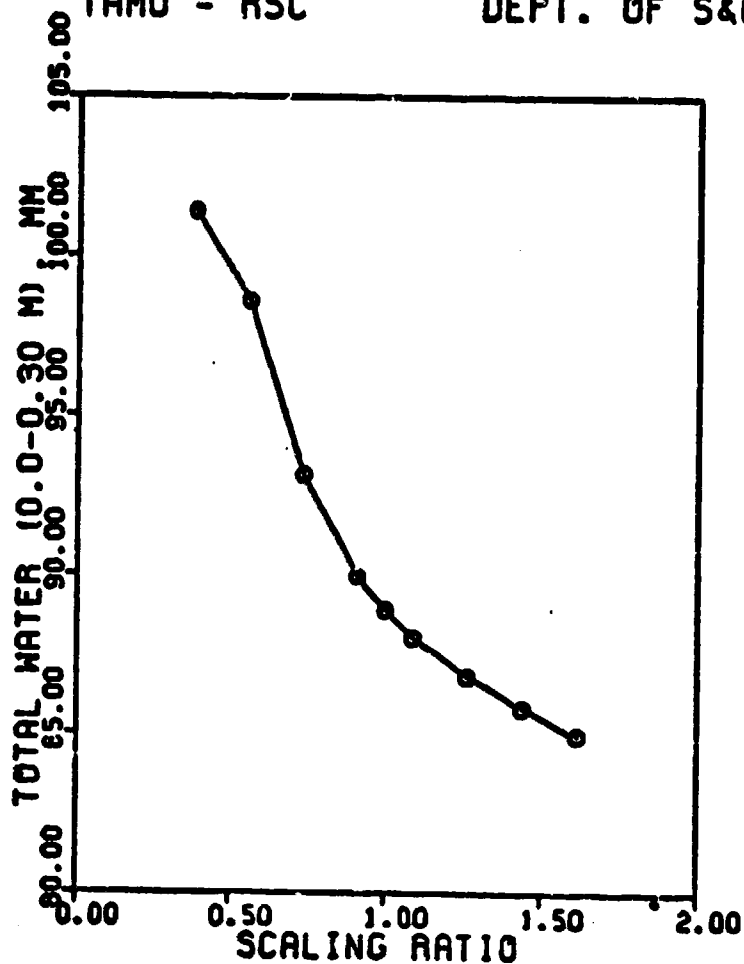


Figure 24. Total water (mm) in the top 0.30 m of the soil profile as a function of scaling ratio (day 11).

the consequences of a more relaxed criterion. For instance, if we demand that the simulation of the hydrologic behavior of a field would have to be within a 90% confidence domain, the range of α would be from 0.589 to 1.411. This, in turn, corresponds to a precision of estimation of the surface (0 - .30 m) water content of about 3 to 5%, according to Figures 23 and 24. If we consider the potential accuracy of both ground and radar measurement of the same property, it appears that what is needed is not so much to improve the input to the model, but rather the accuracy of the measurement, on a whole-field basis, in validating the model and justifying its modification or use. We emphasize, though, that the approach to sensitivity analysis as given is preliminary and that, at this time, only the highlights of current, incomplete studies are presented.

Summary of Model Tests with Field Notes

Model Input: Choice of Daily vs. 30 Minute Weather Data

The present version of CONSERVB is designed to calculate the heat and water balance of a soil system from total maximum, minimum, and average time-dependent weather variables. These variables are:

1. total daily radiation,
2. daily maximum and minimum air temperatures and their corresponding dewpoint temperatures,
3. average windspeed, and
4. amount and duration of precipitation.

It was of interest to evaluate the effect on the predicted results when using 30-minute input data for the weather variables. For this purpose, CONSERVB was modified and the data for two different days was simulated and the results compared.

Table 3 summarizes the daily meteorological data for the two days used in the simulations. The data were obtained at the Agronomy Farm of Texas A&M University.

The results from 24-hour simulations are presented in Figures 25 through 28. Also included are the results when daily meteorological input data are used with windspeed as a function of time, in the form of a FUNCTION table.

The results of the calculated profiles of soil water content and temperature for different frequencies of the weather input data for two days indicate that the accuracy of the output are not significantly affected. Soil water content variations are negligible (Figures 25 and 26), and soil temperature variations are confined to the upper 0.20 m of the soil profile (Figures 27 and 28). However, the maximum difference of soil temperature for the three frequencies of weather input data is of the order of 1-2°C. Therefore, we have concluded that the input of daily weather data used to predict the heat and water balance of a soil system is satisfactory.

Comparison of Measured and Simulated Results

The model, CONSERVB, was used to simulate water content profiles of a bare Norwood silt loam soil for a period of 33 days using as weather input data collected on the Agronomy Farm of Texas A&M University. The meteorological data are summarized in Table 4.

The initial water content and temperature profiles as a function of depth used for the simulation are summarized in Table 5. The initial water content used in the simulation was obtained from measured values in the Agronomy Farm of Texas A&M University during April 16, 1979. The initial soil temperature data used in the simulation had to

Table 3. Daily meteorological data used to evaluate the frequency of weather input data used with CONSERVB.

Weather Input Data	Julian Day 93 (April 3, 1979)	Julian Day 126 (May 6, 1979)
Day length (hours)	12.40	13.33
Total global radiation (MJ/m ²)	3.44	27.30
Maximum air temperature (c)	18.30	28.70
Minimum air temperature (c)	14.20	12.70
Maximum dewpoint temperature (c)	12.5	12.0
Minimum dewpoint temperature (c)	9.6	4.6
Average windspeed (m/s)	2.24	2.20
Rainfall (mm)	0.0	0.0

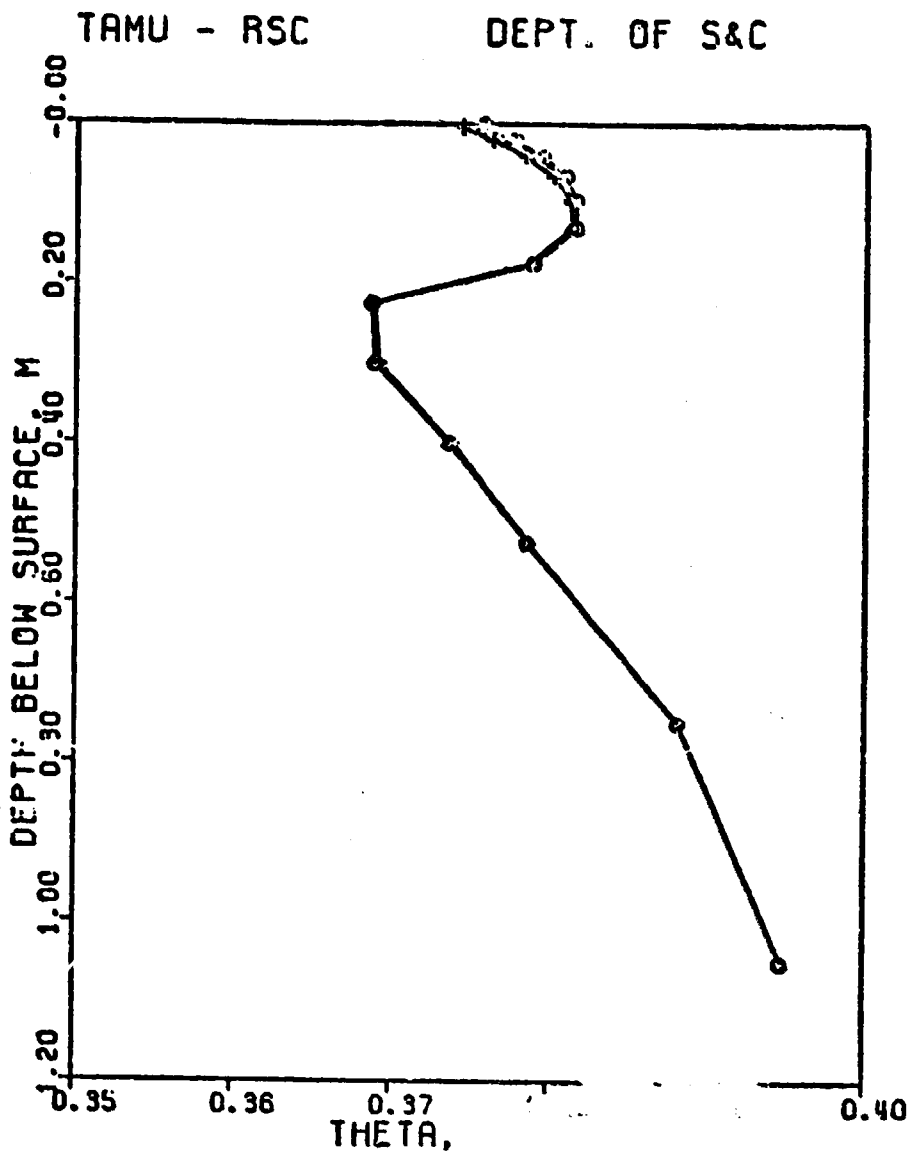


Figure 25. Volumetric water content (m^3/m^3) as a function of depth (m) and frequency of weather input data for Julian day 93, at 4:00 p.m. The symbol (o) is for daily weather input data, (Δ) is for daily and windspeed as a function of time, and (+) is for 30 minute data.

TAMU - RSC

DEPT. OF S&C

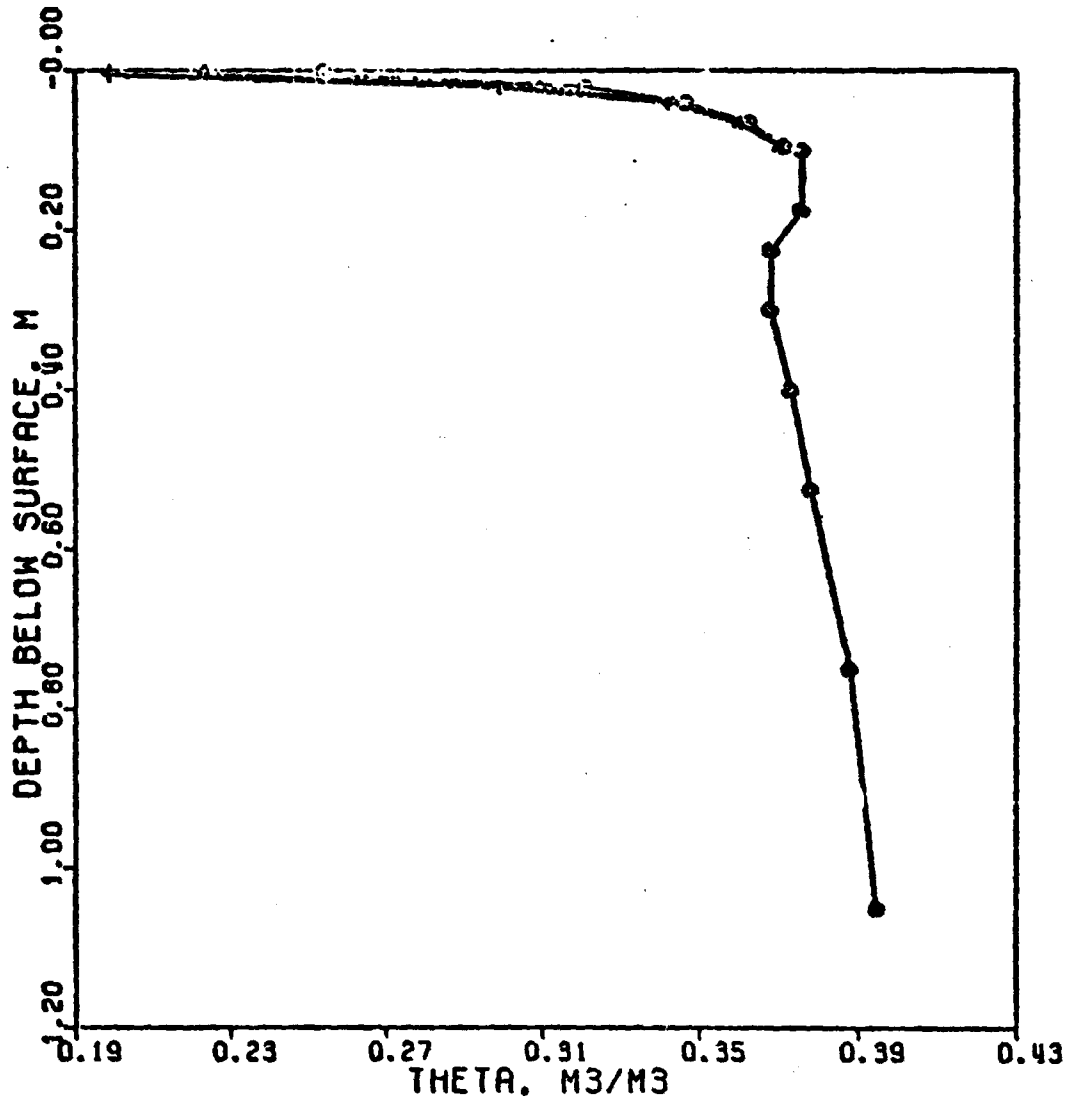


Figure 26. Volumetric water content (m^3/m^3) as a function of depth (m) and frequency of weather input data for Julian day 126 at 4:00 p.m. The symbol (O) is for daily weather input data (Δ) is for daily and windspeed as a function of time, and (+) is for 30-minute data.

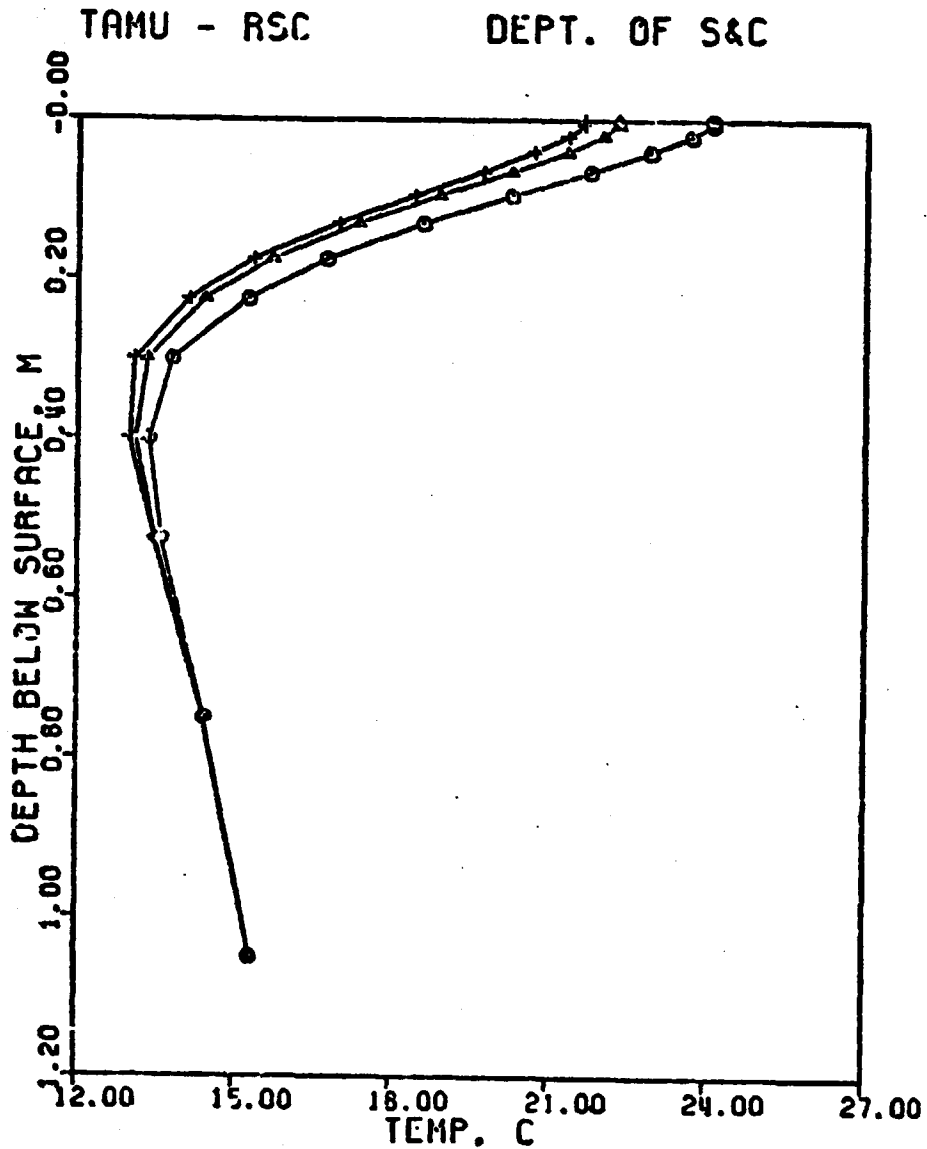


Figure 27. Soil temperature ($^{\circ}\text{C}$) as a function of depth (m) and frequency of weather input data for Julian day 93 at 4:00 p.m. The symbol (O) is for daily weather input, (Δ) is for daily and windspeed as a function of time, and (+) is for 30-minute data.

ORIGINAL PAGE IS
OF POOR QUALITY

TAMU - RSC

DEPT. OF S&C

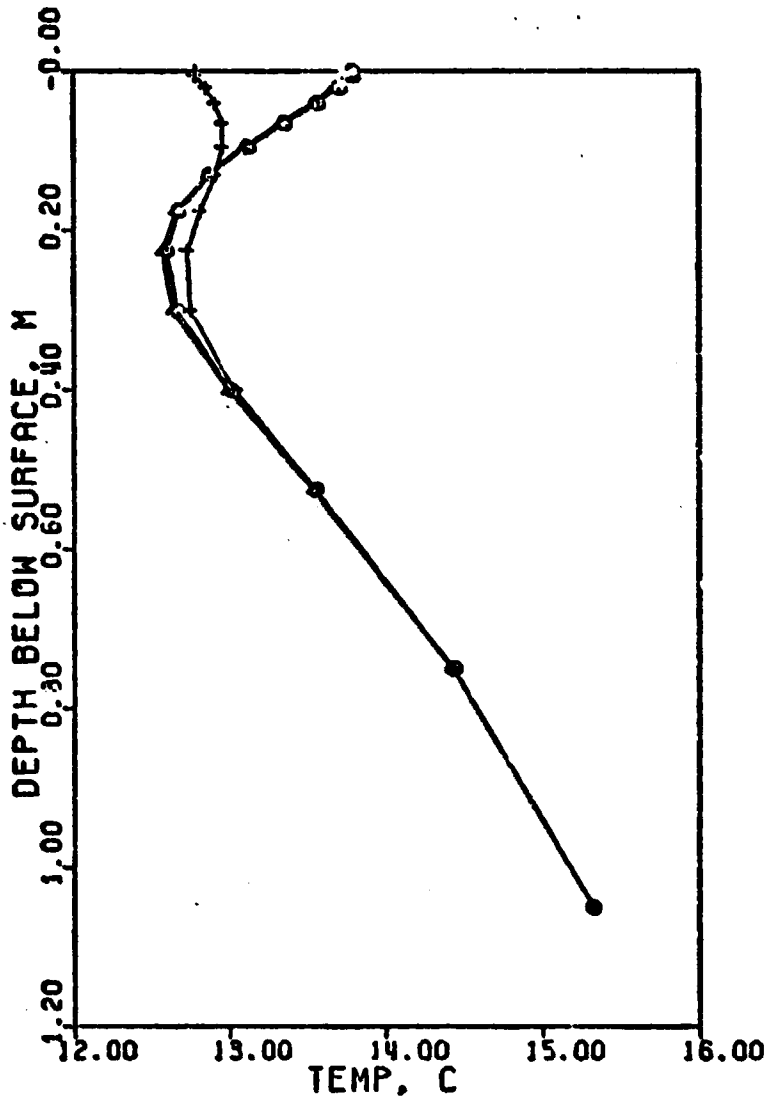


Figure 28. Soil temperature (C) as a function of depth (m) and frequency of weather input data for Julian day 126 at 4:00 p.m. The symbol (O) is for daily weather input data, (Δ) is for daily and windspeed as a function of time, and (+) is for 30-minute data.

Table 4. Weather input data used for the simulation of the heat and water balance of Norwood silt loam soil over a period of 33 days. The data was recorded at the Agronomy farm of Texas A&M University between April 16 and May 18, 1979.

◆ JNM INPUT	DL	DGR	TMAX	TMIN	DMAX*	DMIN*	SA	BEGIN	END	RFT
106.	12.78	15.9	31.5	18.1	20.0	11.7	2.46	0.00	0.00	0.00
107.	12.81	2.6	23.6	20.2	20.0	13.3	2.87	10.0	21.5	24.1
108.	12.84	5.0	23.6	19.5	18.9	16.1	2.86	2.50	13.5	20.3
109.	12.87	6.3	26.6	19.4	21.1	17.2	2.28	13.5	16.5	3.80
110.	12.90	11.2	28.5	19.6	20.6	17.2	1.32	0.00	0.00	0.00
111.	12.93	5.3	22.7	19.5	17.2	15.6	2.25	0.00	0.00	0.00
112.	12.96	4.3	21.8	18.9	16.1	15.0	2.92	0.00	0.00	0.00
113.	12.99	20.5	26.2	18.2	15.6	14.4	1.74	0.00	0.00	0.00
114.	13.01	24.3	29.8	15.2	16.7	12.2	0.80	0.00	0.00	0.00
115.	13.04	25.7	32.0	17.3	17.8	14.4	2.77	0.00	0.00	0.00
116.	13.07	19.5	26.0	15.7	20.0	7.8	2.49	0.00	0.00	0.00
117.	13.09	13.2	26.8	11.7	13.3	7.2	1.41	0.00	0.00	0.00
118.	13.12	25.6	27.6	14.2	15.6	8.9	2.22	0.00	0.00	0.00
119.	13.15	6.1	22.1	16.7	16.1	13.9	2.25	1.00	6.00	14.0
120.	13.18	17.3	27.0	16.8	20.6	12.8	1.03	0.00	0.00	0.00
121.	13.20	6.9	25.8	17.8	19.4	15.0	2.30	11.0	11.5	5.10
122.	13.23	9.8	29.1	21.5	21.7	18.3	3.09	6.50	8.00	3.30
123.	13.25	8.9	30.9	18.0	23.9	14.4	3.50	9.00	9.50	8.90
124.	13.28	6.6	17.7	14.3	14.4	8.9	4.46	0.50	3.00	8.90
125.	13.30	20.5	24.3	14.5	13.9	10.0	1.26	0.00	0.00	0.00
126.	13.33	27.3	28.7	12.7	17.2	10.0	2.25	0.00	0.00	0.00
127.	13.35	24.9	31.9	13.0	19.4	16.1	3.81	0.00	0.00	0.00
128.	13.38	25.9	32.9	20.5	19.4	17.2	4.01	0.00	0.00	0.00
129.	13.40	8.5	28.9	21.2	22.2	18.9	3.52	0.00	0.00	0.00
130.	13.43	12.6	33.0	25.2	23.9	21.7	3.74	0.00	0.00	0.00
131.	13.45	1.2	25.5	13.5	21.1	8.9	2.91	6.00	14.0	20.6
132.	13.47	28.7	25.7	12.0	12.2	8.9	2.75	0.00	0.00	0.00
133.	13.49	28.9	28.5	11.8	12.2	8.9	1.06	0.00	0.00	0.00
134.	13.52	28.1	30.4	13.4	14.4	11.1	0.74	0.00	0.00	0.00
135.	13.54	28.6	31.1	15.2	16.1	12.2	0.89	0.00	0.00	0.00
136.	13.56	24.7	31.6	16.3	16.7	12.8	1.07	0.00	0.00	0.00
137.	13.58	18.1	31.1	17.1	16.7	13.9	1.29	0.00	0.00	0.00
138.	13.60	25.6	32.1	16.6	20.0	13.3	2.85	0.00	0.00	0.00

* The dewpoint data was taken from Easterwood Airport (United States Department of Commerce, National Oceanic and Atmospheric Administration, Environmental Data Service, National Climatic Center, Asheville, N.C. 28801).

Table 5. Initial water content and temperature profiles as a function of depth used in the simulation.

Depth (m)	Water Content (m ³ /m ³)	Temperature (°C)
0.005	0.224	8.6
0.020	0.224	9.2
0.040	0.225	10.7
0.100	0.269	12.6
0.200	0.307	16.3
0.300	0.329	18.1
0.400	0.337	17.6
0.525	0.344	17.0
0.700	0.348	16.7
0.900	0.346	16.7
1.100	0.345	16.8
1.300	0.346	16.9
1.500	0.364	17.1

be generated with a computer program because measured values were not available. This computer program predicts the soil temperature for any given day as a function of depth from specific soil physical properties (Van Bavel, unpublished data).

In our calculations we have assumed that the initial measured values of soil water content correspond to those at midnight of April 16. The initial calculated soil temperatures do correspond to midnight of the first day of the simulation.

Calculated and measured values of soil water content and matric potential for several days of the 33-day simulation period are given in Table 6. Measured values of soil water content were obtained from neutron readings and values of matric potentials were obtained from mercury-type tensiometers. Again, we have assumed that measured values of water content and also matric potential were taken at 8:00 a.m.

Calculated and measured values of the total water content of the top 0.30 m for several days are given in Table 7. The calculated values of water content are for midnight of the given day.

The calculated and measured profiles of water content and matric potential given in Table 6 show that, in general, the calculated water content of the top 0.30 m is slightly overestimated while the water content at lower depths is underestimated. The results suggest that perhaps the hydraulic properties used as input for horizon II in the simulation and the boundary of unit gradient assumed for flow of water at the bottom of the profile are not correct. However, the comparison of calculated and measured total water content in the top 0.30 m given in Table 6 show a good agreement.

Table 6. Calculated and measured values of water content and matric potential for several days of the 33-day simulation period.

Day 106 (First day)

Depth (m)	Calculated Water Content (m^3/m^3)	Measured Water Content (m^3/m^3)	Calculated Matric Potential (mb)	Measured Matric Potential (mb)
0.005	0.181		25000	
0.020	0.223		5499	
0.040	0.230		4559	
0.1	0.269	0.224	1857	280
0.2	0.307	0.254	771	285
0.3	0.328	0.269	390	176
0.4	0.338	0.307	260	162
0.525	0.350	0.329	120	153
0.70	0.334	0.344	102	132
0.9	0.342	0.351	92	106
1.1	0.346	0.344	87	74
1.3	0.349	0.348	83	44
1.5	0.353	0.364	78	67

Day 113

0.005	0.338		267	
0.02	0.345		180	
0.04	0.348		140	
0.1	0.358	0.295	96	122
0.2	0.366	0.301	73	110
0.3	0.368	0.300	68	100
0.4	0.364	0.329	77	90
0.525	0.348	0.344	147	79
0.70	0.306	0.353	141	59
0.90	0.311	0.361	134	78
1.1	0.315	0.348	128	78
1.3	0.317	0.356	125	64
1.5	0.318	0.371	123	68

Table 6. Continued

Day 115

Depth (m)	Calculated Water Content (m ³ /m ³)	Measured Water Content (m ³ /m ³)	Calculated Matric Potential (mb)	Measured Matric Potential (mb)
0.005	0.173		33400	
0.02	0.249		3108	
0.04	0.300		909	
0.1	0.334	0.279	314	251
0.2	0.350	0.287	119	139
0.3	0.359	0.293	93	116
0.4	0.357	0.319	98	106
0.525	0.346	0.340	164	96
0.7	0.298	0.352	155	77
0.9	0.304	0.358	144	82
1.1	0.308	0.346	137	79
1.3	0.311	0.351	133	65
1.5	0.313	0.371	131	61

Day 117

0.005	0.118		1478000	
0.02	0.207		17700	
0.04	0.270		2340	
0.1	0.316	0.274	749	568
0.2	0.341	0.279	281	183
0.3	0.348	0.288	189	129
0.4	0.350	0.321	169	117
0.525	0.345	0.343	188	107
0.7	0.292	0.352	174	100
0.9	0.297	0.360	162	100
1.1	0.302	0.346	153	86
1.3	0.306	0.354	147	70
1.5	0.308	0.375	144	62

Table 6. Continued

ORIGINAL PAGE IS
OF POOR QUALITY

Day 120				
Depth (m)	Calculated Water Content (m ³ /m ³)	Measured Water Content (m ³ /m ³)	Calculated Matric Potential (mb)	Measured Matric Potential (mb)
0.005	0.340		240	
0.02	0.344	0.298	190	103
0.04	0.346		167	
0.1	0.348		141	
0.2	0.344	0.299	187	194
0.3	0.343	0.286	204	156
0.4	0.344	0.323	196	146
0.525	0.343	0.353	199	135
0.7	0.283	0.367	184	118
0.9	0.290	0.376	171	128
1.1	0.294	0.362	161	91
1.3	0.298	0.374	155	74
1.5	0.300	0.390	151	73

Day 127				
0.005	0.1789		27620	
0.02	0.256	0.299	2639	120
0.04	0.304		840	
0.1	0.337		272	
0.2	0.356	0.311	103	109
0.3	0.362	0.303	84	103
0.4	0.358	0.328	96	93
0.525	0.343	0.360	200	83
0.7	0.275	0.375	200	70
0.9	0.278	0.376	194	106
1.1	0.282	0.365	187	104
1.3	0.284	0.372	182	87
1.5	0.286	0.389	179	73

Table 7. Measured and calculated values of total water content (mm) in the top 0.30 m of the Norwood silt loam soil.

Julian Day	Measured Water (mm)	Calculated Water (mm)
106	75	69
113	90	90
115	86	82
117	84	77
120	88	87
127	91	83
130	88	76

These results are not conclusive and further evaluation of the hydraulic properties of the Norwood silt loam soil is necessary. It must also be pointed out that the period chosen for this evaluation was characterized by frequent rainfall events, totaling about 100 mm. Thus the range of the test was limited. Additional data for 1979 are available for further model evaluation, but no work has been done on these, pending the outcome of the studies reported at this time.

References

Jackson, R. D. 1972. On the calculation of hydraulic conductivity. Soil Sci. Soc. Amer. Proc. 36:380-382.

Nielsen, D. R., J. W. Biggar, and K. T. Erh. 1973. Spatial variability of field-measured soil-water properties. Hilgardia 42:215-260.

Peck, A. J., R. J. Luxmoore, and J. L. Stolzy. 1977. Effects of spatial variability of soil hydraulic properties in water budget modeling. Water Res. Res. 13:348-354.

Controlled Field Experiment Test Site

Summary

A system for acquiring both weather and soil moisture data has been developed on several field plots at the Texas A&M University Farm. The data acquired from this system are to be used in conjunction with two projects. The first project deals with experimental measurements of soil moisture using a truck-mounted radiometer system. The second project deals with verification of an algorithm for simulating soil moisture in the root-zone.

The weather data are being collected to provide an assessment of the atmospheric condition (evaporation, transpiration, infiltration) at the soil surface. The soil moisture data are being collected to provide an assessment of the moisture status in the soil profile.

The weather data portion of the system acquires weather information including net radiation, solar radiation, air temperature and dewpoint temperature, windspeed at 2 meters and 4 meters, rainfall and evaporation. Difficulties with the weather data acquisition have resulted from power surges caused by electrical storms. These difficulties have been corrected and the system is now operating properly. The data acquired by the system is considered to be of good quality.

The soil moisture data portion of the system consists of tensiometers located at various depths and neutron access tubes for a neutron probe. The tensiometers measure the capillary potential in the soil profile to a depth of 150 centimeters. The neutron probe is used to measure soil moisture in the profile to the same depth.

Difficulties with the soil moisture data system are caused by maintenance problems with the tensiometers located in the top 30 cm of the soil profile. These tensiometers often become inoperable due to large capillary suction (>700 millibars) when the surface profile dries. Extreme care has to be taken in maintaining these tensiometers and interpreting the acquired data.

The weather and soil moisture data are placed on data files as they are acquired. The data files are made available by the Data Processing Center at Texas A&M University. Example summaries of data acquired to date are included in this report.

Some physical characteristics of the soil at the Farm have been determined by Humphreys in Technical Report RSC-124 (Appendix D). These characteristics are included in this report.

Introduction

The development of remote sensing techniques to measure soil moisture status requires field experimentation under carefully controlled conditions. The information requires in the experimental process includes weather and soil moisture data. The objective of this portion of the soil moisture project was to collect these data for a set of experimental plots.

Field Site Description

The field plots used for the soil moisture experiments are located on the Texas A&M University Farms approximately 8 miles west of College Station on Highway 60. Four plots are used for the experiments. One of the plots is continually fallow while the other three plots are in a wheat-grain sorghum rotation.

The fallow plot is 50 feet by 150 feet and has a North-South orientation. The plot is kept free of vegetation by use of a herbicide. A photograph of the fallow plot is given in Figure 1. The view in this photograph is in the northern direction.

The difference between the vegetated plots is the applied water management practice. One plot is sprinkle irrigated, a second is furrow irrigated (wet) while the third receives no irrigation (dryland). The sprinkle irrigated plot is 120 feet by 120 feet, and the wet and dryland plots are both 40 feet by 120 feet. All three vegetated plots have an east-west orientation. A view across the width dimension of the vegetated plots is given in Figure 2. There are a number of other plots shown in this photograph. Although it is difficult to differentiate between plots in this photograph the three vegetated plots of interest are in the foreground.

A plan view of the experimental site is given in Figure 3. This figure illustrates the location of the various components of the experimental system.

Data System

The system for collection of soil moisture and climatic data is located adjacent to the experimental plots. The data system consists of a weather station and instruments to acquire soil moisture data. The weather station and soil moisture equipment will be described separately.

Weather Station - The weather station consists of the following components:

- 1) net radiometer (over the fallow plot),
- 2) solar radiometer,

ORIGINAL PAGE
BLACK AND WHITE PHOTOGRAPH

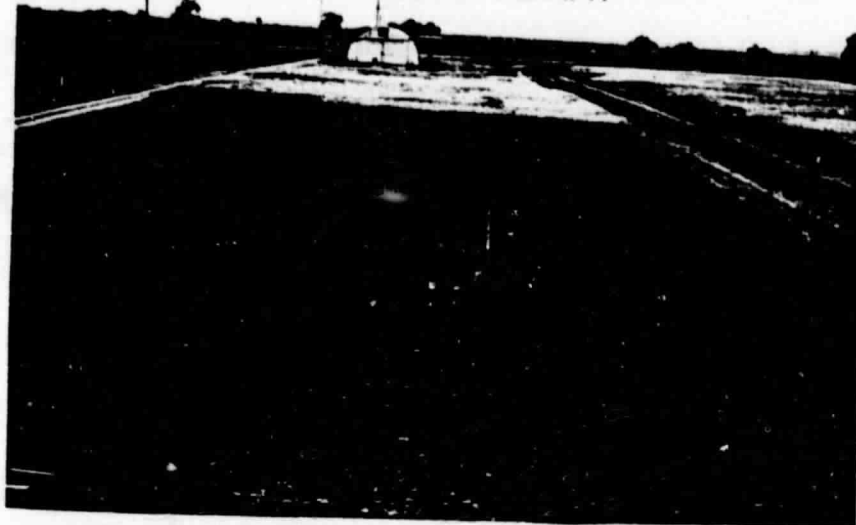


Figure 1. Photographic Illustration of the Fallow Plot at the Texas A&M University Farm.



Figure 2. Photographic Illustration of the Vegetated Plots at the Texas A&M University Farm.

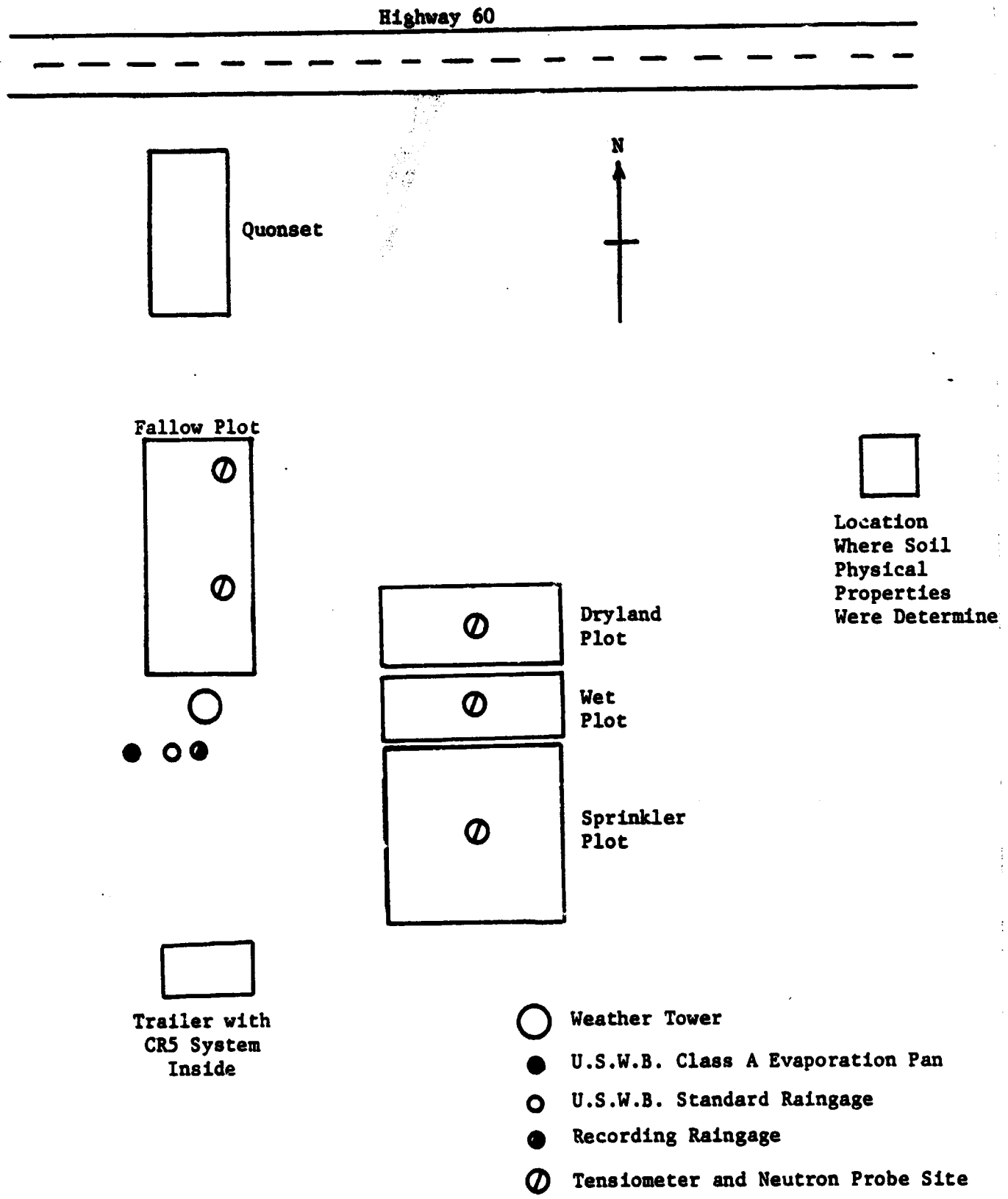


Figure 3. Plan View of the Experimental Site Illustrating the Location of the Experimental Plots and the Data Acquisition Systems.

- 3) ambient air temperature and dewpoint temperature probes,
- 4) anemometers at 2 and 4 meters above the ground surface,
- 5) recording raingage,
- 6) U. S. Weather Bureau Standard raingage, and
- 7) U. S. Weather Bureau Class A evaporation pan.

A tower supports the net radiometer, the solar radiometer, the ambient and dew point temperature sensors, and the 2 meter and 4 meter anemometers. A photograph of the tower is given in Figure 4. The standard and recording raingages are illustrated in Figure 5. The Class A evaporation pan is illustrated in Figure 6.

The outputs from the radiometers, anemometers and the temperature sensors are recorded by a Campbell CR5 data acquisition system. The output is recorded on paper as well as on a cassette tape. At present the data is recorded at half-hour intervals. The recorded radiation and wind speed data are the result of an integration over the recording interval. The recorded temperature data are the average of the temperatures over the recording interval. An illustration of the CR5 system is given in Figure 7.

A continuous record of rainfall amounts is provided by the recording raingage. Rainfall amounts are recorded automatically onto a revolving chart by an ink pen. The charts are removed once a week and the recorded information is transferred to data files for permanent storage.

The amount of rainfall caught by the U.S.W.B. standard raingage is read and recorded manually each day. The amount of evaporation from the evaporation pan is also read and recorded manually on a daily basis.

ORIGINAL PAGE
BLACK AND WHITE PHOTOGRAPH

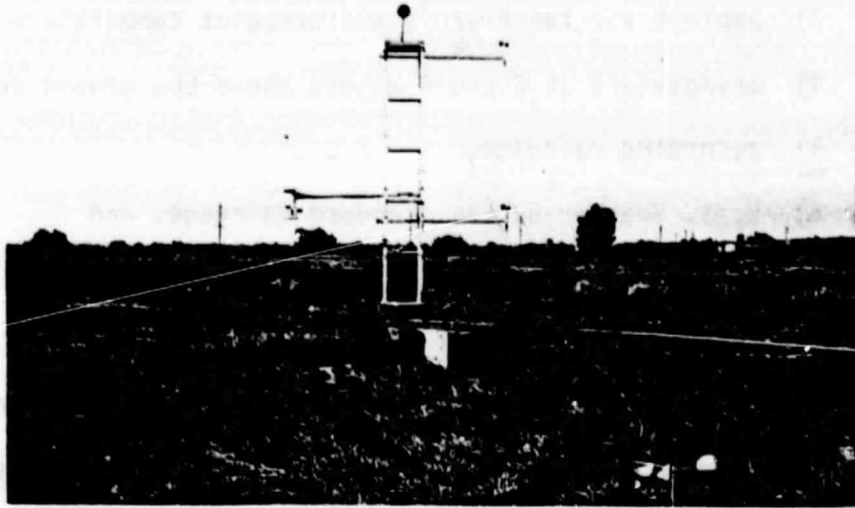


Figure 4. Photographic Illustration of the Weather Station Tower at the Texas A&M University Farm.



Figure 5. Photographic Illustration of the Recording Raingage and U.S.W.B. Standard Raingage at the Texas A&M University Farm.

ORIGINAL PAGE
BLACK AND WHITE PHOTOGRAPH

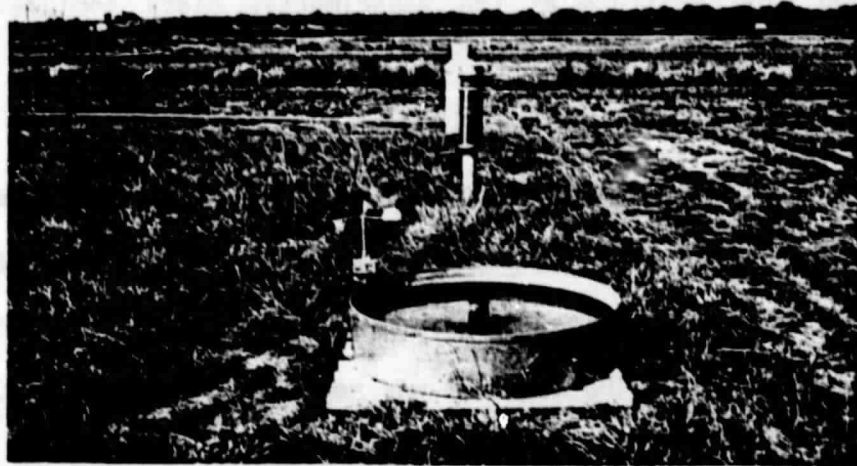


Figure 6. Photographic Illustration of the U.S.W.B. Class A Evaporation Pan.

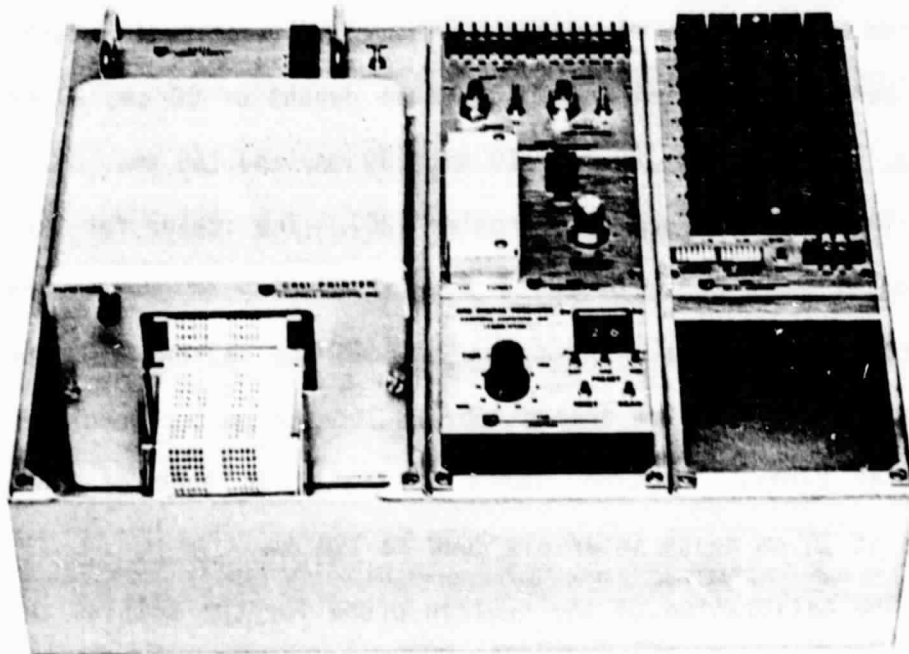


Figure 7. Photographic Illustration of the CR5 Data Acquisition System.

Soil Moisture Equipment - The equipment used to determine the status of soil moisture at the experimental plots includes tensiometers and a neutron probe.

The tensiometers are constructed from standard porous cups (1 bar) and 3/4 inch PVC tubing. The output from the tensiometers is indicated by a mercury manometer which is connected to the tensiometers by plastic tubing (0.063 inch I.D.) filled with a mixture of water and methanol. The methanol was necessary to prevent freezing of the manometer and tensiometer during the colder months. An illustration of the tensiometer-manometer arrangement is given in Figure 8. A field illustration of a manometer is illustrated in Figure 9.

There are two banks of tensiometers on the fallow plots and one bank on each of the vegetated plots. Each tensiometer bank consists of a series of tensiometers located at depths of 10 cm, 20 cm, 30 cm, 40 cm, 50 cm, 70 cm, 90 cm, 110 cm, 130 cm, and 150 cm.

The neutron probe is a Troxler 1257. The scaler for the probe is a Troxler 2651 and provides a digital display of the neutron count. Neutron access tubes are located on both the fallow field and on the vegetated fields. One access tube is located next to each of the tensiometer banks. Neutron counts are taken in each of these access tubes at 10 cm depth intervals down to 150 cm.

The calibration of the neutron probe for the soil at the experimental site is given by Humphreys (1979). The calibration curves for the probe are illustrated in Figure 10. Note that there are two calibration curves, one for 0-10 cm depth and the other for depths greater than 10 cm. The curve for the 0-10 cm depth takes into account the loss of fast neutrons at the soil surface when the probe is within 10 cm of the soil surface.

ORIGINAL PAGE IS
OF POOR QUALITY

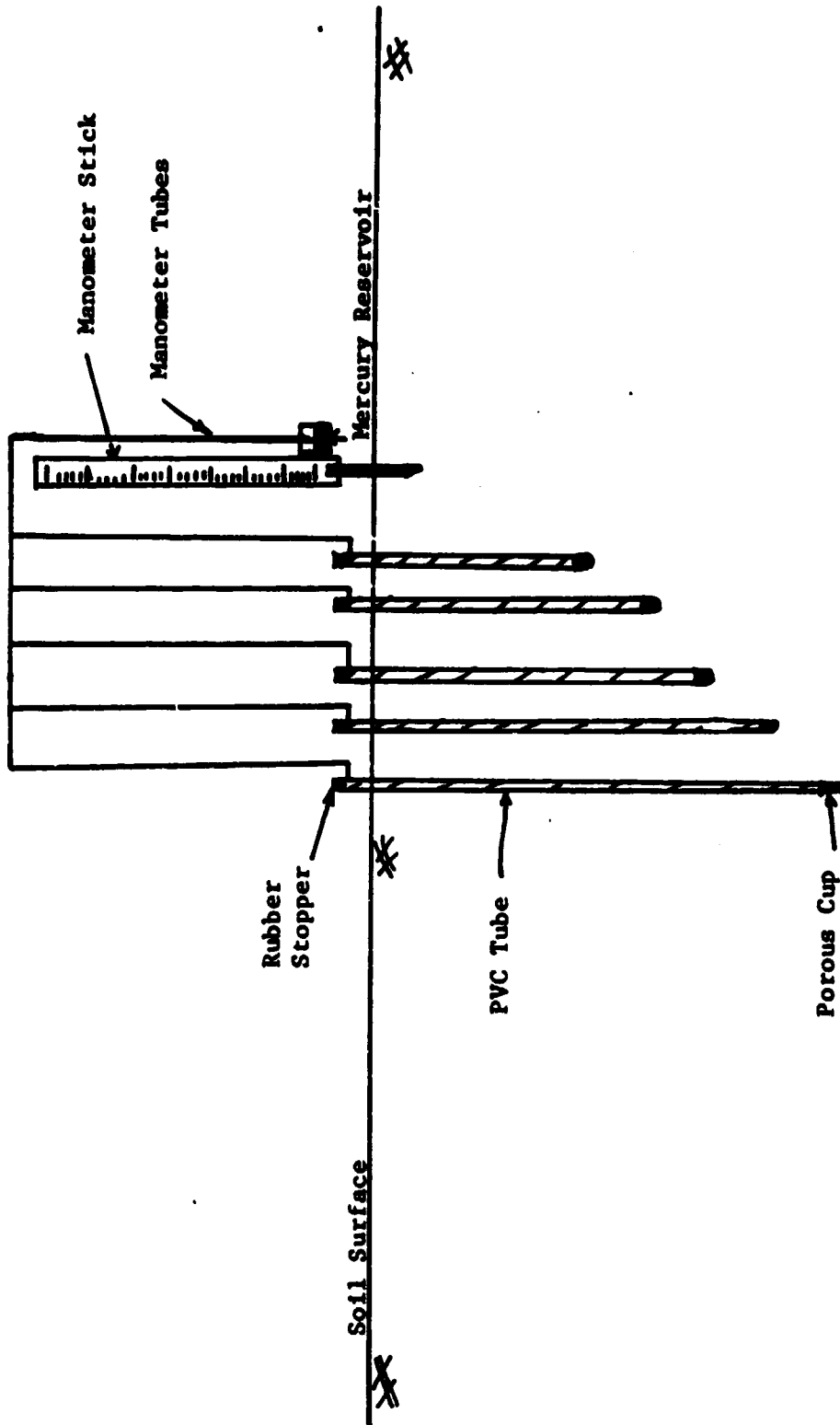


Figure 8. Illustration of the Tensiometer-Manometer Arrangement.



Figure 9. Photographic Illustration of the Field Installation of a Tensiometer-Manometer Bank.

ORIGINAL PAGE
BLACK AND WHITE PHOTOGRAPH

ORIGINAL PAGE IS
OF POOR QUALITY

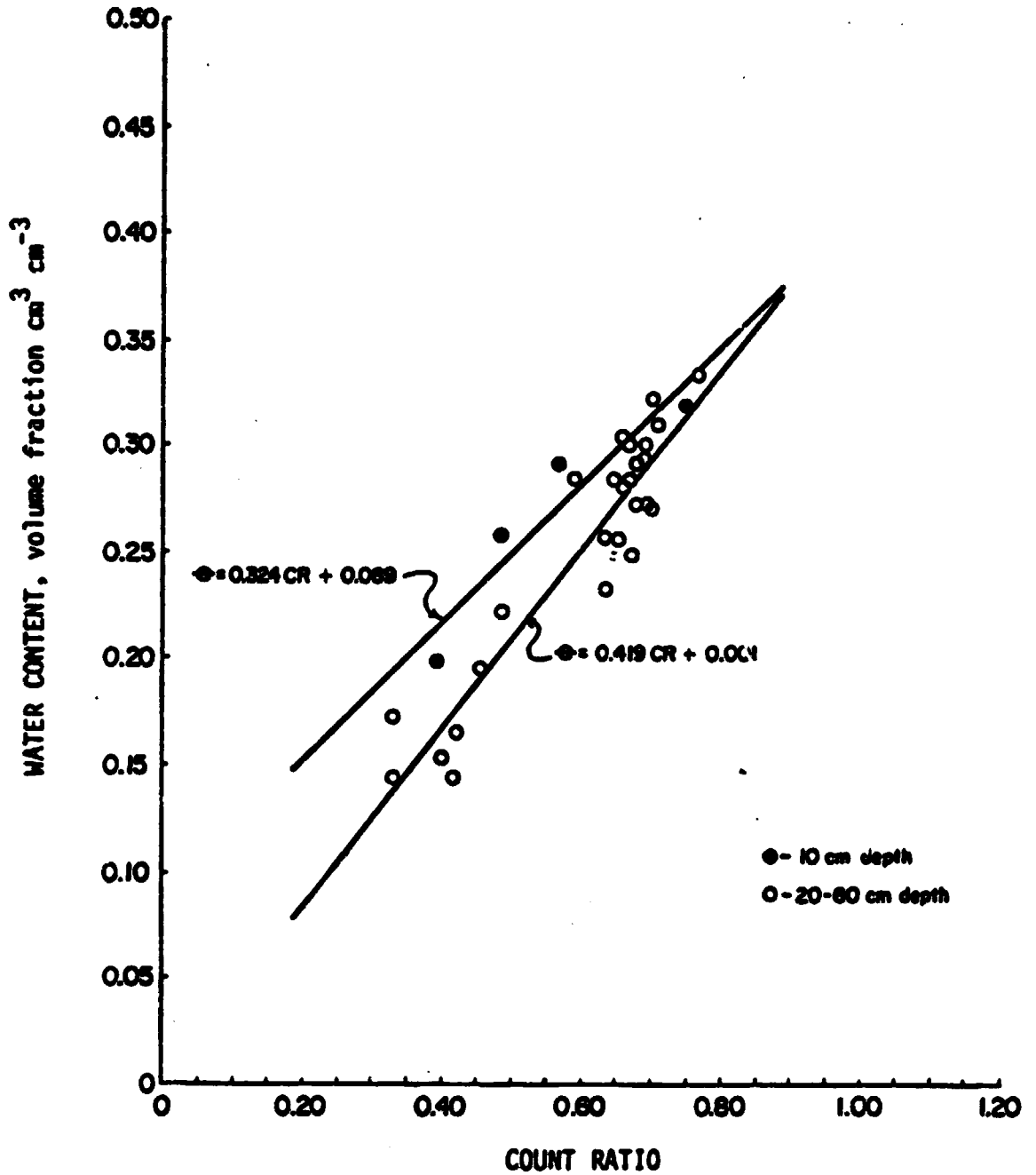


Figure 10. Calibration curve for neutron soil moisture probe.
(From Humphreys, 1979.)

The mercury levels in the manometers are read and recorded manually on a daily basis. The neutron probe is used to measure soil moisture at the plots twice each week.

Data Acquisition Problems

In the early portion of this project there was a period when there were several difficulties in maintaining the Campbell data acquisition system. On numerous occasions components of the system had to be sent to the manufacturer for repair. The problems with the data acquisition system resulted after a major electrical storm produced a power surge in the system. The system has now been properly grounded to prevent recurrence of this type of event.

The data acquisition problems caused by the electrical storm persisted throughout the summer and early fall of 1979. All of the system components did not fail simultaneously. Instead they failed at different times and were sent immediately to the factory for repair. An identical data acquisition system was available during this period of time and components of this system were used while components of the project system were being repaired. Most of the system components have been repaired at the factory and at present the system appears to be operating without difficulty.

Data Files

All of the data collected at the field site are continuously being placed into a data file on the AMDAHL 370 computer system at Texas A&M University. Any portion of these data is then readily available for direct access whenever needed for analysis.

Quality of Data

This investigator is confident that the data for most of the variables measured are of good quality. There were the data acquisition problems associated with the failure of components of the Campbell CR5 but beyond that all weather data is considered to be high quality.

The data associated with soil moisture contents as measured with the neutron probe are considered to be consistent and of high quality. The limitations in the soil moisture status system is the tensiometer data for the tensiometers at depths of 10 cm, 20 cm, and 30 cm. The difficulty with these tensiometers is that the upper portion of the soil profile (0-30 cm) dries down to fairly low moisture levels. The low moisture contents produce large capillary suctions on the tensiometers within this surface profile. The suctions frequently reach a value above 500 mb. Since tensiometers have a practical operating limit of 700 ml. it is difficult to keep the surface tensiometers maintained in good operating condition. Once the practical limit is exceeded air bubbles form in the tensiometer or in the manometer tubing. This air has to be purged from the tensiometer-manometer system. The purging process eliminates the use of a purged tensiometer for one or two days. Therefore, it is difficult to acquire reliable tensiometer data under conditions of high capillary potential unless extreme care is taken in handling the equipment. Extreme care also has to be taken in the interpretation of the acquired tensiometer data.

TABLE 1 *

Field Measurement of Bulk Density

<u>Depth</u> (cm)	<u>Gamma Probe</u> (g/cm ³)	<u>Avg. Gravimetric</u> (g/cm ³)
10	1.570	1.590
	1.562	
20	1.643	1.497
	1.631	
	1.592	
30	1.610	1.439
35		1.458
40	1.470	1.465
	1.560	
50	1.465	1.426
	1.467	
60	1.486	1.505
	1.491	
65		1.520
70	1.550	1.430
	1.491	
75		1.436
80	1.550	
	1.495	
90	1.591	
	1.551	
100	1.610	
	1.605	
11	1.660	
	1.664	
120	1.669	
	1.686	
130	1.674	
	1.653	
140	1.690	
	1.660	
150	1.681	
	1.672	
160	1.665	
	1.643	
170	1.663	

* From Humphreys, 1979.

sieving the dried samples. The derived textural characteristics are given in Table 2. As indicated by the textural classification the profile is dominated by silt loam.

Soil samples were taken from the 0-15 cm, 15-55 cm and 55-90 cm depth increments for determination of the desorption curve for the soil. The desorption curves were developed using a pressure plate extractor. The soil samples placed in the extractor were disturbed. The derived desorption curves are illustrated in Figures 11 to 13.

The relationship between hydraulic conductivity and moisture content was determined in the field. The experiment was performed on a 2 meter by 2 meter plot instrumented with tensiometers and neutron access tubes. The plot was saturated and allowed to drain while soil moisture and hydraulic head data were taken. These data were analyzed to yield the hydraulic conductivity versus moisture content relationship. The derived relationships for different depth increments are given in Figures 14 to 18. Note that most of these relationships do not span a significant portion of the moisture content range. The reasons is that when the experiments were being performed the weather was quite wet and significant drainage of the soil profile did not occur.

The saturated hydraulic conductivity of the soil was determined for three depth locations in the soil profile. These determinations were made with a double-tube apparatus (Bouwer, 1961). The determined saturated hydraulic conductivities for the three depths are given in Table 3.

TABLE 2 *

Texture Profile of Field Site

Depth	% Sand	% Silt	% Clay	Textural Class
0-15	6.40	61.84	31.76	Silty clay loam
15-25	4.00	69.86	26.14	Silt loam
25-35	9.32	74.54	16.14	Silt loam
35-55	10.55	76.84	12.58	Silt loam
55-85	32.20	55.66	12.14	Silt loam
85-95	14.30	73.81	11.39	Silt loam
95-105	23.60	66.16	10.24	Silt loam
105-115	6.95	75.79	17.26	Silt loam
115-145	4.20	71.21	24.59	Silt loam
145-155	10.00	70.00	20.00	Silt loam
155-165	1.75	58.23	40.02	Silty clay
165-185	30.00	56.00	14.00	Silt loam

* From Humphreys, 1979.

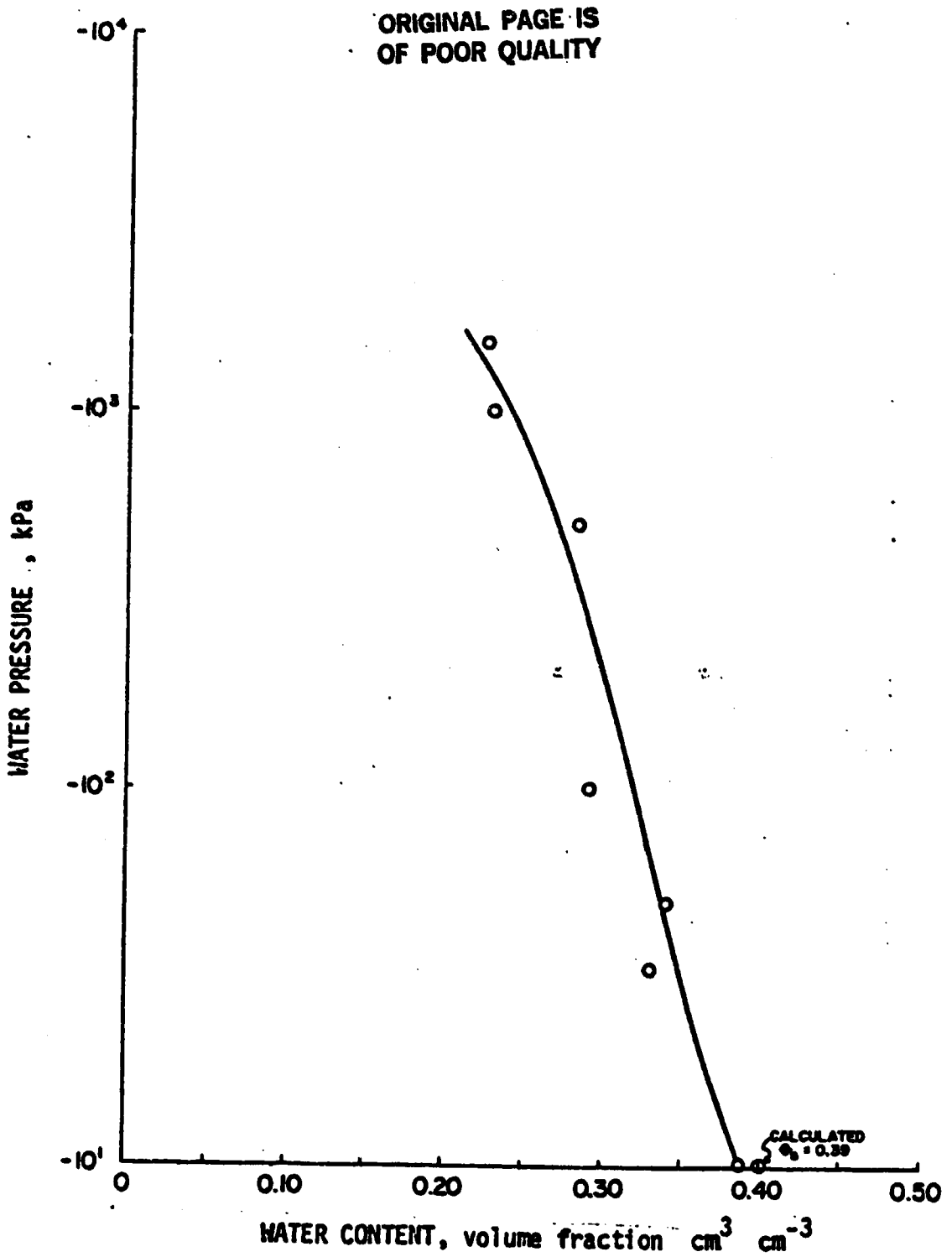


Figure 11. Water retentivity determined in the laboratory, 0-15 cm soil depth. (From Humphreys, 1979.)

ORIGINAL PAGE IS
OF POOR QUALITY

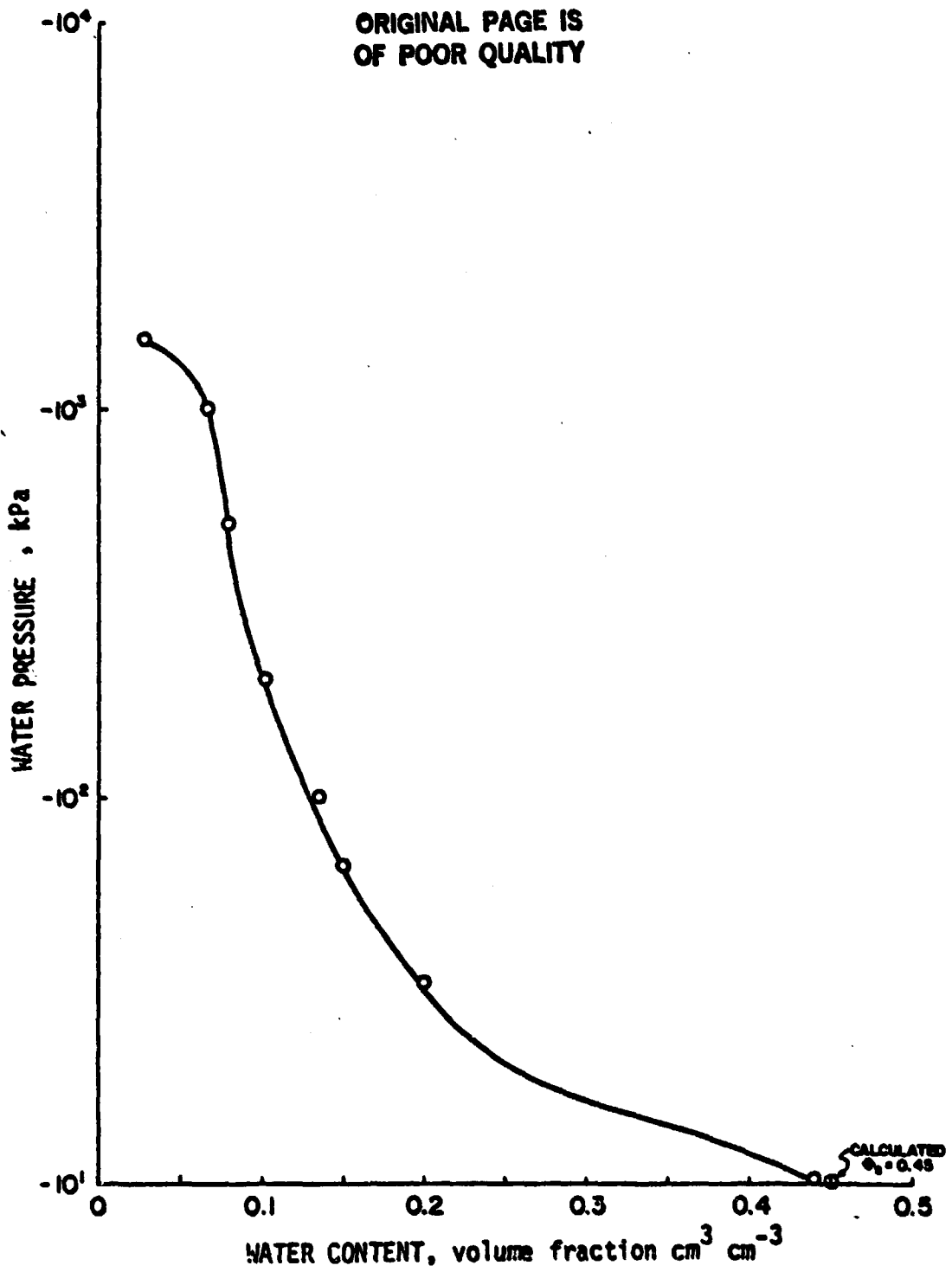


Figure 12. Water retentivity determined in the laboratory, 15-55 cm soil depth. (From Humphreys, 1979.)

ORIGINAL PAGE IS
OF POOR QUALITY

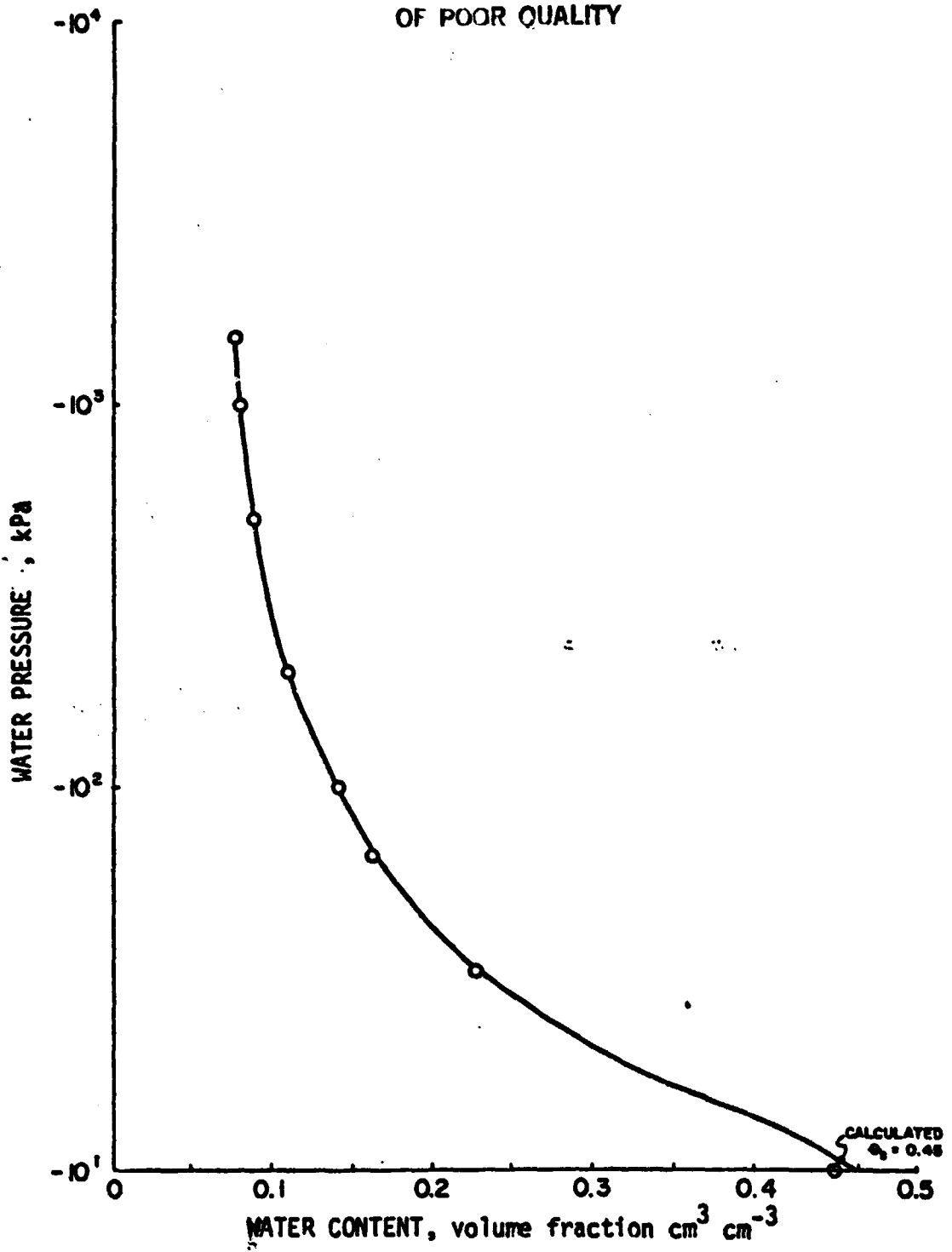


Figure 13. Water retentivity determined in the laboratory, 55-90 cm soil depth. (From Humphreys, 1979.)

ORIGINAL PAGE 137
OF POOR QUALITY

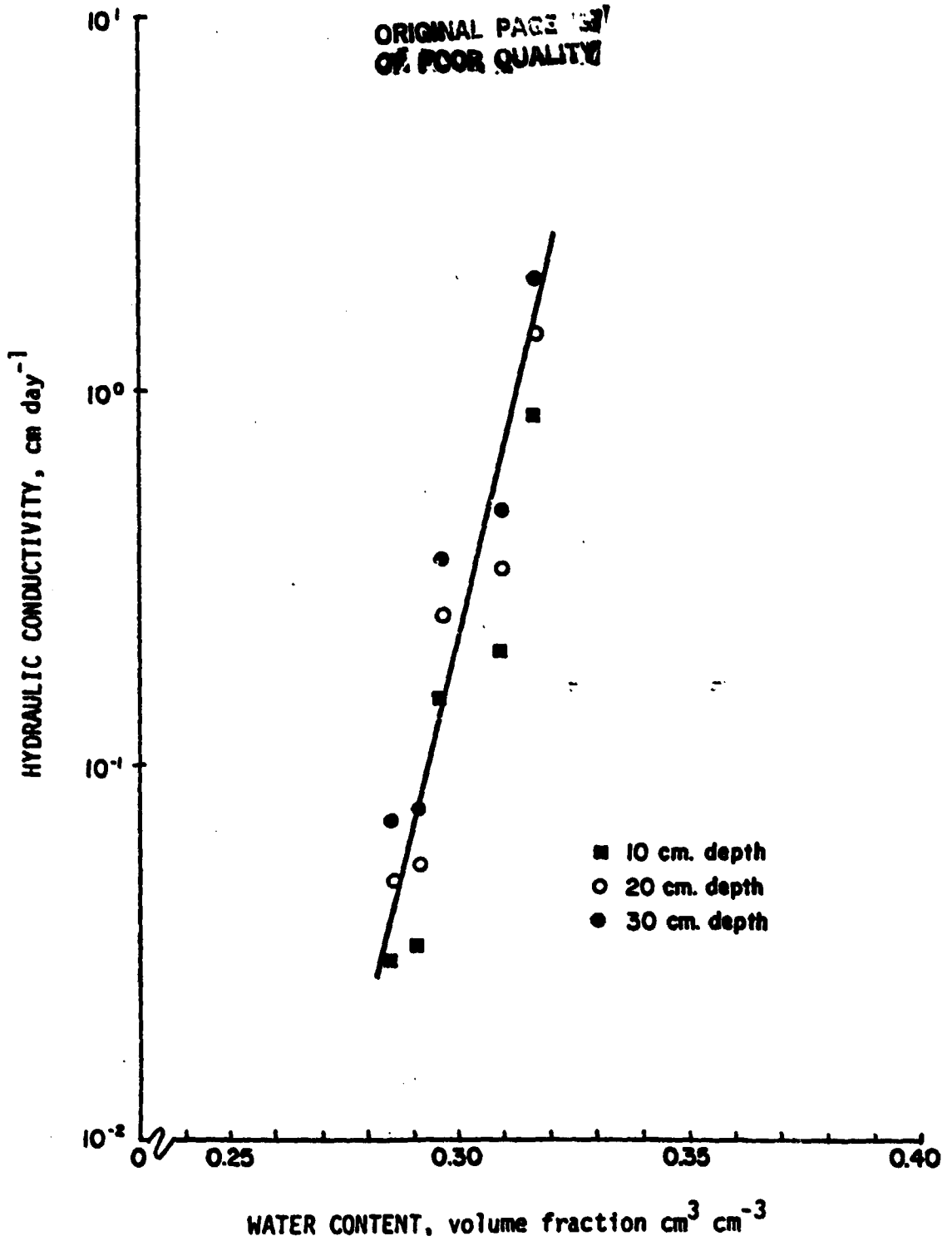


Figure 14. Relationship between hydraulic conductivity and water content determined from field measurements for 10-30 cm soil depth. (From Humphreys, 1979.)

ORIGINAL PAGE IS
OF POOR QUALITY

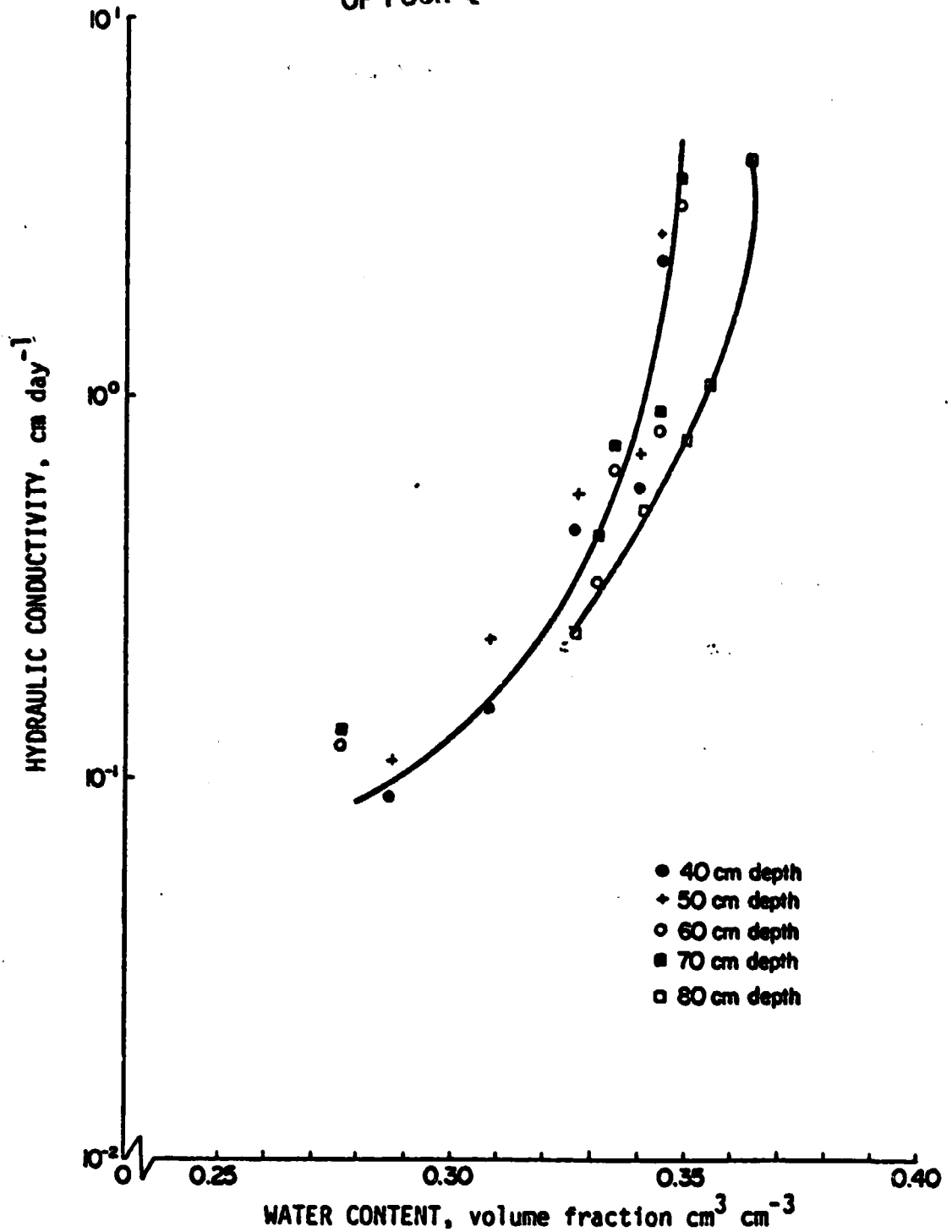


Figure 15. Relationship between hydraulic conductivity and water content determined from field measurements for 40-80 cm soil depth. (From Humphreys, 1979.)

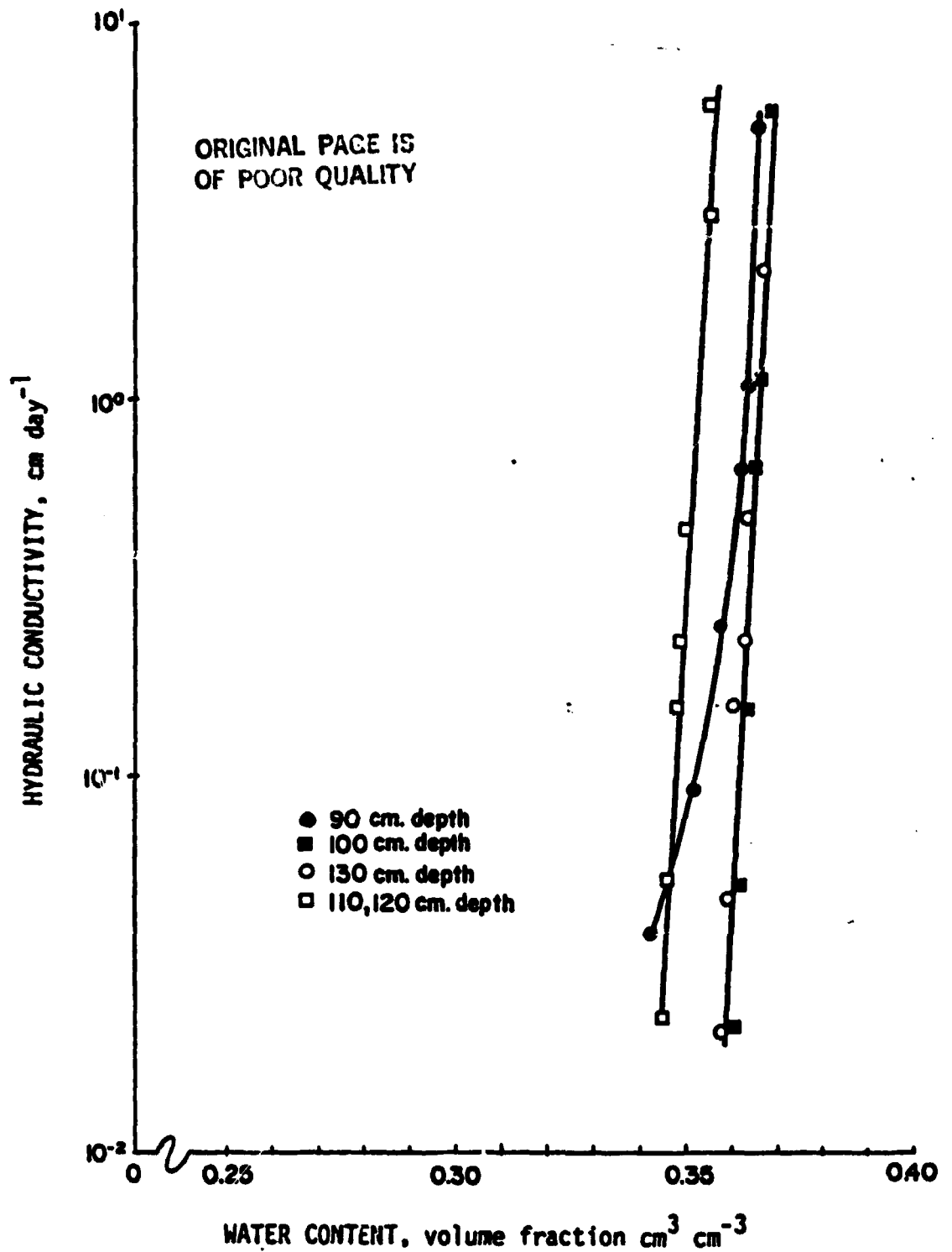


Figure 16. Relationship between hydraulic conductivity and water content determined from field measurements for 90-120 cm soil depth. (From Humphreys, 1979.)

ORIGINAL PAGE IS
OF POOR QUALITY

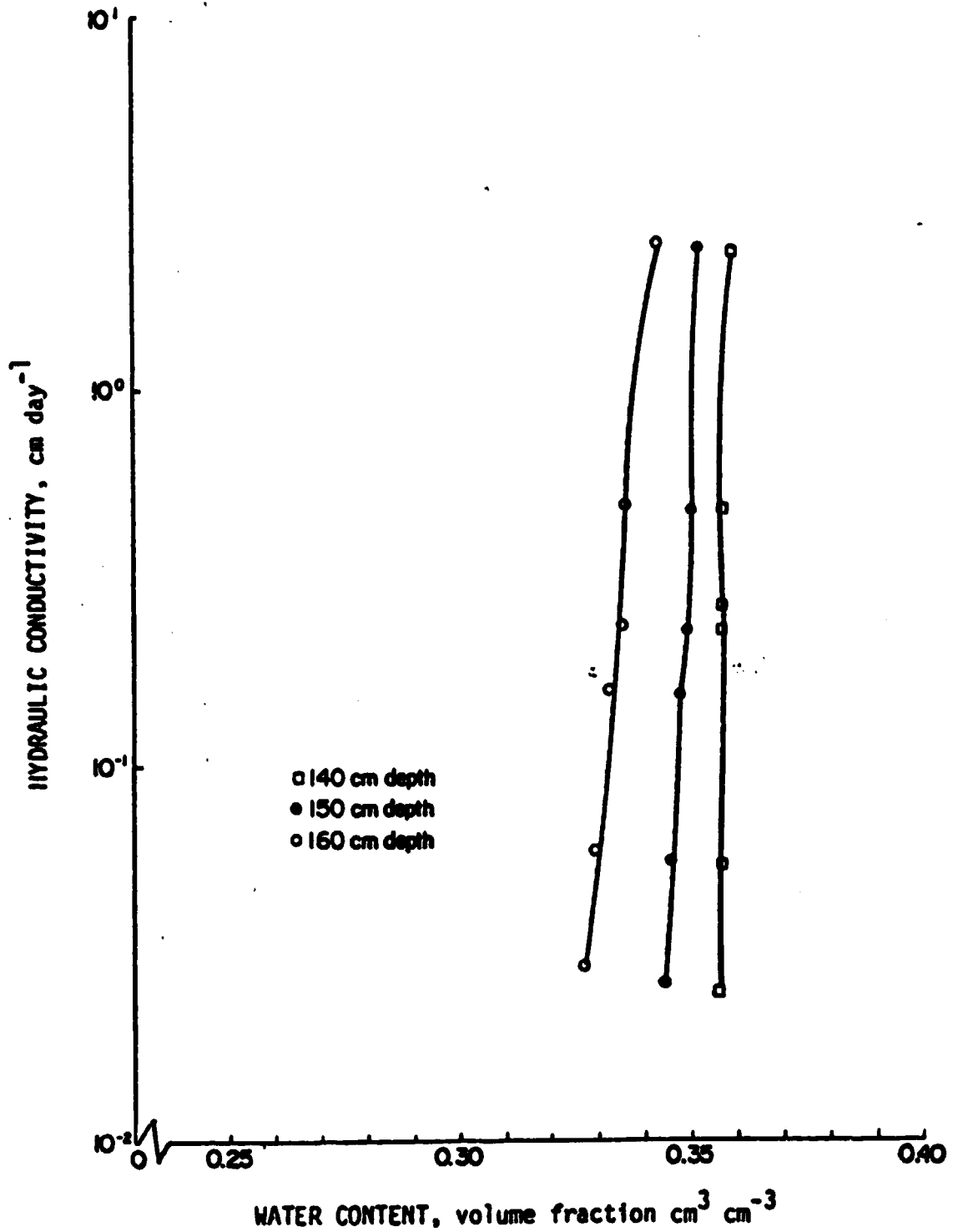


Figure 17. Relationship between hydraulic conductivity and water content determined from field measurements for 140-160 cm soil depth. (From Humphreys, 1979.)

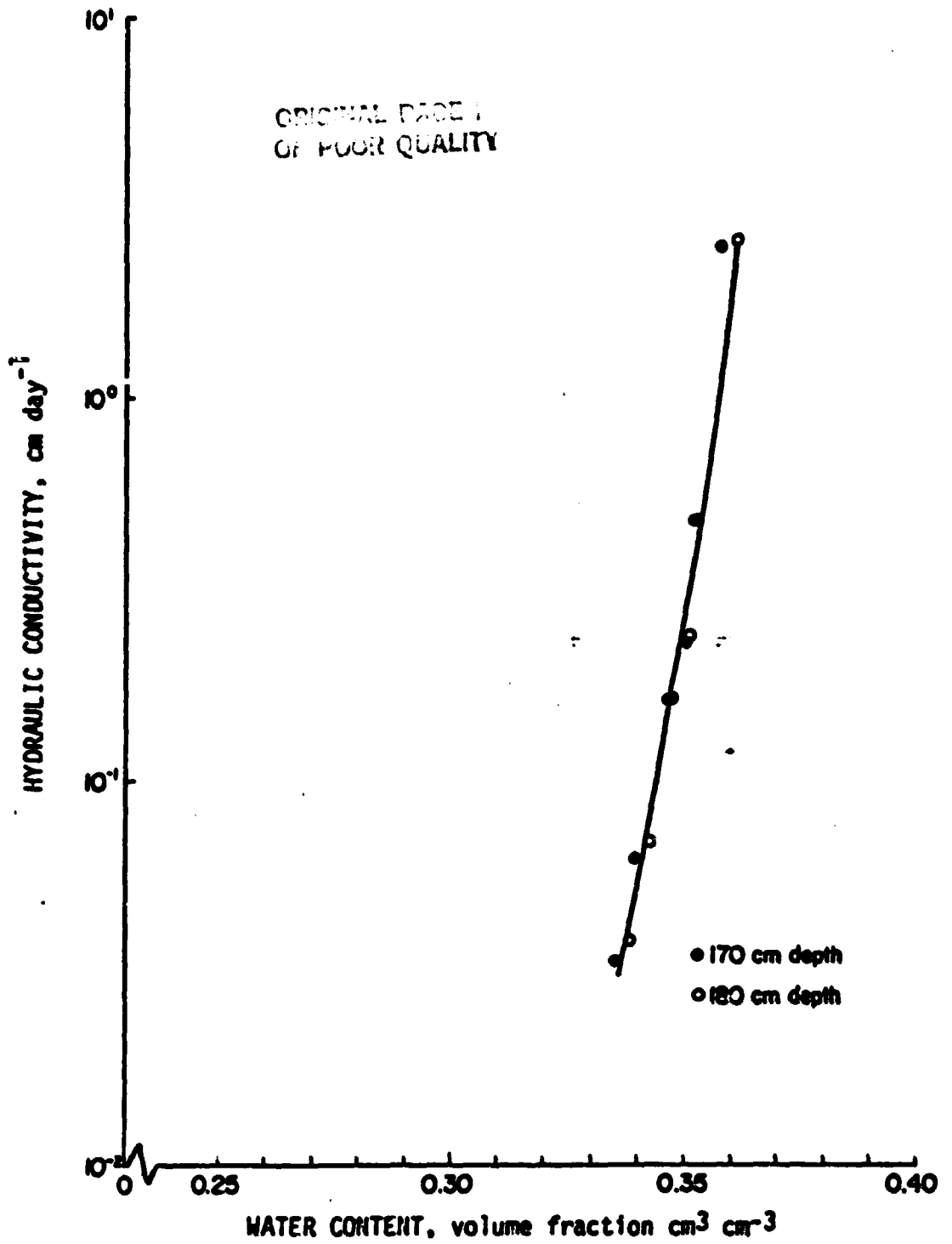


Figure 18. Relationship between hydraulic conductivity and water content determined from field measurements for 170-180 cm soil depth. (From Humphreys, 1979.)

Table 3. Saturated Hydraulic Conductivities Determined* in the Field with the Double-Tube Method

<u>Depth (cm)</u>	<u>K_s (cm/day)</u>
10	4.25
40	40.90
70	53.44

***from Humphreys (1979)**

The physical properties information reported by Humphreys (1979) will be useful as input to the verification of van Bavel's moisture flow model associated with this project. The information will also be useful in the verification of a simplified water balance model to be tested in the next contract period.

Further research will have to be done to complete the determinations of physical properties initiated by Humphreys (1979). For instance, the unsaturated hydraulic conductivity versus moisture content relationship should be derived for a wider range of moisture contents. Laboratory techniques may have to be used to make the appropriate determinations for this information.

Projected Research Plans

Tasks to be completed are listed below.

1. Thorough analysis of the data set to identify limitations of the composite weather and soil moisture data system.
2. Addition of a temperature sensor subsystem to the data acquisition system to monitor soil temperature profiles on the experimental plots.
3. Simulation of the water balance on the experimental plots using a selected water balance model. A model has been chosen and the card deck of the program is on hand.
4. Perform intensive short-term experiments at the data collection sites to provide Dr. van Bavel with data to test the moisture-temperature simulation model developed for this project.
5. Perform intensive short-term experiments during the periods when the truck-mounted passive microwave system is being operated on the experimental plots.

6. Make additional determinations of soil physical properties at the experimental site to supplement the information already acquired.

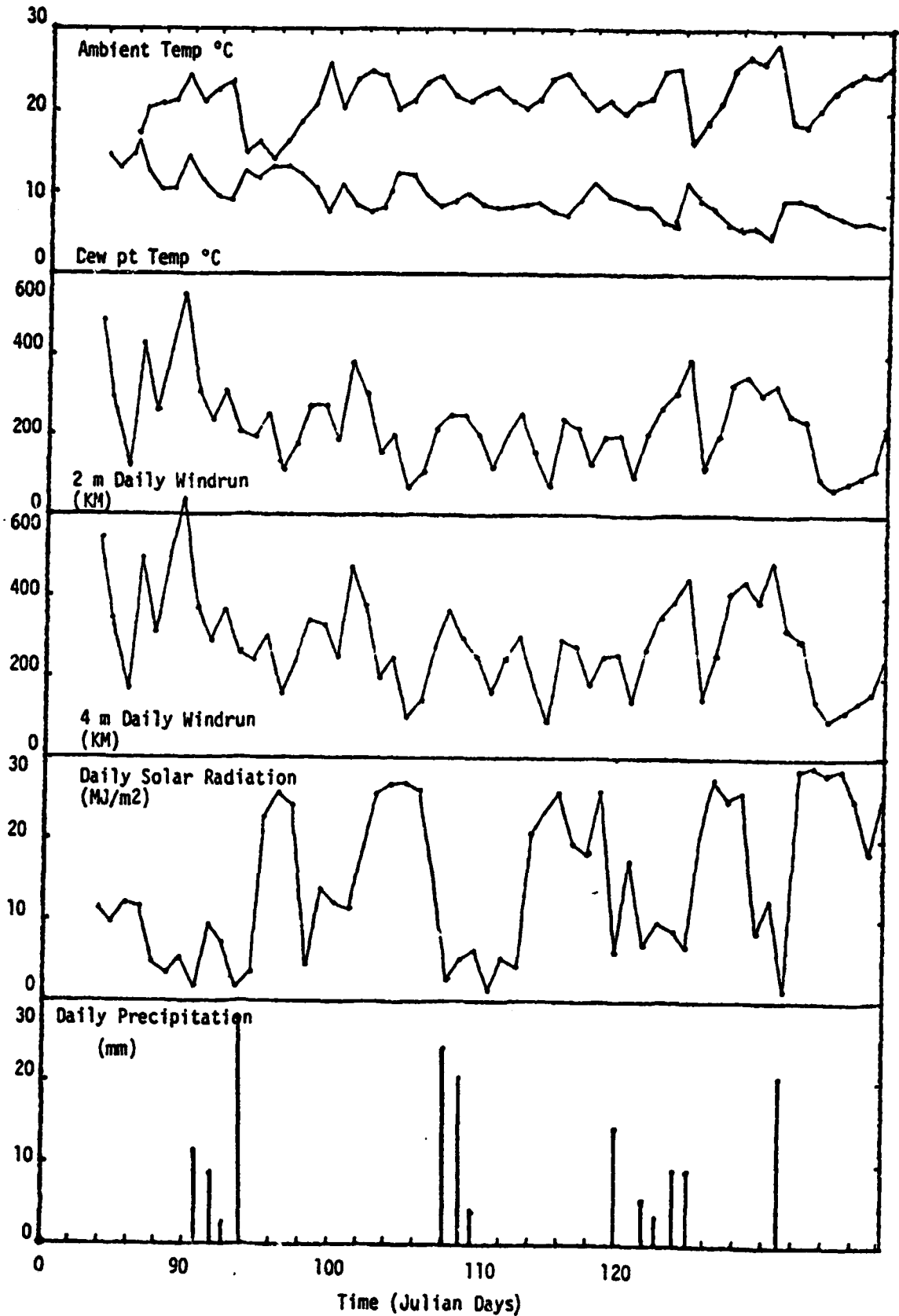
References

Bower, H., A double tube method for measuring hydraulic conductivity of soil in situ above a water table, Proc. Soil Science Society of America. 25: 334-349, 1961.

Hymphreys, K. B., Comparison of methods for determining soil hydraulic characteristics, Technical Report RSC-124, Remote Sensing Center, Texas A&M University, College Station, Texas 77843, 91 pp. May 1979.

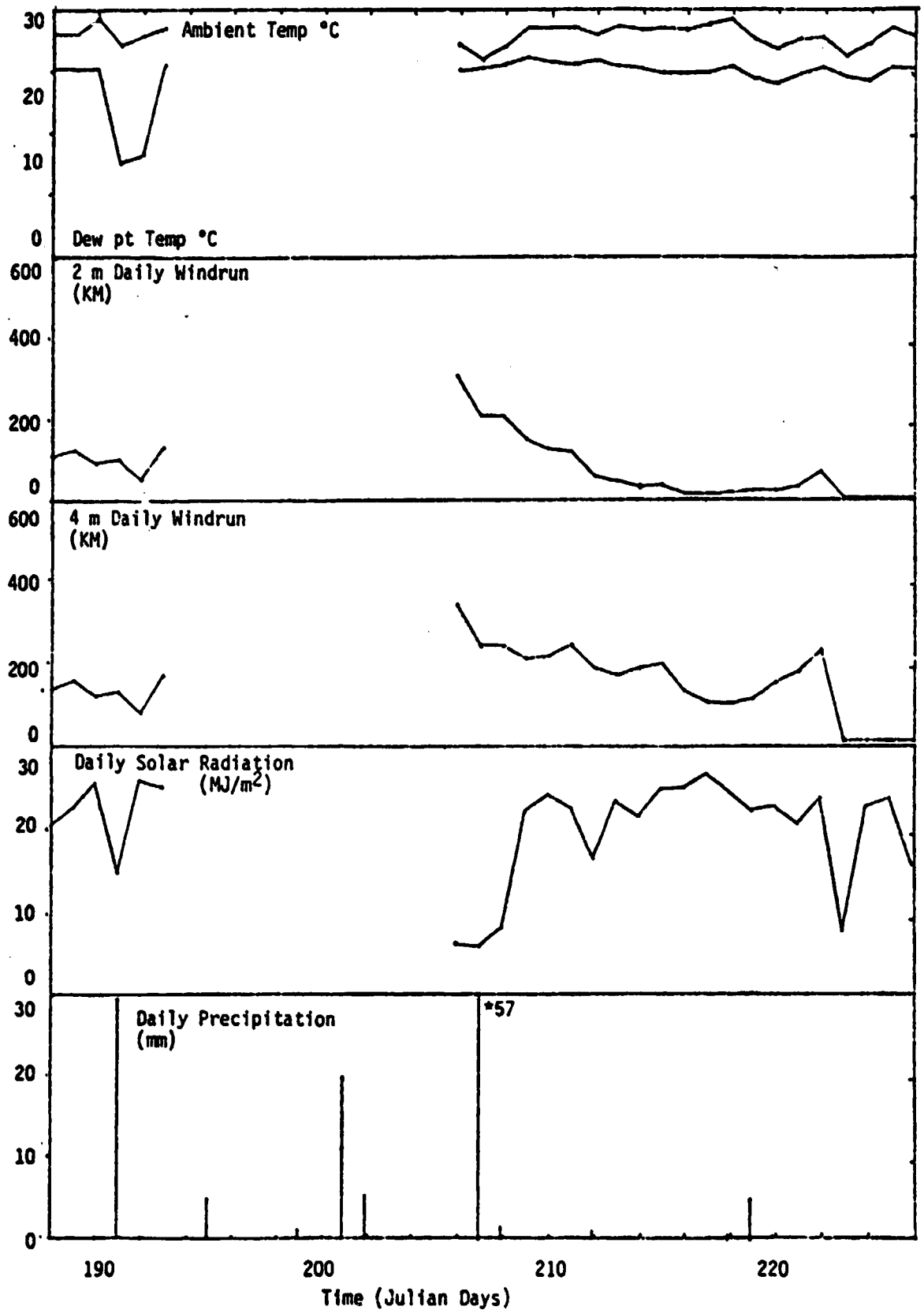
Attachment A
Weather Data Summary

Climatological Data

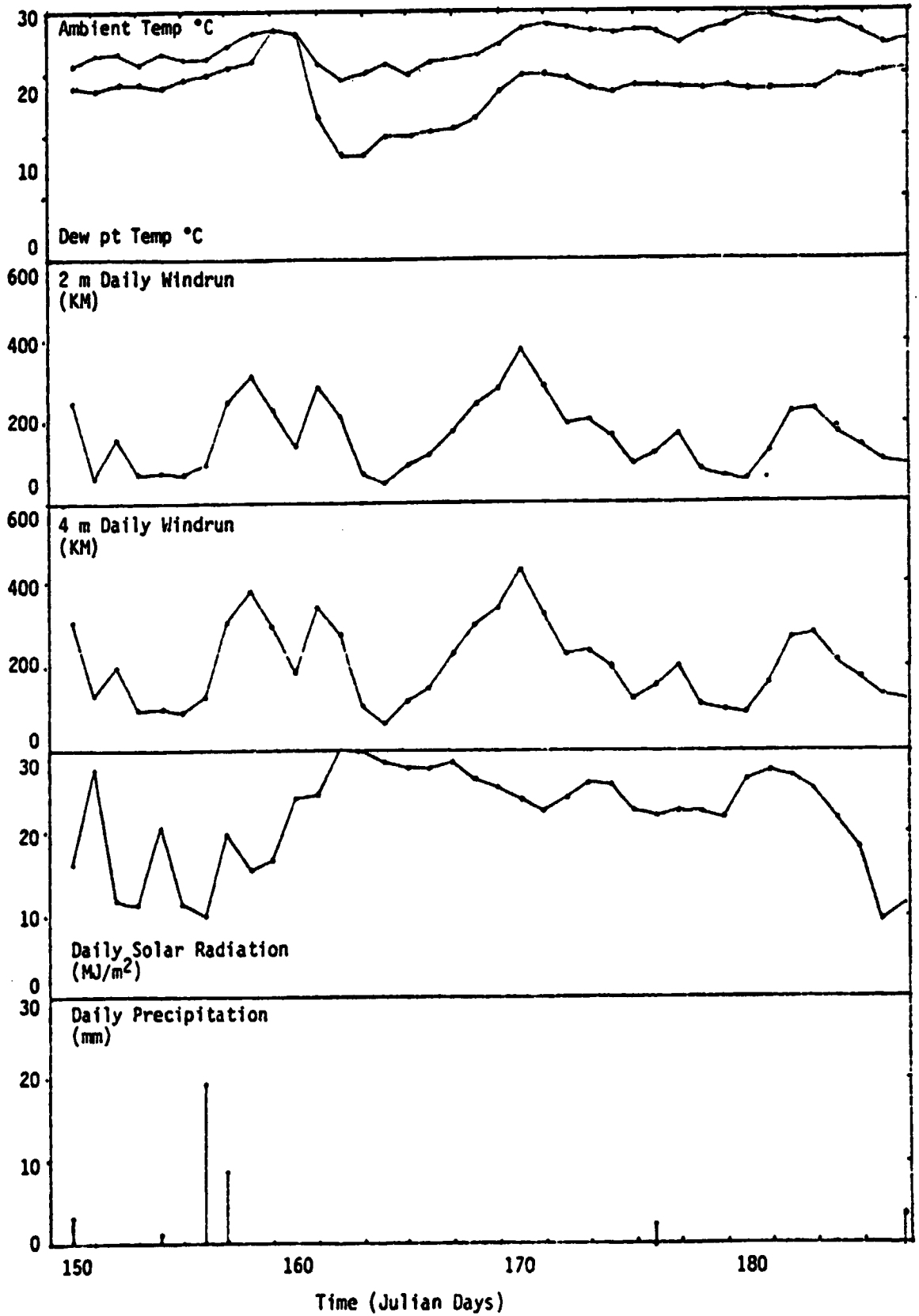


ORIGINAL PAGE IS
OF POOR QUALITY.

Climatological Data



Climatological Data

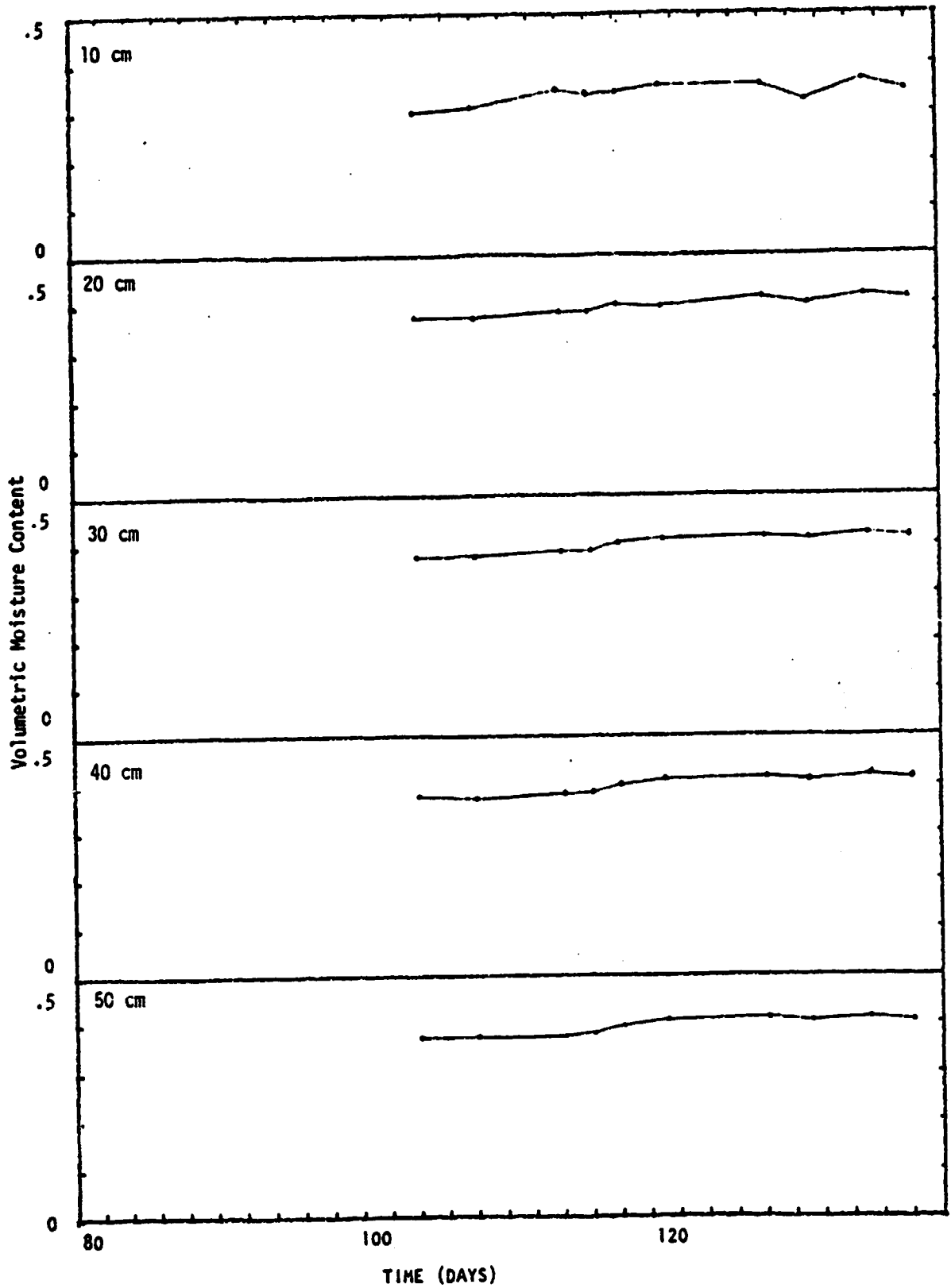


PRECEDING PAGE BLANK NOT FILMED

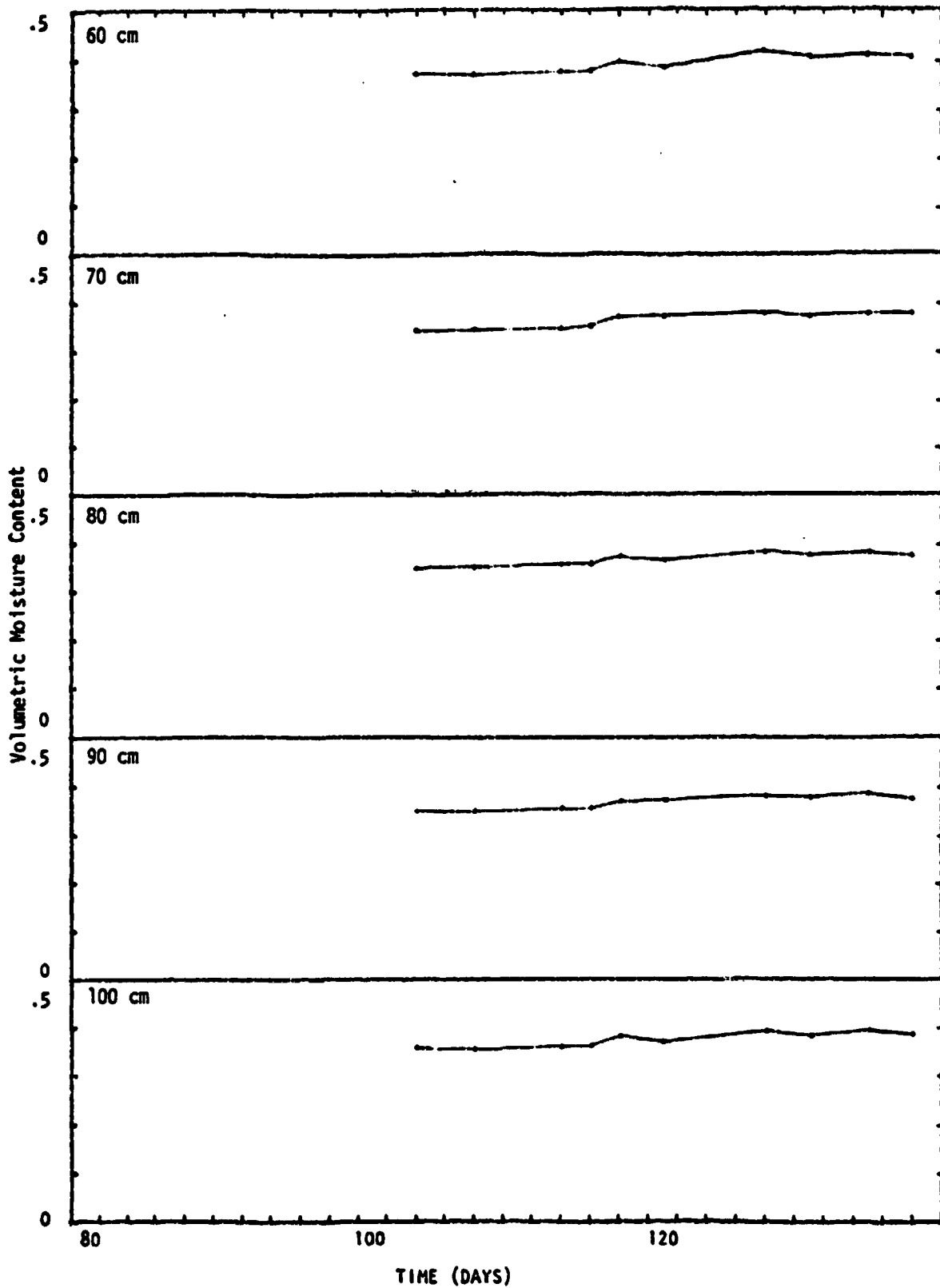
Attachment B

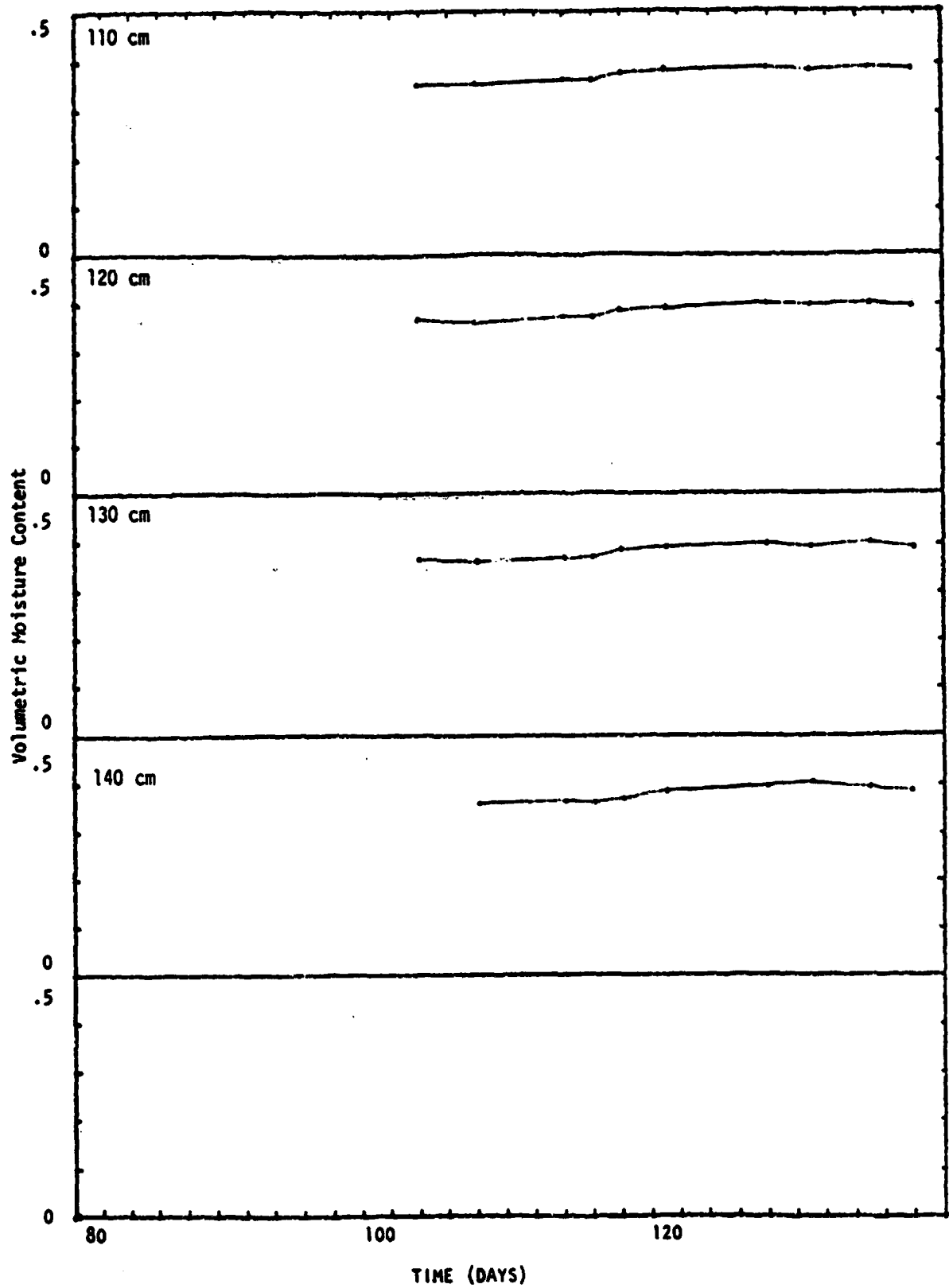
**Soil Moisture Data Summary
for Fallow Plot (Southern Location)**

South Fallow Plot



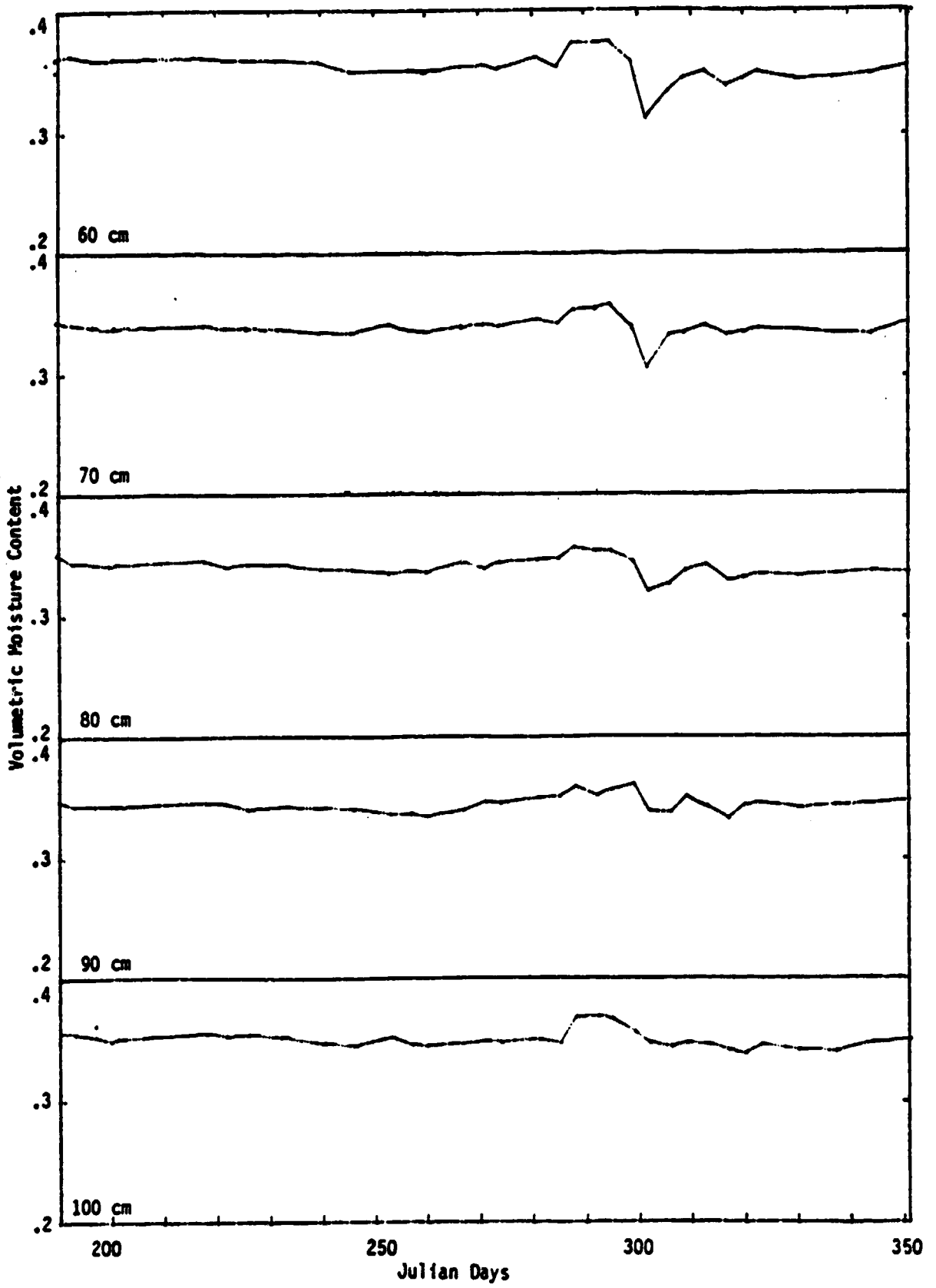
South Fallow Plot



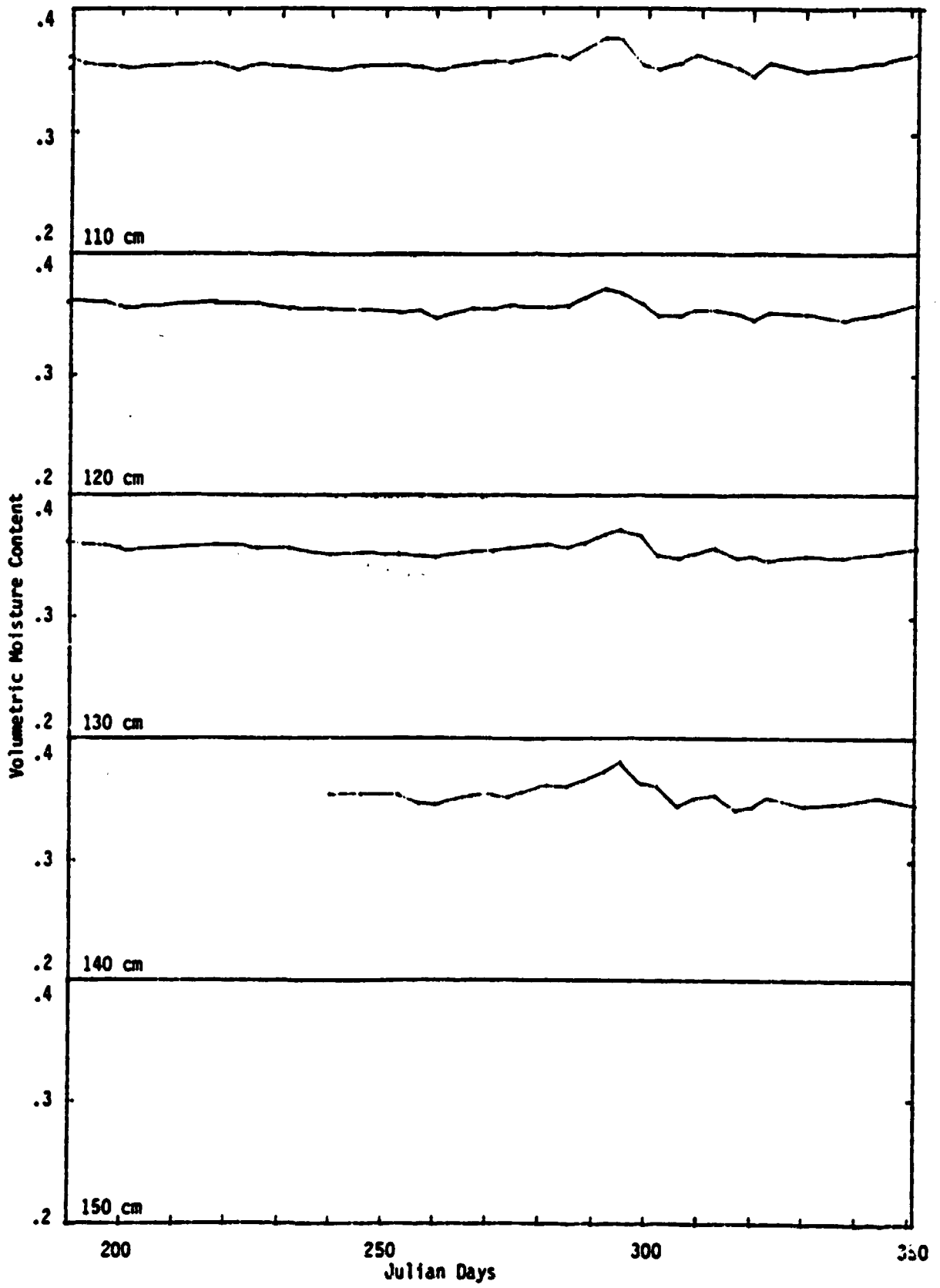


South Fallow Plot

ORIGINAL PAGE IS
OF POOR QUALITY



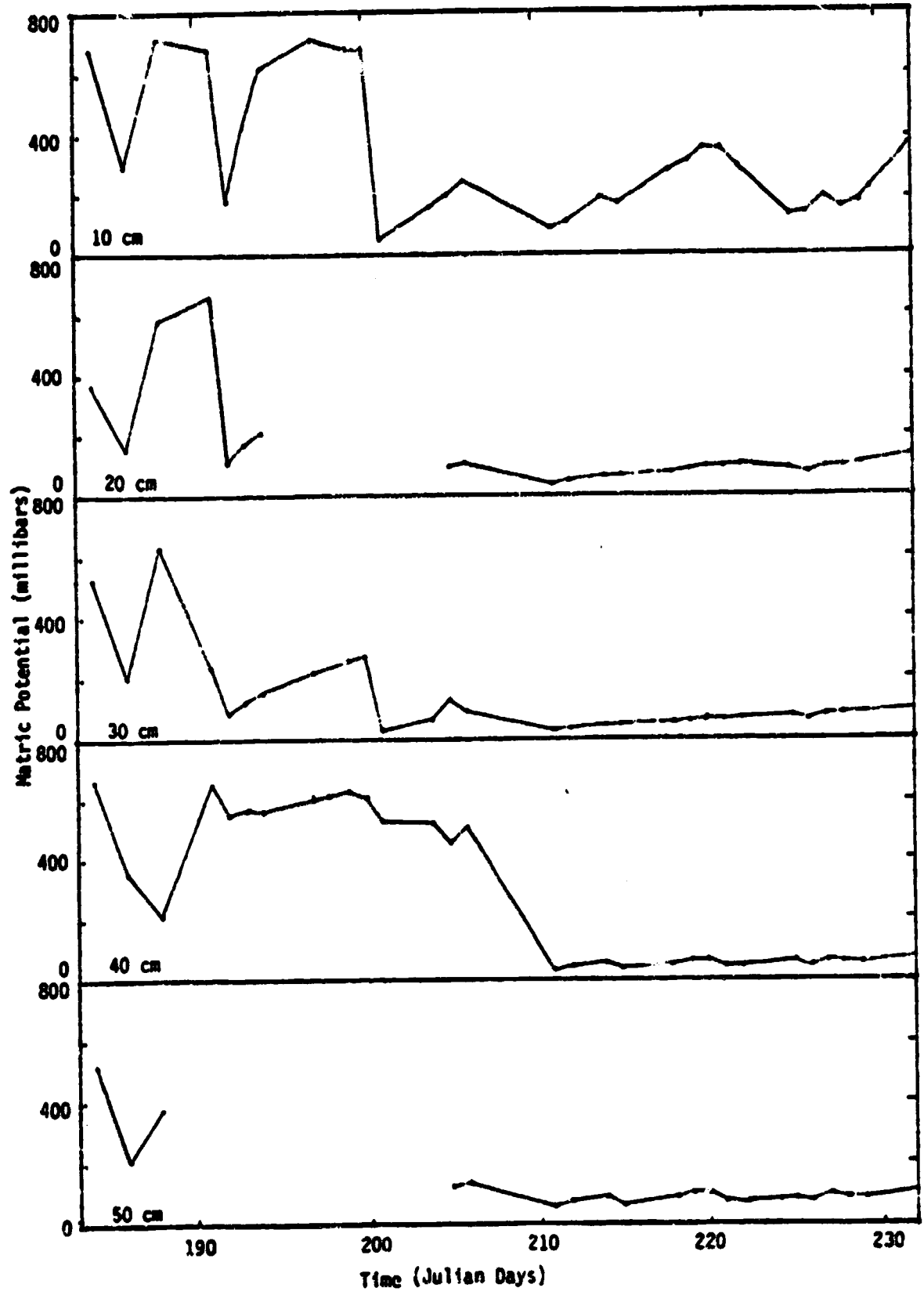
South Fallow Plot



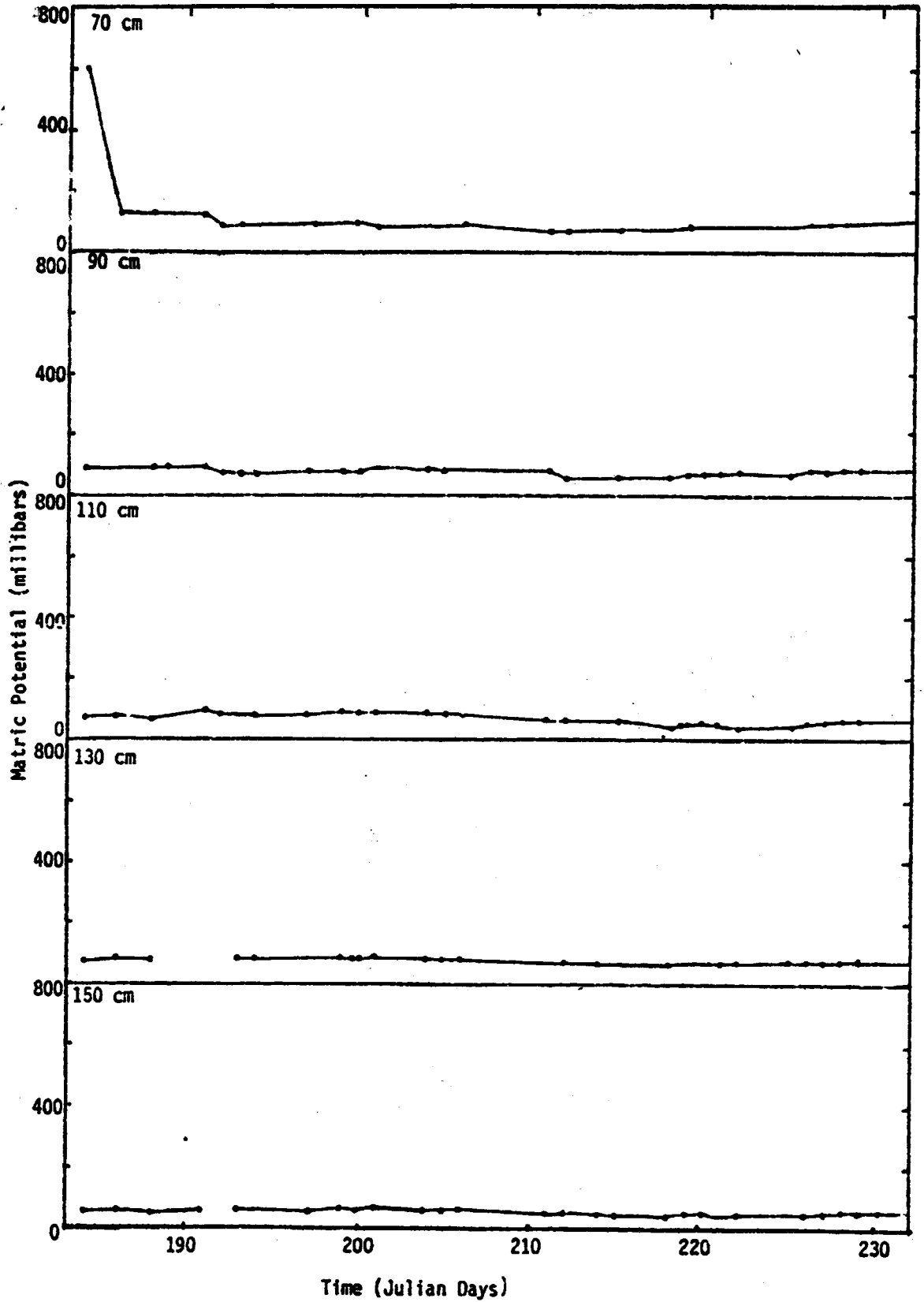
~~PRECEDING PAGE BLANK NOT FILMED~~

Attachment C
Matric Potential Data
for Fallow Plot (Southern Location)

South Fallow Plot



South Fallow Plot



Appendix A: Ground Data Report: 1978 Colby MSAS Experiment

**GROUND DATA REPORT
1978 COLBY, KANSAS EXPERIMENT**

by

**R. W. Newton
Steve Hodapp**

**Remote Sensing Center
Texas A&M University
College Station, Texas 77843**

Supported by:

NASA Contract NAS 9-13904

December 1979

TABLE OF CONTENTS

	Page
INTRODUCTION	1
FIELD MEASUREMENTS AND SAMPLING TECHNIQUES	3
Soil Moisture	3
Soil Temperature	8
Vegetation	8
Density	9
LABORATORY PROCESSING OF SAMPLES	9
COMPARISON OF CONVENTIONAL AND MICROWAVE OVENS	10
Sampling Cup Seal Test	11
Microwave Over Drying	11
CONCLUSION	14
APPENDIX A	17
B	30
C	43
D	54
E	59

LIST OF FIGURES

Figure		Page
1	Photograph of the Microwave Signature Acquisition System (MSAS)	4
2	Experimental Layout with Sampling Locations Identified.	5
3	Paper cup sample container showing the plastic wrap sealer and lid in place.	6
4	"Wing Tool" Type Instruments for Obtaining Soil Samples.	7

LIST OF TABLES

Table		Page
1	Field Descriptions	2
2	Sampling Cup Seal Test12
3	Microwave Over Drying13
4	Microwave vs. Conventional Oven Drying16

GROUND DATA REPORT:

1978 Colby, Kansas MSAS Experiment

by

S. Hodapp and R. W. Newton

INTRODUCTION

This report documents the ground truth acquired by Texas A&M University (TAMU) personnel during the Agriculture Soil Moisture Experiment conducted in Colby, Kansas by NASA/Johnson Space Center (NASA/JSC), TAMU, University of Kansas, University of Arkansas, and Lockheed Electronics Co., Inc. The experiment was funded by the NASA Johnson Space Center (NASA/JSC) and lasted from July 12 to July 22, 1978. Ground based passive microwave data were gathered by TAMU using the Microwave Signature Acquisition System (MSAS) and active microwave data by the University of Kansas using the MSAS. Also, both passive and active aircraft data were taken by a NASA C-130 airplane every three days. This report only documents the ground truth information obtained by Texas A&M University (TAMU) in support of the MSAS measurements. This ground truth information included soil moisture, soil temperature, vegetation cover, moisture content, and bulk density. In addition, weather conditions and general comments were recorded.

Passive microwave measurements and ground truth samples were obtained from five different fields: 11, 13, 18', 30 and 24. Field 24 was the only field with significant vegetation. This field contained corn stalks 4 feet tall which were being irrigated at the time of measurement. Descriptions of these fields are given in Table 1.

TABLE 1. Field Descriptions

<u>Field</u>	<u>Description and Comments</u>
11	Contains harvested wheat stubble with small rows and furrows. Row spacing runs perpendicular to the antenna look direction.
13	A rough, bare field with no rows. There was a moist plateau at a depth of about 15 cm.
18'	Contains scattered vegetation, alfalfa with some dry straw. The plants are approximately aligned, but there are no troughs nor crests in the soil. The rows formed by the plants run parallel with the antenna look direction.
24	Contains corn with irrigation running through the furrows. Unspoiled soil samples were difficult to take because of the irrigation as indicated by the soil moisture standard deviations for this field (see Appendix A).
30	Contains a layer of crushed corn stalks approximately 5 cm thick under standing wheat stubble. The row spacing runs perpendicular to the antenna look direction.

Soil, bulk density, and vegetation samples gathered in the fields were brought to the laboratory to be weighed, dried, and reweighed. Microwave ovens and sealed paper cups were used for drying the soil samples. Tests were performed to demonstrate that the soil moisture measurements obtained through the use of microwave ovens were comparable to ones obtained through the use of conventional ovens. Conventional ovens were used to dry the vegetation.

FIELD MEASUREMENTS AND SAMPLING TECHNIQUES

During one day, measurements could be taken at two or three different fields. First, the trucks carrying the radiometer system were parked alongside one of the fields (Figure 1). When the radiometer antennas had been mounted and positioned over the edge of the field, two teams of two men each proceeded to take ground truth data. In addition, one person stayed with the trucks taking brightness temperature readings.

The antenna marked the center of the front edge of the field, as shown in Figure 2. A tape measure and small flags were used to mark out the locations for soil moisture, bulk density, and vegetation samples. Soil moisture samples were acquired at 12 locations, bulk density at four, and vegetation at two.

Soil Moisture

Soil moisture samples were placed in small 8 oz paper cups and sealed with a lid and a piece of plastic wrap from a perforated roll as shown in Figure 3. Three different types of tools were used to obtain samples from depths of 0-2, 2-5, 5-9, 9-15, 15-30, and 0-15 cm. "Wing tool" type instruments as shown in Figure 4 were used to

ORIGINAL PAGE
COLOR PHOTOGRAPH

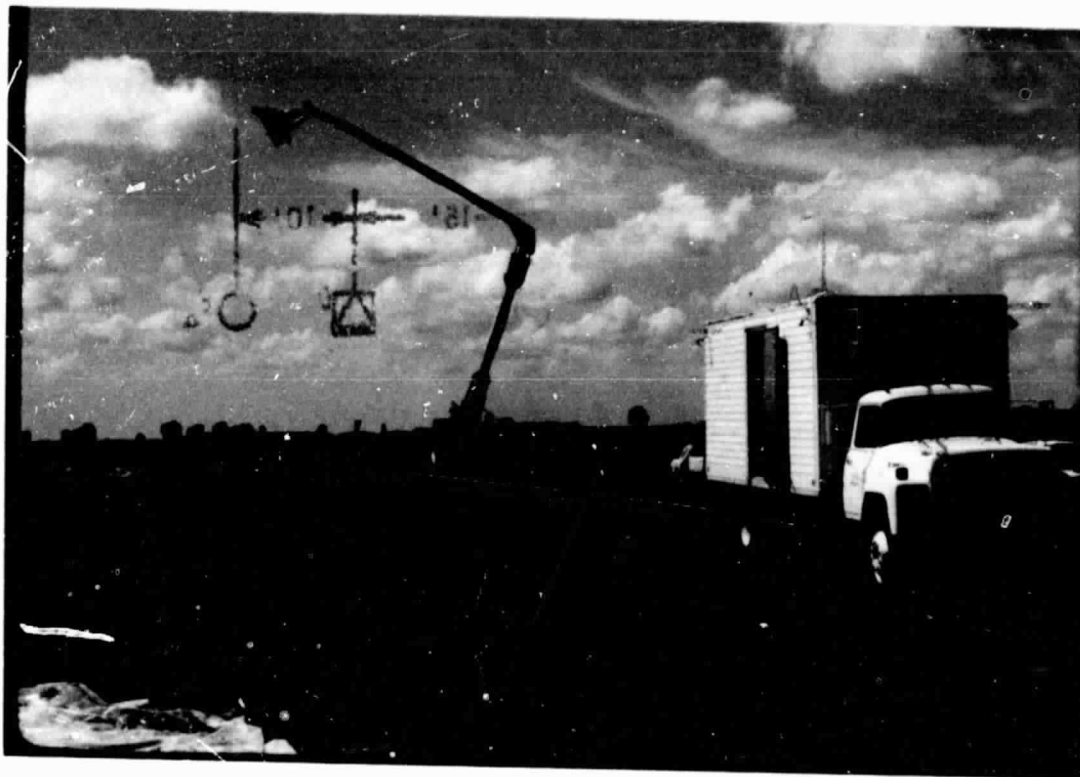


Figure 1. Photograph of the Microwave
Signature Acquisition System (MSAS).

ORIGINAL PAGE IS
OF POOR QUALITY

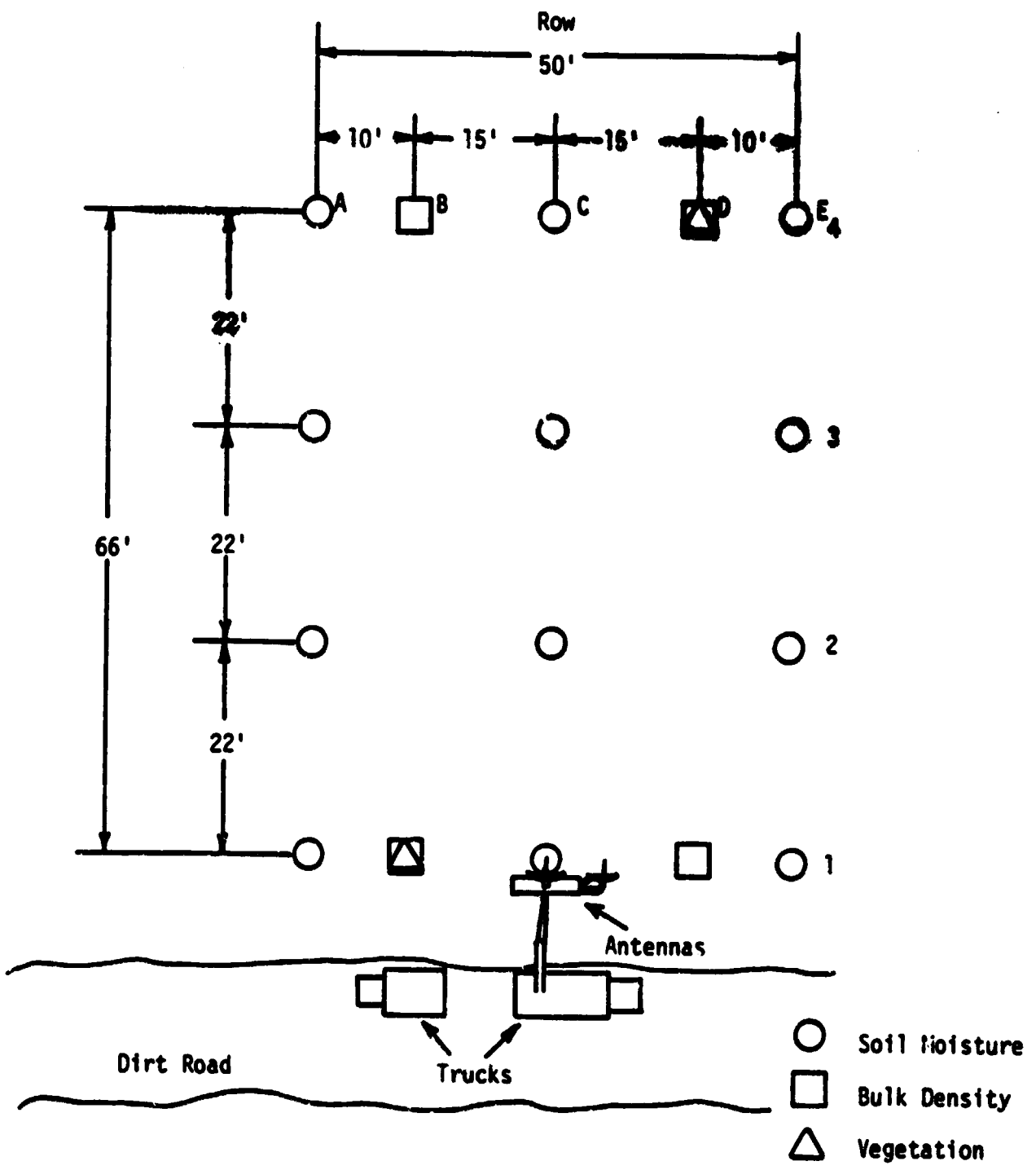


Figure 2 Experimental layout with sampling locations identified.

ORIGINAL PAGE
COLOR PHOTOGRAPH



Figure 3. Paper cup sample container showing the plastic wrap sealer and lid in place

ORIGINAL PAGE IS
OF POOR QUALITY

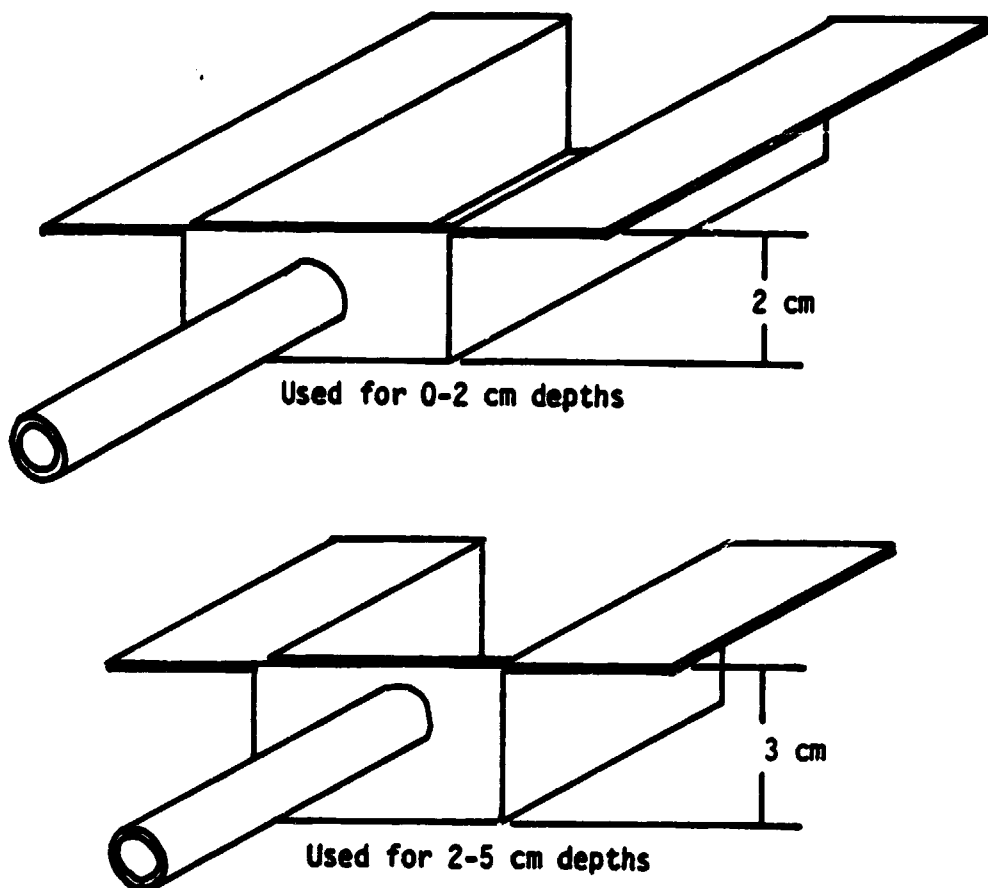


Figure 4 "Wing Tool" type instruments for obtaining soil samples.

obtain the 0-2 and 2-5 cm samples. A trowel was used to obtain the 5-9 and 9-15 cm samples. Standard 1 inch "Soil test" core tubes were used for the 15-30 and 0-15 cm depths. Immediately after acquisition the samples were placed in a box or bag which helped prevent direct exposure of the cups to sunlight and premature moisture loss. They were then loaded in the ground truth van for transport to the lab.

Soil Temperature

In order to obtain surface soil temperature data, a hand held precision radiation thermometer (PRT5) was used at each soil moisture test location. The PRT5, which was borrowed from NASA/JSC, measures thermal infrared radiation which is related to the surface temperature of the soil. Appendix C gives surface soil temperature by field experiment number, field, date, time and location in the field. Some weather comments are also included. No temperature measurements were taken before July 16 because the PRT5 was not available at that time. Although the PRT5 was available for Field 24, the large corn stalks prevented measurements from being taken. For some of the field experiments a "retake" was done on the soil temperature as indicated next to the times. This was done because problems with the MSAS caused some of the microwave readings to be taken much later than the first soil temperature measurements.

Vegetation

At two sites in each field vegetation samples were clipped and placed in paper sacks and then into Ziploc bags to keep in moisture. The height, row spacing, and plant spacing were estimated and recorded. Appendix D shows the vegetation data by field experiment number, field, date, time, and location in the field.

Density

The procedure for obtaining bulk density samples was much like that for soil moisture except that a known volume of soil was needed. Methods for measuring bulk density have been inaccurate because of the difficulty in obtaining a noncompressed known volume of soil. A small can of 100 ml volume was used for samples at depths of 0-3, 3-9, and 9-15 cm. An aluminum cylinder with a line marking at 100 ml was used for the more difficult 15-20 cm depths. The can had hard, sharp, thin edges in order to prevent compression of the soil as it was pressed into the side of a hole. The can was then carefully dug out and the end scraped off to obtain 100 ml of soil. The samples were placed in paper cups and sealed to keep in moisture.

LABORATORY PROCESSING OF SAMPLES

All wet samples brought from the fields to the lab were immediately weighed and recorded. Soil moisture and bulk density samples were placed in microwave ovens and the samples dried until the change in mass over a five minute period was about .05 g. Numerous tests were run to determine drying curves as a fraction of soil wetness and microwave overloading. Soil moisture drying curves shown in Appendix E demonstrate that little change in percent moisture occurred after this point was reached. Test samples M1 through M6 were taken from a cornfield and dried together in the same oven. Test samples F1 through F5 were obtained outside the experiment team's apartment residence and were also dried together. It should be noted that drying times are longer when more samples are placed in the oven. Drying a set of twelve samples usually took about 30 to 60 minutes as compared

with the standard 24 hour period for a conventional oven filled with samples. Previously determined average weights of cups, lids, wraps, and dried cups were used in calculations of soil moisture and bulk density. Calculations were done with programmable calculators. Appendix A gives soil moisture and Appendix B gives bulk density, each by field experiment number, field, date, time and location in the field.

Vegetation samples were weighed wet in the Ziploc bags and paper sacks. Then the samples were dried in a conventional oven in just the paper sack for about 24 hours and reweighed. The vegetation moisture content was computed using these weights and the average weights of the paper sack and Ziploc bag previously determined. The conventional oven was used for vegetation moisture because the microwave ovens were constantly being used for soil moisture and bulk density samples.

COMPARISON OF CONVENTIONAL AND MICROWAVE OVENS

In Colby, microwave ovens were used to dry the soil samples. The standard method for drying, however, is to use metal sample containers and heat the samples in a conventional oven at 105°C for 24 hours. In microwave ovens twelve samples could be dried in 30 to 60 minutes. Because measurements for just one field required 100 samples, microwave ovens were chosen as being more practical.

To eliminate any doubts about the method used, two experiments were conducted to test the accuracy of the microwave drying procedure. One measured the amount of moisture lost through the cups in taking samples from the field to the laboratory to be weighed. Another experiment compared the moisture content obtained using the microwave oven to that obtained using the conventional oven for soil

samples containing different amounts of moisture. The microwave ovens were 600 watt ovens purchased at Montgomery Wards (model KTM-8186-10). It should be noted that the soil drying times when using a microwave oven are highly dependent on the power output of the oven. As a result, the drying times reported below are only valid for the ovens tested.

Sampling Cup Seal Test

In the sampling cup seal test, ten soil samples of varying moisture content were weighed, left in direct sunlight for three hours, then in the ground truth van for three hours, and reweighed. The samples were then dried to get the dry weight. Soil moisture calculated from the initial wet weight and the wet weight after six hours showed little change in the soil moisture as indicated in Table 2. The average difference between the true percent moisture and that after the cups had been left out 6 hours is .57 percent.

Microwave Over Drying

To test theories that microwave ovens dry out soil samples more than conventional ovens, seven samples were initially placed in a conventional oven for about 9 hours (see Table 3). Four were left in the conventional oven while the other three were placed in microwave ovens to see if more moisture could be driven out. Samples left in the conventional oven indicate that drying over 9 hours in that oven produces little change in weight. The samples placed in the microwave oven were dried until they began to burn. The maximum change in weight was 4 g. Wet weights had been neglected to be measured, so changes in percent moistures cannot be given.

TABLE 2. Sampling Cup Seal Test.

Sample Number	Initial* Wet Wt.	Wet Wt.* After 6 Hrs	Dry Wt.*	%Moisture for Initial Wet Wt.	%Moisture for Wet Wt. After 6 hrs.	Difference
1	150.70	150.40	141.00	5.23	5.00	.23
2	113.70	113.05	96.75	15.80	15.08	.72
3	117.30	116.72	94.90	22.28	21.63	.65
4	217.19	216.70	175.65	22.96	22.67	.29
5	146.15	145.50	120.42	20.22	19.65	.57
6	148.60	148.00	121.90	20.80	20.28	.52
7	149.90	149.35	121.90	21.92	21.44	.48
8	84.78	84.50	78.35	5.23	4.84	.39
9	59.00	58.40	48.30	19.14	17.71	1.43
10	182.10	181.50	146.80	23.23	22.80	.43

Average Difference = .57%

*Wet weights include cups, lids, and wraps (8.96 g.).

Dry weights include dry cups (6.3 g.).

TABLE 3. Microwave Over Drying

Date/Time	1	2	3	4	5	6	7
7/25 5:30 P.M.	Placed in conventional oven - no wet weight taken						
7/26 11:00 A.M.	85.40	144.15	141.70	189.58	121.35	137.55	156.55
12:00 P.M.	85.40	144.15	141.70	189.50	121.35	137.55	156.50
2:10 P.M.	85.45	144.20	141.70	189.40	121.40	137.55	156.50
2:10 P.M.	Put in microwave oven			Left in conventional oven			
2:45 P.M.	84.55	142.85	137.70				
2:50 P.M.	84.55	142.50	Burned up				
2:55 P.M.	84.55	141.80					
	Slightly brown	Burned up					
3:50 P.M.				189.35	121.40	137.55	156.55
7/27 5:45 P.M.				188.95	121.30	137.40	145.30
				Total drying time 48 hours			

Further experimentation was conducted to compare the amount of drying in microwave and conventional ovens. Eleven samples were taken from an irrigated corn field. Six were dried in a microwave oven and five in a conventional oven. The average soil moisture from the microwave oven was 34.59 percent moisture and from the conventional oven was 34.0 percent moisture. The change was .59 percent, the microwave oven indicating a higher moisture content.

Later, a similar experiment whose data are shown in Table 4 was done under controlled laboratory conditions with all samples having the same moisture content. The average moisture for microwave oven dried samples was 23.5 percent moisture and for conventional ovens was 22.91 percent moisture, a different of .59 percent moisture. Again, the microwave oven dried out the soil slightly more, giving a measured percent moisture greater than the standard value.

CONCLUSION

The ground truth techniques used in Colby, Kansas were found to be accurate and convenient for the large number of samples processed. Four people assigned to ground truth work were able to keep up with the drying and calculations each day so that new samples could be brought in. This would not have been possible with conventional ovens in which drying would have occupied a great amount of time after the experiment was finished. Questions about loss of moisture during transportation of sealed paper cups and over drying in microwave ovens were investigated. Errors associated with these problems were discarded as being insignificant. Improved techniques might be looked for in sampling 0-15 cm depths where loss of loose topsoil often

occurred. Also, in measuring bulk density there were difficulties in obtaining an accurate known volume of noncompressed soil. However, the instruments and procedures used are thought to be the best that were available at the time of the Colby experiment.

TABLE 4. Microwave vs. Conventional Oven Drying

Dried Microwave Samples

Sample #	Wet Wt.*	Dry Wt.*	% Moisture
1	150.00	122.50	23.37
2	213.75	173.65	23.76
3	103.40	84.70	23.42
4	158.40	129.25	23.43

Average Moisture = 23.50%

Conventional Oven Dried Samples

Sample #	Wet. Wt.*	Dry Wt.*	% Moisture
1	153.10	125.40	22.97
2	218.80	178.75	23.03
3	100.90	83.00	23.89
4	164.85	135.20	22.74

Average Moisture = 22.91%

*Wet weights include cups, lids, and wraps (8.96 g.).
Dry weights include dry cups (6.3 g.).

APPENDIX A
Soil Moisture Listings

SOIL MOISTURE
Field Experiment #: 1

Field #: 11

Date: 7/12/78

Time: 3:40 - 7:00 p.m.

LOCATION	0-2 CM	2-5 CM	5-9 CM	9-15 CM	15-30 CM	30-45 CM	0-15 CM
A1		3.88	5.86				
A2		5.48			17.73		9.32
A3		4.59	7.25				11.56
A4	2.22	3.48			20.82	20.45	13.62
C1							
C2							
C3			6.29		19.57		19.25
C4	2.16		6.52		19.45	18.23	
E1	1.62 3.08	3.75	5.55	8.64			
E2	2.80	5.29	11.22	17.13			11.53
E3	2.41	5.09	10.49			17.86	11.09
E4	2.02	4.91	8.05	17.81	19.73	17.74	10.30
MEAN	2.32	4.50	7.82	14.53	19.46	18.57	12.18
S.D.	0.30	0.84	2.25	5.11	1.11	1.27	3.57

SOIL MOISTURE
Field Experiment #: 2

Field #: 30

Date: 7/13/78

Time: 3:50 - 6:00 p.m.

LOCATION	0-2 CM	2-5 CM	5-9 CM	9-15 CM	15-30 CM	30-45 CM	0-15 CM
A1	5.00	5.89	8.23	10.37	11.71	13.69	12.51
A2	13.60	15.53	15.21	12.39	12.39	14.39	13.08
A3	8.86	13.61	14.73	12.56	13.38	14.48	14.12
A4	4.35	5.03	8.72	11.04	13.35	12.50	12.65
C1	5.84	5.53	9.40	10.85	11.35	12.91	12.63
C2	8.64	9.72	12.34	11.58	12.67	14.61	10.66
C3	5.82	5.09	10.18	12.19	13.50	14.05	12.39
C4	5.57	7.95	13.37	12.67	13.91	14.62	11.92
E1	5.57	5.23	8.66	10.17	11.44	13.15	12.11
E2	8.98	12.35	13.59	11.58	11.86	13.12	13.07
E3	5.61	7.64	13.75	12.17	13.77	15.01	12.40
E4	5.01	6.97	13.74	11.99	15.65	16.08	9.72
MEAN	6.90	8.38	11.83	11.63	12.92	14.05	12.27
S.D.	2.65	3.63	2.60	0.85	1.26	1.02	1.14

SOIL MOISTURE
Field Experiment #: 3

Field #: 13

Date: 7/15/78

Time: 12:10 - 1:30 p.m.

LOCATION	0-2 CM	2-5 CM	5-9 CM	9-15 CM	15-30 CM	30-45 CM	0-15 CM
A1	3.66	5.09	19.13	22.98	22.36	22.96	13.02
A2	4.21	4.46	6.12	17.78	23.28	23.02	11.18
A3	2.87	5.40	11.61	22.85	25.00	24.56	17.70
A4	3.88		21.41	23.36	25.58	25.25	19.14
C1	3.14	5.72	16.50	23.01	22.12	23.29	18.44
C2	3.42	4.19	6.32	17.88	24.54	22.30	15.21
C3	3.58	3.57	5.38	14.48	24.49	24.08	15.01
C4	3.34	4.34	5.73	12.36	24.62	23.36	17.05
E1	3.37	5.89	18.41	20.85	21.41	22.48	12.70
E2	8.66	15.43*	21.57	25.85	26.79	25.36	23.27
E3	4.55	5.41	9.96	22.91	27.36	25.09	13.88
E4	3.39	5.39	18.97	25.67	26.66	25.24	22.96
MEAN	4.01	4.95	13.43	20.83	24.52	23.92	16.63
S.D.	1.54	0.76	6.54	4.29	1.93	1.15	3.88

* not used to find the mean.

SOIL MOISTURE
Field Experiment #: 4

Field #: 13

Date: 7/15/78

Time: 5:00 - 6:20 p.m.

LOCATION	0-2 CM	2-5 CM	5-9 CM	9-15 CM	15-30 CM	30-45 CM	0-15 CM
A1	2.06	4.49	16.40	20.15	22.68	23.69	11.53
A2	3.18	4.59	12.36	19.70	23.73	23.90	16.42
A3	1.94	4.10	9.96	23.64	24.00	24.11	15.01
A4	2.35	5.87	13.04	20.44	24.04	23.18	13.74
C1	1.74	3.12	6.67	17.07	19.45	19.58	10.20
C2	2.44	4.57	14.04	22.84	23.80	22.55	12.15
C3	2.25	3.24	8.57	23.98	23.26	22.18	22.06
C4	2.45	4.77	20.35	23.64	22.11	13.87	17.45
E1	1.80	3.53	10.50	14.17	14.65	15.25	9.64
E2	1.75	3.56	10.52	20.56	21.88	21.08	11.46
E3	2.61	4.87	12.14	22.14	25.30	23.87	19.52
E4	2.00	3.56	8.94	23.81	23.78	23.02	20.04
MEAN	2.21	4.19	11.96	21.01	22.39	21.36	14.94
S.D.	0.42	0.81	3.72	3.02	2.85	3.45	4.15

SOIL MOISTURE
Field Experiment #: 5

Field #: 24

Date: 7/16/78

Time: 2:00 - 4:30 p.m.

LOCATION	0-2 CM	2-5 CM	5-9 CM	9-15 CM	15-30 CM	30-45 CM	0-15 CM
A1	2.93	4.62	7.18	11.27	11.75	14.48	9.22
A2	14.72	20.32	27.83	29.77	31.81	28.21	17.20
A3	10.70	26.63	31.51	33.69	29.95	31.19	19.96
A4	4.10	17.91	25.88	32.98	31.25	28.60	16.78
C1	3.07	4.65	8.25	11.69	21.00	18.50	21.48
C2	8.30	9.39	22.35	22.86	20.08	21.30	16.31
C3	12.31	26.97	30.81	33.80	30.44	29.74	17.78
C4	11.86	17.44	31.14	32.77	31.11	30.70	18.99
E1	4.41	6.13	7.25	10.42	20.61	24.32	24.43
E2	8.95	29.29	31.32	32.64	29.95	26.70	25.35
E3	19.90	22.79	29.52	28.44	22.47	23.60	23.12
E4	33.54	37.61	38.38	34.53	31.53	31.73	32.68
MEAN	11.25	18.65	23.87	26.24	26.0	26.75	20.11
S.D.	8.71	10.71	10.72	9.65	6.56	5.45	5.70

SOIL MOISTURE
Field Experiment #: 6

Field #: 18

Date: 7/17/78

Time: 2:45 - 4:05 p.m.

LOCATION	0-2 CM	2-5 CM	5-9 CM	9-15 CM	15-30 CM	30-45 CM	0-15 CM
A1	3.60	4.57	9.17	11.39	10.99	11.84	7.75
A2	3.25	5.20	9.86	13.62	12.98	13.62	9.51
A3	3.70	6.71	11.02	13.36	17.35	20.55	12.52
A4	3.92	5.78	10.05	14.84	16.35	18.12	11.52
C1	3.19	5.98	8.14	10.27	11.37	12.17	8.11
C2	3.67	5.33	10.61	13.46	14.97	18.52	10.88
C3	2.83	5.29	9.15	13.98	16.13	19.07	10.80
C4	2.94	6.53	10.37	13.83	16.86	18.55	10.78
E1	4.35	7.71	11.58	14.26	15.21	20.62	12.42
E2	2.86	5.18	9.52	13.60	13.82	14.41	10.24
E3	3.44	6.48	9.90	11.48	13.41	14.07	9.43
E4	2.89	4.64	7.88	12.03	17.32	16.27	8.87
MEAN	3.47	5.78	9.77	13.01	14.73	16.48	10.24
S.D.	0.52	0.93	1.09	1.38	2.21	3.16	1.55

SOIL MOISTURE
Field Experiment #: 7

Field #: 11

Date: 7/18/78

Time: 9:00 -9:40 a.m.

LOCATION	0-2 CM	2-5 CM	5-9 CM	9-15 CM	15-30 CM	30-45 CM	0-15 CM
A1	4.03	4.64	8.95	12.27	13.98	12.84	10.01
A2	3.79	5.28	10.15	15.62	17.32	17.00	14.85
A3	4.01	5.64	9.88	16.79	16.02	15.39	12.42
A4	3.83	4.42	9.96	18.98	18.84	18.05	14.69
C1	3.95	4.98	7.02	12.70	16.02	13.70	7.78
C2	3.70	4.71	7.82	13.66	17.76	16.66	10.01
C3	4.08	5.17	9.66	16.74	17.36	16.45	13.42
C4	3.83	4.79	11.99	19.19	17.46	15.07	16.37
E1	3.70	4.39	7.30	10.75	13.65	13.40	8.52
E2	4.08	5.93	11.85	19.27	21.36	20.66	12.32
E3	3.69	4.96	8.21	16.98	19.07	17.55	10.78
E4	4.09	4.44	7.91	14.33	16.16	16.13	10.97
MEAN	3.90	4.95	9.20	15.61	17.08	16.24	18.85
S.D.	0.16	0.49	1.64	2.87	2.14	2.38	2.64

SOIL MOISTURE
Field Experiment #: 8

Field #: 13

Date: 7/18/78

Time: 3:30 - 4:15 p.m.

LOCATION	0-2 CM	2-5 CM	5-9 CM	9-15 CM	15-30 CM	30-45 CM	0-15 CM
A1	1.74	2.66	8.84	18.71	20.22	21.53	5.08
A2	2.06	3.25	11.92	21.01	19.46	20.02	13.54
A3	2.09	4.17	13.41	23.00	21.78	22.80	21.39
A4	2.33	4.37	16.94	25.06	18.33	17.59	14.03
C1	1.89	3.93	15.02	19.63	21.00	20.29	12.38
C2	3.24	2.42	9.30	19.34	22.77	22.38	8.25
C3	1.97	4.27	15.77	22.49	23.48	20.47	22.19
C4	2.41	4.15	12.11	21.76	18.66	20.70	9.71
E1	2.49	3.07	5.78	21.02	98.09*	21.76	11.25
E2	2.05	3.93	18.97	21.49	22.30	116.79*	7.88
E3	2.51	4.38	9.49	21.32	23.71	24.09	15.00
E4	1.91	3.34	6.02	17.17	23.35	22.90	13.19
MEAN	2.22	3.66	11.96	21.00	21.37	21.32	12.82
S.D.	0.41	0.69	4.22	2.09	1.96	1.77	5.10

* not used to find the mean

SOIL MOISTURE
Field Experiment #: 9

Field #: 11

Date: 7/20/78

Time: 9:00 - 9:50 a.m.

LOCATION	0-2 CM	2-5 CM	5-9 CM	9-15 CM	15-30 CM	30-45 CM	0-15 CM
A1	25.98	25.13	22.97	10.90	12.62	13.98	22.33
A2	29.08	27.91	25.29	15.10	17.33	16.02	19.89
A3	30.67	28.45	26.22	20.99	19.55	18.18	21.58
A4	29.73	27.61	25.73	21.48	20.09	19.87	23.57
C1	27.73	26.27	23.65	9.42	12.86	14.27	19.75
C2	28.45	27.11	26.18	16.42	19.14	18.13	19.96
C3	29.68	27.84	22.77	18.38	20.94	19.32	21.75
C4	28.25	27.75	25.59	17.30	20.48	18.98	24.59
E1	25.12	25.22	21.22	12.07	17.77	16.94	19.11
E2	27.87	27.71	25.23	12.42	17.82	17.49	19.05
E3	27.94	27.72	20.89	13.84	17.61	16.23	20.38
E4	27.27	26.72	22.17	18.36	15.14	16.53	22.87
MEAN	28.09	27.12	23.99	15.64	17.61	17.16	21.24
S.D.	1.52	1.08	1.95	3.92	2.79	1.87	1.83

SOIL MOISTURE
Field Experiment #: 1J

Field #: 13

Date: 7/20/78

Time: 1:30 - 2:30 p.m.

LOCATION	0-2 CM	2-5 CM	5-9 CM	9-15 CM	15-30 CM	30-45 CM	0-15 CM
A1	22.86	22.09	21.10	19.73	21.43	21.89	21.8
A2	30.38	27.00	24.84	22.06	22.96	22.31	20.65
A3	24.43	24.26	21.91	19.09	23.23	24.27	22.67
A4	24.39	25.44	22.85	18.6	22.99	24.64	22.65
C1	23.96	24.35	19.46	20.84	22.10	20.73	21.94
C2	25.18	24.50	21.04	21.62	23.50	22.85	22.01
C3	27.17	25.57	25.84	22.94	25.06	25.32	22.59
C4	24.59	23.49	17.04	17.02	24.76	24.19	23.53
E1	19.35	23.51	18.1	8.82*	19.77	21.76	19.69
E2	23.25	23.23	21.61	22.38	23.32	24.41	21.46
E3	25.09	23.99	22.53	25.41	24.99	25.29	24.66
E4	22.52	22.41	19.21	18.08	25.04	24.97	22.83
MEAN	24.43	24.16	21.29	20.71	23.26	23.55	22.29
S.D.	2.65	1.38	2.59	2.47	1.62	1.57	1.27

* not used to find the mean

SOIL MOISTURE
Field Experiment #: 11

Field #: 11

Date: 7/22/78

Time: 2:20 - 3:40 p.m.

LOCATION	0-2 CM	2-5 CM	5-9 CM	9-15 CM	15-30 CM	30-45 CM	0-15 CM
A1	24.22	23.70	25.20	23.38	14.36	15.72	25.03
A2	24.58	25.66	26.54	24.25	16.50	17.42	27.09
A3	25.97	27.17	26.11	22.15	19.04	19.94	22.54
A4	18.64	21.55	23.23	16.01	14.25	13.91	18.67
C1	19.73	22.96	24.27	19.35	14.96	13.95	24.77
C2	22.26	24.59	25.26	21.93	15.78	17.32	23.61
C3	21.01	23.27	24.40	15.53	15.52	16.38	21.40
C4	21.82	23.67	25.35	25.86	16.47	17.52	27.14
E1	17.69	21.51	20.09	9.77	11.32	13.68	21.00
E2	16.87	21.95	23.68	18.75	13.10	13.29	21.97
E3	21.24	24.15	24.63	22.40	14.89	14.99	19.79
E4	23.86	26.00	26.27	22.64	18.04	19.79	27.90
MEAN	21.49	23.85	24.59	20.17	15.35	16.16	23.41
S.D.	2.87	1.79	1.74	4.54	2.08	2.30	3.02

SOIL MOISTURE
Field Experiment #: 12

Field #: 13

Date: 7/22/78

Time: 6:15 - 7:10 p.m.

LOCATION	0-2 CM	2-5 CM	5-9 CM	9-15 CM	15-30 CM	30-45 CM	0-15 CM
A1	18.48	25.93	23.33	23.04	24.36	25.35	23.15
A2	19.39	22.81	23.31	23.26	23.99	23.36	23.52
A3	23.80	23.37	24.43	20.67	23.63	22.54	23.83
A4	20.27	23.22	23.26	19.99	23.88	23.45	22.07
C1	18.23	22.58	20.78	20.51	22.52	22.90	19.44
C2	17.76	22.84	22.85	22.01	24.18	22.60	25.02
C3	21.59	23.39	24.28	27.21	25.33	22.89	24.54
C4	19.68	23.00	23.22	23.47	22.77	22.04	24.18
E1	19.13	27.37	26.45	23.90	24.13	22.86	21.92
E2	18.27	22.01	21.47	20.95	23.23	22.16	23.58
E3	22.82	23.43	24.45	26.44	23.53	22.16	20.73
E4	22.75	22.96	23.76	21.72	23.00	22.57	23.49
MEAN	20.18	23.58	23.47	22.76	23.71	22.91	22.96
S.D.	2.06	1.52	1.45	2.29	0.78	0.89	1.63

APPENDIX B
Bulk Density/Soil Moisture Listings

BULK DENSITY/SOIL MOISTURE
Field Experiment #: 1

Field #: 11

Date: 7/12/78

Time: 6:10 - 9:45 p.m.

LOCATION	0-3 CM		4-11* CM		11-18* CM		18-23* CM	
	DEN.	MOIST.	DEN.	MOIST.	DEN.	MOIST.	DEN.	MOIST.
B1	1.071	3.17	0.950	7.10	0.937	13.38	1.167	15.46
B4	0.916	3.05	0.945	8.24	1.215	17.23	1.185	20.41
D1	0.991	2.97	0.955	6.85	1.061	12.38	1.230	16.29
D4	0.989	3.38	1.006	7.93	1.143	17.63	1.120	18.36
MEAN	0.992	3.14	0.964	7.53	1.089	15.16	1.176	17.63
S.D.	0.063	0.18	0.028	0.66	0.119	2.66	0.046	2.22

* -On this first field different depths were used.

BULK DENSITY/SOIL MOISTURE
Field Experiment #: 2

Field #: 30

Date: 7/13/78

Time: 6:05 - 7:00 p.m.

LOCATION	0-3 CM		4-11* CM		11-18* CM		18-23* CM	
	DEN.	MOIST.	DEN.	MOIST.	DEN.	MOIST.	DEN.	MOIST.
B1	0.942	4.82	0.982	7.07	0.919	10.16	1.388	11.45
B4	1.035	6.32	1.075	12.09	1.030	14.46	1.292	13.03
D1	1.003	3.88	0.946	7.86	0.902	8.91	1.227	9.41
D4	0.902	7.59	0.944	13.81	1.119	12.55	1.038	11.45
MEAN	0.971	5.65	0.987	10.21	0.993	11.52	1.236	11.34
S.D.	0.060	1.64	0.061	3.26	0.102	2.47	0.148	1.48

BULK DENSITY/SOIL MOISTURE

Field Experiment #: 3

Field #: 13

Date: 7/15/78

Time: 1:35 - 1:55 p.m.

LOCATION	0-3 CM		4-11* CM		11-18* CM		18-23* CM	
	DEN.	MOIST.	DEN.	MOIST.	DEN.	MOIST.	DEN.	MOIST.
B1	1.311	21.92	0.830	3.96	0.979	21.96	1.386	21.33
B4								
D1	0.945	5.45	0.956	16.05	1.065	26.39	1.009	29.41
D4								
MEAN	1.128	13.69	0.893	10.01	1.022	24.18	1.198	25.37
S.D.	0.259	11.65	0.089	8.55	0.061	3.13	0.267	5.71

BULK DENSITY/SOIL MOISTURE**Field Experiment #: 4**

Field #: 13

Date: 7/15/78

Time: 6:30 - 6:55 p.m.

LOCATION	0-3 CM		4-11* CM		11-18* CM		18-23* CM	
	DEN.	MOIST.	DEN.	MOIST.	DEN.	MOIST.	DEN.	MOIST.
B1	1.021	2.88	1.000	6.14	0.848	23.16	0.861	21.42
B4	1.085	1.88	0.936	8.80	1.159	22.82	1.156	23.17
D1	0.979	1.78	0.905	8.11	1.026	10.37	0.944	13.13
D4	0.988	1.81	0.858	9.49	1.047	18.62	1.071	25.34
MEAN	1.018	2.09	0.925	8.14	1.020	18.74	1.008	20.77
S.D.	0.048	0.53	0.060	1.44	0.129	5.95	0.131	5.34

BULK DENSITY/SOIL MOISTURE
Field Experiment #: 5

Field #: 24

Date: 7/16/78

Time: 2:00 - 3:00 p.m.

LOCATION	0-3 CM		4-11* CM		11-18* CM		18-23* CM	
	DEN.	MOIST.	DEN.	MOIST.	DEN.	MOIST.	DEN.	MOIST.
B1	1.012	6.25	1.213	22.04	1.101	24.37	1.061	24.18
B4	0.874	19.92	0.769	27.23	0.998	32.30	1.298	32.54
D1	1.081	8.51	1.034	23.44	1.075	26.66	1.269	24.59
D4	0.659	33.86	0.683	33.29	0.855	35.31	0.868	32.02
MEAN	0.907	17.14	0.925	26.50	1.007	29.66	1.124	28.33
S.D.	0.186	12.65	0.243	5.03	0.111	5.03	0.201	4.57

BULK DENSITY/SOIL MOISTURE
Field Experiment #: 6

Field #: 18'

Date: 7/17/78

Time: 4:45 - 5:05 p.m.

LOCATION	0-3 CM		4-11* CM		11-18* CM		18-23* CM	
	DEN.	MOIST.	DEN.	MOIST.	DEN.	MOIST.	DEN.	MOIST.
B2*	0.831	2.94	1.187	10.61	1.094	14.13	1.216	13.32
B4	0.917	3.99	1.104	10.87	1.186	14.31	1.191	15.32
D2*	0.893	3.24	1.079	8.13	1.076	13.33	1.191	14.69
D4	0.694	5.68	1.077	13.27	1.233	15.29	1.154	15.81
MEAN	0.834	3.96	1.132	10.72	1.147	14.27	1.188	14.79
S.D.	0.100	1.23	0.063	2.10	0.075	0.81	0.026	1.08

* Samples were mistakenly taken at a different location.

BULK DENSITY/SOIL MOISTURE
Field Experiment #: 7

Field #: 11

Date: 7/18/78

Time:

Bulk density assumed not to have changed since previous measurement.

LOCATION	0-3 CM	4-11* CM	11-18* CM	18-23* CM
	DEN. MOIST.	DEN. MOIST.	DEN. MOIST.	DEN. MOIST.

BULK DENSITY/SOIL MOISTURE

Field Experiment #: 8

Field #: 13

Date: 7/18/78

Time: 4:40 - 4:55 p.m.

LOCATION	0-3 CM		4-11* CM		11-18* CM		18-23* CM	
	DEN.	MOIST.	DEN.	MOIST.	DEN.	MOIST.	DEN.	MOIST.
B1	0.980	2.29	0.859	6.80	0.836	18.95	1.018	21.26
B4	0.879	1.98	1.007	7.59	1.186	21.62	1.050	22.70
D1	0.929	3.27	0.938	7.72	0.926	20.13	0.945	24.38
D4	1.039	2.37	1.003	8.81	1.116	15.36	1.138	23.23
MEAN	0.957	2.48	0.952	7.73	1.016	19.02	1.038	24.14
S.D.	0.069	0.55	0.069	0.83	0.163	2.67	0.080	2.70

BULK DENSITY/SOIL MOISTURE

Field Experiment #: 9

Field #: 11

Date: 7/20/78

Time: 9:15 - 11:05 a.m.

LOCATION	0-3 CM		4-11* CM		11-18* CM		18-23* CM	
	DEN.	MOIST.	DEN.	MOIST.	DEN.	MOIST.	DEN.	MOIST.
B1	1.053	25.25	1.141	24.22	0.940	8.55	1.336	11.11
B4	0.993	27.13	0.891	25.07	1.032	14.53	1.144	19.00
D1	1.124	25.39	1.161	21.48	1.017	10.17	1.221	12.24
D4	1.145	26.93	1.160	24.09	1.017	11.51	1.171	15.96
MEAN	1.079	26.18	1.088	24.19	1.017	11.99	1.218	14.58
S.D.	0.069	0.99	0.132	1.19	0.069	2.53	0.085	3.60

* Bulk density taken again due to rain on the night of 7/19/78.

BULK DENSITY/SOIL MOISTURE

Field Experiment #: 9

Field #: 11

Date: 7/20/78

Time: 9:15 - 11:05 a.m.

LOCATION	0-3 CM		4-11* CM		11-18* CM		18-23* CM	
	DEN.	MOIST.	DEN.	MOIST.	DEN.	MOIST.	DEN.	MOIST.
B1	1.053	25.25	1.141	24.22	0.940	8.55	1.336	11.11
B4	0.993	27.13	0.891	25.07	1.032	14.53	1.144	19.00
D1	1.124	25.39	1.161	21.48	1.017	10.17	1.221	12.24
D4	1.145	26.93	1.160	24.09	1.017	11.51	1.171	15.96
MEAN	1.079	26.18	1.088	24.19	1.017	11.51	1.218	14.58
S.D.	0.069	0.99	0.132	2.53	0.069	2.53	0.085	3.60

* Bulk density taken again due to rain on the night of 7/19/78.

BULK DENSITY/SOIL MOISTURE
Field Experiment #: 10

Field #: 13*

Date: 7/20/78

Time: 2:25 - 3:35 p.m.

LOCATION	0-3 CM		4-11* CM		11-18* CM		18-23* CM	
	DEN.	MOIST.	DEN.	MOIST.	DEN.	MOIST.	DEN.	MOIST.
B1	1.108	20.26	1.140	21.15	0.944	13.68	1.183	20.79
B4	1.043	20.47	1.048	22.33	1.233	21.82	1.153	22.68
D1	0.965	18.95	0.979	21.79	1.061	22.06	0.964	22.41
D4	0.892	24.22	1.066	25.55	1.108	21.43	1.090	23.76
MEAN	1.002	20.98	1.058	22.70	1.087	19.75	1.098	22.41
S.D.	0.094	2.27	0.066	1.96	0.120	4.05	0.097	1.23

* Bulk density taken again due to rain on the night of 7/19/78.

BULK DENSITY/SOIL MOISTURE

Field Experiment #: 11

Field #: 11

Date: 7/22/78

Time: 4:15 - 4:50 p.m.

LOCATION	0-3 CM		4-11* CM		11-18* CM		18-23* CM	
	DEN.	MOIST.	DEN.	MOIST.	DEN.	MOIST.	DEN.	MOIST.
B1	1.116	20.78	0.988	23.42	1.238	14.54	1.362	13.32
B4	1.124	28.33	1.185	27.73	1.077	21.67	1.425	16.45
D1	1.079	22.28	0.905	24.20	0.967	21.30	1.145	12.92
D4	1.072	28.46	1.098	27.14	1.193	24.43	1.587	18.97
MEAN	1.098	24.96	1.044	25.62	1.119	20.49	1.380	15.42
S.D.	0.026	4.01	0.123	2.13	0.122	4.20	0.183	2.85

BULK DENSITY/SOIL MOISTURE
Field Experiment #: 12

Field #: 13

Date: 7/22/78

Time: 7:00 - 7:35 p.m.

LOCATION	0-3 CM		4-11* CM		11-18* CM		18-23* CM	
	DEN.	MOIST.	DEN.	MOIST.	DEN.	MOIST.	DEN.	MOIST.
B1	0.765	16.47	0.837	22.75	0.786	21.96	0.886	21.38
B4	0.877	20.34	0.948	23.57	1.116	24.05	0.989	23.66
D1	0.814	17.13	0.686	23.09	0.846	22.74	1.066	23.49
D4	0.656	24.15	0.847	23.20	0.899	23.74	1.043	23.49
MEAN	0.778	19.52	0.830	23.15	0.912	23.12	0.996	23.00
S.D.	0.093	3.52	0.108	0.34	0.143	0.96	0.080	1.09

APPENDIX C
Soil Temperature and Weather

SOIL TEMPERATURE AND WEATHER

Field Experiment #: 6

Field #: 18

Date: 7/17/78

Time: 4:12 - 4:20 p.m.

LOCATION	SOIL TEMP.	WEATHER COMMENTS
A1	61.5	Very hot.
A2	47.0	
A3	52.5	
A4	54.5	
C1	56.0	
C2	56.0	
C3	55.5	
C4	52.0	
E1	60.5	
E2	56.0	
E3	40.5	
E4	56.0	
MEAN	54.0	
S.D.	5.7	

SOIL TEMPERATURE AND WEATHER

Field Experiment #: 7

Field #: 11

Date: 7/18/78

Time: 9:55 a.m.

LOCATION	SOIL TEMP.	WEATHER COMMENTS
A1	34.5	Cloudy.
A2	31.0	
A3	35.5	
A4	36.0	
C1	42.5	
C2	44.0	
C3	37.5	
C4	39.0	
E1	31.5	
E2	34.5	
E3	35.0	
E4	33.5	
MEAN	36.2	
S.D.	4.0	

SOIL TEMPERATURE AND WEATHER
Field Experiment #: 7

Field #: 11

Date: 7/18/78

Time: 11:30 - 11:45 a.m. (Retake)

LOCATION	SOIL TEMP.	WEATHER COMMENTS
A1	34.5	Sunny.
A2	37.2	
A3	35.6	
A4	32.8	
C1	34.2	
C2	34.8	
C3	39.4	
C4	39.8	
E1	38.1	
E2	38.4	
E3	39.8	
F4	35.8	
MEAN	36.7	
S.D..	2.4	

SOIL TEMPERATURE AND WEATHER
Field Experiment #: 8

Field #: 13

Date: 7/18/78

Time: 4:30 p.m.

LOCATION	SOIL TEMP.	WEATHER COMMENTS
A1	51.0	Sunny.
A2	50.5	
A3	50.0	
A4	49.0	
C1	52.0	
C2	50.5	
C3	50.0	
C4	48.5	
E1	52.0	
E2	49.0	
E3	50.5	
E4	51.5	
MEAN	50.4	
S.D.	1.2	

SOIL TEMPERATURE AND WEATHER

Field Experiment #: 8

Field #: 13

Date: 7/18/78

Time: 7:20 ~ 7:50 p.m. (Retake)

LOCATION	SOIL TEMP.	WEATHER COMMENTS
A1	66.0	
A2	64.5	
A3	65.5	
A4	66.0	
C1	67.0	
C2	62.5	
C3	65.5	
C4	66.5	
E1	67.0	
C2	65.0	
E3	67.5	
E4	65.5	
MEAN	65.7	
S.D.	1.3	

SOIL TEMPERATURE AND WEATHER

Field Experiment #: 9

Field #: 11

Date: 7/20/78

Time: 10:10 - 10:17 a.m.

LOCATION	SOIL TEMP.	WEATHER COMMENTS
A1	25.5	Very Cloudy (90%). Cool. Rained the previous night (the night of 7/19/78), receiving approximately .75 inches.
A2	26.2	
A3	25.6	
A4	26.2	
C1	25.5	
C2	25.8	
C3	26.0	
C4	25.8	
E1	25.5	
E2	25.7	
E3	26.2	
E4	26.5	
MEAN	25.9	
S.D.	0.3	

SOIL TEMPERATURE AND WEATHER

Field Experiment #: 9

Field #: 11

Date: 7/20/78

Time: 12:05 - 12:11 p.m. (Retake)

LOCATION	SOIL TEMP.	WEATHER COMMENTS
A1	34.2	50% clouds. Warming.
A2	37.0	
A3	36.4	
A4	32.8	
C1	32.5	
C2	32.6	
C3	30.4	
C4	34.2	
E1	30.8	
E2	32.2	
E3	31.1	
E4	31.4	
MEAN	33.0	
S.D.	2.1	

SOIL TEMPERATURE AND WEATHER

Field Experiment #: 10

Field #: 13

Date: 7/20/78

Time: 3:29 - 3:35 p.m.

LOCATION	SOIL TEMP.	WEATHER COMMENTS
A1	36.5	30% cumulus clouds.
A2	33.0	
A3	32.0	
A4	32.0	
C1	34.0	
C2	34.25	
C3	35.0	
C4	33.5	
E1	33.5	
E2	32.0	
E3	35.25	
E4	32.0	
MEAN	33.6	
S.D.	1.5	

C-3

SOIL TEMPERATURE AND WEATHER

Field Experiment #: 11

Field #: 11

Date: 7/22/78

Time:

Neglected to take Soil Temperature.

LOCATION	SOIL TEMP.	WEATHER COMMENTS
----------	------------	------------------

SOIL TEMPERATURE AND WEATHER

Field Experiment #: 12

Field #: 13

Date: 7/22/78

Time: 8:00 - 8:05 a.m.

LOCATION	SOIL TEMP.	WEATHER COMMENTS
A1	18.25	40% cumulus clouds. Air temperature - 72° F. Winds 12 - 18 knots from N.E.
A2	17.75	
A3	17.25	
A4	18.00	
C1	17.75	
C2	17.50	
C3	18.50	
C4	18.00	
E1	17.75	
E2	18.25	
E3	17.50	
E4	17.25	
MEAN	17.8	
S.D.	0.4	

APPENDIX D
Vegetation Parameters

VEGETATION
Field Experiment #: 1

Field #: 11

Date: 7/12/78

Time: 6:20 - 7:00 p.m.

LOCATION	HEIGHT	PLANT SPACING	ROW SPACING	SAMPLE TYPE	% MOIST
B1	30 cm	15 cm	30 cm	wheat stubble	13.69
D4	30 cm	15 cm	30 cm	wheat stubble	

VEGETATION
Field Experiment #: 2

Field #: 30

Date: 7/13/78

Time: 5:15 - 5:50 p.m.

LOCATION	HEIGHT	PLANT SPACING	ROW SPACING	SAMPLE TYPE	% MOIST
B1	30 cm	solid	20 cm	wheat	8.24
B1	5 cm*	solid		corn stalk	6.69
C4		solid	20 cm		6.73
E3	30 cm	solid	20 cm		

* A layer of crushed corn stalks along with some fallen wheat stubble. Other wheat stubble is still standing.

VEGETATION
Field Experiment #: 5

Field #: 24

Date: 7/16/78

Time: 4:00 - 5:30 p.m.

LOCATION	HEIGHT	PLANT SPACING	ROW SPACING	SAMPLE TYPE	% MOIST
D1	120 cm	15 cm	79 cm	corn	87.02
D4	120 cm	15 cm	79 cm	corn	85.58

VEGETATION
Field Experiment #: 6

Field #: 18

Date: 7/17/78

Time: 5:50 p.m.

LOCATION	HEIGHT	PLANT SPACING	ROW SPACING	SAMPLE TYPE	% MOIST
B1	7 cm			Alfalfa stubble	46.81
C4	15 cm			Alfalfa plants	75.94

VEGETATION
Field Experiment #: 7

Field #: 11

Date: 7/18/78

Time: 10:05 - 10:10 a.m.

LOCATION	HEIGHT	PLANT SPACING	ROW SPACING	SAMPLE TYPE	% MOIST
B1	20 cm	15 - 20 cm	30 cm	wheat stubble	9.84
D4	25 cm	10 - 15 cm	30 cm	wheat stubble	8.79

VEGETATION
Field Experiment #: 9

Field #: 11

Date: 7/20/78

Time: 10:20 - 10:30 a.m.

LOCATION	HEIGHT	PLANT SPACING	ROW SPACING	SAMPLE TYPE	% MOIST
B1	20 cm	15 - 20 cm	30 cm	wheat stubble	29.79*
D4	25 cm	10 - 15 cm	30 cm	wheat stubble	26.75*

* Higher moisture due to rain on the night of 7/19/78.

VEGETATION
Field Experiment #: 11

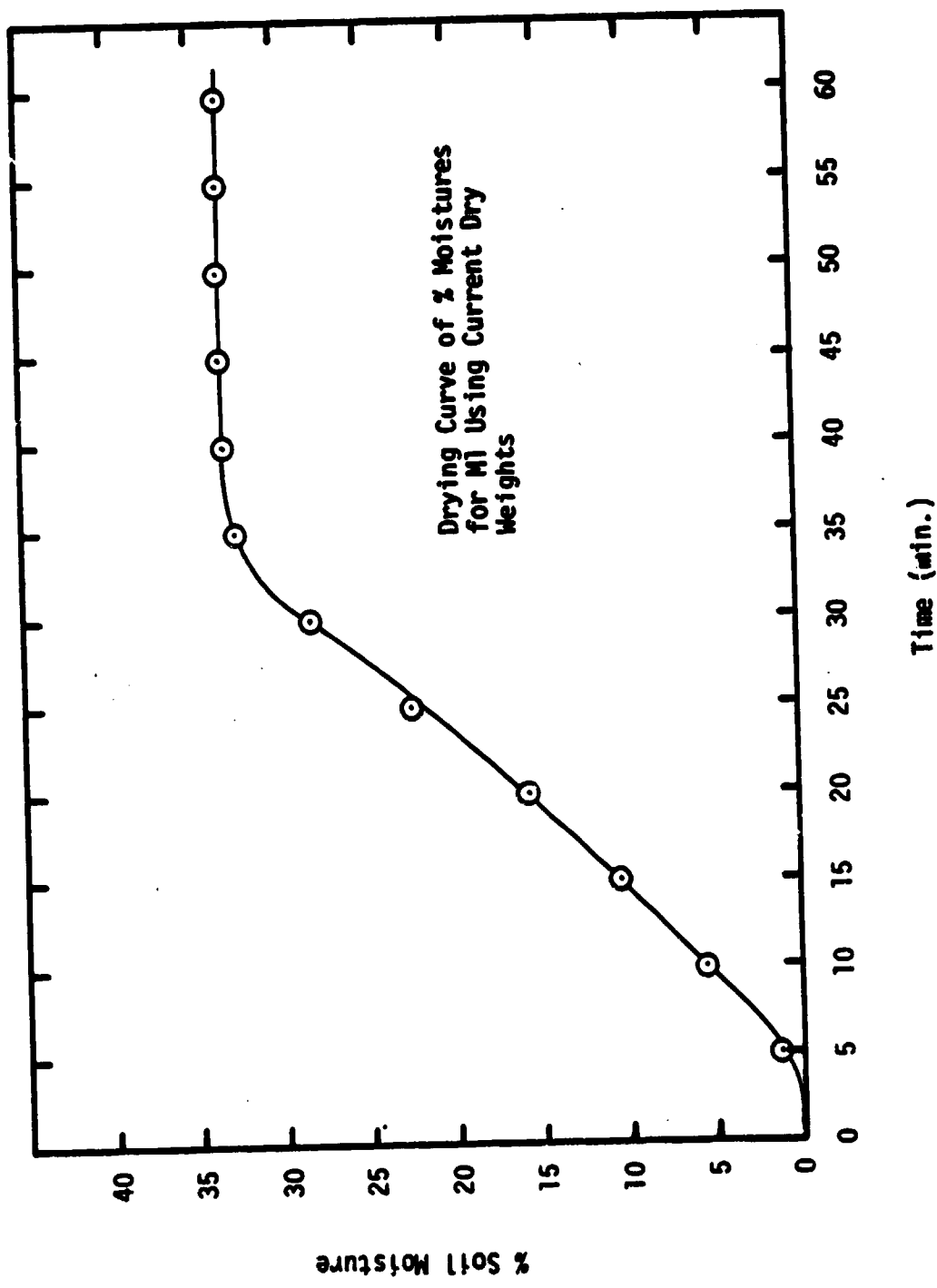
Field #: 11

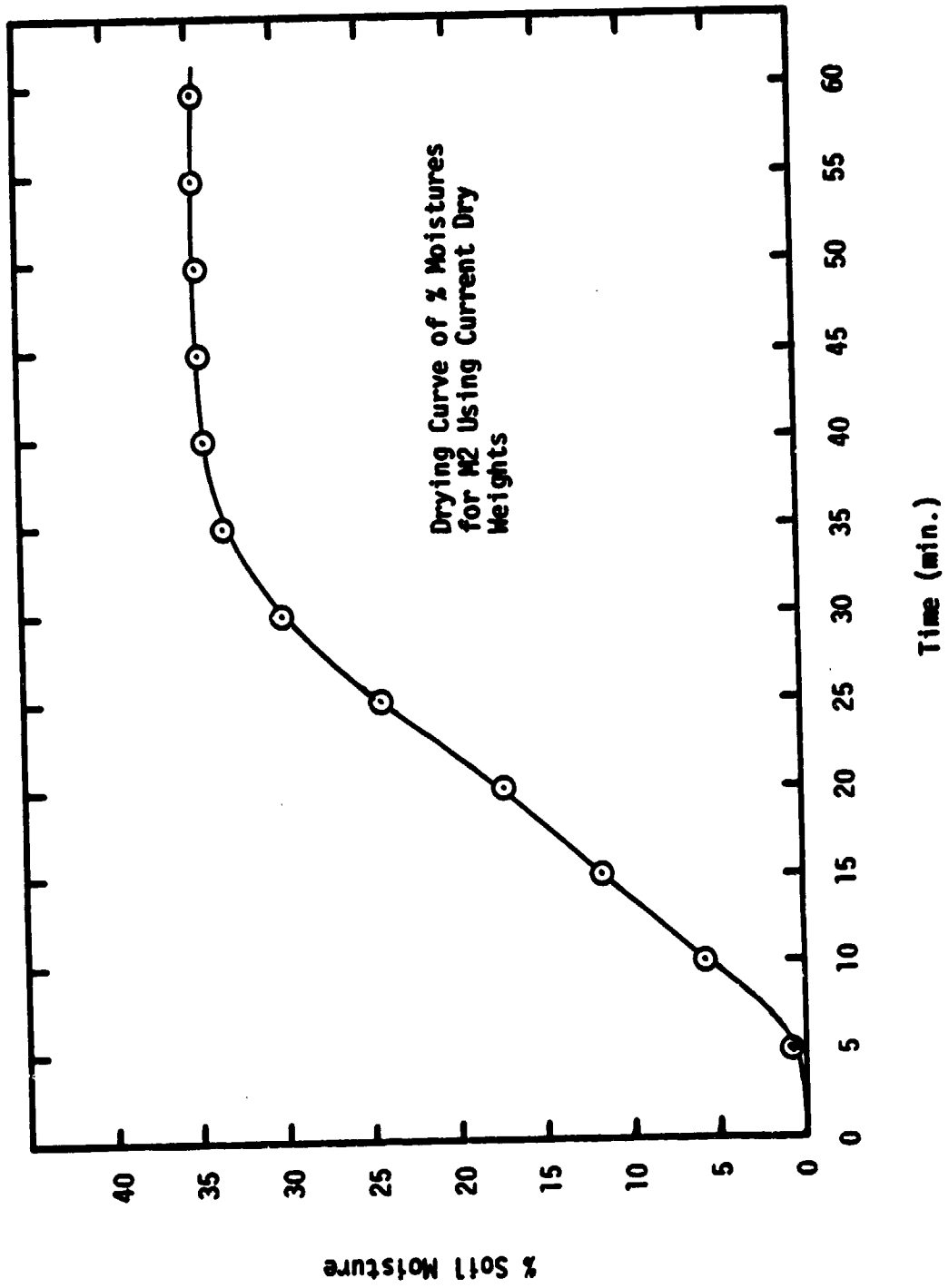
Date: 7/22/78

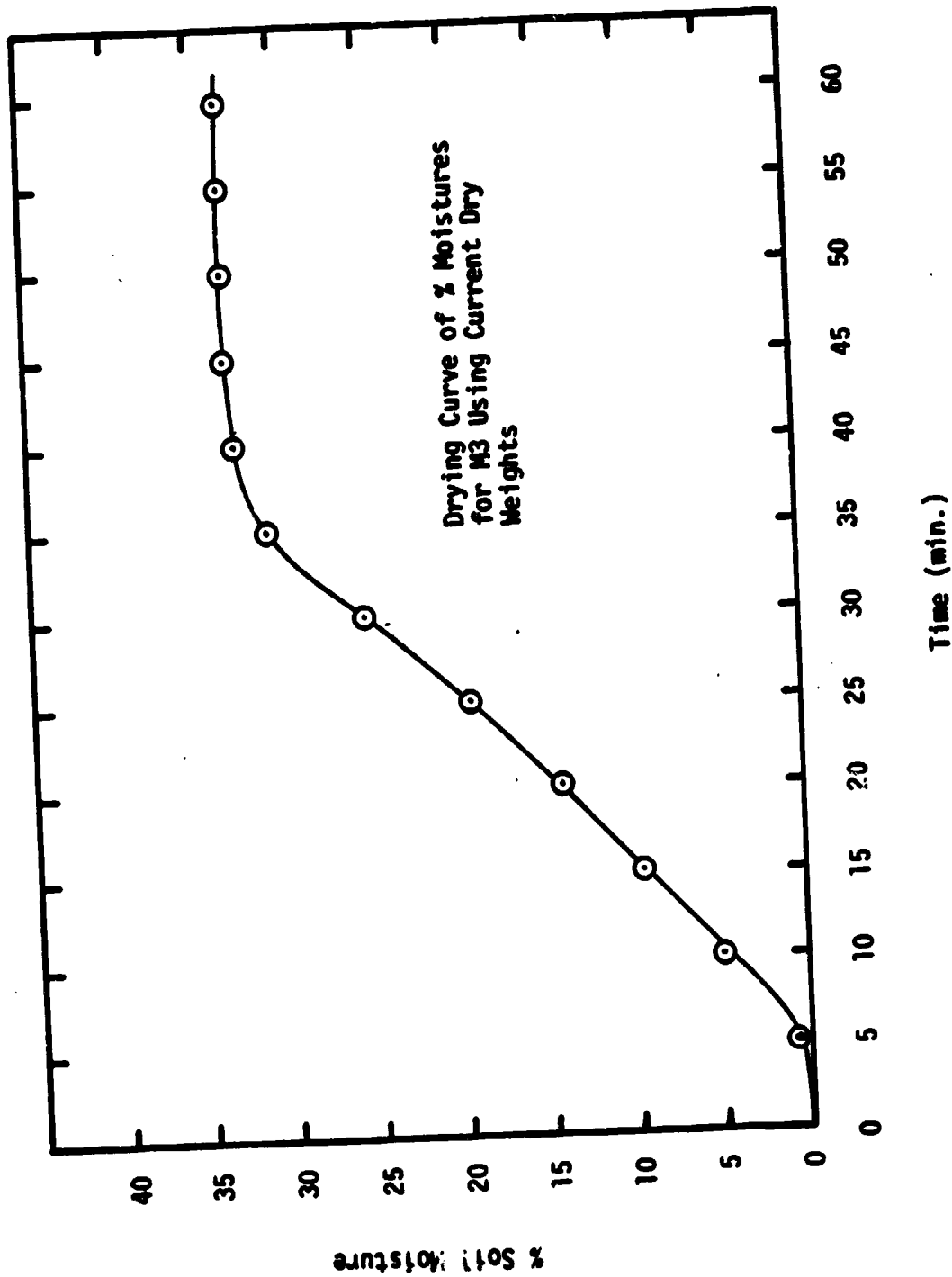
Time: 3:45 - 4:45 p.m.

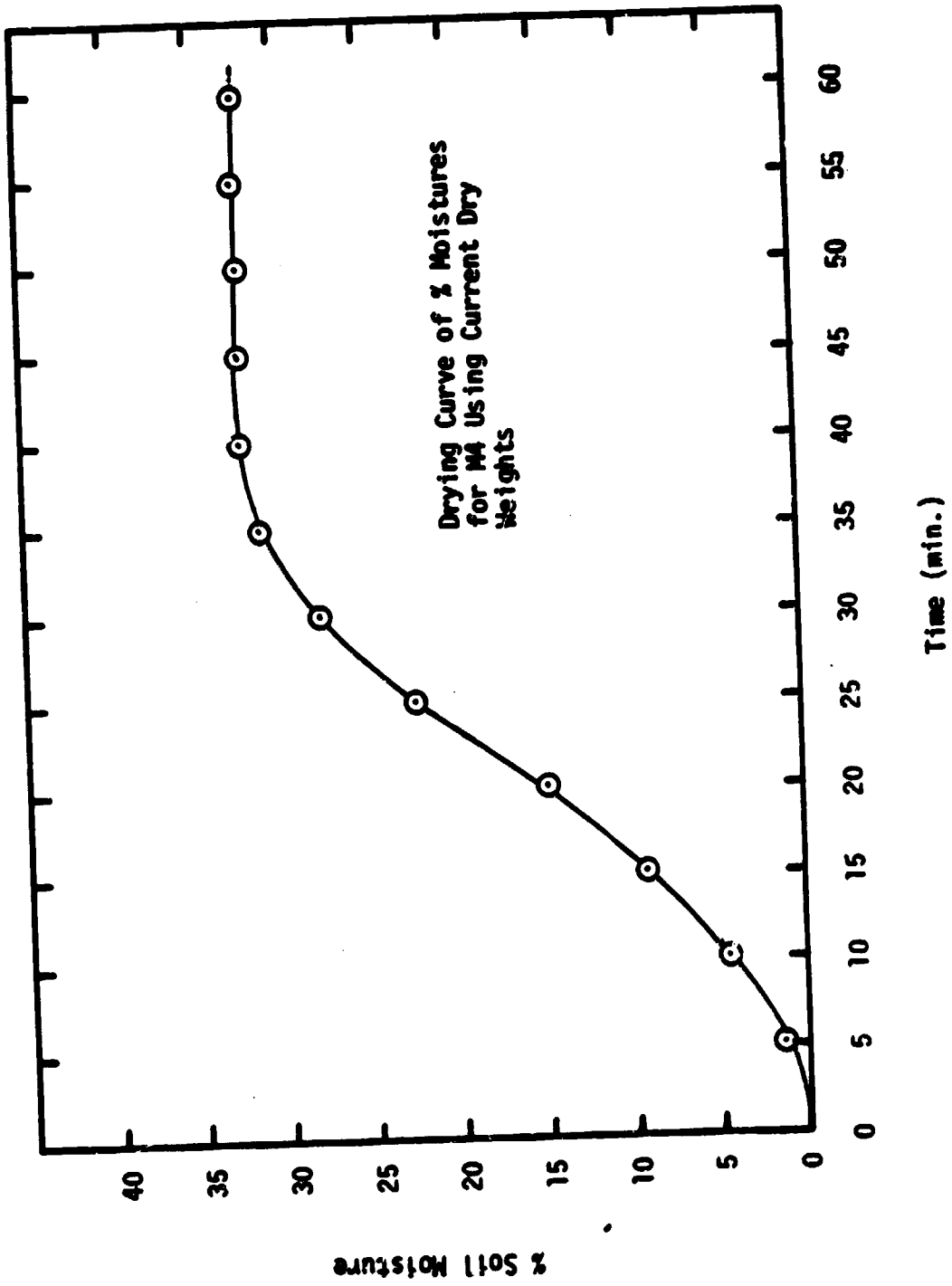
LOCATION	HEIGHT	PLANT SPACING	ROW SPACING	SAMPLE TYPE	% MOIST
B1	28 cm	15 cm	30 cm	wheat stubble	14.68
B4	32 cm	15 cm	30 cm	wheat stubble	10.22

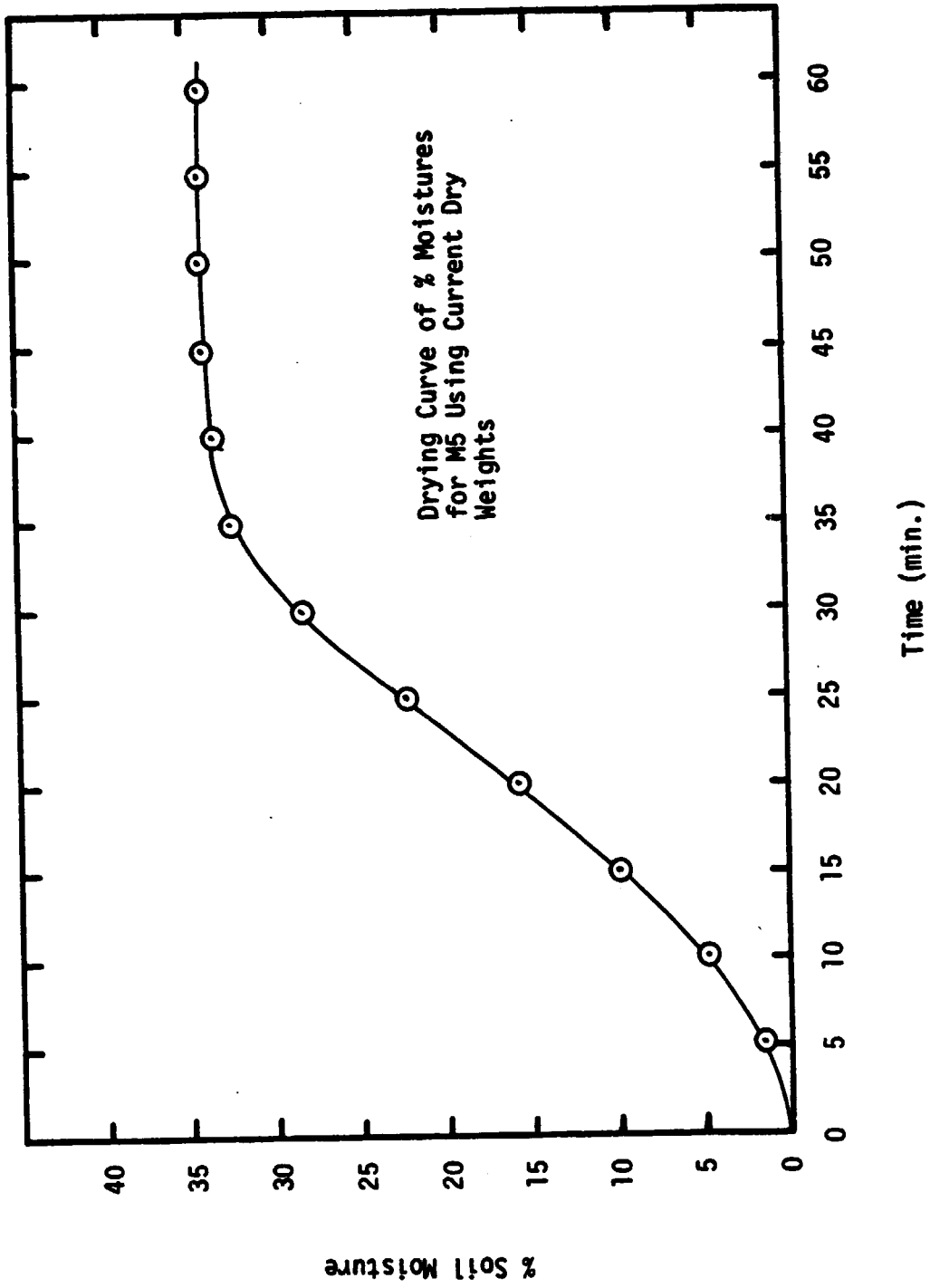
APPENDIX E
Drying Curves

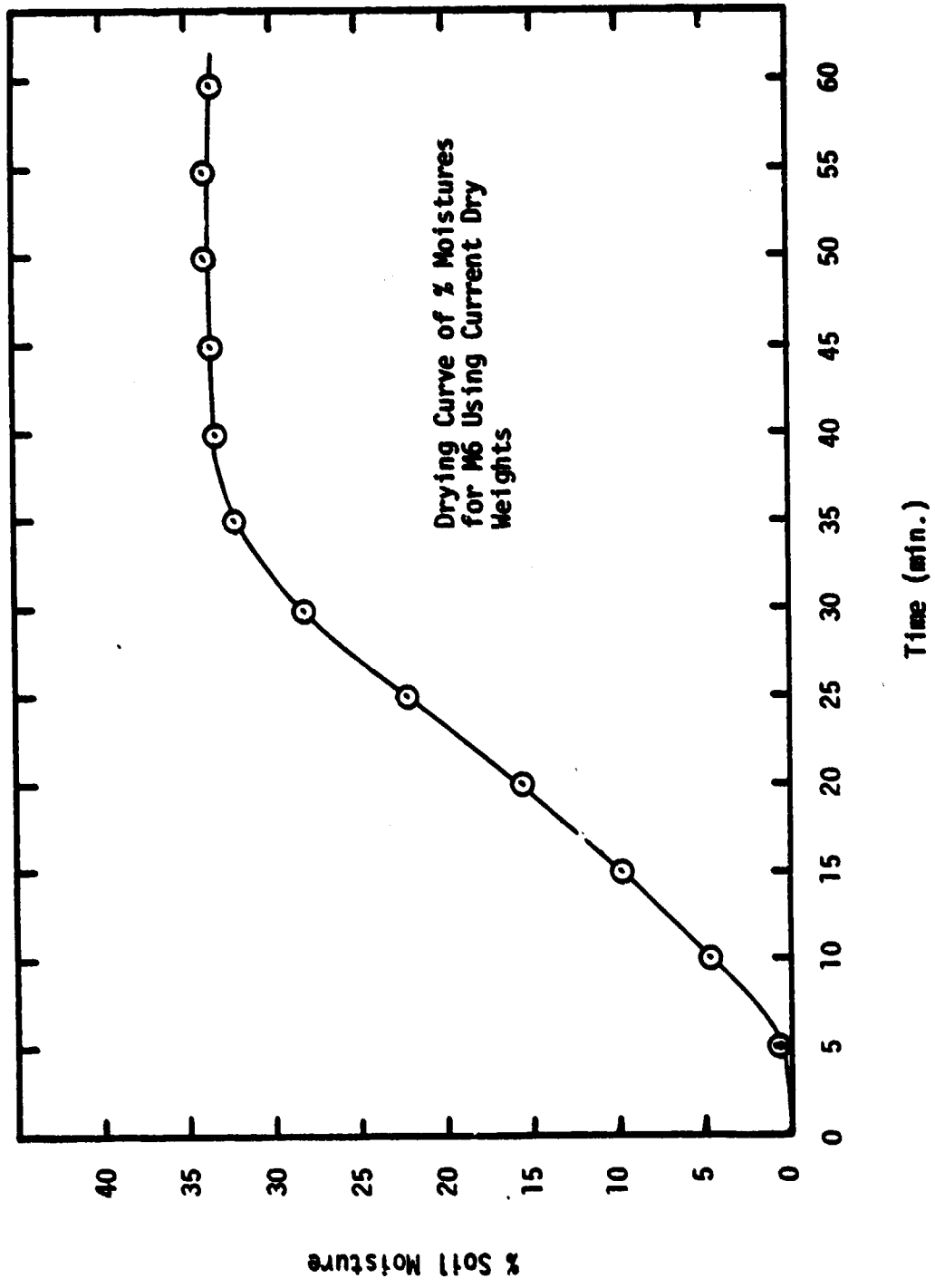


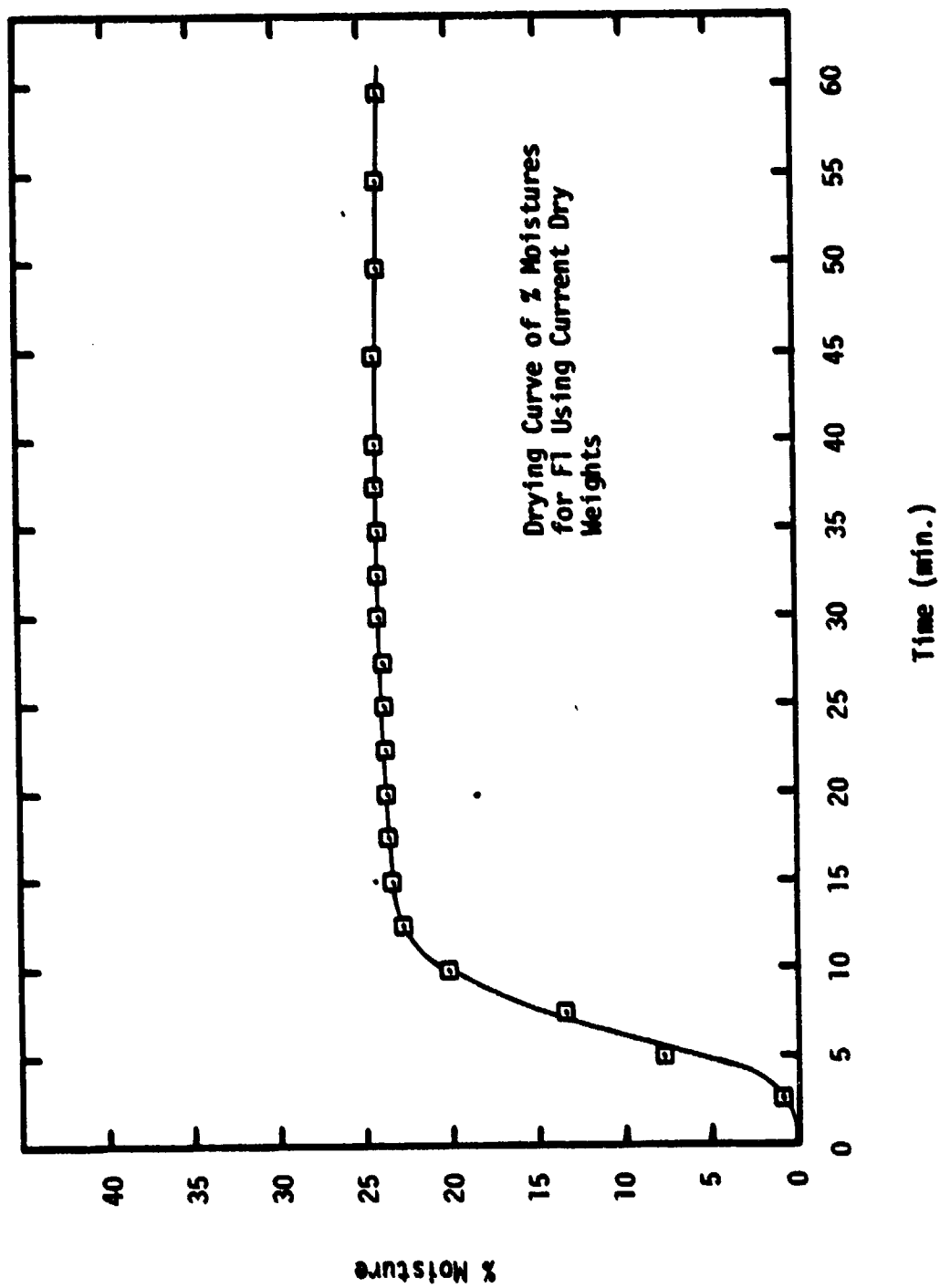


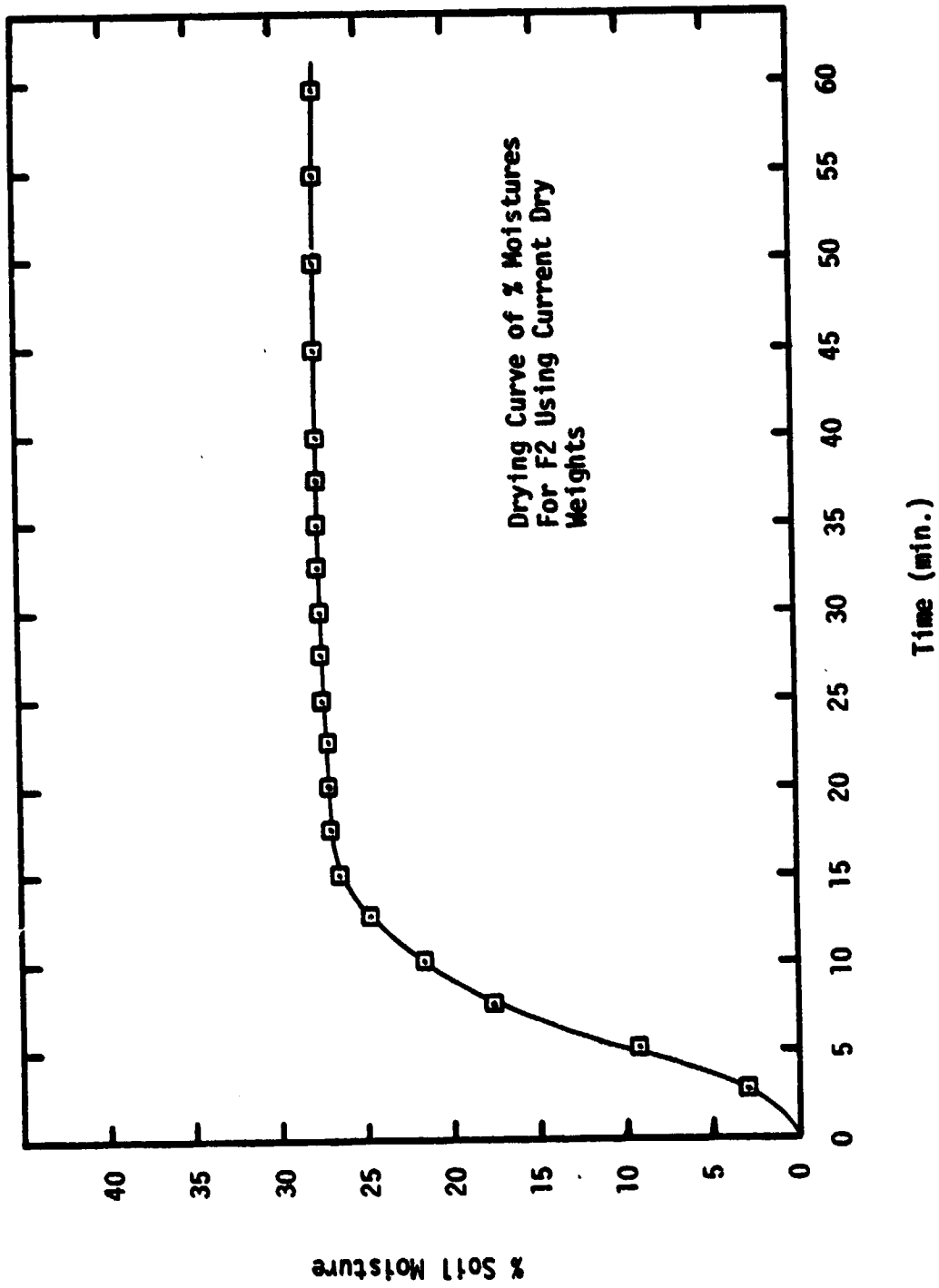


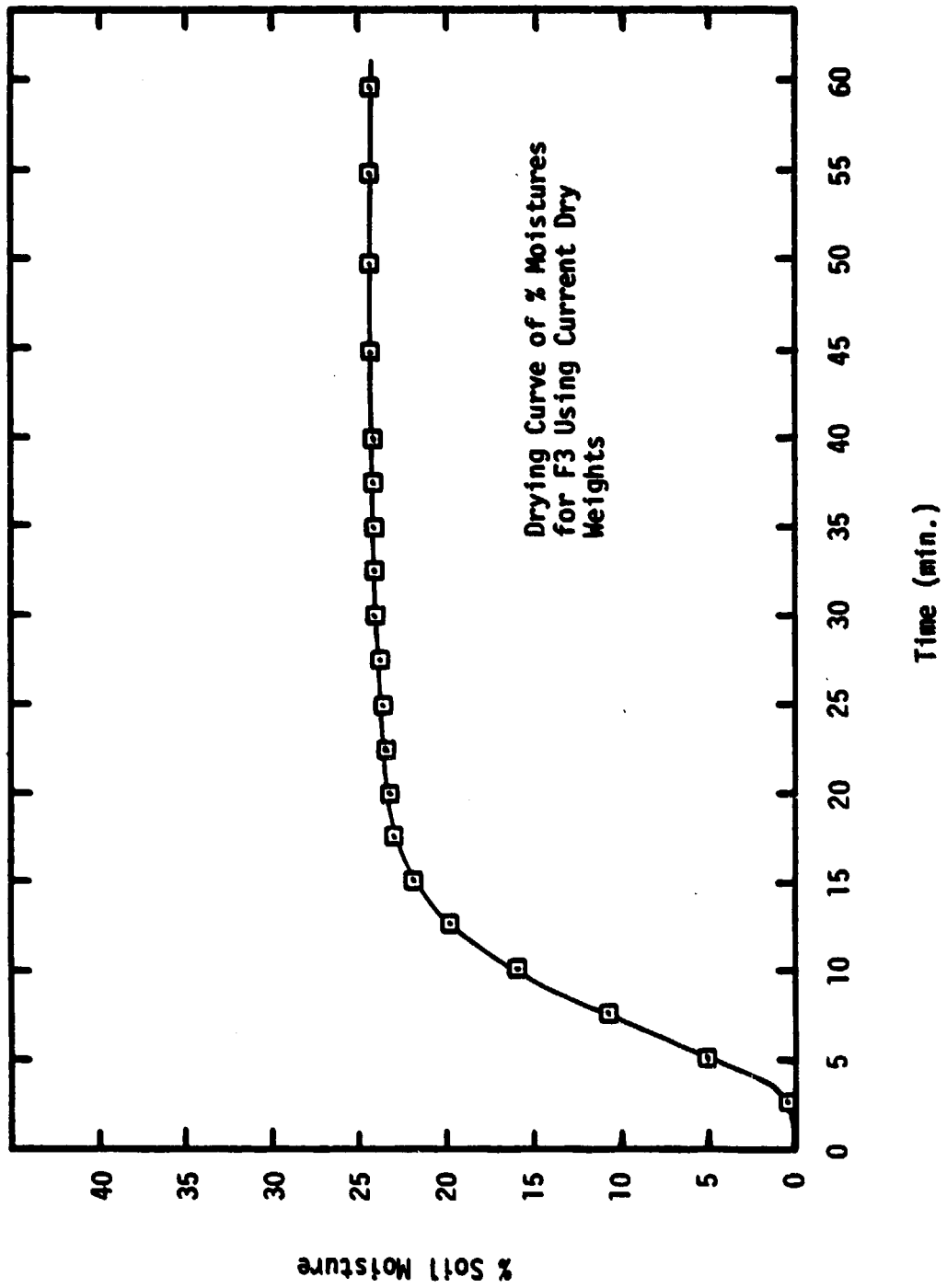


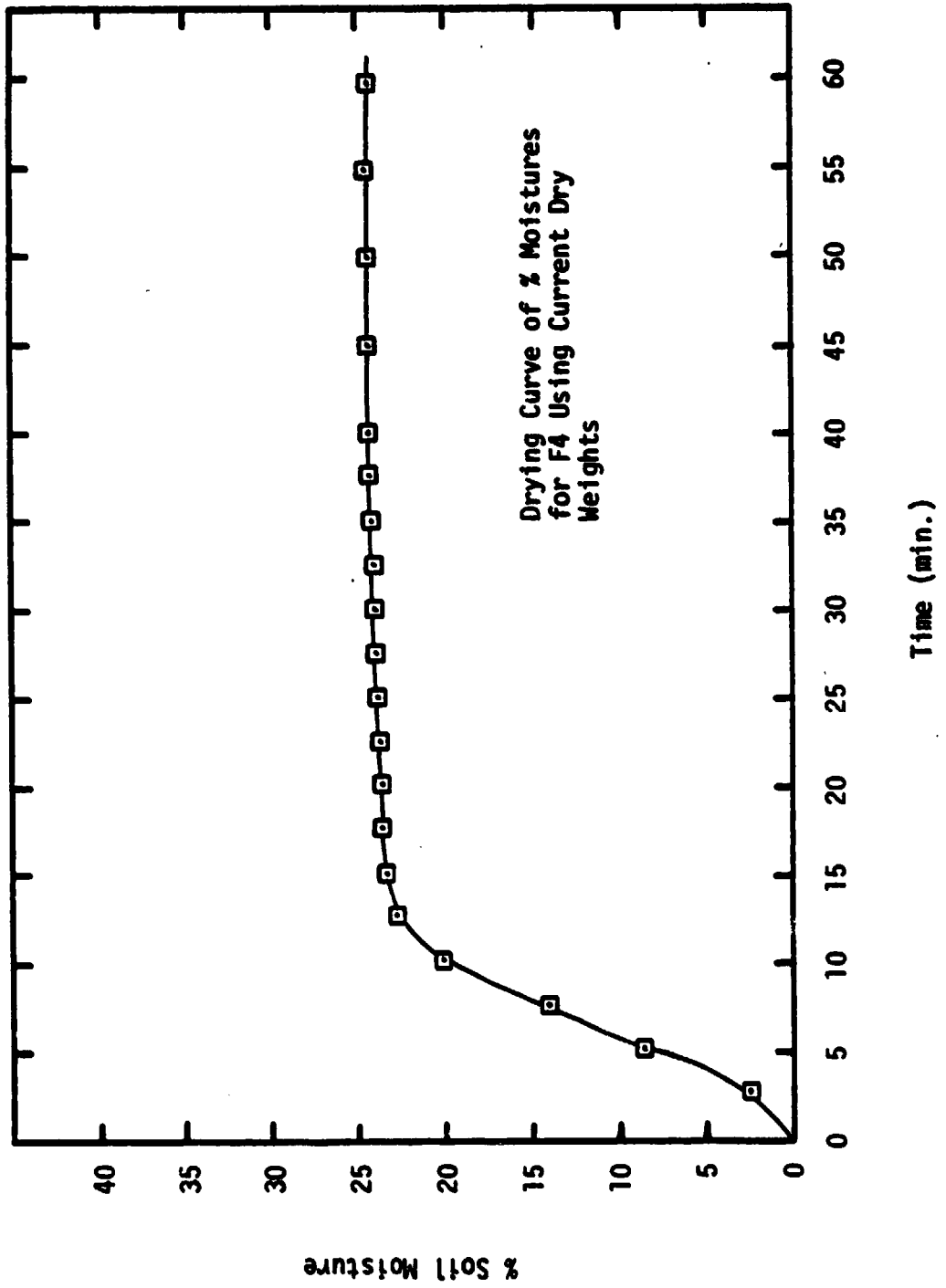


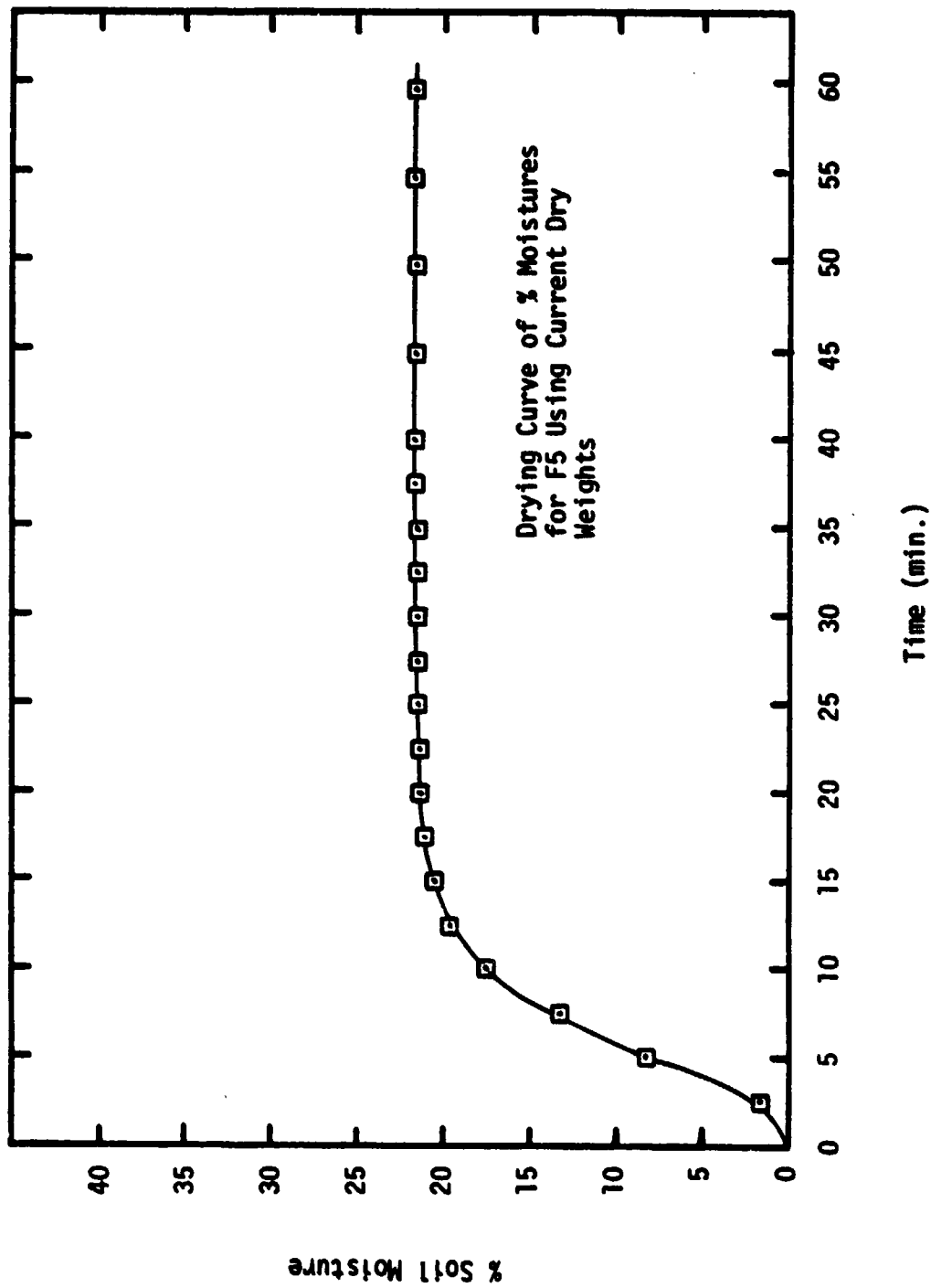












**Appendix B: A Numerical Method To Compute Soil Water
Content and Temperature Profiles Under
a Bare Surface**

TABLE OF CONTENTS

	PAGE
PREFACE	1
CHAPTER	
I INTRODUCTION	5
II INPUTS AND INITIAL VALUES FOR THE COMPUTER SIMULATION	5
III DESCRIPTION OF THE SOIL	6
IV DESCRIPTION OF THE MODEL	12
Introduction to CSMP III	12
Description	13
A) Job Control Language	13
B) Title, Memory Organization, and Allocation	14
C) INITIAL Section	14
D) DYNAMIC Section	20
E) TERMINAL Section	42
V DESCRIPTION OF OUTPUT OF THE MODEL	44
VI REFERENCES	48
VII APPENDICES	50
A. Glossary of Variable Names	51
B. Program Listing	55
C. Calculation of Unsaturated Hydraulic Conductivity	64

PREFACE

Under a contract with the National Aeronautics and Space Administration (NASA, Johnson Space Center in Houston), Texas A&M University, through its Remote Sensing Center, is one of a small group of contractors, evaluating the feasibility of remotely sensing the status of soil moisture.

At present, the most promising technology is the measurement of microwave emission by the earth's surface or the backscattering of microwave radiation emitted by an airborne source. In either case, the signals characterize a rather shallow layer, variously estimated between 0.05 and 0.25 m deep. Surface configuration, moisture content, or perhaps more accurately, the specific free energy of the water present, affect not only the signal strength, but also the depth of perception.

To support such efforts, a closely related study of the moisture movement and the water balance of deeper layers is indispensable. This classical problem of agricultural and natural hydrology has always been made intractable by the lack of facts on the surface moisture regime. Thus, the two areas of research and application are currently merging. Evidence of this trend is the development of theories, in the form of numerical models, that are combinations of atmospheric and soil physics. These may provide the foundation for models of microwave physics as well as a practical means to interpret radar signatures.

As one step in that direction, we present here a comprehensive, yet fairly simple model of water disposition in a bare soil profile under the sequential impact of rain storms and other atmospheric influences, as they occur from hour to hour. This model is intended mostly to support field

studies of soil moisture dynamics by our current team, to serve as a background for the microwave measurements, and, eventually, to serve as a point of departure for soil moisture predictions or estimates based in part upon airborne measurements.

The main distinction of the current model is that it accounts not only for the moisture flow in the soil-atmosphere system, but also for the energy flow and, hence, calculates system temperatures. Also, the model is of a dynamic nature, capable of supporting any required degree of resolution in time and space.

This work is the precursor of similar work for vegetated areas. It should be emphasized, however, that much critical testing of the simple case is needed before the complexities of the hydrology of a vegetated surface can be related meaningfully to microwave observations.

The present model is given in full detail, so as to invite its use by others and to make it possible to make adaptations, changes, and improvements. The program, as listed, can be obtained from the authors in the form of punched cards or a cassette.

Texas A&M University
Department of Soil and Crop Sciences

C.H.M. van Bavel, Professor and Principal Investigator

R. Lascano, Research Associate

I INTRODUCTION

A simulation model is documented for calculating the water content and temperature profiles of a bare soil, from known initial conditions and a set of ordinary, time-dependent weather data, over a period of several days to several weeks. The model is dynamic, because the properties of the system are updated as the temperature and water content are changing in time.

The present model was adapted from a set of algorithms devised for the study of dry mulching as a water conserving treatment in the dryland farming areas of North Texas (Horton, 1977). In turn, the latter model was derived from a simulation of the concurrent flow of water and heat in soil proposed by Van Bavel and Hillel (1975, 1976) and of the infiltration and detention of rainfall suggested by Hillel et al. (1975).

The model provides a comprehensive method for the simultaneous solution of the equations of continuity for water and heat in a soil system. The solution is obtained at frequent, fixed intervals and the moisture and temperature profiles are printed when desired. The distinguishing characteristic of the model is that it does not assume a typical or average rate of evaporation, but that it, rather, generates the instantaneous rate, from the ambient weather and the momentary values of the soil moisture and temperatures. The evaporative flux is found by a combination method, that is, a combination of a surface energy balance and a model of the fluxes above and below that surface.

The model is written in the Continuous System Modeling Program III (CSMP III) language (IBM, 1975), a specific numerical simulation language suitable for time-variant systems. The model was developed for execution on the AMDAHL 470V/6 computer operated by Texas A&M University at

College Station, Texas. This system is operated with the IBM S-370 operating system.

A basic knowledge of physics and FORTRAN is desirable to understand the model. To assist the user, a glossary of variable names with their units has been provided as Appendix A, and a complete listing of the program is presented in Appendix B. Furthermore, since CSMP III is used throughout, a brief explanation will be given when CSMP III statements are used.

II- INPUTS AND INITIAL VALUES FOR THE COMPUTER SIMULATION

The inputs to calculate the heat and water balance of a soil system are divided in two parts: constant and variable inputs.

Constant inputs to the model refer to the hydraulic characteristics of the soil and the relationship between albedo (short-wave reflectance) and volumetric water content of the soil surface. The hydraulic characteristics of the soil are the functions relating pressure potential and hydraulic conductivity to volumetric water content.

Variable inputs to the model refer to the time-dependent weather variables. These are:

1. daily global radiation, based on either daily total or hourly data,
2. daily maximum and minimum air temperatures and their corresponding relative humidities, or, hourly temperature and dewpoint data (2.0 m height),
3. average daily wind speed, or hourly data if available (2.0 m height), and
4. amount and duration of precipitation.

Initial values that must be known are the initial soil moisture and heat content of the soil as a function of depth. These are obtained as follows:

1. initial heat content are calculated from an initial measured or estimated soil temperature profile, and
2. initial water contents as measured in the field.

The way in which the constant and time-dependent inputs, and the initial values are manipulated in the model will be considered in detail in section IV of this document.

III- DESCRIPTION OF THE SOIL

This simulation model is being applied to describe the heat and water balance of a soil classified in the Norwood series (Mixed (Calcareous), Thermic Typic Udifluvents). Specifically, the hydraulic characteristics in the model were obtained from three unpublished theses from Texas A&M University (Saffaf, 1966; Marek, 1977; and Humphreys, 1979). These reports deal with the field determination of the hydraulic conductivity of the soil and with the hydraulic characteristics of irrigation furrows. The experimental work was done on the Agronomy farm of Texas A&M University, on a Norwood soil.

In terms of its hydraulic characteristics, the soil profile being used in this simulation can be divided into two horizons (Humphreys, 1979). The characteristics of each horizon are listed below:

A. Horizon number 1:

- | | |
|---|----------------------------|
| a. Depth | 0.0 - 0.20 m |
| b. Texture | silty clay loam |
| c. Average dry bulk density | 1.54 g/cm ³ |
| d. Saturated hydraulic conductivity | 5.0 x 10 ⁻⁷ m/s |
| e. Relationship of pressure potential versus volumetric water content as plotted in Figure 1, and | |
| f. Calculated hydraulic conductivity versus volumetric water content as plotted in Figure 2. | |

B. Horizon number 2:

- | | |
|-----------------------------|------------------------|
| a. Depth | 0.20 - 1.20 m |
| b. Texture | silt loam |
| c. Average dry bulk density | 1.46 g/cm ³ |

ORIGINAL PAGE IS
OF POOR QUALITY

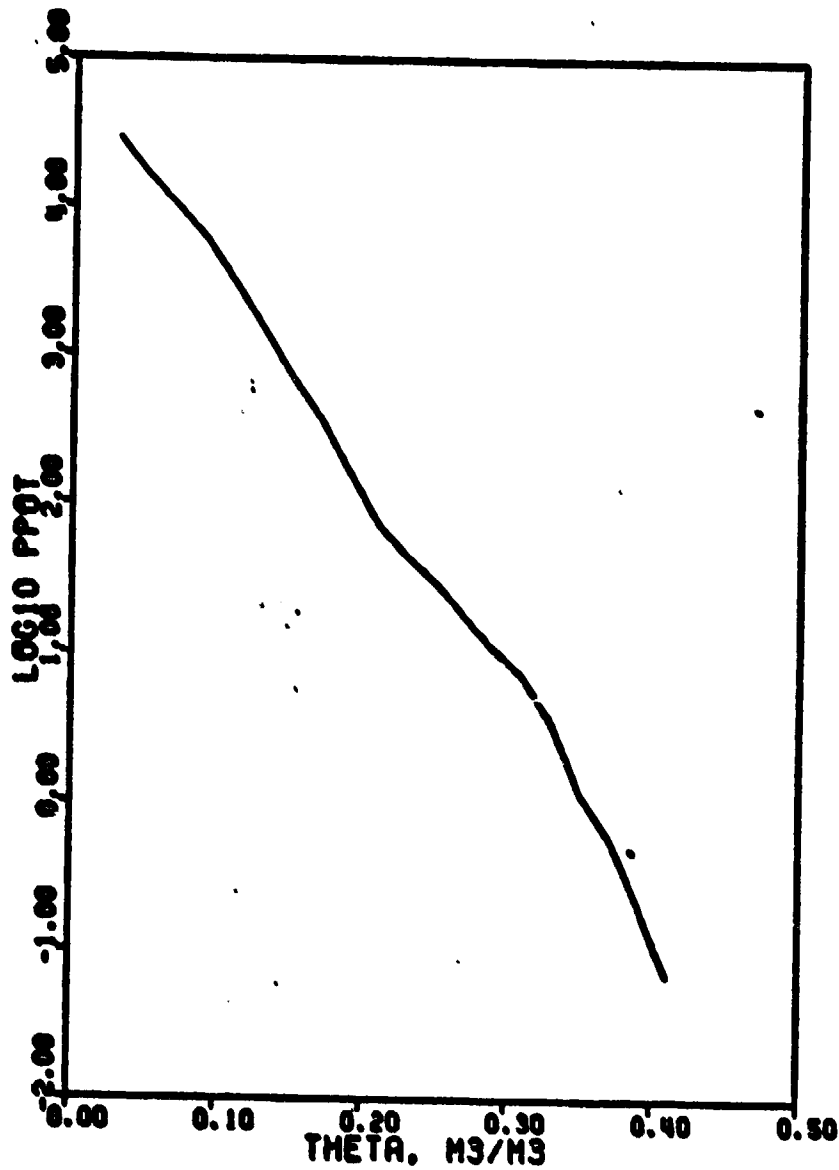


Figure 1. Relationship between the Log_{10} of pressure potential (-m of water column) and volumetric water content for the surface horizon, 0.0 - 0.20 m, of the Norwood soil (FUNCTION TVSP1).

ORIGINAL PAGE IS
OF POOR QUALITY

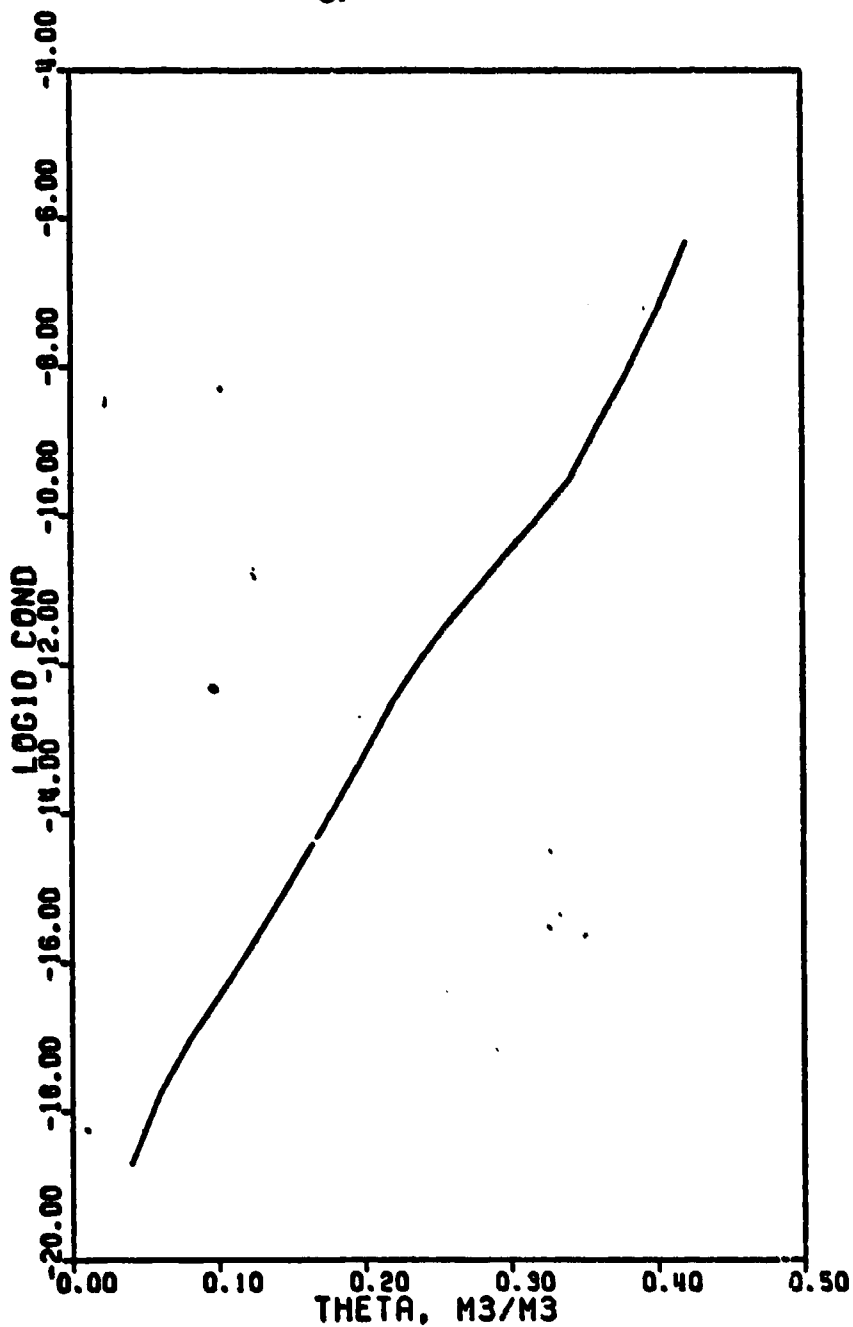


Figure 2. Relationship between the calculated hydraulic conductivity in m/s and the volumetric water content of the surface horizon, 0.0 - 0.20 m, of the Norwood soil (FUNCTION TVSC1).

- d. Average saturated hydraulic conductivity 6.0×10^{-6} m/s
- e. Relationship of pressure potential versus volumetric water content as plotted in Figure 3, and
- f. Calculated hydraulic conductivity versus volumetric water content as plotted in Figure 4.

The hydraulic conductivity as a function of volumetric water content for both horizons was calculated by the method of Jackson (Jackson, 1972). The WATFIV algorithm used for this calculation is included in Appendix C.

ORIGINAL PAGE IS
OF POOR QUALITY

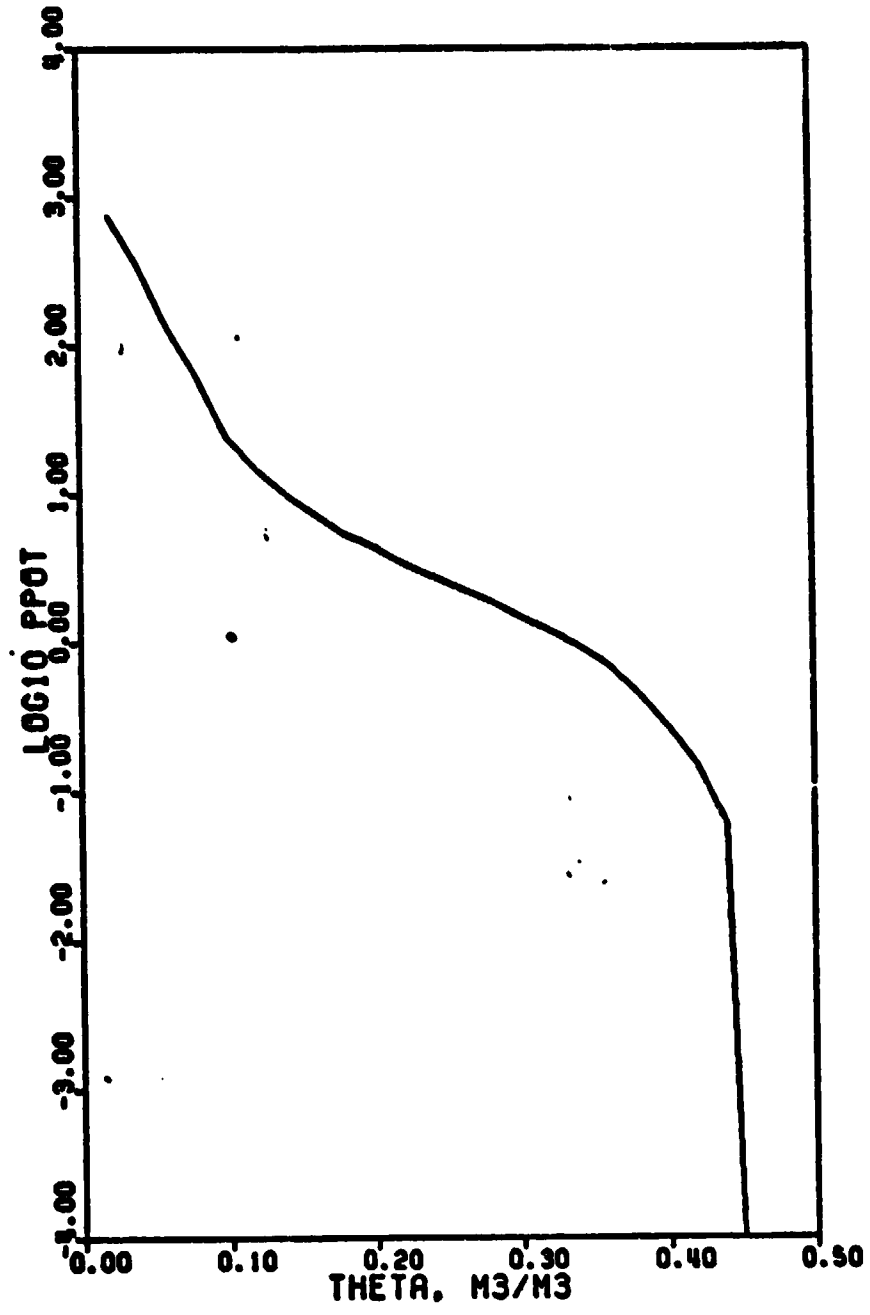


Figure 3. Relationship between the Log₁₀ of pressure potential (-m of water column) and volumetric water content for the sub-soil horizon, 0.20 - 1.20 m, of the Norwood soil (FUNCTION TVSP2).

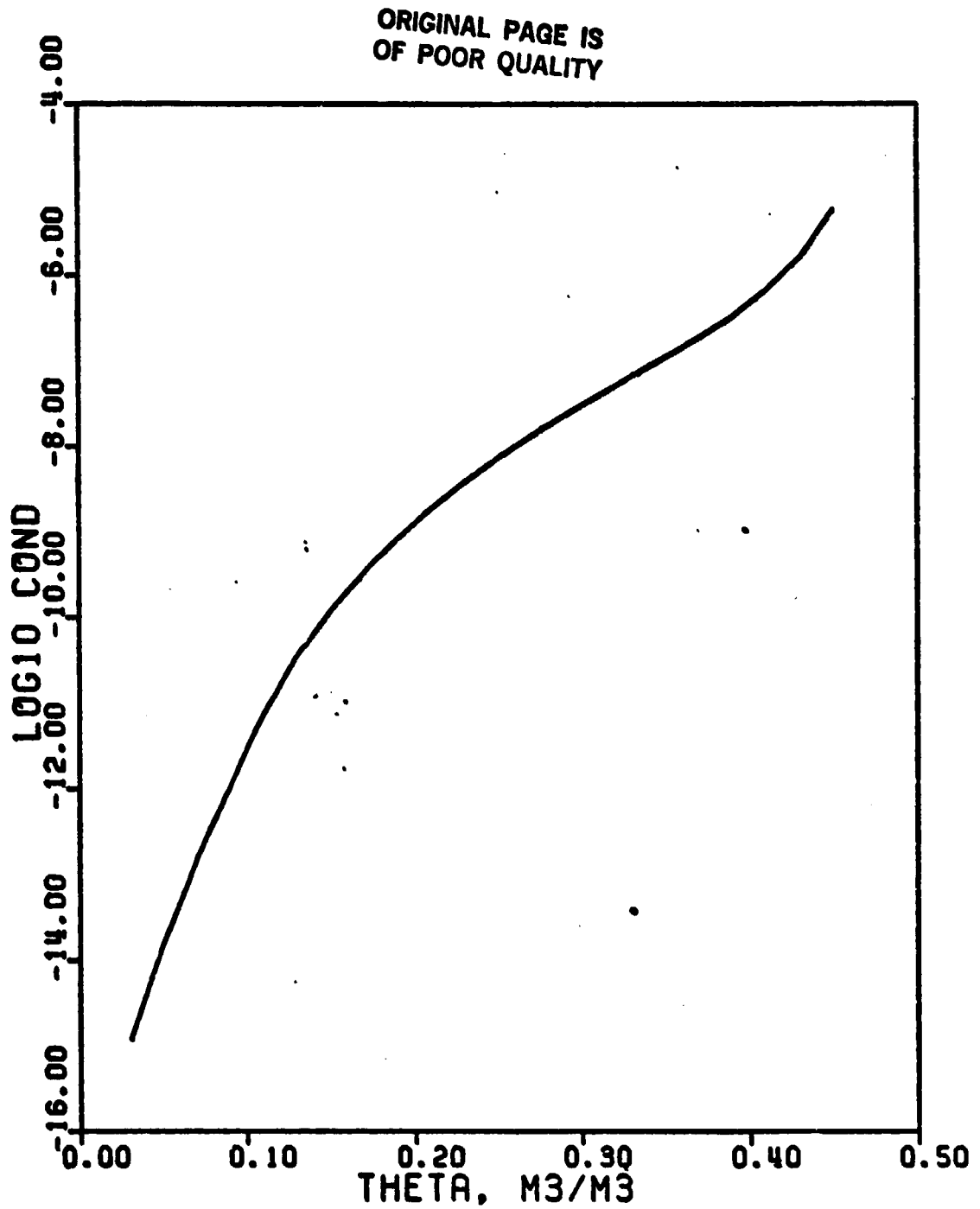


Figure 4. Relationship between calculated hydraulic conductivity in m/s and volumetric water content for the sub-soil horizon, 0.20 - 1.20 m, of the Norwood soil (FUNCTION TVSC2).

IV- DESCRIPTION OF THE MODEL

Introduction to CSMP III:

Program statements in CSMP III can be divided into three categories: data, structure, and control statements. Data statements assign numeric values to the parameters, constants, and initial conditions of the system. Structure statements define the functional relationship between the variables of the model. Control statements deal with the duration of the simulation, the integration increment, type of output, and with the translation and execution of the program. The user does not need to specify the category of each statement.

The structure of the program can be divided into three sections: INITIAL, DYNAMIC, and TERMINAL sections. The major characteristics of these translation control statements are the following:

A. INITIAL section:

1. Operations specified in this section are executed only at the onset of the simulation,
2. it contains the equations that define the invariable geometry of the system, and
3. it contains values and tables for specified parameters, and provides the initial values of specified variables.

B. DYNAMIC section

1. It contains the equations that are needed to update the system at every time interval, and
2. it uses an iterative procedure for the solution of implicit functions of certain variables.

C. **TERMINAL** section:

1. it specifies the finish time for simulation,
2. it specifies the time interval for output and the variables to be printed in the output, and
3. it specifies the method of integration that is to be used and the integration time interval.

Description

The program will be described in the sequence given in the listing in Appendix B. To assist the user with the identification of variables refer to Appendix A where a glossary of the variables with their corresponding units are given. The International System of Units (SI) is used throughout the program with the exception of water potential values, which are given in terms of m water column. In principle, the water potential should be specified in kPa, but the approximation that $1 \text{ kPa} = 0.1 \text{ m water column}$ is sufficiently accurate and simplifies the dimensions of the units throughout. For the purpose of the description, the program is divided into five parts:

A. **JOB CONTROL LANGUAGE (JCL)** (lines 4-10)

The JCL statements are the ones used at the Texas A&M University computer installation (AMDAHL 470V/6, IBM S370 system). The user should consult the instructions of the local installation and make the necessary changes. Note that the program requires at least 128K bytes of memory.

B. TITLE, MEMORY ORGANIZATION AND ALLOCATION (lines 16-30)

Lines 16-19 are TITLE statements. This is a CSMP III label statement and allows the user to specify a heading that will appear at the top of the first page of printed output. Lines 14 and 15 are CSMP III comment statements, and can be identified by an asterisk (*) in column 1. Lines 21-30 are translation control statements to organize the memory and to initialize arrays. Lines 21-23 are the CSMP III STORAGE statement, and they represent subscripted variables with the appropriate number of storage locations contained within the parentheses. Lines 24-27 are DIMENSION statements, and are handled as in FORTRAN with the exception that a virgule (/) must appear in column 1. The virgule indicates that the DIMENSION instruction is a FORTRAN specification statement. Lines 27 and 28 are EQUIVALENCE statements and are treated in the same manner as the DIMENSION statements. The EQUIVALENCE statement allows that the variables within the parentheses be assigned to the same storage locations in the memory, that is, the variables are synonymous. Line 30 are variables specified as integers with the statement FIXED.

C. INITIAL section (lines 36-210)

The INITIAL section begins with the lines (the numbers to the left refer to the corresponding number of the listing in Appendix B):

36. INITIAL

38. NOSORT

The NOSORT is a CSMP III translation control statement and it means that the subsequent statements are to be executed in the order in which they

appear. The INITIAL section will be described in paragraphs as indicated by the comment cards in the listing (Appendix B).

*** 1) DEFINITION OF PARAMETERS (lines 40-50)

Lines 40 and 42-50 are data control statements. The PARAMETER statement (lines 40-50) is used to assign numerical values to the following variables (the number to the right in parenthesis refers to the corresponding number of the variable as given in the glossary in Appendix A):

40.	PARAMETER	NL	= 13	(68)
42.	PARAMETER	KONDS	= 4.20	(61)
43.	PARAMETER	KNODW	= 0.57	(63)
44.	PARAMETER	KONDA	= 0.025	(60)
45.	PARAMETER	VHCAPS	= 1.925E-06	(102)
46.	PARAMETER	VHCAPW	= 4.186E06	(103)
47.	PARAMETER	SIGMA	= 5.67E-08	(82)
48.	PARAMETER	Z0	= 0.01	(108)
49.	PARAMETER	SATCON	= 0.60E-06	(80)
50.	PARAMETER	PORSTY	= 0.50	(71)

The values for the heat conductivity of soil (KONDS), water (KONDW), heat conductivity by air (KONDA) and volumetric heat capacity of the soil (VHCAPS) and of water (VHCAPW) were obtained as suggested by De Vries (1966).

The value for the total porosity (PORSTY) of the soil was calculated from the average dry bulk density of the soil layers i.e.

$$\text{PORSTY} = 1.0 - \frac{\text{Average dry bulk density}}{\text{Particle density}}$$

*** 2) DAILY COUNTERS (lines 52-54)

Lines 52-54 initialize day counters, which are used to keep track of the daily input data that is read with lines 56-61 in the third paragraph.

*** 3) READ INPUT DATA (lines 56-61)

The input data is stored in a two dimensional array (WINPUT), and is

read in with a FORTRAN READ statement (line 57).

*** 4) SPECIFICATION OF THE GEOMETRY OF THE SYSTEM, INITIAL WATER CONTENT AND TEMPERATURE (lines 64-68)

In CSMP III, the TABLE statement is used to assign values to the subscripted variables listed on a STORAGE card. Thus, lines 64, 66, and 67 are used to initialize the values for the thickness of the compartment (TCOM), initial volumetric water content (ITHETA), and initial soil temperatures (ITEMP). Since the number of layers (NL) is 13, one value for each soil layer must be specified with the TABLE statement. Three periods (...) are used as continuation to following lines.

*** 5) CALCULATIONS OF DISTANCE AND DEPTH (lines 70-75)

The depth (DEPTH(I)) and the distance (DIST(I)) of each soil layer is calculated in lines 70-75. The depth of each layer is the vertical distance between its midpoint and the soil surface, and the distance between midpoint of adjacent layers is given by DIST(I) (lines 72-75). The depth of the first layer (DEPTH(1)) is half its thickness (line 70), and the distance of the first layer (DIST(1)) is set equal to its depth (line 71).

```

70.     DEPTH(1) = 0.5*TCOM(1)
71.     DIST(1) = DEPTH(1)
72.     DO 20 I = 2,NL
73.     DIST(I) = 0.5*(TCOM(I-1)+TCOM(I))           (21)
74.     DEPTH(I) = DEPTH(I-1)+0.5*(TCOM(I-1)+TCOM(I)) (17)
75. 20 CONTINUE

```

Figure 5 shows the geometry of the system and symbols used in the program, and Table 1 lists the corresponding values of TCOM, DIST, and DEPTH.

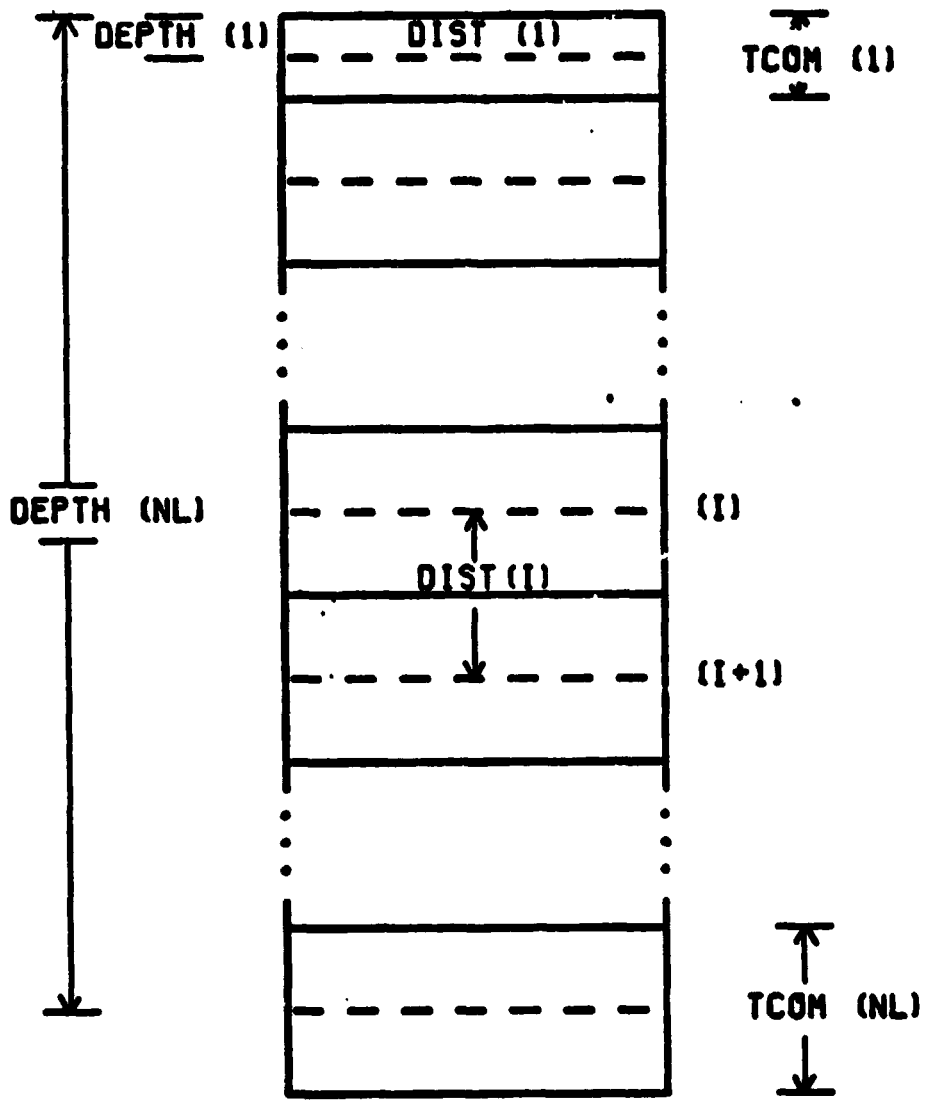


Figure 5. Geometry of the system and symbols used in the program.

TABLE 1. Invariable geometry of the soil system.

Layer N (I)	Thickness of compartment TCOM(I) (m)	Distance DIST(I) (m)	Depth DEPTH(I) (m)
1	0.01	0.005	0.005
2	0.02	0.015	0.020
3	0.02	0.020	0.040
4	0.03	0.025	0.065
5	0.03	0.030	0.095
6	0.04	0.038	0.130
7	0.05	0.045	0.175
8	0.05	0.050	0.225
9	0.10	0.075	0.300
10	0.10	0.100	0.400
11	0.15	0.125	0.525
12	0.30	0.225	0.750
13	0.30	0.300	1.050

*** 6) CALCULATIONS OF INITIAL WATER AND TEMPERATURE CONDITIONS (lines 79-87)

From the parameters given, the following initial conditions for water and temperature in the soil system are calculated:

1) the initial volumetric heat capacity of each soil layer (IVHCAP(I)) is calculated from the soil porosity and its water content as suggested by De Vries (1966).

$$81. \quad IVHCAP(I) = VHCAPW * ITHETA(I) + (1.0 - PORSTY) * VHCAPS \quad (54)$$

2) the initial water content (IWATER) for the entire soil profile is calculated by,

$$82. \quad IWATER = IWATER + TOOM(I) * ITHETA(I) \quad (57)$$

3) the initial volume of heat of each soil layer (IVOLH (I)) is calculated by,

$$83. \quad IVOLH(I) = ITEMP(I) * TCGH(I) * IVHCAP(I) \quad (55)$$

4) the net difference between influx and outflux of soil water (NFLUX) and inflow and outflow of heat (NFLOW) is set equal to zero respectively by,

$$84. \quad NFLUX(I) = 0.0 \quad (67)$$

$$85. \quad NFLOW(I) = 0.0 \quad (66)$$

5) and the initial volume of water in each soil layer (IVOLW(I)) is calculated by,

$$86. \quad IVOLW(I) = ITHETA(I) * TOOM(I) \quad (56)$$

In CSMP III, a graphical relationship between pairs of x - y coordinates can be represented by the data control statement FUNCTION. Thus, lines 93, 116, 139, 164, 188, and 198 represent the following relationships:

1) FUNCTION TVSP1: Volumetric water content versus pressure potential. These data characterize the first soil horizon as given in Figure 1.

2) FUNCTION TVSC1: Volumetric water content versus calculated hydraulic conductivity. These data characterize the first soil horizon as

given in Figure 2.

3) FUNCTION TVSP2: Volumetric water content versus pressure potential. These data characterize the second soil horizon as given in figure 3.

4) FUNCTION TVSC2: Volumetric water content versus calculated hydraulic conductivity. These data characterize the second soil horizon as given in figure 4.

5) FUNCTION TEVSKO: Soil temperature versus heat conductivity by water vapor. This relationship is plotted in Figure 6.

6) FUNCTION TIVSAL: Volumetric water content of the first soil layer versus albedo (shortwave reflectance). This relationship is plotted in Figure 7.

*** 7) TABLE OF THE GEOMETRY OF THE SYSTEM AND ITS INITIAL STATE
(lines 206-210)

The INITIAL section ends with an output of a table of the geometry of the system as given in Table 1.

D. DYNAMIC SECTION (lines 216-428)

The equations which update the system at every time interval and to perform integrations are given in the DYNAMIC section. The DYNAMIC section will be described in paragraphs as indicated by the comment cards in the listing (Appendix B).

The DYNAMIC section begins with the lines,

216. DYNAMIC

218. NOSORT

ORIGINAL PAGE IS
OF POOR QUALITY

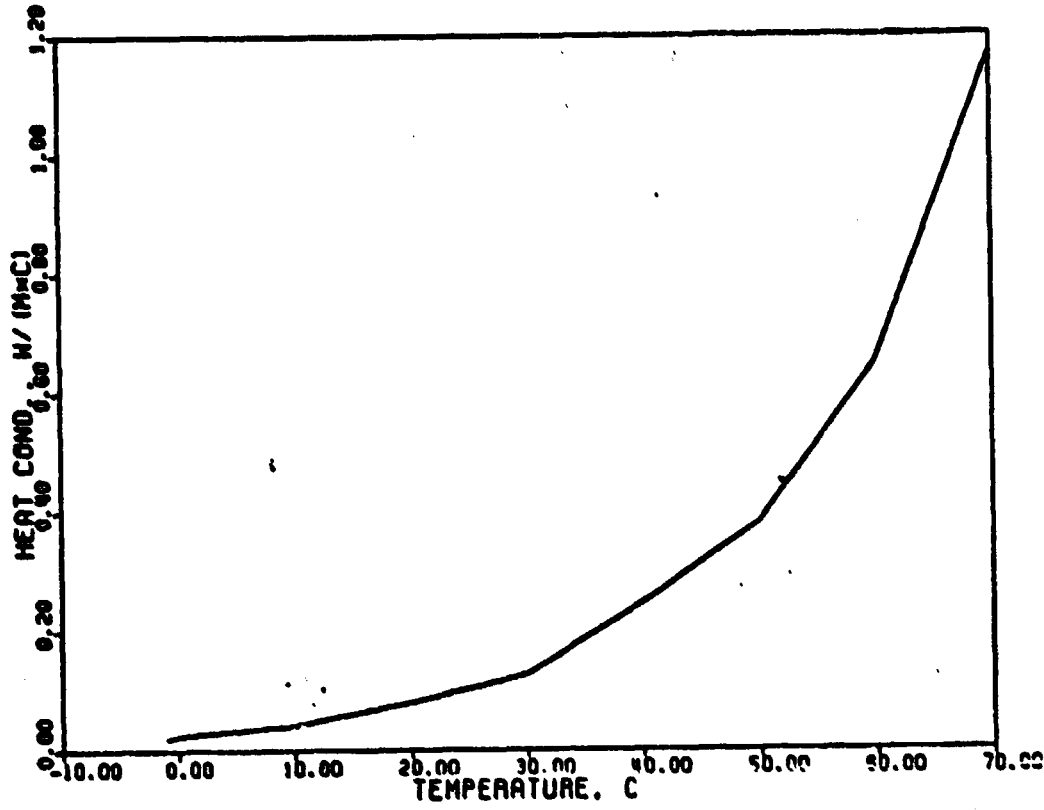


Figure 6. Heat conductivity by water vapor versus soil temperature (FUNCTION TEVSKO).

ORIGINAL PAGE IS
OF POOR QUALITY

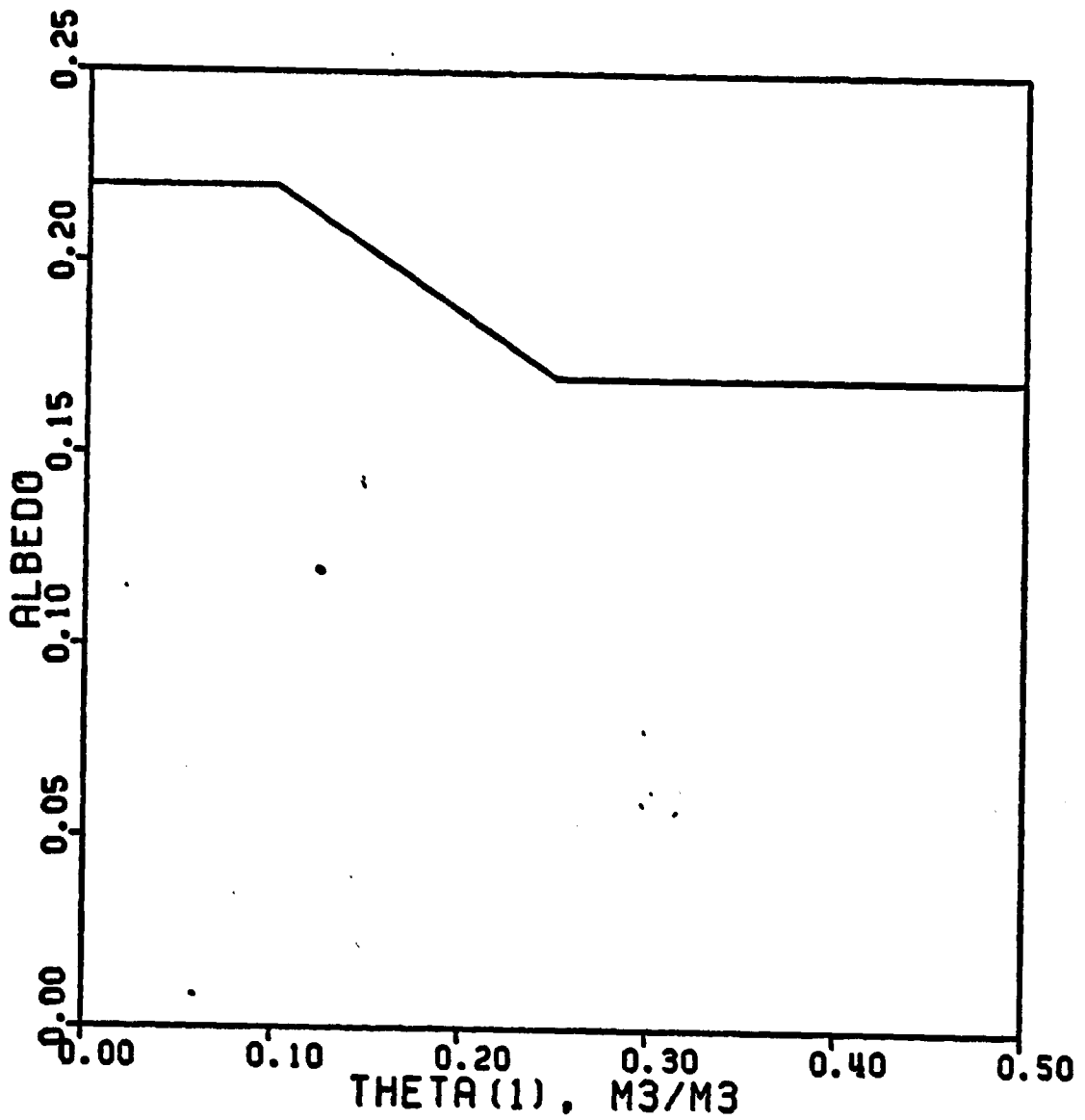


Figure 7. Albedo versus volumetric water content of first soil layer (FUNCTION TIVSAL).

As explained before, the NOSORT statement indicates that the statements are executed in the order in which they are listed.

The paragraphs are:

*** 1) DEFINITION OF TIME RELATED VARIABLES (lines 221-230)

This paragraph defines the time related variables: time in hours (HTIME) and standard time of the day in hours (STIME). Also defined is an impulse generator (IMPULS).

223. Y = IMPULS(86400., 86400.)

which increments the day index (DNUM), which is used to reference WINPUT. The first value in parentheses in the IMPULS statement is the time in seconds to the first pulse, and the second value is the time interval in seconds between pulses.

The variables DNUM, DNUM1, and DNUM2 are daily counters that are used to keep track of the input data read from the array WINPUT where the data are stored. The method used to determine to what Julian day number (JDNUM) the input data corresponds is given by line 230.

230. JDNUM = WINPUT(1, DNUM) (58)

*** 2) CALCULATION OF HYDRAULIC CHARACTERISTICS OF THE FIRST HORIZON (lines 232-237)

The volumetric water content (THETA(I)), hydraulic conductivity (COND(I)), pressure potential (PPOT(I)), and hydraulic potential (HPOT(I)), for the first 8 layers of the soil profile (horizon #1) are calculated from the following equations:

1) THETA(I) of each layer is obtained from the ratio of the volume of water (VOLW(I)) to the layer volume per unit area:

$$233. \quad \text{THETA}(I) = \text{VOLW}(I)/\text{TCOM}(I) \quad (93)$$

2) COND(I) at the center of each layer is obtained by linear interpolation of the values in the FUNCTION TVSCI using the water content (THETA(I)) of each layer.

$$234. \quad \text{COND}(I) = \text{ARGEN}(\text{TVSCI}, \text{THETA}(I)) \quad (7)$$

ARGEN (Arbitrary Function Generator) is a CSMP III statement that allows linear interpolation from a relationship specified with a FUNCTION statement.

3) PPOT(I) is obtained by linearly interpolating values in the FUNCTION TVSP1 using THETA(I) of each layer.

$$235. \quad \text{PPOT}(I) = \text{ARGEN}(\text{TVSP1}, \text{THETA}(I)). \quad (72)$$

4) HPOT(I) is the sum of PPOT(I) and the elevation (-DEPTH(I)) of each layer.

$$236. \quad \text{HPOT}(I) = \text{PPOT}(I) - \text{DEPTH}(I) \quad (45)$$

*** 3) CALCULATION OF HYDRAULIC CHARACTERISTICS OF SECOND HORIZON
(lines 239-244)

The same calculations outlined in paragraph #2 are performed for the bottom five layers of the soil profile, that is, the second horizon. In this case, FUNCTIONS TVSP2 and TVSC2 are used with the ARGEN statements.

*** 4) CALCULATION OF THERMAL PROPERTIES (lines 246-253)

In this paragraph, the volumetric heat capacity (VHCAP(I)), temperature (TEMP(I)), and thermal conductivity (KOND(I)) are calculated for the 13 layers in the soil profile. The equations used are:

1) VHCAP(I) is calculated from the porosity (PORSTY) and the water

content (THETA(I)) as suggested by De Vries (1966). Soil air is not considered in the calculation.

$$247. \quad \text{VHCAP}(I) = \text{VHCAPW} * \text{THETA}(I) + (1.0 - \text{PORSTY}) * \text{VHCAPS} \quad (101)$$

2) TEMP(I) of each soil layer is calculated by dividing the volumetric heat content per unit area (VOLH(I)) by the product of volumetric heat capacity (VHVAP(I)) and layer thickness (TCOM(I)).

$$248. \quad \text{TEMP}(I) = \text{VOLH}(I) / (\text{VHCAP}(I) * \text{TCOM}(I)) \quad (91)$$

3) The contribution of the water vapor phase to the thermal conductivity (KONDV) is obtained by linear interpolation of values in FUNCTION TEVSKO and TEMP(I) for each layer.

$$249. \quad \text{KONDV} = \text{AFGEN}(\text{TEVSKO}, \text{TEMP}(I)) \quad (62)$$

4) KOND(I) of each soil layer is found by the formula suggested by De Vries (1966) using the values of KONDS, KONDA, and KONDW assigned in the INITIAL section.

$$250. \quad \text{KOND}(I) = ((1. - \text{PORSTY}) * \text{KONDS} * 0.4 + \text{THETA}(I) * \text{KONDW} + \dots \quad (59) \\ (\text{PORSTY} - \text{THETA}(I)) * 1.4 * (\text{KONDA} + \text{KONDV})) / \dots \\ ((1. - \text{PORSTY}) * 0.4 + \text{THETA}(I) + (\text{PORSTY} - \text{THETA}(I)) * 1.4)$$

*** 5) CALCULATIONS OF AVERAGE CONDUCTIVITIES (lines 255-260)

The average thermal conductivity (AVKOND) and average hydraulic conductivity (AVCOND) for transport between adjacent layers is taken to be the average of layer conductivities, weighted according to their relative thickness.

For the flow of heat, AVKOND(I) is calculated from:

$$256. \quad \text{AVKOND}(I) = (\text{TCOM}(I-1) + \text{TCOM}(I)) / (\text{TCOM}(I-1) / \text{KOND}(I-1) + \text{TCOM}(I) / \text{KOND}(I)) \quad (4)$$

For the flux of liquid water, AVCOND(I) is calculated from:

$$258. \quad AVCOND(I) = (COND(I-1) * TCOM(I-1) + COND(I) * TCOM(I)) / (TCOM(I-1) + TCOM(I)) \quad (3)$$

*** 6) SPECIFICATIONS OF BOUNDARY CONDITIONS FOR FLOW OF HEAT AND FLUX OF WATER (lines 263-264)

The boundary conditions at the bottom layer (NLL) of the soil profile are defined by the following:

1) The flux of water at the bottom boundary is taken to be equal to the hydraulic conductivity of the bottom layer. That is, the flux of water is driven by unit hydraulic potential gradient

$$263. \quad FLUX(NLL) = COND(NL) \quad (39)$$

2) The flow of heat at the bottom boundary is calculated by Fourier's law assuming that the temperature at 1.20 m depth remains constant, and that this temperature is set equal to ITEMP(NL).

$$264. \quad FLOW(NL) = (TEMP(NL) - ITEMP(NL) * KOND(NL)/TCOM(NL)/2.0) \quad (37)$$

*** 7) CALCULATION OF FLOW OF HEAT AND FLUX OF WATER (lines 266-269)

The flow of heat between layers is calculated by Fourier's law.

$$267. \quad FLOW(I) = (TEMP(I-1) - TEMP(I)) * AVKOND(I)/DIST(I) \quad (36)$$

The flux of water between layers is calculated by Darcy's law.

$$268. \quad FLUX(I) = (HPOT(I-1) - HPOT(I)) * AVCOND(I)/DIST(I) \quad (33)$$

Note that flow of heat and flux of water is calculated for all layers except the top one.

*** 8) USE DAILY RAINFALL DATA, AND CALCULATE DAILY RAINFALL DISTRIBUTION (lines 272-285)

The daily rainfall distribution is assumed to follow the pattern illustrated in Figure 8. The necessary inputs to calculate the rainfall distribution are given by,

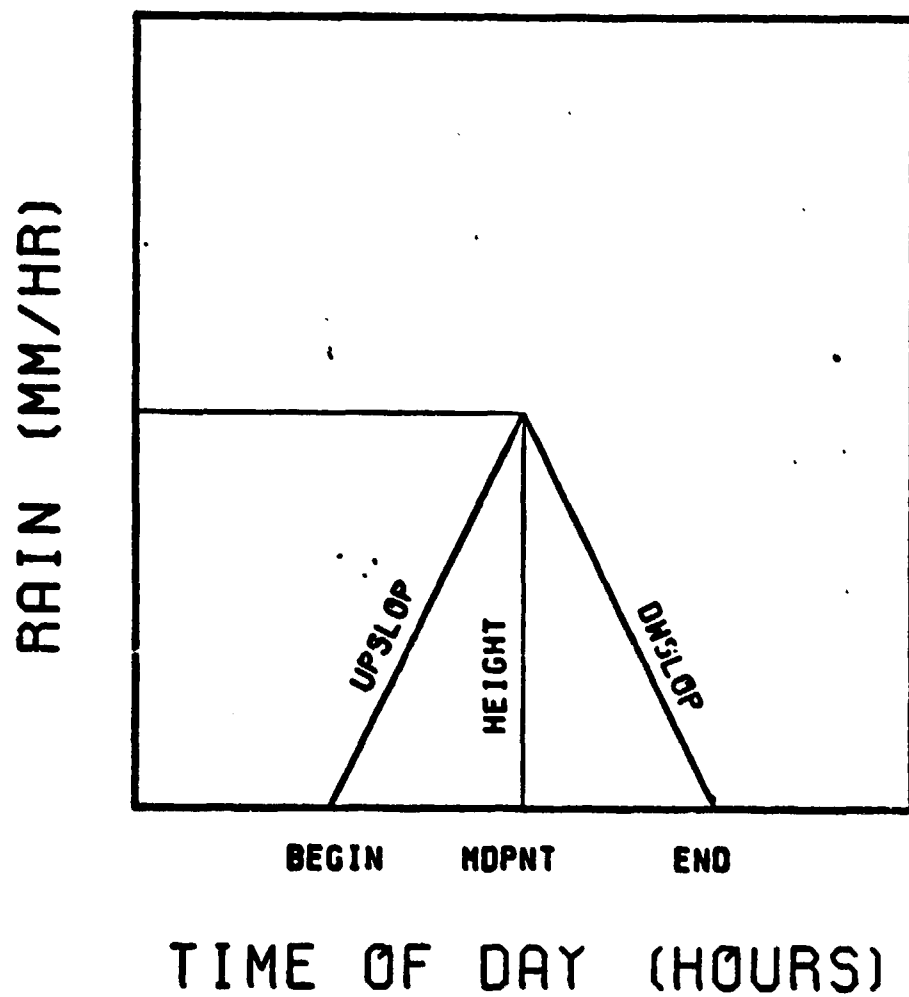


Figure 8. Pattern of daily rainfall distribution. For definition of symbols see text.

272. BEGIN = WINPUT(9, DNUM) (6)
 273. END = WINPUT(10, DNUM) (32)
 274. RFT = WINPUT(11, INUM) (75)

The logical branching used to calculate the rainfall distribution as a function of time is illustrated by the flow chart of Figure 9. In the program this is calculated by lines 272-285.

*** 9) USE DAY LENGTH AND CALCULATE DAILY DISTRIBUTION OF GLOBAL RADIATION (lines 288-292)

The daily distribution of global radiation (GR) is spread out over the daylength (DL) period using a sine function. An example of this distribution is given in Figure 10. *

290. GR = 436.33*WINPUT(3, DNUM)/DL * SIN((STIME -12. + DL/2.) *3.141/DL) (41)

Note: 436.33 is a simplification of $(24 \times 10^6 / 86400) \times (\pi/2)$

***10) CALCULATION OF ALBEDO (lines 294-295)

Albedo (ALB) is obtained by linear interpolation of values in TABLE T1VSAL and the volumetric water content of the first soil layer(T1).

294. T1 = THETA(1) (85)
 295. ALB = AFGEN (T1VSAL, T1) (2)

***11) CALCULATION OF WINDSPEED AND BOUNDARY LAYER RESISTANCE (lines 297-305)

Values of the average windspeed (SA) are set at noon (line 297) and linear interpolation produces values at other times (lines 299-302). The boundary layer resistance (RA) is calculated as the quotient of the logarithm of 2.0 divided by the roughness factor (ZO) squared and the

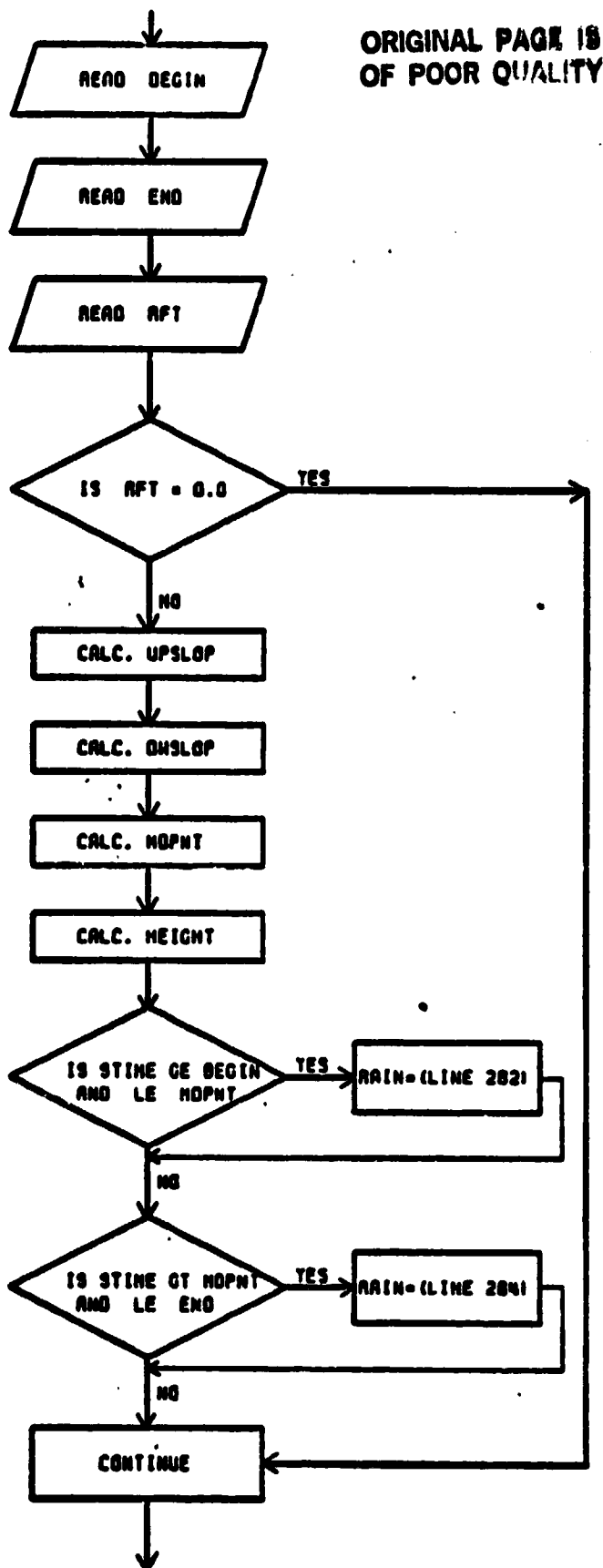


Figure 9. Flow chart showing the logical branching used to calculate the pattern of rainfall distribution.

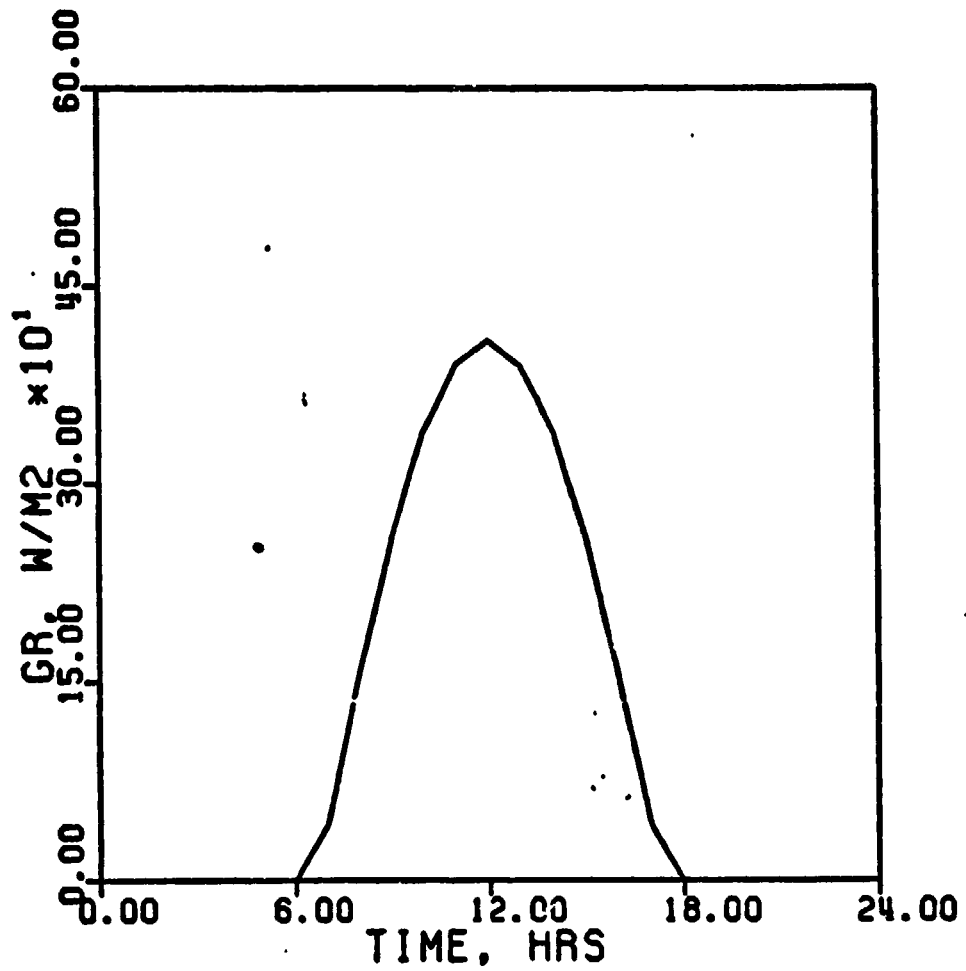


Figure 10. Example of daily distribution of global radiation (GR) over time. (Total irradiance 10.0 MJ/m², day length = 10.7 hours).

product of windspeed at 2.0 meters and a stability factor (Sellers, 1965).

$$305. \quad RA = (ALOG(2.0/ZO)**2.0)/(0.16*SA) \quad (73)$$

***12) CALCULATION OF DEWPOINT TEMPERATURE AND ABSOLUTE HUMIDITY

(lines 307-314)

Dewpoints at time of minimum air temperature (DPMIN) are set at 5:00 hours standard time and dewpoints at time of maximum air temperature (DPMAX) are set at 15:00 hours standard time allowing linear interpolation of dewpoints (DPTC) at other times (line 311 and 313).

The absolute humidity of the air (HA) is calculated from the equation (Murray, 1967), and is plotted in Figure 11.

$$314. \quad HA = 1.323*EXP(17.27*DPTC/(237.3+DPTC))/(273.16+DPTC) \quad (42)$$

***13) CALCULATION OF TEMPERATURE OF THE AIR AND VOLUMETRIC HEAT

CAPACITY OF THE AIR (lines 316-324)

Minimum air temperature values (TAMIN) are set at 5:00 hours standard time and maximum air temperatures (TAMAX) are set at 15:00 hours standard time allowing linear interpolation of air temperatures (TAC) at other times.

The volumetric heat capacity of the air (SH), as a function of air temperature in degrees Kelvin (TAK) is calculated from the following equation, and is plotted in Figure 12.

$$324. \quad SH = (1154.8*303.16)/(TAK) \quad (81)$$

***14) CALCULATION OF SKY IRRADIANCE (line 326)

The sky irradiance (SKL) is found from a formula suggested by Brunt (1932), as modified by Sellers (1965).

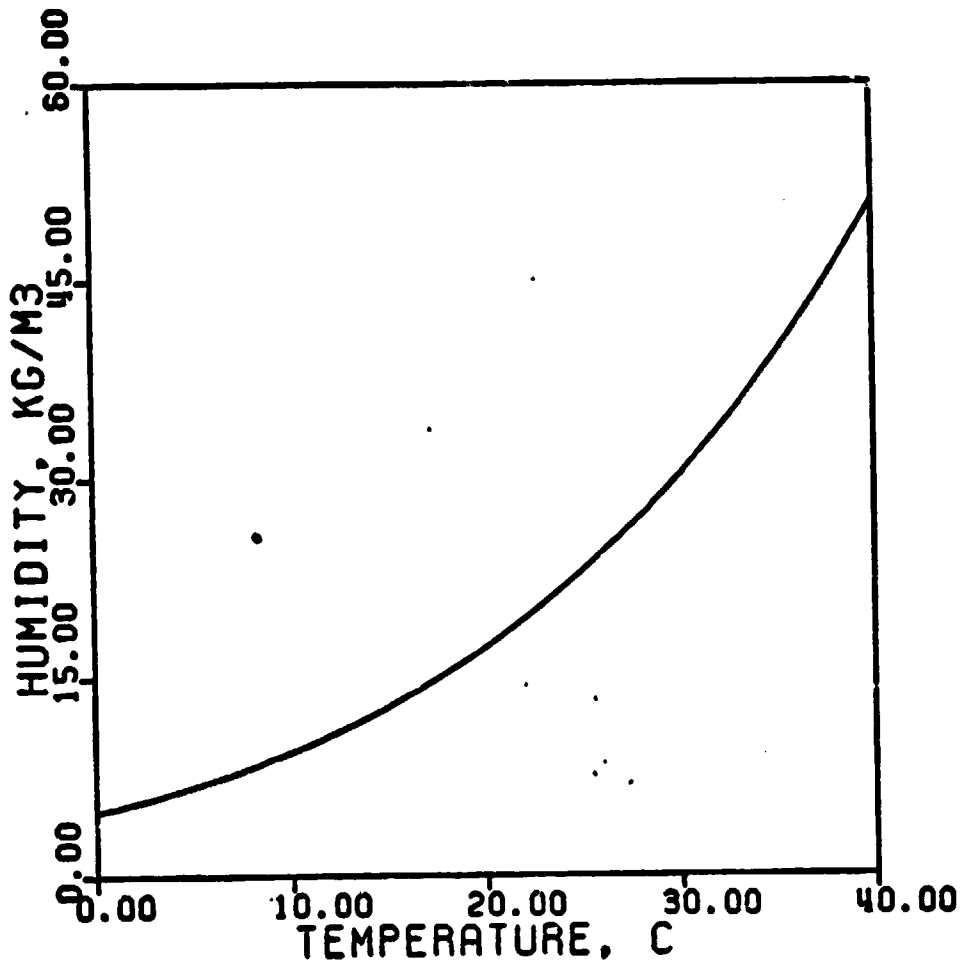


Figure 11. Relationship between absolute humidity of the air (HA) and temperature as calculated with Murray's equation.

ORIGINAL PAGE IS
OF POOR QUALITY

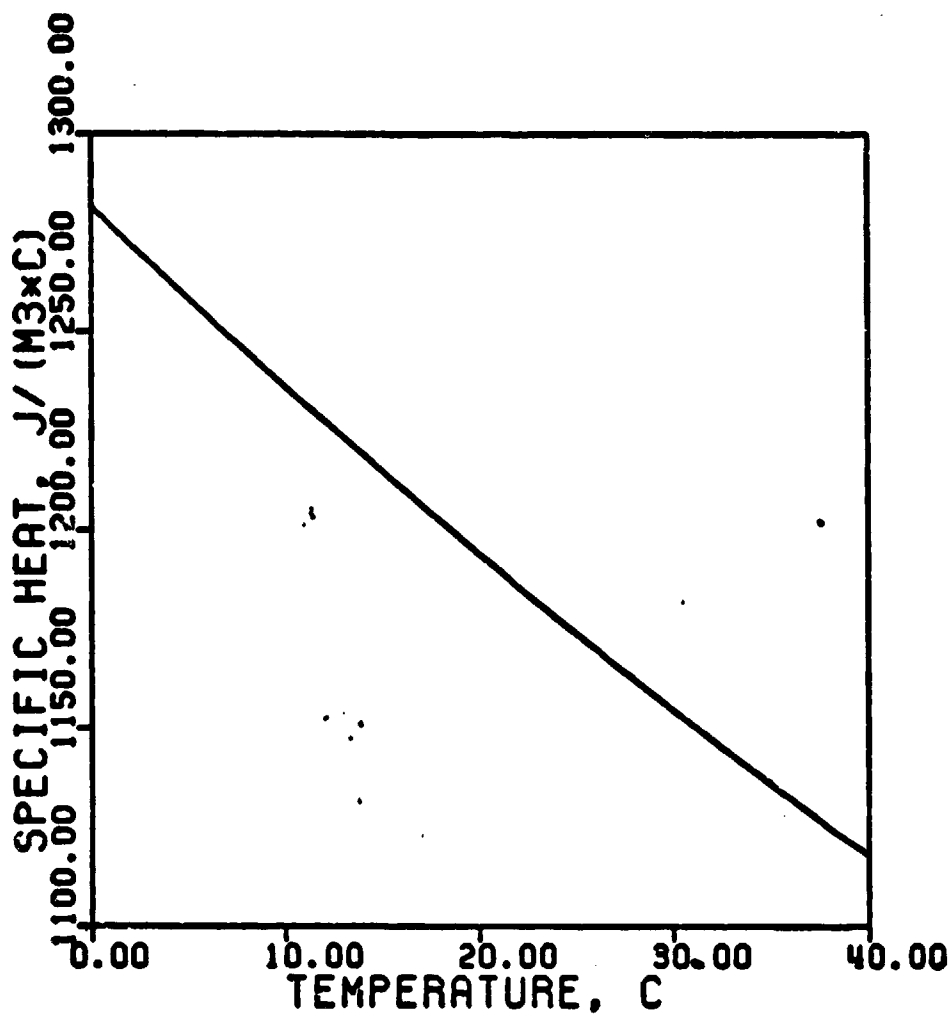


Figure 12. Volumetric heat capacity or specific heat of the air (SH) as a function of temperature.

$$326. \quad SKL = (SIGMA * TAK^{**4}) * (0.605 + 0.039 * SQRT(410. * HA)) \quad (83)$$

***15) IMPLICIT CALCULATION OF THE SOIL SURFACE TEMPERATURE (lines 328-335)

The temperature of the soil surface (TSC) is calculated by an implicit function (line 328) using the air temperature (TAC) as a first estimate and calculating the energy balance at the surface:

- 1) Sensible heat flux (A)

$$329. \quad A = (TSC - TAC) * SH / RA \quad (1)$$

2) Murray's equation (Murray, 1967) to calculate the saturated humidity (HO) at the soil surface.

$$330. \quad HO = 1.323 * EXP(17.27 * TSC / (273.3 + TSC)) / (273.16 * TSC) \quad (44)$$

3) Absolute humidity is calculated as suggested by Van Bavel and Hillel (1976).

$$33. \quad HO = HO * EXP(PPOT(1) / (46.97 * (TSC + 273.16))) \quad (44)$$

4) The evaporation (EV) is the quotient of the difference in humidities of surface and atmosphere and the boundary layer resistance.

$$332. \quad EV = (HO - HA) / (RA * 1000.) \quad (33)$$

5) The conduction into the soil (S) is calculated as the difference in net radiation and the sum of sensible and latent heat fluxes.

$$333. \quad S = GR * (1. - ALB) + SKL - SIGMA * (TSC + 273.16)^{**4} - A - LH * EV \quad (78)$$

6) The final temperature of the soil surface (FTSC) as calculated in the implicit loop is given by Fourier's law for conduction.

$$335. \quad FTSC = TEMP(1) + S * DEPTH(1) / KOND(1) \quad (40)$$

***16) CALCULATIONS OF EVAPORATION AND NET RADIATION (lines 337-344)

The flow of heat into the center of layer one (FLOW(1)) is calculated as the product of heat conductivity (KOND(1)) and the differences in surface (TSC) and layer temperatures (TEMP(1)) divided by

distance (DIST(1)).

$$337. \quad \text{FLOW}(1) = (\text{TSC} - \text{TEMP}(1)) * \text{KOND}(1) / \text{DIST}(1).$$

The saturated humidity of the air at the soil surface (HS) is calculated with Murray's equation.

$$338. \quad \text{HS} = 1.323 * \text{EXP}(17.27 * \text{TSC} / (237.3 + \text{TSC})) / (273.16 + \text{TSC}) \quad (46)$$

The absolute humidity (HS) is calculated by,

$$340. \quad \text{HS} = \text{HS} * \text{EXP}(\text{PPOT}(1)) / (46.97 * (\text{TSC} + 273.16)) \quad (46)$$

Evaporation (EVAP) is the quotient of the difference in humidities of soil surface and the atmosphere and the boundary layer resistance.

$$342. \quad \text{EVAP} = (\text{HS} - \text{HA}) / (\text{RA} * 1000.0) \quad (34)$$

The latent heat of vaporization (LH) as a function of the soil surface temperature is given by (Forsythe, 1964).

$$343. \quad \text{LH} = 2.94963\text{E}09 - 2.247\text{E}06 * \text{TSC} \quad (64)$$

and LH as a function of temperature is plotted in Figure 13.

Net radiation (NR) at the soil surface is calculated by difference from the energy balance equation.

$$344. \quad \text{NR} = \text{FLOW}(1) + (\text{TSC} - \text{TAC}) * \text{SH} / \text{RA} + \text{LH} * \text{EVAP} \quad (70)$$

A diagram illustrating the energy and water flux in the top two layers of the soil system is given in Figure 14.

***17) CALCULATION OF DETAIN, INFILTRATION, AND INCAP (lines 346-359)

The amount of water that remains on the soil surface (DETAIN) is defined as the integral between the initial value and the difference between the rainfall rate (RAIN) and the infiltration rate (INFILT). In CSMP III, this is accomplished by an INTGRL statement.

$$346. \quad \text{DETAIN} = \text{INTGRL}(0.0, \text{RAIN} - \text{INFILT}) \quad (18)$$

The infiltration capacity (INCAP) is the Darcian flux to the center

ORIGINAL PAGE IS
OF POOR QUALITY

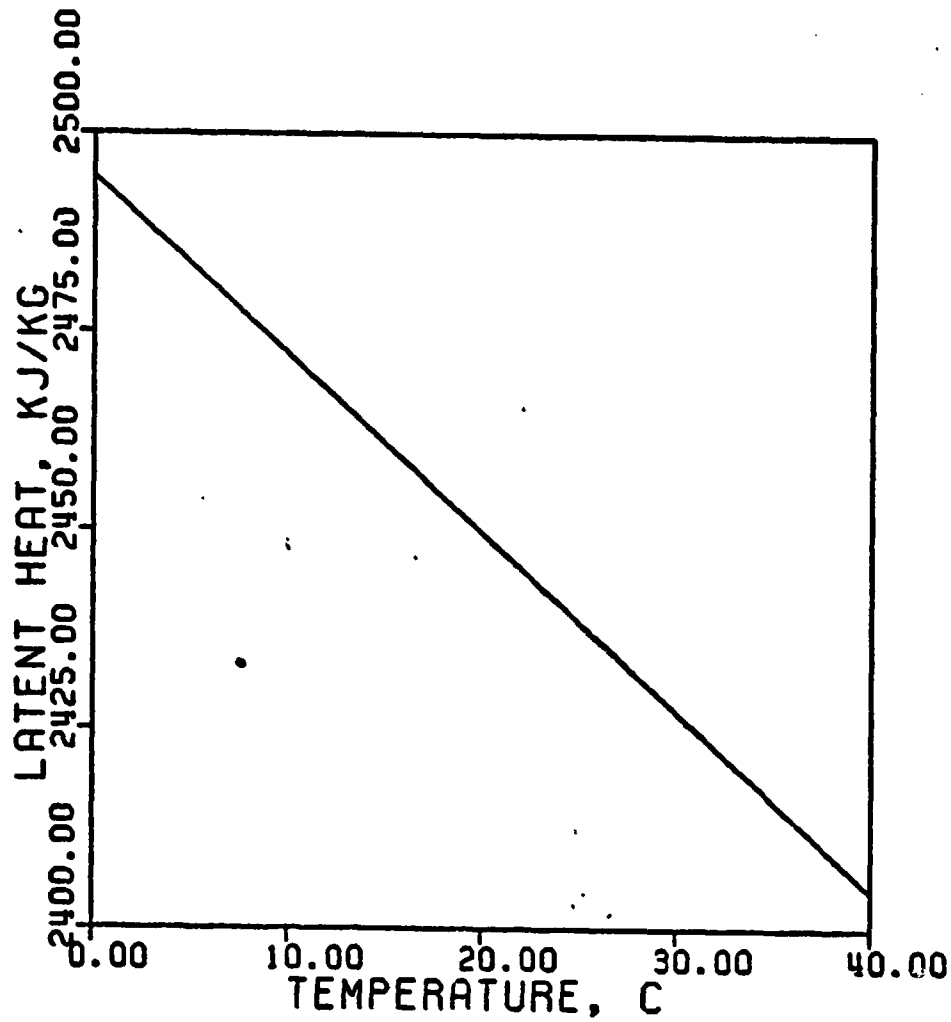


Figure 13. Latent heat of vaporization (LH) as a function of temperature.

ORIGINAL FIGURE 13
OF POOR QUALITY

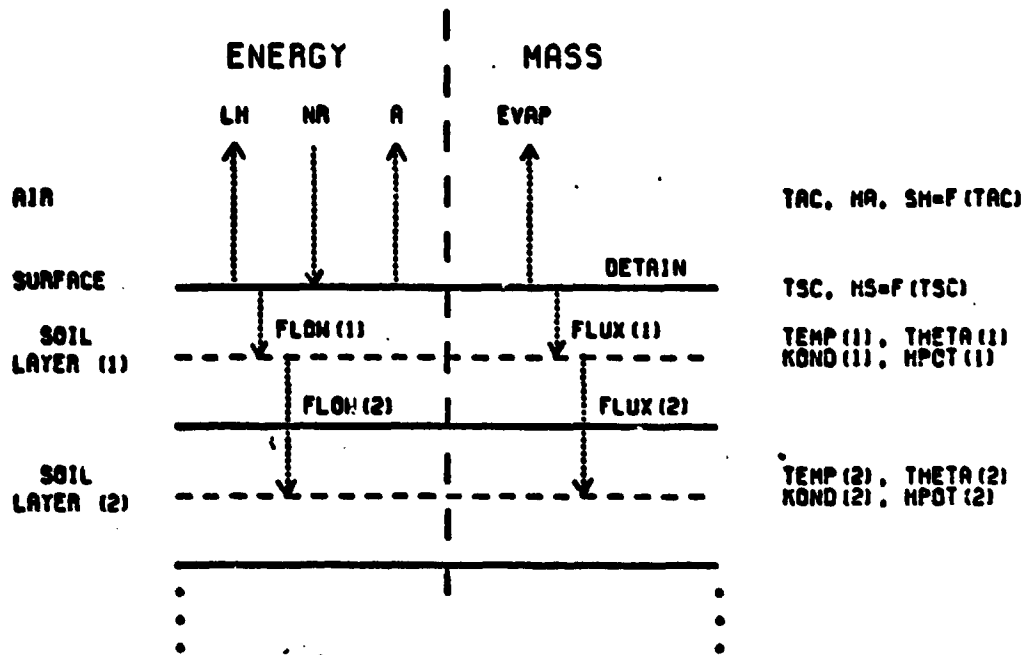


Figure 14. Schematic diagram of the energy and mass flux in the top two layers of the soil system.

of the first layer from the saturated soil surface, at which the pressure potential is assigned a value of zero.

$$347. \quad \text{INCAP} = (0.0 - \text{HPOT}(1)) * 0.5 * (\text{SATCON} + \text{COND}(1)) / \text{DIST}(1) \quad (49)$$

Since the model assumes no runoff, only two possibilities exist with rainfall, and these are:

1) When the rainfall rate does not exceed the infiltration capacity and there is no detention on the soil surface, then the rainfall rate controls the infiltration rate.

$$358. \quad \text{IF}(\text{RAIN.LT.INCAP.AND.DETAIN.LE.0}) \text{INFILT}=\text{RAIN}$$

2) When the rainfall rate exceeds the infiltration capacity of the soil and water is detained on the soil surface, the infiltration capacity controls the infiltration rate.

$$357. \quad \text{INFILT} = \text{INCAP} \quad (51)$$

The logical branching of the above calculations is illustrated by the flow chart in Figure 15.

***18) CALCULATION OF NET FLOW OF HEAT AND NET FLUX OF WATER (lines 361-365)

The flux of water into the middle of the soil surface layer is equal to the difference in the rate of infiltration and the rate of evaporation.

$$361. \quad \text{FLUX}(1) = \text{INFILT} - \text{EVAP}$$

The heat flow into the bare soil surface ($\text{FLOW}(1)$) was previously defined as,

$$337. \quad \text{FLOW}(1) = (\text{TSC} - \text{TEMP}(1)) * \text{KOND}(1) / \text{DIST}(1)$$

The flux of water ($\text{FLUX}(I)$) and flow of heat ($\text{FLOW}(I)$) for the rest of the layers must obey the continuity equation that is,

$$\text{NFLOW}(I) = \text{FLOW}(I) - \text{FLOW}(I-1) \quad (66)$$

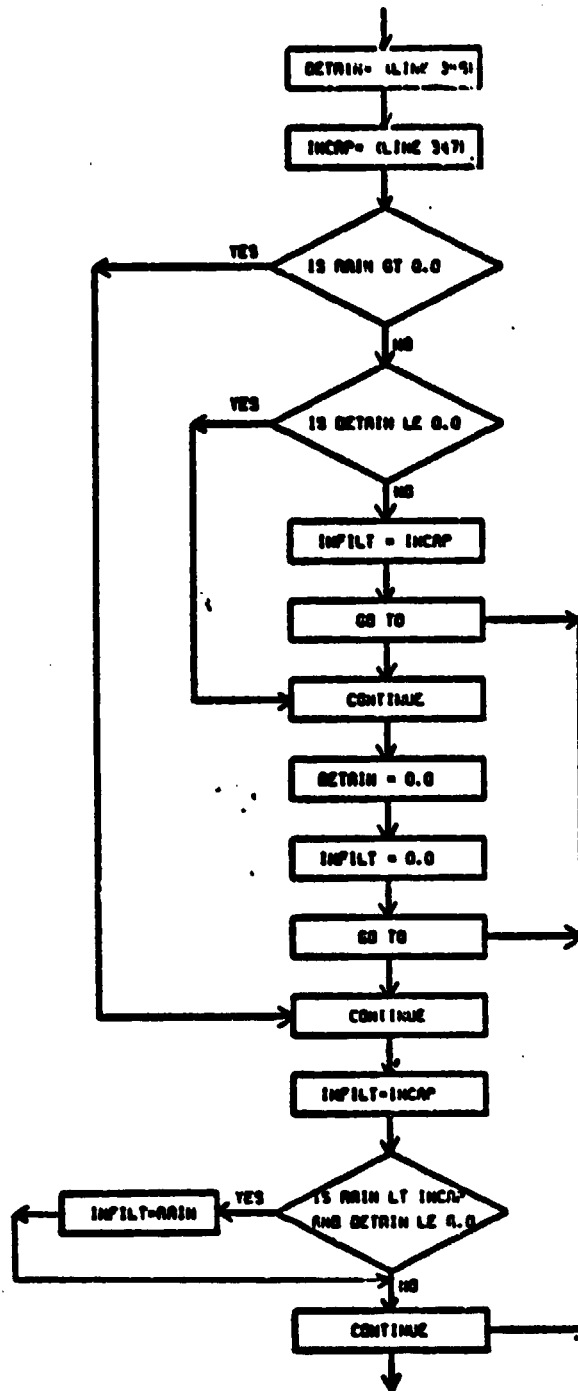


Figure 15. Flowchart showing the logical branching used to calculate INFILT and DETAIN.

$$\text{NFLUX}(I) = \text{FLUX}(I) - \text{FLUX}(I+1) \quad (67)$$

***19) INTEGRATION OF VOLUMETRIC HEAT CONTENT AND VOLUMETRIC WATER CONTENT (lines 368-369)

The 13 integrations to keep track of the volumetric heat contents (VOLH(I)) and volumetric water contents (VOLW(I)) are carried out by the CSMP III INTGRL function.

$$368. \quad \text{VOLH1} = \text{INTGRL}(\text{IVOLH1}, \text{NFLOW1}, 13) \quad (105)$$

$$369. \quad \text{VOLW1} = \text{INTGRL}(\text{IVOLW1}, \text{NFLUX1}, 13) \quad (106)$$

The third argument of the integral function indicates that there are 13 integrals to keep track of the volumetric heat content and water content of the 13 layers. The heat contents are stored in an array VOLH(I) and the water contents are stored in an array VOLW(I). Note that these arrays are named in the INITIAL section (lines 23 and 29). The first argument of the integral function states that the initial value of the volumetric heat content and volumetric water content is given by an array IVOLH(I) and IVOLW(I), respectively. The second argument states that the flow and flux rate into the integral is given by the array NFLOW(I) for heat and NFLUX(I) for water.

***20) CALCULATION OF CUMULATIVE RAIN, INFILTRATION, EVAPORATION, AND DRAINAGE (lines 372-375)

Cumulative rain (CUMRN), cumulative infiltration (CUMINF), cumulative evaporation (CUMEVP), and cumulative drainage (CUMDRN) are calculated with the CSMP III INTGRL function.

$$372. \quad \text{CUMRN} = \text{INTGRL}(0.0, \text{RAIN}) \quad (11)$$

$$373. \quad \text{CUMINF} = \text{INTGRL}(0.0, \text{INFILT}) \quad (10)$$

374. CUMEVP = INTGRL(0.0, EVAP) (9)

375. CUMDRN = INTGRL(0.0, FLXNLL) (8)

***21) CALCULATION OF TOTAL WATER FOR DIFFERENT LAYERS (lines 377-392)

The integrated volume of water in the profile, from a given depth to the bottom of the profile, is the sum of the volume of water in each layer starting at the specified depth.

1) From 0.0 - 1.20 m (CUMWTR) (I=1, NL)

382. CUMWTR = CUMWTR+VOLW(I) (12)

2) From 0.13 - 1.20 m (CUMWT1) (I = 6,NL)

385. CUMWT1 = CUMWT1 + VOLW(I) (13)

3) From 0.30 - 1.20 m (CUMWT2) (I=9,NL)

388. CUMWT2 = CUMWT2+VOLW(I) (14)

4) From 0.75 - 1.20 m (CUMWT3) (I=12,NL)

391. CUMWT3 = CUMWT3 + FLOW(I) (15)

***22) CALCULATION OF DAILY TOTALS (lines 394-404)

The daily totals of infiltration (DINF), rain (DRN), evaporation (DEVP), and drainage (DDRN) are calculated by difference from the accumulated totals and the values at the previous midnight.

400. DINF = CUMINF - INF(DNUM - 2) (20)

401. DRN = CUMRN - RN(DNUM - 2) (30)

402. DEVP = CUMEVP - EVP(DNUM - 2) (19)

403. DDRN = CUMDRN - DRAIN(DNUM - 2) (16)

The daily totals are calculated only at the end of a day and the calculations are controlled by the IMPULS statement.

394. ZBHJS = IMPULS(86400.,86400.),

***23) CHECK WATER BALANCE (line 406)

The water balance for the soil system (BALANS) is calculated as the difference in the sum of cumulative water in the profile (CUMWTR), cumulative evaporation (CUMEVP), and cumulative drainage (CUMDRN) and the sum of the initial water content (IWATER) and the cumulative infiltration (CUMINF).

$$406. \quad \text{BALANS} = \text{CUMWTR} - \text{IWATER} - \text{CUMINF} + \text{CUMEVP} + \text{CUMDRN} \quad (5)$$

The deviation of BALANS from zero provides an indication of the error produced in the solution of the equations in the model.

***24) OUTPUT OF DESIRED VARIABLE (lines 408-428)

The last paragraph of the DYNAMIC section deals with output of calculated variables. Specifically, the following variables are printed at 8:00 and 16:00 hours, standard time: DEPTH(I), THETA(I), PPOT(I), FLUX(I), NFLUX(I), and TEMP(I)

The output at 8:00 hours is controlled by the IMPULS statement.

$$408. \quad Z = \text{IMPULS}(28800.0., 86400.)$$

and the output at 16.0 hours is controlled by the IMPULS statement.

$$425. \quad \text{ZZ} = \text{IMPULS}(57600.0., 86400.0)$$

E. TERMINAL SECTION (lines 433-466)

The terminal section is mainly composed of execution control statements. The statements that appear in the TERMINAL section are:

$$1) \quad \text{TIMER} \quad \text{FINTIM} = 259200., \text{PRDEL} = 84600.0, \text{DELT} = 100.0$$

The **TIMER** card is used to specify the variables that control the run-time, print increment, and integration interval (step-size):

a) **FINTIM** determines the value of **TIME** (independent variable) at which the run is terminated. **FINTIM** is set equal to the desired simulation time.

b) **PRDEL**. This **TIMER** variable controls the increment for the output of the **PRINT** statement.

c) **DELT**. This **TIMER** variable specifies the integration interval.

2) **PRINT**. The **PRINT** card is used to specify the variables that will be printed at each specified interval (**PRDEL**) during the simulation.

3) **METHOD TRAPZ**. The integration technique is specified by the use of the **METHOD** card with the appropriate **CSMP III** integration name. In this case, the selected method is the trapezoidal (**TRAPZ**) method that uses a fixed integration interval (**DELT**).

4) **END**. The **END** card specifies the end of the program.

The last segment of the program is a list of the input data stored in the two dimensional array **WINPUT**. It is specified between the lines **INPUT** and **ENDINPUT**. This array must match the **FORMAT** statement of line 58.

The program ends with the lines

```
464.    STOP
465.    ENDJOB
466.    /*END
```

The **ENDJOB** card must begin in the first column.

V DESCRIPTION OF OUTPUT OF THE MODEL

To provide the user with an example of the output of this model, the program described in section IV of this document was executed for a period of three days.

The output of the model consists of two parts:

1) The first part is generated in the DYNAMIC section (paragraph 24), and for each simulated day an output at 8:00 am and 4:00 pm is printed. The variables printed for each soil layer are: DEPTH, THETA, PPOT, FLUX, NFLUX, and TEMP.

2) The second part of the output is generated with the PRINT card the TERMINAL section. The variables printed for midnight at the end of each day of the simulation period are: JDNUM, XDNUM, DRN, DINF, DEVP, DDRN, CUMWTR, CUMWT1, CUMWT2, CUMWT3, BALANS, CUMRN, CUMDRN, CUMINF, CUMEVP, and FLOW(14).

It should be noted that for a fixed integration method, such as TRAPZ, the integration interval (DELT) necessary for execution of the model may have to be adapted to the input data. Our experience with this model, using TRAPZ, suggests a DELT of 100 seconds for input data with rain, and 200 seconds for input data with no rain. However, the user has a choice of other integration methods and should consult the CSMP III manual for proper use.

ORIGINAL PAGE IS OF POOR QUALITY

WATER AND HEAT BALANCE OF BARE SOIL- NO RUNOFF
VAN GAVEL - LASCANO 21 MAY 1979
PROGRAM USED FOR USER'S GUIDE PREPARATION
CONSERVATION VARIATIONS

JULIAN DAY NUMBER	1. TIME	26000.0 ROMAN	PPOT	FLUX	NET FLUX	TEMP
1	0.5000E-02	0.3400E 00	-0.3334E 00	-0.2674E-07	-0.6991E-08	0.3430E 01
1	0.2100E-01	0.3450E 00	-0.3204E 00	-0.1075E-07	-0.1114E-07	0.3494E 01
2	0.4000E-01	0.3470E 00	-0.2767E 00	-0.8406E-03	-0.9771E-08	0.3433E 01
4	0.6500E-01	0.3403E 00	-0.2828E 00	0.1165E-03	-0.1445E-07	0.4009E 01
5	0.9500E-01	0.3400E 00	-0.2390E 00	0.1562E-07	-0.1506E-07	0.5506E 01
6	0.1300E 00	0.3469E 00	-0.2911E 00	0.3145E-07	-0.2124E-07	0.6776E 01
7	0.1750E 00	0.3465E 00	-0.2857E 00	0.5272E-07	-0.2670E-07	0.8319E 01
8	0.2250E 00	0.3770E 00	-0.4673E 00	0.7341E-07	-0.1768E-07	0.9744E 01
9	0.3000E 00	0.3640E 00	-0.4288E 00	0.9109E-07	-0.1768E-07	0.1141E 02
10	0.4000E 00	0.3875E 00	-0.3829E 00	0.1604E-03	-0.6343E-07	0.1254E 02
11	0.5250E 00	0.3425E 00	-0.2375E 00	0.2238E-03	-0.8779E-07	0.1328E 02
12	0.7100E 00	0.4021E 00	-0.2374E 00	0.3116E-04	-0.8779E-07	0.1418E 02
13	0.1050E 01	0.4092E 00	-0.2149E 00	0.5131E-03	-0.1443E-06	0.1522E 02

JULIAN DAY NUMBER	1. TIME	57600.0 ROMAN	PPOT	FLUX	NET FLUX	TEMP
1	0.5000E-02	0.342E 00	-0.1806E 01	-0.6558E-07	-0.3551E-06	0.1050E 02
1	0.2000E-01	0.354E 00	-0.1039E 01	-0.6240E-07	-0.2117E-07	0.1064E 02
2	0.4000E-01	0.360E 00	-0.7075E 00	-0.413E-07	-0.1193E-07	0.1068E 02
4	0.6500E-01	0.374E 00	-0.5441E 00	-0.2948E-07	-0.1790E-07	0.1033E 02
5	0.9500E-01	0.371E 00	-0.444E 00	-0.1199E-07	-0.1255E-07	0.1032E 02
6	0.1300E 00	0.3788E 00	-0.435E 00	0.9470E-03	-0.1293E-07	0.1010E 02
7	0.1750E 00	0.377E 00	-0.4673E 00	0.1300E-07	-0.1408E-07	0.1001E 02
8	0.2250E 00	0.3403E 00	-0.447E 00	0.2858E-07	-0.6353E-08	0.1021E 02
9	0.3000E 00	0.3642E 00	-0.5075E 00	0.3493E-07	-0.3501E-07	0.1084E 02
10	0.4000E 00	0.3731E 00	-0.5345E 00	0.7594E-07	-0.3036E-07	0.1195E 02
11	0.5250E 00	0.3781E 00	-0.4732E 00	0.143E-04	-0.5620E-07	0.1313E 02
12	0.7500E 00	0.365E 00	-0.374E 00	0.1704E-04	-0.1213E-04	0.1439E 02
13	0.1050E 01	0.3647E 00	-0.3100E 00	0.2919E-03	-0.1205E-04	0.1533E 02

JULIAN DAY NUMBER	2. TIME	115200.0 ROMAN	PPOT	FLUX	NET FLUX	TEMP
1	0.5000E-02	0.344E 00	-0.1891E 01	-0.2637E-07	-0.6333E-08	0.3055E 01
1	0.2000E-01	0.347E 00	-0.1513E 01	-0.1603E-07	-0.4164E-08	0.2902E 01
2	0.4000E-01	0.350E 00	-0.1192E 01	-0.1367E-07	-0.3300E-08	0.3190E 01
4	0.6500E-01	0.3570E 00	-0.9634E 00	-0.1004E-07	-0.3150E-08	0.3626E 01
5	0.9500E-01	0.362E 00	-0.833E 00	-0.6710E-03	-0.4102E-06	0.4451E 01
6	0.1300E 00	0.364E 00	-0.7670E 00	-0.2612E-03	-0.5290E-08	0.5541E 01
7	0.1750E 00	0.364E 00	-0.7545E 00	0.2806E-03	-0.6101E-08	0.6930E 01
8	0.2250E 00	0.360E 00	-0.8720E 00	0.8707E-03	-0.5004E-08	0.8304E 01
9	0.3000E 00	0.350E 00	-0.8104E 00	0.1307E-07	-0.2478E-07	0.1003E 02
10	0.4000E 00	0.354E 00	-0.7417E 00	0.3865E-07	-0.2420E-07	0.1155E 02
11	0.5250E 00	0.342E 00	-0.669E 00	0.6205E-07	-0.2324E-07	0.1284E 02
12	0.7500E 00	0.370E 00	-0.5632E 00	0.9608E-07	-0.6014E-07	0.1436E 02
13	0.1050E 01	0.370E 00	-0.4890E 00	0.1422E-04	-0.7512E-07	0.1520E 02

ORIGINAL PAGE IS
OF PCOR QUALITY

JULIAN DAY NUMBER	DEPTH	2. TIME	14400.0 XMMUM	PPOT	FLUX	NET FLUX	TEMP
1	0.500E-02	0.4372 00	0.0	0.4373-04	-0.3510E-04	0.1013E 02	
2	0.200E-01	0.4186E 00	-0.9466E-02	0.7891E-04	-0.5392E-04	0.1023E 02	
3	0.400E-01	0.4202E 00	0.0	0.2495E-04	-0.5732E-04	0.1003E 02	
4	0.500E-01	0.4172L 00	-0.1945E-01	0.8232E-04	0.3111E-04	0.5774E 01	
5	0.950E-01	0.4166E 00	-0.2526E-01	0.5121E-04	-0.8085E-07	0.0349E 01	
6	0.1300E 00	0.4136E 00	-0.4456E-01	0.5970E-04	0.1720E-07	0.8981E 01	
7	0.170E 00	0.4046E 00	-0.9460E-01	0.5797E-04	0.4392E-08	0.0714E 01	
8	0.225E 00	0.3937E 00	-0.3019E 00	0.5733E-04	0.1678E-07	0.0722E 01	
9	0.300E 00	0.3747E 00	-0.5660E 00	0.5645E-04	0.1186E-06	0.0280E 01	
10	0.400E 00	0.3710E 00	-0.6430E 00	0.4380E-04	0.1434E-04	0.1057E 02	
11	0.525E 00	0.3643E 00	-0.6464E 00	0.2946E-04	0.1414E-04	0.1223E 02	
12	0.750E 00	0.3440E 00	-0.6246E 00	0.1331E-04	0.7117E-04	0.1470E 02	
13	0.1050E 01	0.3708E 00	-0.6449E 00	0.1466E-04	-0.4681E-07	0.1521E 02	

JULIAN DAY NUMBER	DEPTH	3. TIME	20160.0 XMMUM	PPOT	FLUX	NET FLUX	TEMP
1	0.500E-02	0.3734E 00	-0.5247E 00	-0.2242E-07	-0.7506E-08	0.2695E 01	
2	0.200E-01	0.3749L 00	-0.4474E 00	-0.1591E-07	-0.6970E-08	0.2742E 01	
3	0.400E-01	0.3791E 00	-0.4496E 00	-0.6446E-08	-0.5744E-08	0.2901E 01	
4	0.500E-01	0.3796E 00	-0.4202E 00	-0.1195E-08	-0.6248E-08	0.3298E 01	
5	0.950E-01	0.3831E 00	-0.4082E 00	0.5833E-08	-0.5835E-08	0.4491E 01	
6	0.1300E 00	0.3796E 00	-0.4167E 00	0.1004E-07	-0.9243E-08	0.5039E 01	
7	0.170E 00	0.3740E 00	-0.4467E 00	0.2011E-07	-0.1368E-07	0.6323E 01	
8	0.225E 00	0.3645E 00	-0.7517E 00	0.3301E-07	-0.7444E-08	0.7560E 01	
9	0.300E 00	0.3593E 00	-0.7801E 00	0.4121E-07	-0.3835E-07	0.9145E 01	
10	0.400E 00	0.3494E 00	-0.6579E 00	0.7643E-07	-0.3188E-07	0.1056E 02	
11	0.525E 00	0.3470E 00	-0.6124E 00	0.1601E-06	-0.3926E-07	0.1184E 02	
12	0.750E 00	0.3708E 00	-0.5449E 00	0.1471E-06	-0.4222E-07	0.1344E 02	
13	0.1050E 01	0.3715E 00	-0.5540E 00	0.1091E-06	-0.6329E-08	0.1484E 02	

JULIAN DAY NUMBER	DEPTH	3. TIME	23040.0 XMMUM	PPOT	FLUX	NET FLUX	TEMP
1	0.500E-02	0.3544 00	-0.2955E 01	-0.6377E-07	-0.0777E-00	0.1023E 02	
2	0.200E-01	0.3496E 00	-0.1547E 01	-0.6550E-07	-0.1384E-07	0.1023E 02	
3	0.400E-01	0.3596E 00	-0.9924E 00	-0.4094E-07	-0.1613E-07	0.1309E 02	
4	0.500E-01	0.3672E 00	-0.843E 00	-0.2401E-07	-0.1201E-07	0.0400E 01	
5	0.950E-01	0.3716E 00	-0.5304E 00	-0.1291E-07	-0.1291E-07	0.937E 01	
6	0.1300E 00	0.3726E 00	-0.5502E 00	0.8101E-06	-0.1173E-07	0.6961E 01	
7	0.170E 00	0.3646E 00	-0.608E 00	0.1254E-07	-0.9526E-08	0.0637E 01	
8	0.225E 00	0.3614E 00	-0.6546E 00	0.2244E-07	-0.5467E-08	0.6431E 01	
9	0.300E 00	0.3586E 00	-0.6105E 00	0.2713E-07	-0.2559E-07	0.9663E 01	
10	0.400E 00	0.3534E 00	-0.7538E 00	0.2331E-07	-0.2424E-07	0.1016E 02	
11	0.525E 00	0.3603E 00	-0.6082E 00	0.7717E-07	-0.3178E-07	0.1194E 02	
12	0.750E 00	0.3440E 00	-0.6190E 00	0.1049E-06	-0.4697E-07	0.1341E 02	
13	0.1050E 01	0.3695E 00	-0.5811E 00	0.1543E-06	-0.2903E-07	0.1470E 02	

ORIGINAL PAGE IS
OF POOR QUALITY

TIME	00-100.	1.7200E 03	2.5020E 03
JONAS	1.0000	3.0000	4.0000
RONAN	1.0000	3.0000	4.0000
CON	0.0	2.0000E-02	0.3
DIAP	0.0	2.50310E-02	0.0
CEVP	0.0	3.26261E-03	3.2303E-03
DSM	0.0	1.92001E-02	1.53041E-02
CUMST8	0.0	0.0000	0.13030
CUMST1	0.0	0.00738	0.39107
CUMST2	0.0	0.35391	0.51001
CUMST3	0.0	0.22201	0.21043
BALANS	0.0	-1.30203E-04	-2.1000E-04
CUMSRN	0.0	2.0990E-02	2.0990E-02
CUMSR	0.0	7.21317E-02	8.0330E-02
CUMSTP	0.0	2.50310E-02	2.50310E-02
FLOW(10)	3.9100E-03	0.7750E-03	1.0010E-02
	1.1000	-2.0000	-5.5330

REFERENCES

1. Brunt, D. 1932. Notes on radiation in the atmosphere. *Quarterly J. of Royal Met. Society.* 58:380-420.
2. De Vries, D.A. 1966. Thermal properties of soils. In: Van Wijk (Ed), *Physics of Plant Environment*, 2nd edition, pp 210-235. N. Holland Publ. Co.
3. Forsythe, W.E. 1964. *Smithsonian Physical Tables*. Smithsonian Institution. Publication 4169. 827pp.
4. Hillel, D.I., C.H.M. van Bavel, and H. Talpaz. 1975. Dynamic simulation of water storage in fallow soil as affected by mulch of hydrophobic aggregates. *Soil Sci. Soc. Amer. Proc.* 39:826-833.
5. Horton, Robert. 1977. Field test of hydrophobic soil clod mulch for soil water conservation in a semiarid area. M.S. Thesis, Texas A&M University, 114pp.
6. Humphreys, K.B. 1979. Comparison of methods for determining soil hydraulic characteristics. M.S. Thesis, Texas A&M University, 91pp.
7. IBM Corporation. 1975. Continuous System Modeling Program III (CSMP III). Program Reference Manual. SH19-7001-3. Data Processing Division, 112 East Post Road, White Plains, New York 10601, 205pp.
8. Jackson, R.D. 1972. On the calculation of hydraulic conductivity. *Soil Sci. Soc. Amer. Proc.* 36:380-382.
9. Marek, T.H. 1977. Hydraulic characteristics of short, blocked irrigation furrows. M.S. Thesis, Texas A&M University, 135pp.
10. Murray, F.W. 1967. On the computation of saturation vapor pressure. *J. of Appl. Met.* 6:203-205.
11. Saffaf, A.Y. 1966. Field determination of hydraulic conductivity of Norwood silt loam. M.S. Thesis, Texas A&M University, 111pp.
12. Sellers, W.D. 1965. *Physical Climatology*. U. of Chicago Press. 272pp.
13. Van Bavel, C.H.M., and D.I. Hillel. 1975. A simulation study of soil heat and moisture dynamics as affected by a dry mulch. *Proc. 1975 Summer Computer Simulation Conf.*, pp815-821, San Francisco, Cal. Simulation Councils, Inc., La Jolla, Cal.

14. Van Bavel, C.H.M., and D.I. Hillel. 1976. Calculating potential and actual evaporation from a bare soil surface by simulation of concurrent flow of water and heat. Agric. Meteorol. 17:453-476.

VII APPENDICES

APPENDIX A - GLOSSARY OF VARIABLE NAMES

TITLE: GLOSSARY FOR HEAT AND WATER BALANCE MODEL

NO.....	TERM.....	DEFINITION.....	UNITS
1.	A.....	SENSIBLE HEAT FLUX INTO THE AIR.....	W/M**2
2.	ALB.....	ALBEDO.....	-
3.	AVCOND(I) ..	AVERAGE HYDRAULIC CONDUCTIVITY..... .. BETWEEN ADJACENT LAYERS.....	M/S
4.	AVKOND(I) ..	AVERAGE THERMAL CONDUCTIVITY..... .. BETWEEN ADJACENT LAYERS.....	W/(M*C)
5.	BALANS.....	WATER BALANCE.....	M
5.	BEGIN.....	BEGINNING OF RAINFALL PERIOD.....	HOURS
7.	COND(I)	HYDRAULIC CONDUCTIVITY OF LAYER (I)	M/S
8.	CUMDRN.....	CUMULATIVE DRAINAGE.....	M
9.	CUMEV.....	CUMULATIVE EVAPORATION.....	M
10.	CUMINF.....	CUMULATIVE INFILTRATION.....	M
11.	CUMRN.....	CUMULATIVE RAIN.....	M
12.	CUMWTR.....	TOTAL WATER IN SOIL PROFILE.....	M
13.	CUMWT1.....	TOTAL WATER (I=6,NL).....	M
14.	CUMWT2.....	TOTAL WATER (I=9,NL).....	M
15.	CUMWT3.....	TOTAL WATER (I=12,NL).....	M
16.	DDRN.....	DAILY DRAINAGE.....	M
17.	DEPTH(I)	VERTICAL DISTANCE BETWEEN MIDPOINT.. .. OF LAYER (I) AND THE SURFACE.....	M
18.	DETAIN.....	DEPTH OF WATER ON THE SOIL SURFACE..	M
19.	DEVAP.....	DAILY EVAPORATION.....	M
20.	DINF.....	DAILY INFILTRATION.....	M
21.	DIST(I)	DISTANCE BETWEEN MIDPOINTS OF	M
		.. ADJACENT SOIL LAYERS (I,I+1).....	M
22.	DL.....	DAY LENGTH	HOURS
23.	DNUM.....	DAY COUNTER.....	-
24.	DNUM1.....	DAY COUNTER.....	-
25.	DNUM2.....	DAY COUNTER.....	-
26.	DPMAX.....	DEWPOINT TEMP. AT TIME OF TMAX.....	C
27.	DPKIN.....	DEWPOINT TEMP. AT TIME OF TMIN.....	C
28.	DPTC.....	DEWPOINT TEMPERATURE.....	C
29.	DRAIN.....	DRAINAGE.....	M/S
30.	DRN.....	DAILY RAIN.....	M
31.	DWSLOP.....	RAINFALL SLOPE BETWEEN MIDPOINT AND.END.....	MM/HR**2
32.	END.....	END OF RAINFALL PERIOD.....	HOURS
33.	EV.....	EVAPORATION (DUMMY VARIABLE).....	M/S
34.	EVAP.....	EVAPORATION.....	M/S
35.	EVP.....	EVAPORATION (DUMMY VARIABLE).....	M/S
36.	FLOW(I)	FLOW OF HEAT INTO LAYER (I)	W/M**2
37.	FLOW(NLL) ..	FLOW OF HEAT ACROSS THE LOWER..... .. BOUNDARY.....	W/M**2
38.	FLUX(I)	FLUX OF WATER INTO LAYER (I)	M/S
39.	FLUX(NLL) ..	FLUX OF WATER ACROSS THE LOWER.....	

40. ..BOUNDARY.....M/S
FTSC.....FINAL TEMPERATURE OF SOIL SURFACE...
.....AS CALCULATED IN THE IMPLICIT LOOP..C
41. GR.....GLOBAL RADIATION.....W/H**2
42. HA.....ABSOLUTE HUMIDITY OF THE AIR.....KG/H**3
43. HEIGHT.....RAINFALL RATE AT MIDPOINT.....MM/HOUR
44. HD.....SATURATED HUMIDITY AT THE SOIL.....
.....SURFACE AND ABSOLUTE HUMIDITY.....KG/H**3
45. HPOT(I).....HYDRAULIC POTENTIAL OF SOIL LAYER...M OF WATER
46. HS.....ABSOLUTE HUMIDITY.....KG/H**3
47. HSO.....ABSOLUTE HUMIDITY, DUMMY VARIABLE...KG/H**3
48. HTIME.....TIME.....HOURS
49. INCAP.....INFILTRATION CAPACITY.....M/S
50. INF.....INFILTRATION.....M
51. INFILT.....INFILTRATION RATE.....M/S
52. ITEMP(I)...INITIAL TEMPERATURE OF LAYER (I)....C
53. IPHETA(I)..INITIAL VOLUMETRIC WATER CONTENT....
.....OF LAYER (I).....M**3/H**3
54. IVHCAP(I)..INITIAL VOLUMETRIC HEAT CAPACITY....
.....OF LAYER (I).....J/(M**3*C)
55. IVOLH(I)...INITIAL AMOUNT OF HEAT IN LAYER (I).J/H**2
56. IVOLW(I)...INITIAL VOLUME OF WATER IN
.....LAYER (I).....M
57. IWATER.....INITIAL TOTAL WATER CONTENT OF.....
.....THE SOIL PROFILE.....M
58. JDNUM.....JULIAN DAY NUMBER..... -
59. KOND(I)....THERMAL CONDUCTIVITY OF LAYER (I)...W/(M*C)
60. KONDA.....THERMAL CONDUCTIVITY OF AIR.....W/(M*C)
61. KONDS.....THERMAL CONDUCTIVITY OF SOIL.....W/(M*C)
62. KONDV.....THERMAL CONDUCTIVITY BY WATER VAPOR.W/(M*C)
63. KONDW.....THERMAL CONDUCTIVITY BY WATER.....W/(M*C)
64. LH.....LATENT HEAT OF VAP. OF WATER.....J/H**3
65. HDPNT.....MIDPOINT OF RAINFALL PERIOD.....HOURS
66. NFLOW(I)...NET FLOW OF HEAT INTO LAYER (I)....W/H**2
67. NPLUX(I)...NET FLUX OF WATER INTO LAYER (I)....M/S
68. NL.....NUMBER OF LAYERS..... -
69. NLL.....NL + 1..... -
70. NR.....NET RADIATION AT THE SOIL SURFACE...W/H**2
71. PORSTY.....POROSITY OF THE SOIL..... -
72. PPOT(I)....PRESSURE POTENTIAL OF LAYER (I).....M OF WATER
73. RA.....BOUNDARY LAYER RESISTANCE.....S/M

74. RAIN.....RAINFALL RATE.....M/S
75. RFT.....TOTAL RAINFALL BETWEEN BEGIN AND ...
.....END.....MM
76. RHS.....RELATIVE HUMIDITY OF THE SOIL SURFACE -
78. RN.....RAIN (DUMMY VARIABLE).....M
78. S.....CONDUCTION OF ENERGY INTO THE SOIL..
.....SURFACE.....W/M**2
79. SA.....WINDSPEED.....M/S
80. SATCON.....SATURATED HYDRAULIC CONDUCTIVITY OF.
.....THE SURFACE HORIZON.....M/S
81. SH.....VOLUMETRIC HEAT CAPACITY OF THE AIR.J/(M**3*C)
82. SIGMA.....STEPAN-BOLTZMAN CONSTANT.....W/(M**2*K**4)
83. SKL.....SKY RADIANCE.....W/M**2
84. STINE.....TIME.....HOURS
85. T1.....WATER CONTENT OF FIRST LAYER.....
.....(DUMMY VARIABLE).....M**3/M**3
86. IAC.....TEMPERATURE OF THE AIR.....C
87. TAK.....TEMPERATURE OF THE AIR.....K
88. TAMAX.....MAXIMUM AIR TEMPERATURE.....C
89. TANIN.....MINIMUM AIR TEMPERATURE.....C
90. ICON(I).....THICKNESS OF LAYER (I).....M
91. TENP(I).....TEMPERATURE OF LAYER(I).....C
92. TEVSKO.....SOIL TEMPERATURE VS. THERMAL.....
.....CONDUCTIVITY BY WATER VAPOR.....C VS. W/(M*C)
93. THETA (I).....VOLUMETRIC WATER CONTENT OF LAYER...
.....(I).....M**3/M**3
94. T1V5AL.....VOLUMETRIC WATER CONTENT OF FIRST...
.....SOIL LAYER VS ALHEDO..... -
95. TSC.....TEMPERATURE OF THE SOIL SURFACE.....C
96. TVSC1.....VOLUMETRIC WATER CONTENT VS. HYDRAULIC
.....CONDUCTIVITY FOR FIRST HORIZON..... -
97. TVSC2.....VOLUMETRIC WATER CONTENT VS. HYDRAULIC
.....CONDUCTIVITY FOR SECOND HORIZON..... -
98. TVSP1.....VOLUMETRIC WATER CONTENT VS. PRESSURE
.....POTENTIAL FOR FIRST HORIZON..... -
99. TVSP2.....VOLUMETRIC WATER CONTENT VS. PRESSURE
.....POTENTIAL FOR SECOND HORIZON..... -
100. UPSLOP.....RAINFALL SLOPE BETWEEN BEGIN AND
.....MIDPOINT.....MM/HR**2
101. VHCAP(I).....VOLUMETRIC HEAT CAPACITY OF LAYER (I).J/(M**3*C)
102. VHCAPS.....VOLUMETRIC HEAT CAPACITY OF THE SOIL.J/(M**3*C)
103. VHCAPW.....VOLUMETRIC HEAT CAPACITY OF WATER.....J/(M**3*C)
104. VOLH(I).....VOLUMETRIC HEAT CONTENT OF LAYER (I).....J/M**2
105. VOLW(I).....VOLUME OF WATER PER UNIT AREA OF LAYER
.....(I).....M**3/M**2
106. WINPUT.....ARRAY FOR WEATHER INPUT DATA..... -
107. ZC.....SURFACE ROUGHNESS COEFFICIENT..... -

APPENDIX B - PROGRAM LISTING

```

1.      **** A.....JOB CONTROL LANGUAGE
2.      ****
3.      ****
4.      //SCSDRYJA JOB (R042,403A,003,020,RL),* VAN BAVEL - LASCANO*
5.      /*LEVEL          0
6.      /*JOBPARM R=128
7.      // EXEC CSM@JCLG
8.      //COMPRINT DD DUMMY
9.      //SYSPRINT DD DUMMY
10.     //SYSIN DD *
11.     ****
12.     ****
13.     **** B.....TITLE, MEMORY ORGANIZATION AND ALLOCATION
14.     ****
15.     ****
16.     TITLE          WATER AND HEAT BALANCE OF BARE SOIL- NO RUNOFF
17.     TITLE          VAN BAVEL - LASCANO  21 MAY 1979
18.     TITLE          PROGRAM USED FOR USER'S GUIDE PREPARATION
19.     TITLE          CONSERVB VARIATION#6
20.     ****
21.     STORAGE        TCOM(25),ITHETA(25),DEPTH(25),COND(25),HPOT(25)
22.     STORAGE        AVCOND(25),FLUX(25),PPOT(25),DIST(25)
23.     STORAGE        AVKOND(25),FLOW(25),KOND(25),TEMP(25),VHCAP(25),IVHCAP(25)
24.     /      DIMENSION  VOLW(25),IVOLW(25),NFLUX(25),THETA(25)
25.     /      DIMENSION  TEMP(25),IVOLH(25),VOLH(25),NFLOW(25)
26.     /      DIMENSION  WINPUT(11,37)
27.     /      DIMENSION  INF(38),RN(38),EVP(38),DRAIN(38)
28.     /      EQUIVALENCE (VOLW1,VOLW(1)),(IVOLW1,IVOLW(1)),(NFLUX1,NFLUX(1))
29.     /      EQUIVALENCE (VOLH1,VOLH(1)),(IVOLH1,IVOLH(1)),(NFLOW1,NFLOW(1))
30.     FIXED          I,J,K,NI,NII,ONUM,ONUM1,ONUM2
31.     ****
32.     ****
33.     **** C.....INITIAL SECTION
34.     ****
35.     ****
36.     INITIAL
37.     ****
38.     NOSORT
39.     **** 1) DEFINITION OF PARAMETERS
40.     PAPAMETER      NL=13
41.                   NLL= NL + 1
42.     PARAMETER      KONDS = 4.2
43.     PARAMETER      KONDW = 0.57
44.     PARAMETER      KONDA = 0.025
45.     PARAMETER      VHCAPS= 1.925E06
46.     PARAMETER      VHCAPW= 4.186E06
47.     PARAMETER      SIGMA = 5.67E-08
48.     PARAMETER      ZO    = 0.01
49.     PARAMETER      SATCON= 0.50E-06
50.     PARAMETER      PORSTY= 0.42
51.     **** 2) DAILY COUNTERS
52.                   DNUM = 1
53.                   DNUM1= 2
54.                   DNUM2= 3
55.     **** 3) READ INPUT DATA
56.                   DO 10 K=1,37
57.                   READ(5,1000)(WINPUT(J,K),J=1,11)
58.                   1000 FORMAT(F5.0,1X,F5.2,9(1X,F4.1))
59.                   IF(WINPUT(1,K).EQ.0.0) GO TO 11
60.                   10 CONTINUE

```

ORIGINAL PAGE IS
OF POOR QUALITY

```

61.          11 CONTINUE
62.      **** 4) SPECIFICATION OF THE GEOMETRY OF THE SYSTEM,
63.      **** INITIAL WATER CONTENT AND TEMPERATURE
64.      TABLE      TCOM(1-13)=0.01,0.02,0.02,0.03,0.03,0.04,0.05,0.05....
65.                      0.10,0.10,0.15,0.30,0.30
66.      TABLE      ITHETA(1-13)=13*0.42
67.      TABLE      ITEMP(1-13)=3.57,4.92,6.52,8.17,9.66,10.84,11.69....
68.                      12.08,12.18,12.26,12.69,13.81,15.22
69.      **** 5) CALCULATION OF DISTANCE AND DEPTH
70.          DEPTH(1) = 0.5*TCOM(1)
71.          DIST(1) = DEPTH(1)
72.          DO 20 I=2,NL
73.          DIST(I) = 0.5*(TCOM(I-1)+TCOM(I))
74.          DEPTH(I) = DEPTH(I-1) + 0.5*(TCOM(I-1)+TCOM(I))
75.      20 CONTINUE
76.      **** 6) CALCULATION OF INITIAL WATER AND TEMPERATURE CONDITIONS
77.      **** FLUX REFERS TO WATER
78.      **** FLOW REFERS TO HEAT
79.          IWATER = 0.0
80.          DO 30 I=1,NL
81.          IVHCAP(I) = VHCAPW*ITHETA(I)+(1.0-PORSTY)*VHCAPS
82.          IWATER = IWATER + TCOM(I)*ITHETA(I)
83.          IVOLH(I) = ITEMP(I)*TCOM(I)*IVHCAP(I)
84.          NFLUX(I) = 0.0
85.          NFLOW(I) = 0.0
86.          IVOLW(I) = ITHETA(I)*TCOM(I)
87.      30 CONTINUE
88.      ****
89.      ****
90.      **** HYDRAULIC CHARACTERISTICS OF FIRST HORIZON 0.0-0.20 M
91.      **** VOLUMETRIC WATER CONTENT VS. PRESSURE POTENTIAL
92.      **** IN M WATER COLUMN
93.      FUNCTION TVSP1 = ( 0.030, -29000.00), ...
94.                      ( 0.050, -16000.00), ...
95.                      ( 0.070, -10000.00), ...
96.                      ( 0.090, -6000.00), ...
97.                      ( 0.110, -3000.00), ...
98.                      ( 0.130, -1500.00), ...
99.                      ( 0.150, -700.00), ...
100.                     ( 0.170, -370.00), ...
101.                     ( 0.190, -160.00), ...
102.                     ( 0.210, -74.00), ...
103.                     ( 0.230, -45.00), ...
104.                     ( 0.250, -30.00), ...
105.                     ( 0.270, -18.00), ...
106.                     ( 0.290, -11.00), ...
107.                     ( 0.310, -7.20), ...
108.                     ( 0.330, -3.60), ...
109.                     ( 0.350, -1.20), ...
110.                     ( 0.370, -0.60), ...
111.                     ( 0.390, -0.22), ...
112.                     ( 0.410, -0.07), ...
113.                     ( 0.420, 0.00), ...
114.                     ( 1.000, 0.00)
115.      **** VOLUMETRIC WATER CONTENT VS. HYDRAULIC CONDUCTIVITY IN M/S
116.      FUNCTION TVSCI = ( 0.040, 0.1980432E-18), ...
117.                      ( 0.060, 0.1867095E-17), ...
118.                      ( 0.080, 0.9215115E-17), ...
119.                      ( 0.100, 0.3565605E-16), ...
120.                      ( 0.120, 0.1411493E-15), ...
121.                      ( 0.140, 0.6032844E-15), ...

```

ORIGINAL PAGE IS
OF POOR QUALITY

122.	(0.160, 0.2846457E-14), ...
123.	(0.180, 0.1263317E-13), ...
124.	(0.200, 0.6312881E-13), ...
125.	(0.220, 0.3265092E-12), ...
126.	(0.240, 0.1312614E-11), ...
127.	(0.260, 0.4195633E-11), ...
128.	(0.280, 0.1239914E-10), ...
129.	(0.300, 0.3590753E-10), ...
130.	(0.320, 0.9914647E-10), ...
131.	(0.340, 0.3065372E-09), ...
132.	(0.360, 0.1694214E-08), ...
133.	(0.380, 0.8728055E-08), ...
134.	(0.400, 0.5553067E-07), ...
135.	(0.420, 0.5000000E-06), ...
136.	(1.000, 0.5000000E-06)

**** HYDRAULIC CHARACTERISTICS OF SECOND HORIZON 0.20-1.20 M
**** VOLUMETRIC WATER CONTENT VS. PRESSURE POTENTIAL

139.	FUNCTION TVSP2 = (0.020, -760.00), ...
140.	(0.040, -340.00), ...
141.	(0.060, -130.00), ...
142.	(0.080, -60.00), ...
143.	(0.100, -24.00), ...
144.	(0.120, -15.00), ...
145.	(0.140, -10.00), ...
146.	(0.160, -7.40), ...
147.	(0.180, -5.40), ...
148.	(0.200, -4.40), ...
149.	(0.220, -3.40), ...
150.	(0.240, -2.80), ...
151.	(0.260, -2.30), ...
152.	(0.280, -1.90), ...
153.	(0.300, -1.50), ...
154.	(0.320, -1.20), ...
155.	(0.340, -0.94), ...
156.	(0.360, -0.70), ...
157.	(0.380, -0.45), ...
158.	(0.400, -0.27), ...
159.	(0.420, -0.15), ...
160.	(0.440, -0.06), ...
161.	(0.450, 0.00), ...
162.	(1.000, 0.00)

**** VOLUMETRIC WATER CONTENT VS. HYDRAULIC CONDUCTIVITY
FUNCTION TVSC2 =

163.	(0.030, 0.1200167E-14), ...
164.	(0.050, 0.1599529E-13), ...
165.	(0.070, 0.1516890E-12), ...
166.	(0.090, 0.1062001E-11), ...
167.	(0.110, 0.7476516E-11), ...
168.	(0.130, 0.3470373E-10), ...
169.	(0.150, 0.1199559E-09), ...
170.	(0.170, 0.3375351E-09), ...
171.	(0.190, 0.8332817E-09), ...
172.	(0.210, 0.1842094E-08), ...
173.	(0.230, 0.3760615E-08), ...
174.	(0.250, 0.7218816E-08), ...
175.	(0.270, 0.1315320E-07), ...
176.	(0.290, 0.2300420E-07), ...
177.	(0.310, 0.3924749E-07), ...
178.	(0.330, 0.6606643E-07), ...
179.	(0.350, 0.1105485E-06), ...
180.	(0.370, 0.1868858E-06), ...
181.	(0.390, 0.3336319E-06), ...
182.	(0.390, 0.3336319E-06), ...

```

183.          ( 0.410, 0.6711355E-06), ...
184.          ( 0.430, 0.1617800E-05), ...
185.          ( 0.450, 0.6000000E-05), ...
186.          ( 1.000, 0.6000000E-05)
187.  ****      SOIL TEMPERATURE VS. HEAT CONDUCTIVITY BY VAPOR IN W/(M°C)
188.  FUNCTION TEVSKD = ( -1.000, 0.02000), ...
189.          ( 0.000, 0.02470), ...
190.          ( 10.000, 0.04190), ...
191.          ( 20.000, 0.07990), ...
192.          ( 30.000, 0.12600), ...
193.          ( 40.000, 0.24700), ...
194.          ( 50.000, 0.38100), ...
195.          ( 60.000, 0.65000), ...
196.          ( 70.000, 1.17000)
197.  ****      VOLUMETRIC WATER CONTENT OF FIRST LAYER VS. ALBEDO
198.  FUNCTION TIVSAL = ( 0.00, 0.22), ...
199.          ( 0.10, 0.22), ...
200.          ( 0.25, 0.17), ...
201.          ( 1.00, 0.17)
202.  ****
203.  ****
204.  ****  7) TABLE OF THE GEOMETRY OF THE SYSTEM AND ITS INITIAL STATE
205.  ****
206.          WRITE(6,1100)
207.          1100 FORMAT('0 I      TCOM      DEPTH      ITHETA      ITEMP')
208.          DO 40 I=1,NLL
209.              40 WRITE(6,1200) I,TCOM(I),DEPTH(I),ITHETA(I),ITEMP(I)
210.              1200 FORMAT('1H .12,4F10.5)
211.  *****
212.  ****
213.  ****  D.....DYNAMIC SECTION
214.  ****
215.  ****
216.  DYNAMIC
217.  *****
218.  NOSORT
219.  ****
220.  ****  1) DEFINITION OF TIME RELATED VARIABLES
221.          HTIME=TIME/3600.
222.          STIME=AMOD(HTIME,24.)
223.          Y=IMPULS(86400.,86400.)
224.          IF(Y.LT.0.5) GO TO 22
225.          DNUM = DNUM + 1
226.          DNUM1 = DNUM1 + 1
227.          DNUM2 = DNUM2 + 2
228.          22 CONTINUE
229.          XDNUM=FLOAT(DNUM)
230.          JDNUM = WINPUT (1,DNUM)
231.  ****  2) CALCULATION OF HYDRAULIC CHARACTERISTICS OF FIRST HORIZON
232.          DO 50 I=1,8
233.              THETA(I) = VOLW(I)/TCOM(I)
234.              COND(I)=AFGEN( TVSC1,THETA(I))
235.              PPOT(I)=AFGEN( TVSP1,THETA(I))
236.              HPOT(I)=PPOT(I)-DEPTH(I)
237.          50 CONTINUE
238.  ****  3) CALCULATION OF HYDRAULIC CHARACTERISTICS OF SECOND HORIZON
239.          DO 60 I=9,NL
240.              THETA(I) = VOLW(I)/TCOM(I)
241.              COND(I)=AFGEN( TVSC2,THETA(I))
242.              PPOT(I)=AFGEN( TVSP2,THETA(I))
243.              HPOT(I)=PPOT(I)-DEPTH(I)

```

```

244.      60 CONTINUE
245.      **** 4)  CALCULATION OF THERMAL PROPERTIES
246.              DO 70 I=1,NL
247.              VHCAP(I) = VHCAP*THETA(I) + (1.0 - PORSTY)*VHCAPS
248.              TEMP(I) = VOLH(I)/(VHCAP(I)*TCOM(I))
249.              KONDV = AFGEN (TEVSKO,TEMP(I))
250.              KOND(I) = ((1. -PORSTY)*KONDS*0.4 + THETA(I)*KONOW + ...
251.                      (PORSTY - THETA(I))*1.4*(KONOA + KONDV))/ ...
252.                      ((1.-PORSTY)*.4+THETA(I)+(PORSTY-THETA(I))*1.4)
253.      70 CONTINUE
254.      **** 5)  CALCULATION OF AVERAGE CONDUCTIVITIES
255.              DO 80 I = 2,NL
256.              AVKOND(I) = (TCOM(I-1)+TCOM(I))/(TCOM(I-1)/KOND(I-1) ...
257.                      + TCOM(I)/KOND(I))
258.              AVCOND(I)=(COND(I-1)*TCOM(I-1)+COND(I)*TCOM(I))/...
259.                      (TCOM(I-1)+TCOM(I))
260.      80 CONTINUE
261.      **** 6)  SPECIFICATION OF BOUNDARY CONDITIONS FOR FLOW OF HEAT
262.      ****      AND FLUX OF WATER
263.              FLUX(NLL)= COND(NL)
264.              FLOW(NLL)=(TEMP(NL)-TEMP(NL))*KOND(NL)/(TCOM(NL)/2.)
265.      **** 7)  CALCULATION OF FLOW OF HEAT AND FLUX OF WATER
266.              DO 90 I = 2,NL
267.              FLW(I) = (TEMP(I-1) - TEMP(I))*AVKOND(I)/DIST(I)
268.              FLUX(I)=(HPOT(I-1)-HPOT(I))*AVCOND(I)/DIST(I)
269.      90 CONTINUE
270.      **** 8)  USE DAILY RAINFALL DATA, AND CALCULATE DAILY
271.      ****      RAINFALL DISTRIBUTION
272.              BEGIN = WINPUT(9,DNUM)
273.              END = WINPUT(10,DNUM)
274.              RFT = WINPUT(11,DNUM)
275.              RAIN=0.0
276.              IF(RFT.EQ.0.0) GO TO 33
277.              UPSLOP=(4.0*RFT)/((END-BEGIN)**2)
278.              DWSLOP=-UPSLOP
279.              MDPNT=(BEGIN+END)/2.0
280.              HEIGHT=(2.0*RFT)/(END-BEGIN)
281.              IF(STIME.GE-BEGIN.AND.STIME.LE.MDPNT)RAIN=...
282.              (UPSLOP*(STIME-BEGIN))/3600000.0
283.              IF(STIME.GT.MDPNT.AND.STIME.LE.END)RAIN=...
284.              (DWSLOP*(STIME-END))/3600000.0
285.      33 CONTINUE
286.      **** 9)  USE DAY LENGTH AND CALCULATE DAILY DISTRIBUTION OF
287.      ****      GLOBAL RADIATION
288.              DL=WINPUT(2,DNUM)
289.      ****      OGR/86400.*1.E06*24./DL*PI/2.=436.33*OGR/DL
290.              GR=436.33*WINPUT(3,DNUM)/DL*SIN((STIME-12.+DL/2.)...
291.              *3.141/DL)
292.              IF (GR.LE.0.0) GR = 0.0
293.      **** 10) CALCULATION OF ALBEDO
294.              T1 = THETA(I)
295.              ALB =AFGEN(T1VSAL,T1)
296.      **** 11) CALCULATION OF WINDSPEED AND BOUNDARY LAYER RESISTANCE
297.              IF(HTIME.LE.12.) SA=WINPUT(8,DNUM)
298.              IF(HTIME.LE.12.) GO TO 44
299.              IF(STIME.LE.12.)SA=WINPUT(8,DNUM-1)+(STIME+12.)/24.* ...
300.              (WINPUT(8,DNUM)-WINPUT(8,DNUM-1))
301.              IF(STIME.LE.12.) GO TO 44
302.              SA=WINPUT(8,DNUM)+(STIME-12.)/24.*(WINPUT(8,DNUM+1)-...
303.              WINPUT(8,DNUM))
304.      44 CONTINUE

```

```

305.          RA = (ALOG(2.0/20)*2.0)/(0.16*SA)
306.  **** 12)  CALCULATION OF DEWPOINT TEMPERATURE AND ABSOLUTE HUMIDITY
307.          DPMAX=WINPUT(6,DNUM)
308.          DPMIN=WINPUT(7,DNUM)
309.          DPTC=DPMIN+(DPMAX-DPMIN)*(STIME-5.)/10.
310.          IF(STIME.GT.15.)DPMIN=WINPUT(7,DNUM+1)
311.          IF(STIME.GT.15.)DPTC=DPMAX-(DPMAX-DPMIN)*(STIME-15.)/14.
312.          IF(STIME.LT.5.AND.DNUM.GE.2.)DPMAX=WINPUT(6,DNUM-1)
313.          IF(STIME.LT.5.)DPTC=DPMAX-(DPMAX-DPMIN)*(STIME+9.)/14.
314.          MA = 1.323*EXP(17.27*DPTC/(237.3+DPTC))/(273.16+DPTC)
315.  **** 13)  CALCULATION OF TEMPERATURE OF THE AIR AND SH OF THE AIR
316.          TAMAX=WINPUT(4,DNUM)
317.          TAMIN=WINPUT(5,DNUM)
318.          TAC=TAMIN+(TAMAX-TAMIN)*(STIME-5.)/10.
319.          IF(STIME.GT.15.)TAMIN=WINPUT(5,DNUM+1)
320.          IF(STIME.GT.15.)TAC=TAMAX-(TAMAX-TAMIN)*(STIME-15.)/14.
321.          IF(STIME.LT.5.AND.DNUM.GE.2.)TAMAX=WINPUT(4,DNUM-1)
322.          IF(STIME.LT.5.)TAC=TAMAX-(TAMAX-TAMIN)*(STIME+9.)/14.
323.          TAK=TAC+273.16
324.          SH=(1154.8*303.16)/(TAK)
325.  **** 14)  CALCULATION OF SKY IRRADIANCE
326.          SKL=(SIGMA*TAK**4)*(0.605+0.039*SQRT(1410.*MA))
327.  **** 15)  IMPLICIT CALCULATION OF THE SOIL SURFACE TEMPERATURE
328.          TSC = IMPL (TAC,0.01,FTSC)
329.          A = (TSC - TAC)*SH/RA
330.          HO = 1.323*EXP(17.27*TSC / (237.3+TSC )) / (273.16+TSC )
331.          HO=HO*EXP(PPOT(1)/(46.97*(TSC+273.16)))
332.          EV =(HO - MA)/(RA*1000.)
333.          S = GR*(1. - ALB) + SKL - SIGMA*(TSC + 273.16)**4 ...
334.          - A -LH*EV
335.          FTSC = TEMP(1) + S*DEPTH(1)/KOND(1)
336.  **** 16)  CALCULATION OF EVAPORATION AND NET RADIATION
337.          FLOW(1) = (TSC - TEMP(1))*KOND(1)/DIST(1)
338.          HS = 1.323*EXP(17.27*TSC / (237.3+TSC )) / (273.16+TSC )
339.          HSO = HS
340.          HS=HS*EXP(PPOT(1)/(46.97*(TSC+273.16)))
341.          RHS = HS/HSO
342.          EVAP = (HS - MA)/(RA*1000.)
343.          LH=2.49463E09-2.247E06*TSC
344.          NR = FLOW(1) + (TSC - TAC)*SH/RA + LH*EVAP
345.  **** 17)  CALCULATION OF DETAIN, INFILTRATION, AND INCAP
346.          DETAIN = INTGRL (0.0, RAIN-INFILT)
347.          INCAP = (0.-PPOT(1))*0.5*(SATCON+COND(1)) / DIST(1)
348.          IF (RAIN.GT.0.0) GO TO 55
349.          IF (DETAIN.LE.0.0) GO TO 66
350.          INFILT=INCAP
351.          GO TO 77
352.          66 CONTINUE
353.          DETAIN = 0.0
354.          INFILT=0.0
355.          GO TO 77
356.          55 CONTINUE
357.          INFILT = INCAP
358.          IF (RAIN. LT. INCAP. AND. DETAIN. LE. 0.)INFILT=RAIN
359.          77 CONTINUE
360.  **** 18)  CALCULATION OF NET FLOW OF HEAT AND NET FLUX OF WATER
361.          FLUX(1)=INFILT-EVAP
362.          DO 100 I = 1,NL
363.          NFLOW(I) = FLOW(I) - FLOW(I+1)
364.          NFLUX(I)=FLUX(I)-FLUX(I+1)
365.          100 CONTINUE

```

```

366. **** 19) INTEGRATION OF VOLUMETRIC HEAT CONTENT AND VOLUMETRIC
367. **** WATER CONTENT
368. VOLHI=INTGRL(IVOLHI,NFLOW1,13)
369. VOLWI=INTGRL(IVOLWI,NFLUX1,13)
370. **** 20) CALCULATION OF CUMULATIVE RAIN, INFILTRATION, EVAPORATION
371. **** AND DRAINAGE
372. CUMRN = INTGRL (0.0 , RAIN)
373. CUMINF = INTGRL ( 0.0 , INFILT )
374. CUMEVP = INTGRL ( 0.0 , EVAP )
375. CUMDRN = INTGRL ( 0.0 , FLUX(NL) )
376. **** 21) CALCULATION OF TOTAL WATER FOR DIFFERENT LAYERS
377. CUMWTR = 0.0
378. CUMWT1 = 0.0
379. CUMWT2 = 0.0
380. CUMWT3 = 0.0
381. DO 110 I=1,NL
382. CUMWTR=CUMWTR + VOLW(I)
383. 110 CONTINUE
384. DO 120 I=6,NL
385. CUMWT1 = CUMWT1 + VOLW(I)
386. 120 CONTINUE
387. DO 130 I=9,NL
388. CUMWT2 = CUMWT2 + VOLW(I)
389. 130 CONTINUE
390. DO 140 I=12,NL
391. CUMWT3 = CUMWT3 + VOLW(I)
392. 140 CONTINUE
393. **** 22) CALCULATION OF DAILY TOTALS
394. ZBHJS=IMPULS(86400.,86400.)
395. IF(ZBHJS.LT.0.5) GO TO 88
396. INF(DNUM)=CUMINF
397. RN(DNUM)=CUMRN
398. EVP(DNUM)=CUMEVP
399. DRN(DNUM)=CUMDRN
400. DINF=CUMINF-INF(DNUM-2)
401. DRN=CUMRN-RN(DNUM-2)
402. DEVP=CUMEVP-EVP(DNUM-2)
403. DDRN=CUMDRN-DRN(DNUM-2)
404. 88 CONTINUE
405. **** 23) CHECK WATER BALANCE
406. BALANS = CUMWTR - IWATER - CUMINF + CUMEVP + CUMDRN
407. **** 2) OUTPUT OF DESIRED VARIABLES
408. Z=IMPULS(28800.0,86400.)
409. IF(Z.LT.0.5) GO TO 99
410. 222 CONTINUE
411. WRITE(6,1300) *INPUT(1,DNUM),TIME, XDNUM,STIME
412. 1300 FORMAT(' JULIAN DAY NUMBER = ',F4.0,' TIME = ',F10.1,
413. $ ' XDNUM = ',F11.0,' STIME = ',F7.4)
414. WRITE(6,1400)
415. 1400 FORMAT('0 I ',5X,'DEPTH',10X,'THETA',11X,'PPOT',11X,
416. $ 'FLUX',9X,'NET FLUX',10X,'TEMP')
417. DO 150 I=1,NL
418. 150 WRITE(6,1500) I,DEPTH(I),THETA(I),PPOT(I),FLUX(I), ...
419. NFLUX(I),TEMP(I)
420. 1500 FORMAT(13,6E15.4)
421. WRITE(6,1600)
422. 1600 FORMAT(1H ////)
423. GO TO 111
424. 99 CONTINUE
425. ZZ=IMPULS(57600.,86400.)
426. IF(ZZ.LT.0.5) GO TO 111

```

ORIGINAL PAGE IS
OF POOR QUALITY

```

427.          GO TO 222
428.          111 CONTINUE
429.          *****
430.          ****
431.          **** E.....TERMINAL SECTION
432.          ****
433.          TERMINAL
434.          *****
435.          TIMER F=NTIM=259200.0,PRODEL=86400.0,DELT=100.0
436.          PRINT J(NUM, X(NUM, DRN, DINP, DEVP, DDRN, CUMWTR,...
437.          CUMWT1, CUMWT2, CUMWT3, BALANS, CUMRN,CUMDRN,CUMINF,CUMEVP ...
438.          FLOW(14)
439.          METHOD TRAPZ
440.          END
441.          *
442.          *
443.          *
444.          * WEATHER INPUT DATA, STORED IN ARRAY WINPUT(11,37)
445.          * JNM DL DGR TMAX TMIN DMAX DMIN SA BEGIN END RFT
446.          INPUT
447.          1. 10.70 10.0 16.0 0.5 3.0 -2.5 3.0 0.0 0.0 0.0
448.          2. 10.70 10.0 16.0 0.5 3.0 -2.5 3.0 9.0 12.0 25.0
449.          3. 10.70 10.0 16.0 0.5 3.0 -2.5 3.0 0.0 0.0 0.0
450.          4. 10.70 10.0 16.0 0.5 3.0 -2.5 3.0 0.0 0.0 0.0
451.          5. 10.70 10.0 16.0 0.5 3.0 -2.5 3.0 0.0 0.0 0.0
452.          6. 10.70 10.0 16.0 0.5 3.0 -2.5 3.0 0.0 0.0 0.0
453.          7. 10.70 10.0 16.0 0.5 3.0 -2.5 3.0 0.0 0.0 0.0
454.          8. 10.70 10.0 16.0 0.5 3.0 -2.5 3.0 0.0 0.0 0.0
455.          9. 10.70 10.0 16.0 0.5 3.0 -2.5 3.0 0.0 0.0 0.0
456.          10. 10.70 10.0 16.0 0.5 3.0 -2.5 3.0 0.0 0.0 0.0
457.          11. 10.70 10.0 16.0 0.5 3.0 -2.5 3.0 0.0 0.0 0.0
458.          12. 10.70 10.0 16.0 0.5 3.0 -2.5 3.0 0.0 0.0 0.0
459.          13. 10.70 10.0 16.0 0.5 3.0 -2.5 3.0 0.0 0.0 0.0
460.          14. 10.70 10.0 16.0 0.5 3.0 -2.5 3.0 0.0 0.0 0.0
461.          15. 10.70 10.0 16.0 0.5 3.0 -2.5 3.0 0.0 0.0 0.0
462.          0. 10.70 10.0 16.0 0.5 3.0 -2.5 3.0 0.0 0.0 0.0
463.          ENDINPUT
464.          STOP
465.          ENDJCB
466.          /*END

```

APPENDIX C - CALCULATION OF UNSATURATED HYDRAULIC CONDUCTIVITY

CALCULATION OF UNSATURATED HYDRAULIC CONDUCTIVITY

PURPOSE: This WATFIV program is designed to calculate the unsaturated hydraulic conductivity as a function of water content using Jackson's method (Jackson, 1972; Bower and Jackson, 1974). It also states the relationship between water content vs. pressure potential and water content vs. hydraulic conductivity in the form required for a CSMP III FUNCTION statement. Note, that the symbols used for variables in this program are different from those used in the general model.

INTRODUCTION: In order to use this program, three parameters must be known. These are:

1. the saturated hydraulic conductivity of the soil, (COND(1)), in m/s,
2. The relationship between pressure potential, (PP(I)), in m water column and volumetric water content, (TH(I)), and
3. the maximum value of water content, (TH(1)).

The first two parameters are obtained experimentally and the third one is estimated by calculating the porosity of the soil, i.e.

$$TH(1) = \text{porosity} = 1 - DB/PD$$

where DB is the dry bulk density of the soil in g/cm^3 , and PD is the particle density of the soil, usually taken as $2.65 g/cm^3$.

It should be noted that Jackson's method requires detailed information on the relationship between pressure potential vs. water content for high values of pressure potential, i.e. > - 0.50 m.

Experience has shown that this information has a critical effect on the results.

PROCEDURE: This section outlines the procedure that should be followed to obtain the values of pressure potential for different values of water content from experimental data.

1. Plot the relationship between pressure potential vs. volumetric water content for values of pressure potential $> - 5.0$ m on a linear scale. To the value of 0.0 pressure potential assign the maximum water content (TH(1)). A semi-log graph of pressure potential vs. water content is used for the remaining values of pressure potential.

2. Select an increment for the volumetric water content (DELTH), i.e. 0.01, 0.02.

3. Calculate the number of values of water content (M) for which the hydraulic conductivity is to be calculated.

$$M = \frac{TH(\text{MAXIMUM}) - TH(\text{MINIMUM})}{DELTH} + 1.0$$

4. From the graphs, read the values of pressure potential that correspond to the midpoint of each equal increment of volumetric water content. This is illustrated with an example.

EXAMPLE: DELTH = 0.02, TH(1) = 0.42

<u>WATER CONTENT INTERVAL</u>	<u>MIDPOINT</u>	<u>PP(I) (-m)</u>
0.42 - 0.40	0.41	0.07
0.40 - 0.38	0.39	0.22
0.38 - 0.36	0.37	0.60
.	.	.
.	.	.
.	.	.
0.04 - 0.02	0.03	29000.00

INPUT TO THE WATFIV PROGRAM: The following input cards must be specified, in the sequence given, after the //\$DATA card.

<u>DATA CARD NO.</u>	<u>IDENTIFICATION</u>	<u>RESTRICTIONS</u>
1.	TITLE	up to 80 alphabetic or numeric characters
2.	TH(1)	Real variable
3.	DELTH	Real variable
4.	M	Integer
5.	PP(1)	Positive real variables
I+4	PP(I)	.
.	.	.
M+4	PP(M)	.
M+5	COND(1)	Real variable

OUTPUT: The output of the program is in three parts. The first part lists the title and the input data. Note that in the first table the values of PP(I), LOG10 PP(I), and RH(I) correspond to THETAM(I), the midpoint water content. The second part lists the results. Note that in the second table the calculated value of hydraulic conductivity, (COND(I)), corresponds to THETA(I). The maximum hydraulic conductivity (COND(1)) should correspond to the maximum value of water content (TH(1)). The third part is a table of volumetric water content vs. pressure potential, and volumetric water content vs. hydraulic conductivity, in the form required for a CSMP FUNCTION statement.

REFERENCES:

1. Bower, H. and R.D. Jackson. 1974. Determining soil properties. p. 611-672. In: Jan van Schilfgaarde (Ed). Drainage for Agriculture. Agronomy Monograph 17. American Society of Agronomy, Madison, WI.
2. Jackson, R.D. 1972. On the calculation of hydraulic conductivity. Soil Sci. Soc. Amer. Proc. 36: 380-382.

ORIGINAL PAGE IS
OF POOR QUALITY

```

1. //JACKSON JOB (R042,402E,*02,001,PL), LASCANO
2. /*WATPIV
3. C
4. C
5. C      CALCULATE HYDPAULIC CONDUCTIVITY
6. C      JACKSON 1972  SSAP 36 : 390-382
7. C
8. C
9. C*****
10. C      THE NECESSARY INPUT FOR THIS CALCULATION IS GIVEN BELOW
11. C      THE EXPLANATION OF INPUT VARIABLES IS GIVEN IN THE PROGRAM
12. C
13. C
14. C      DATA CARD #      IDENTIFICATION
15. C      1.....TITLE
16. C      2.....TH (1)
17. C      3.....DELTH
18. C      4.....H
19. C      5.....PP (1)
20. C      .
21. C      .
22. C      .
23. C      I+4.....PP (I)
24. C      .
25. C      .
26. C      .
27. C      H+4.....PP (H)
28. C      H+5.....COND (1)
29. C
30. C*****
31. C      REAL NOM1, NOM2, LCOND, LPP
32. C      INTEGER TITLE(40)
33. C      DIMENSION TH(70), PP(70), RELCON(70), COND(70), LCOND(70), PH(70)
34. C      DIMENSION LPP(70), THETA(70), THX(70), CONDX(70), PPX(70), THY(70)
35. C
36. C      INPUT DATA
37. C
38. C      READ TITLE (NAME OF SOIL, DEPTH, OTHER INFORMATION)
39. C      READ(5, 11) TITLE
40. C      11  FORMAT('0A1)
41. C      MAXIMUM VALUE OF WATER CONTENT
42. C      READ, TH(1)
43. C      DEFINE STEP SIZE (INCREMENT)
44. C      READ, DELTH
45. C      N IS THE TOTAL NUMBER OF VALUES OF WATER CONTENT FOR WHICH THE
46. C      HYDRAULIC CONDUCTIVITY IS CALCULATED
47. C      H CAN BE CALCULATED FROM THE FOLLOWING EXPRESSION:
48. C      H = (TH(MAXIMUM) - TH(MINIMUM)) / DELTH + 1.0
49. C      READ, H
50. C
51. C      PROGRAM
52. C
53. C      DO 10 I = 1, N
54. C      TH(I) = TH(1) - (I-1)*DELTH
55. C      THETA(I) = TH(I) - (DELTH/2.0)
56. C      READ PRESSURE POTENTIAL VALUES IN H, CORRESPONDING TO THEIR
57. C      RESPECTIVE VALUES FOR THE CENTER OF EACH INCREMENT THETA.
58. C      READ, PP(I)
59. C      PP(I) = -PP(I)
60. C      RH(I) = EXP(PP(I)/14091.)

```

```

61.          LPP(I) = ALOG10(-PP(I))
62.          10 CONTINUE
63.          DENOM = 0.
64.          DO 20 J = 1, N
65.             DENOMJ = (2*J-1)/(PP(J)**2)
66.             DENOM = DENOM + DENOMJ
67.          20 CONTINUE
68.          C   GIVE MAXIMUM CONDUCTIVITY IN M/S (SAT. CONDUCTIVITY).
69.          READ, COND(1)
70.          C   RECORD OF INPUT DATA
71.          WRITE(6,850) TITLE
72.          850  FORMAT('1',///,20X,'TITLE:',80A1,/)
73.          WRITE(6,900)
74.          900  FORMAT('1',///,45X,'INPUT DATA',/)
75.          WRITE(6,1000) TH(1)
76.          1000 FORMAT('1',20X,'MAXIMUM VALUE OF WATER CONTENT =',F4.2)
77.          WRITE(6,1100) DELTA
78.          1100 FORMAT('1',20X,'INCREMENT OF WATER CONTENT =',F5.3)
79.          WRITE(6,1200) N
80.          1200 FORMAT('1',20X,'NUMBER OF VALUES OF WATER CONTENT, FOR WHICH K IS
81.          SCALCULATED =',I3)
82.          WRITE(6,1300) COND(1)
83.          1300 FORMAT('1',20X,'MAXIMUM CONDUCTIVITY (SAT. COND.) =',E14.5
84.          S,2X,'M/S')
85.          WRITE(6,1400)
86.          1400 FORMAT('0',20X,'THE VALUES OF THETA ARE THE MIDPOINTS',/,
87.          S21X,'OF EACH INCREMENT TO WHICH THE VALUES OF PP(I)',/,
88.          S21X,'CORRESPOND ACCORDING TO EXPERIMENTAL DATA')
89.          WRITE(6,1450)
90.          1450 FORMAT('0',20X,'THE LOG10 VALUE OF PP(I) AND RH(I) CORRESPOND',
91.          S/,21X,'TO THE VALUE OF THETA(J)',/)/)
92.          WRITE(6,1500)
93.          1500 FORMAT('1',20X,'THETA(I)',2X,'THETA(I)',4X,'PP(I) (N)',2X,
94.          S'LOG10 PP(I)',2X,'RH(I)')
95.          DO 50 I=1,N
96.             WRITE(6,1600) TH(I), THETA(I), PP(I), LPP(I), RH(I)
97.          1600 FORMAT(' ',23X,F4.2,6X,F4.2,5X,F9.2,6X,F6.2,2X,F6.2)
98.          50 CONTINUE
99.          DO 30 I = 1, N
100.             NOMI = 0.
101.             DO 40 J = I, N
102.                NOMJ = (2*J + 1 - 2*I)/(PP(J)**2)
103.                NOMI = NOMI + NOMJ
104.             40 CONTINUE
105.             RELCON(I) = (TH(I)/TH(1))*(NOMI /DENOM)
106.             COND(I) = RELCON(I)*COND(1)
107.             LCOND(I) = ALOG10(COND(I))
108.             30 CONTINUE
109.             WRITE(6,1700)
110.          1700 FORMAT('1',////////,45X,'RESULTS',/)
111.             WRITE(6,1800)
112.          1800 FORMAT('1',20X,'THETA(I)',4X,'RELCON(I)',4X,'COND(I)',4X,
113.          S'LOG10 COND(I)')
114.             DO 60 I=1,N
115.                WRITE(6,1900) TH(I), RELCON(I), COND(I), LCOND(I)
116.          1900 FORMAT(' ',21X,F6.4,4X,E10.4,3X,E10.4,4X,F6.2)
117.             60 CONTINUE
118.             WRITE(6,2000)
119.          2000 FORMAT(1H1)
120.             K=0
121.             DO 90 J=1, N

```

ORIGINAL PAGE IS
OF POOR QUALITY

```

122.          KK=N-K
123.          THX (J) =THETAM (KK)
124.          CONDX (J) =COND (KK)
125.          THY (J) =TH (KK)
126.          PPX (J) =PP (KK)
127.          K=K+1
128.          9C CONTINUE
129.          WRITE (6,2100)
130.          2100 FORMAT (1H1)
131.          DO 100 J=1,N
132.          WRITE (6,2200) THX (J),PPX (J)
133.          2200 FORMAT (' ',20X,' (' ,F6.3,' ',' ,F10.2,' ), ... ')
134.          100 CONTINUE
135.          WRITE (6,2300)
136.          2300 FORMAT (1H1)
137.          DO 110 J=1,N
138.          WRITE (6,2400) THY (J),CONDX (J)
139.          2400 FORMAT (' ',20X,' (' ,F6.3,' ',' ,E14.7,' ), ... ')
140.          110 CONTINUE
141.          WRITE (6,2500)
142.          2500 FORMAT (1H1)
143.          STOP
144.          END
145.          //SDATA
146.          MORWOOD SILT LOAM, AGRONOMY FARM, 0.00 - 0.20 M DEPTH
147.          0.02
148.          0.020
149.          20
150.          0.07
151.          0.22
152.          0.60
153.          1.20
154.          3.60
155.          7.20
156.          11.0
157.          18.0
158.          30.0
159.          45.0
160.          78.0
161.          160.0
162.          370.0
163.          700.0
164.          1500.0
165.          3000.0
166.          6000.0
167.          10000.0
168.          16000.0
169.          29000.0
170.          5.0E-07
171.          /*END

```

TITLE: ROEWOOD SILT LOAM, AGRONOMY FARM, 0.00 - 0.20 M DEPTH

INPUT DATA

MAXIMUM VALUE OF WATER CONTENT =0.42

INCREMENT OF WATER CONTENT =0.020

NUMBER OF VALUES OF WATER CONTENT, FOR WHICH K IS CALCULATED =

MAXIMUM CONDUCTIVITY (SAT. COND.) = 0.50000E-06 κ/S

THE VALUES OF THETA_K ARE THE MIDPOINTS
OF EACH INCREMENT TO WHICH THE VALUES OF PP(I)
CORRESPOND ACCORDING TO EXPERIMENTAL DATA

THE LOG₁₀ VALUE OF PP(I) AND PH(I) CORRESPOND
TO THE VALUE OF THETA_K(I)

THETA(I)	THETA _K (I)	PP(I) (M)	LOG ₁₀ PP(I)	PH(I)
0.42	0.41	-0.07	-1.15	1.00
0.40	0.39	-0.22	-0.66	1.00
0.38	0.37	-0.60	-0.22	1.00
0.36	0.35	-1.20	0.08	1.00
0.34	0.33	-3.60	0.56	1.00
0.32	0.31	-7.20	0.96	1.00
0.30	0.29	-11.00	1.04	1.00
0.28	0.27	-18.00	1.26	1.00
0.26	0.25	-30.00	1.48	1.00
0.24	0.23	-45.00	1.65	1.00
0.22	0.21	-74.00	1.87	0.99
0.20	0.19	-160.00	2.20	0.99
0.18	0.17	-370.00	2.57	0.97
0.16	0.15	-700.00	2.85	0.95
0.14	0.13	-1500.00	3.18	0.90
0.12	0.11	-3000.00	3.48	0.81
0.10	0.09	-6000.00	3.78	0.65
0.08	0.07	-10000.00	4.00	0.49
0.06	0.05	-10000.00	4.20	0.32
0.04	0.03	-29000.00	4.46	0.13

RESULTS

THETA (I)	RELCON (I)	COND (I)	LOG10 COND (I)
0.4200	0.1000E-01	0.5000E-06	-6.30
0.4000	0.1111E-01	0.5553E-07	-7.26
0.3800	0.1746E-01	0.8728E-08	-8.06
0.3600	0.3388E-02	0.1694E-08	-8.77
0.3400	0.6131E-03	0.3065E-09	-9.51
0.3200	0.1993E-03	0.9915E-10	-10.00
0.3000	0.7182E-04	0.3591E-10	-10.44
0.2800	0.2480E-04	0.1240E-10	-10.91
0.2600	0.8391E-05	0.4196E-11	-11.38
0.2400	0.2625E-05	0.1313E-11	-11.88
0.2200	0.6530E-06	0.3265E-12	-12.49
0.2000	0.1265E-06	0.6313E-13	-13.20
0.1800	0.2527E-07	0.1263E-13	-13.90
0.1600	0.5693E-08	0.2846E-14	-14.55
0.1400	0.1207E-08	0.6033E-15	-15.22
0.1200	0.2823E-09	0.1411E-15	-15.85
0.1000	0.7131E-10	0.3566E-16	-16.45
0.0800	0.1043E-10	0.9215E-17	-17.04
0.0600	0.3734E-11	0.1667E-17	-17.73
0.0400	0.3961E-12	0.1980E-18	-18.70

ORIGINAL PAGE IS
OF POOR QUALITY

(0.030,	-29000.00),	...
(0.050,	-16000.00),	...
(0.070,	-10000.00),	...
(0.090,	-6000.00),	...
(0.110,	-3000.00),	...
(0.130,	-1500.00),	...
(0.150,	-700.00),	...
(0.170,	-370.00),	...
(0.190,	-160.00),	...
(0.210,	-74.00),	...
(0.230,	-45.00),	...
(0.250,	-30.00),	...
(0.270,	-18.00),	...
(0.290,	-11.00),	...
(0.310,	-7.20),	...
(0.330,	-3.60),	...
(0.350,	-1.20),	...
(0.370,	-0.60),	...
(0.390,	-0.22),	...
(0.410,	-0.07),	...

ORIGINAL VALUES
OF POOR QUALITY

(0.040, 0.1980432E-14), ...
(0.060, 0.1867095E-17), ...
(0.080, 0.9215115E-17), ...
(0.100, 0.3565605E-16), ...
(0.120, 0.1411493E-15), ...
(0.140, 0.6032844E-15), ...
(0.160, 0.2846457E-14), ...
(0.180, 0.1263317E-13), ...
(0.200, 0.6312881E-13), ...
(0.220, 0.3265092E-12), ...
(0.240, 0.1312614E-11), ...
(0.260, 0.4195633E-11), ...
(0.280, 0.1239914E-10), ...
(0.300, 0.3590754E-10), ...
(0.320, 0.9914647E-10), ...
(0.340, 0.3065372E-09), ...
(0.360, 0.1694214E-08), ...
(0.380, 0.8728055E-08), ...
(0.400, 0.5553067E-07), ...
(0.420, 0.5000000E-06), ...

**Appendix C: Improved Water and Nutrient Management
Through High-Frequency Irrigation**

C-4

**IMPROVED WATER AND NUTRIENT MANAGEMENT
THROUGH HIGH-FREQUENCY IRRIGATION**

by

Kathryn Byrd Humphreys

Terry A. Howell

December 1980

Supported by:

**National Aeronautics and Space Administration
Johnson Space Center
Houston, Texas**

Grant No. NAS 9-13904

and

**Office of Water, Research and Technology
U.S. Department of Interior
Washington, D.C.**

Project B-219-TEX

ABSTRACT

An adequate description of soil moisture movement is necessary for solution of agriculturally oriented problems such as irrigation, drainage and runoff control. Three approaches for determining the hydraulic properties of soil are in situ measurements, laboratory measurements and theoretical models. Field measurements, though representative, have the disadvantages of being costly and time consuming. Laboratory and mathematical processes are more practical but require extensive comparison to field results for evaluation. The purpose of this study was to determine the principle hydraulic properties of a soil of the Norwood Series utilizing the three approaches and to compare the results.

The laboratory method selected was centrifugation (Alemi, et al., 1972). Soil cores were centrifuged and the redistribution of water was measured as change in weight with time. Inconsistent results and limited data obtained with this method, consequently, prevented adequate conclusions from being made.

Hydraulic conductivity was obtained by measurement of hydraulic head and moisture content of the soil profile in situ with tensiometers and neutron probe, respectively. The theoretical procedure utilized water retentivity curves in conjunction with values of saturated hydraulic conductivity for computing hydraulic conductivity as a function of water content. Saturated hydraulic conductivity was measured in the field using Bower's (1961) double-tube method. The pressure-water content curves were obtained with disturbed soil samples for 30 to 80 cm depths and with soil cores for 0 to 15 cm

depths using pressureplate extractors. A combination of laboratory and field measured values for these curves was also used for comparison.

The field measurements yielded several relationships between hydraulic conductivity and water content, varying with soil depth. Comparison of calculated values with field data using only the laboratory water retention curves gave mediocre results for the 30 to 80 cm soil depth. However, when the field and laboratory data were combined and the resulting water retention curve was used to calculate hydraulic activity, the correlation was greatly improved. The 0 to 20 cm soil depth showed good results with both curves. Thus, it appears that this theoretical technique is applicable to soils of the type studied, but the accuracy of the calculated values is quite sensitive to the shape of the water retention curve, the saturated water content value and the saturated hydraulic conductivity value. Thus, accurate measurement of these parameters is necessary for its successful use.

TABLE OF CONTENTS

Chapter		Page
I	INTRODUCTION	1
II	LITERATURE REVIEW	3
III	EXPERIMENTAL PROCEDURE	16
	Measurement of Soil Hydraulic Properties in the Laboratory	16
	Pressure Chamber Method	16
	Centrifuge Method	17
	Measurement of Soil Hydraulic Properties in the Field	20
	Double-Tube Method	20
	Instantaneous Profile Method	22
IV	RESULTS AND DISCUSSION	28
	Soil Profile Hydrology	32
	Double-Tube Method	39
	Laboratory Measurements	47
	Centrifuge Measurements	56
V	SUMMARY AND CONCLUSIONS	63
	Recommendations for Future Study	64
	REFERENCES	66
	APPENDIX A	69

LIST OF TABLES

Table		Page
1	Texture profile of field site	29
2	Saturated conductivities measured with double-tube apparatus	45
A-1	Field measurement of bulk density	70
A-2	Neutron probe calibration data	71
A-3	Soil moisture measured at different depths for various times during drainage	73
A-4	Soil-water pressure head (cmH ₂ O) measured at different depths for various times during drainage	74
A-5	Calculation of hydraulic conductivity from field data	75
A-6	Water retentivity values of pressure potential and water content used in the calculation of hydraulic conductivity.	81
A-7	Double-tube data used for calculation of K _s	86
A-8	Centrifuge data	90

LIST OF FIGURES

Figure		Page
1	Detail of double-tube apparatus showing dimensions, inner tube, outer tube and standpipes.	12
2	Values of flow factor, F (Bouwer and Jackson, 1974) . .	14
3	Soil core weighing apparatus for centrifuge method	19
4	Schematic diagram of plot layout showing dimensions, instrumented section and manometer location.	23
5	Schematic diagram of instrument layout showing relative positions of neutron access tubes, tensiometers and tensiometer depths	24
6	Bulk density profile showing gamma probe data, gravimetric results and texture profile.	30
7	Calibration curve for neutron soil moisture probe . . .	31
8	Tensiometry showing pressure head versus drainage period for each depth. (smoothed data)	33
9	Hydraulic head profiles for different times. (smoothed data)	34
10	Soil moisture profiles for different times	36
11	Soil moisture for different depths	37

LIST OF FIGURES (Continued)

Figure		Page
12	Volume flux versus time for various depths	38
13	Relationship between hydraulic conductivity and water content determined from field measurements for 10-30 cm soil depth	40
14	Relationship between hydraulic conductivity and water content determined from field measurements for 40-80 cm soil depth	41
15	Relationship between hydraulic conductivity and water content determined from field measurements for 90-120 cm soil depth	42
16	Relationship between hydraulic conductivity and water content determined from field measurements for 140-160 cm soil depth	43
17	Relationship between hydraulic conductivity and water content determined from field measurements for 170-180 cm soil depth	44
18	Saturated hydraulic conductivity versus depth	46
19	Water retentivity determined in the laboratory, 0-15 cm soil depth	48
20	Water retentivity determined in the laboratory, 15-55 cm soil depth	49
21	Water retentivity determined in the laboratory, 55-90 cm soil depth	50
22	Comparison of calculated to measured hydraulic conductivity, 0-25 cm soil depth	51
23	Comparison of calculated to measured hydraulic conductivity, 30-80 cm soil depth	53

LIST OF FIGURES (Continued)

Figure		Page
24	Water retentivity from field data combined with laboratory data, 0-25 cm soil depth.	54
25	Water retentivity from field data combined with laboratory data, 15-55 cm soil depth	55
26	Comparison of calculated to measured hydraulic conductivity, 0-25 cm soil depth.	57
27	Comparison of calculated to measured hydraulic conductivity, 30-80 cm soil depth	58
28	Hydraulic conductivity versus water content determined from centrifuge data for noted soil depths	60
29	Comparison of laboratory to field hydraulic conductivity, 0-30 cm soil depth	61
30	Comparison of laboratory to field hydraulic conductivity, 40-80 cm soil depth	62
A-1	Double-tube data for 5 cm depth	87
A-2	Double-tube data for 40 cm depth	88
A-3	Double-tube data for 70 cm depth	89

LIST OF SYMBOLS

<u>Symbol</u>	<u>Definition</u>
C	Specific water capacity (1/L).
CR	Count ratio, measured/standard.
D	Depth of slowly permeable material beneath auger hole (L).
Db	Bulk density (M/L ³).
Dp	Depth of highly permeable material beneath auger hole (L).
Dw	Soil water diffusivity (L ² /T).
F	Flow factor, dimensionless.
Fcp	Centripetal force per unit mass (L/T ²).
H	Total head (L).
HB	Head measured in inner-tube standpipe (L).
HB ₁	Head measured in inner-tube standpipe during outer-tube constant measurement (L).
K	Hydraulic conductivity (L/T).
L	Length of soil core (L).
Lm	Total length of bridge to hold soil core (L).
Q _H	Flow moving in or out of inner tube due to head difference between tubes (L ³ /T).
R	Radius from center of centrifuge (L).
R ₁	Reaction measured on balance (M).

LIST OF SYMBOLS (Continued)

<u>Symbol</u>	<u>Definition</u>
Rc	Radius of inner-tube standpipe (L).
Rv	Radius of inner-tube (L).
S	Total porosity (%).
Z	Soil depth (L).
d	Depth of penetration of inner-tube (L).
g	Gravitational acceleration (L/T ² , F/M).
h	Pressure head (L) or (F/L ²).
hg	Gravitational head (L).
i	Summation index.
j	Summation index.
k	Permeability (L ²).
m	Number of water content increments of water retention curve.
n	Summation index.
nm	Number of water content increments of water retention curve from zero to saturation.
p	Particle density (M/L ³).
q	Volume flux (L/T).
s	subscript, denotes saturation.
t	Time (T) or subscript denoting time.
z	Distance between points of flow (L).

LIST OF SYMBOLS (Continued)

<u>Symbol</u>	<u>Definition</u>
γ	Surface tension (F/L).
ρ	Density (M/L ³).
θ	Volumetric water content (L ³ /L ³).
η	Viscosity (FT/L ²).
ω	Angular velocity (1/T).
σ	Exponent of θ_1/θ_s for Jackson's equation.

CHAPTER I

INTRODUCTION

Solutions to problems involving irrigation, runoff control, drainage and water conservation are dependent upon a description of soil moisture movement. With respect to plant water requirements, the water storage capacity of a soil is determined by infiltration, redistribution and drainage processes which also rely on knowledge of soil moisture movement. Three approaches used to determine the relevant hydraulic properties utilized in describing soil moisture patterns are in situ measurements, laboratory processes, and mathematical models.

Field measurements, though more representative of actual conditions, have the disadvantage of being costly and time consuming, whereas laboratory and mathematical processes, though more practical compared to field techniques, require extensive comparison to field results to determine the validity for various soils.

Soil hydraulic characteristics are best described by the relationship between hydraulic conductivity and soil water content. In this study, this relationship will be determined using in situ measurements, with a laboratory technique and by a theoretical procedure. An

evaluation of the laboratory technique and the theoretical procedure will be made by comparing them with field data. Specifically, the objectives of this study were:

1. To determine the unsaturated hydraulic conductivity of a soil in situ using the instantaneous profile method (Watson, 1966, van Bavel, et al., 1968, Hillel, et al., 1972).

2. To determine the pressure head-water content relationship of a soil using the pressure chamber method (Richards, 1947) and to determine the saturated hydraulic conductivity using the double-tube method described by Bouwer (1961). These relationships were then used in a theoretical model developed by Millington and Quirk (1960) and Marshall (1958) as described by Jackson (1972) to predict the relationship between unsaturated hydraulic conductivity versus soil water content for a soil.

3. To determine the unsaturated hydraulic conductivity on soil cores from the field using a simplified centrifugation method described by Alemi, et al., (1976).

4. To compare the results obtained in the field (instantaneous profile) with those acquired in the laboratory (centrifugation) and with the theoretical model (Jackson method).

CHAPTER II

LITERATURE REVIEW

Capillary flow was first analyzed by E. Buckingham in 1907 (Richards, 1931). Since then, it has been realized that the relationships between pressure potential versus soil water content and hydraulic conductivity versus soil water content are extremely important to the comprehension of soil water movement.

The theory of water movement in soil is based on Darcy's Law which states that flow is proportional to the hydraulic gradient. The equation representing one dimensional flow in a homogeneous isotropic media can be written:

$$q = -K \frac{dH}{dz} \quad (1)$$

where q is the volume flux (L/T), K is the hydraulic conductivity (L/T), H is the piezometric head (L), and z is the distance between two points along the axis of the flow (L). The piezometric head is the sum of the gravitational head (h_g) and the pressure head (h) as follows:

$$H = h_g + h. \quad (2)$$

In unsaturated flow, the components of the flow equation, K and H , are both dependent on the water content of the soil. These relationships between soil water content versus hydraulic conductivity or

pressure potential are informative hydrological descriptors of a particular soil and are the primary inputs into most theoretical water balance models. The accuracy of these soil properties has a direct bearing on the validity of the theoretical models; therefore, the method used to determine these relationships should yield accurate and representative results.

Hydraulic conductivity versus water content relationships have been evaluated using both laboratory and field techniques. The reliability of the laboratory procedures is determined by comparison to field measurements. Soil sampling necessary to laboratory procedures is the major reason for discrepancy since the sample size is severely decreased from that in the field and natural environmental factors are absent.

The two approaches generally used to evaluate these relationships in the laboratory are: (1) a steady-state approach and (2) a non-steady-state approach. For steady-state flow, it is necessary that the water content, pressure head and flux remain unchanged with time; whereas, these parameters will vary under unsteady-state conditions.

Most laboratory techniques for determining unsaturated hydraulic conductivity under steady-state conditions are based on the two plate method described by Richards (1931). In this method, the volume flux (q) through a soil column is measured volumetrically and dH/dz

is measured with tensiometers. Utilizing Darcy's Law, the hydraulic conductivity (K) is calculated. Childs and Collis-George (1950) used the idea that in a long column of soil ending in a water table there is a zone of uniform water content with no pressure head gradient. Therefore, a known applied volume flux is equal to the hydraulic conductivity because the piezometric head gradient is equal to one.

When solving for unsaturated hydraulic conductivity with unsteady-state conditions, soil water diffusivity is used (Klute, 1965b).

Diffusivity is related to conductivity by:

$$D_w = K \frac{dh}{d\phi} = \frac{K}{C} \quad (3)$$

where D_w is the soil water diffusivity (L^2/T), h is the pressure head (L), ϕ is the volumetric water content (L^3/L^3), $dh/d\phi$ is the slope of the water characteristic curve (L), C is the specific water capacity ($1/L$), and K is the hydraulic conductivity (L/T).

Several methods have been proposed for measuring diffusivity (Bruce and Klute, 1956, Gardner, 1956, Doering, 1964). The moment method or centrifugation is one of the more recent approaches (Alemi, et al., 1976). When a core of soil is centrifuged at a constant angular velocity for a long time, the centripetal force can be defined as:

$$F_{cp} = R \omega^2 \quad (4)$$

where F_{cp} is the centripetal force per unit mass (L/T^2), R is the radius from the center of the centrifuge (L), and ω is the angular velocity ($1/T$). In this approach a soil core is centrifuged to an equilibrium condition determined by the speed of the centrifuge. The redistribution of soil water is then determined by monitoring the weight change as a function of time along the soil column, which is used for calculation of soil water diffusivity. Assumptions underlying this method are: (1) upon cessation of the centrifuge, soil water pressure head changes as a parabolic function of distance along the soil core, (2) the hydraulic conductivity is constant and (3) a linear relationship exists between water content and pressure head.

Childs and Collis-George (1950) demonstrated that permeability could be predicted from pore size distribution instead of particle size distribution as was previously used. The radius of the largest pores holding water is defined by:

$$r = \frac{2\gamma}{h}, \quad (5)$$

where r is the pore radius (L), γ is the surface tension of water (F/L) and h is the water pressure (F/L^2). Permeability as a function of pore radius could also be defined as a function of pressure head. Hydraulic conductivity is related to permeability by:

$$K = \frac{k \rho g}{\eta} \quad (6)$$

where K is the hydraulic conductivity (L/T), k is the permeability (L^2), ρ is the density (M/L^3), g is gravitational acceleration (F/M) and η is the viscosity (FT/L^2). The calculation of unsaturated hydraulic conductivity was greatly simplified by the use of the water retention curve. Marshall (1958) improved this method by developing the following equation to solve for hydraulic conductivity:

$$K = \frac{30\gamma^2}{\rho g \eta} \left(\frac{\theta}{n}\right)^2 \left[h_1^{-2} + 3h_2^{-2} + 5h_3^{-2} + \dots + (2n-1)h_n^{-2} \right] \quad (7)$$

where K is the hydraulic conductivity (L/T), γ is the surface tension of water (F/L), ρ is the density of water (M/L^3), g is the gravitational acceleration (F/M), η is the viscosity of water (FT/L^2), θ is the volumetric water content (L^3/L^3), n is the number of water content increments, h is the pressure head (L), and 30 is a constant obtained from converting pore radius to pressure head, seconds to minutes and using $1/8$ from Poiseuille's equation for stream-line flow. Millington and Quirk (1959, 1960) developed a similar relationship for computation of hydraulic conductivity as shown in the following equation:

$$K = \frac{30\gamma^2}{\rho g \eta} \left(\frac{\theta^{4/3}}{nm^2}\right) \left[h_1^{-2} + 3h_2^{-2} + 5h_3^{-2} + \dots + (2n-1)h_{nm}^{-2} \right] \quad (8)$$

where nm is the number of water content increments from zero to saturation and K , γ , ρ , g , η and θ are as previously defined.

Several investigators have tested these equations by comparing

calculated to measured values of hydraulic conductivity (Jackson, et al., 1965, Kunze, et al., 1968, Green and Corey, 1971, Jackson, 1972) with good results. Millington and Quirk (1960) found that comparison of a relative hydraulic conductivity (the ratio of unsaturated to saturated hydraulic conductivity) calculated from their equation gave satisfactory agreement with measured values. Jackson determined this ratio with a general equation using Eq. 7 (Marshall's) and Eq. 8 (Millington and Quirk's) to be:

$$\frac{K_u}{K_s} = \left(\frac{\theta_u}{\theta_s} \right)^\sigma \frac{\sum_{j=1}^m \left[(2j + 1 - 2i) h_j^{-2} \right]}{\sum_{j=1}^m \left[(2j - 1) h_j^{-2} \right]}, \quad (9)$$

where K is the unsaturated hydraulic conductivity (L/T), K_s is the saturated hydraulic conductivity (L/T), θ_u is the volumetric water content at the i th increment of the water retention curve (L³/L³), θ_s is the volumetric water content at saturation, σ is 4/3 for the Millington-Quirk equation and 0 for the Marshall equation, h is the pressure head (L), m is the total number of increments used in the calculation, and j and i are summation indices. Comparison of this equation for both values of σ gave reasonable correlation with measured values.

Jackson determined a value for the exponent (σ) of θ_u/θ_s by comparing calculated values of hydraulic conductivity using various values of σ with measured values to obtain the best fit. Values of σ

ranged from 0.82 to 1.24 for sand and 0.74 was the best fit value for a loam. Jackson concluded that a value of 1 for σ was adequate for use with Eq. 9. The variance in σ values appeared to have a greater effect on the sandy soils than on the loam. The deviation of calculated from measured values occurred in the lower water content range, with little or no change for higher water contents. The disagreement for sandy soils appeared to be because values of smaller water content were easier attained with a sand than with a loam, so data in that region of water content was available for comparison. It seems, from Jackson's data then, that this calculating method would be most applicable to agricultural soils which normally maintain higher water contents and any value of σ used, between 0 and 2, has little effect on final values of calculated hydraulic conductivity.

The measurement of soil hydraulic properties in situ eliminates errors associated with soil disturbance which occurs when collecting soil samples for laboratory tests. When the soil is undisturbed, evaluation of soil water flow properties is more representative of actual processes. The instantaneous profile method is a method developed to evaluate soil flow properties under field conditions. This method was originally developed and tested by Watson (1966) on a laboratory model. van Bavel, et al., (1968) and Hillel, et al., (1972) expanded the application to a field situation. Although this procedure

is not valid when horizontal flow is appreciable, it can be used in heterogeneous or layered soil.

To use this method, evaporation from the soil surface is prevented and the soil profile is monitored for changes in soil water content and pressure head while undergoing drainage. Changes in soil water content are obtained with a neutron moisture probe (van Bavel, et al., 1963) and the changes in pressure head are measured with numerous tensiometers located throughout the soil profile (Richards, 1965). The volume flux (q) is determined from each soil layer using the water content data and the gradient in hydraulic head (dH/dz) for each soil layer is determined from the tensiometer data. The hydraulic conductivity for each soil layer is then determined from Darcy's Law ($K=q/dH/dz$). Thus, one of the principle soil hydraulic properties, the dependence of hydraulic conductivity on water content, is determined. This method is associated with the desorption process only.

The range of water contents measured in this method is limited because of the drainage process. Consequently, the hydraulic conductivity and pressure potential as functions of water content are restricted to this narrow range. One method of increasing the water content range is to include evaporation, but boundary conditions become difficult to define. Another solution is to investigate laboratory or theoretical techniques which would adequately describe the field properties. Good correlation with field results is basic for

extrapolation of field data to lower water contents.

Several procedures are available for determining saturated hydraulic conductivity under field conditions (Bouwer and Jackson, 1974). The procedures for measuring saturated hydraulic conductivity above a water table include the shallow well, pump-in, cylinder permeameter and double-tube. The double-tube method considers the geometry of the flow system.

The double-tube method consists of two concentric cylinders with standpipes installed in the field and filled with water as shown in Fig. 1 (p. 12). When saturation is attained, the rate of water level change in the inner tube is measured under two conditions. In condition 1, the head in the outer tube is kept constant and under condition 2 the head in the outer tube is manipulated to maintain an equal head with the inner tube. The water level change in the inner tube represents the net flow in or out of the inner tube. This net flow consists of movement between the tube within the soil (Q_H) plus the actual intake of water by the soil.

When the two head change measurements are plotted as head versus time on the same graph, the distance between the two curves at time t is:

$$\Delta HB = \int_0^t \frac{Q_H}{\pi Rv^2} dt \quad (10)$$

where ΔHB is the head difference between the inner and outer tubes

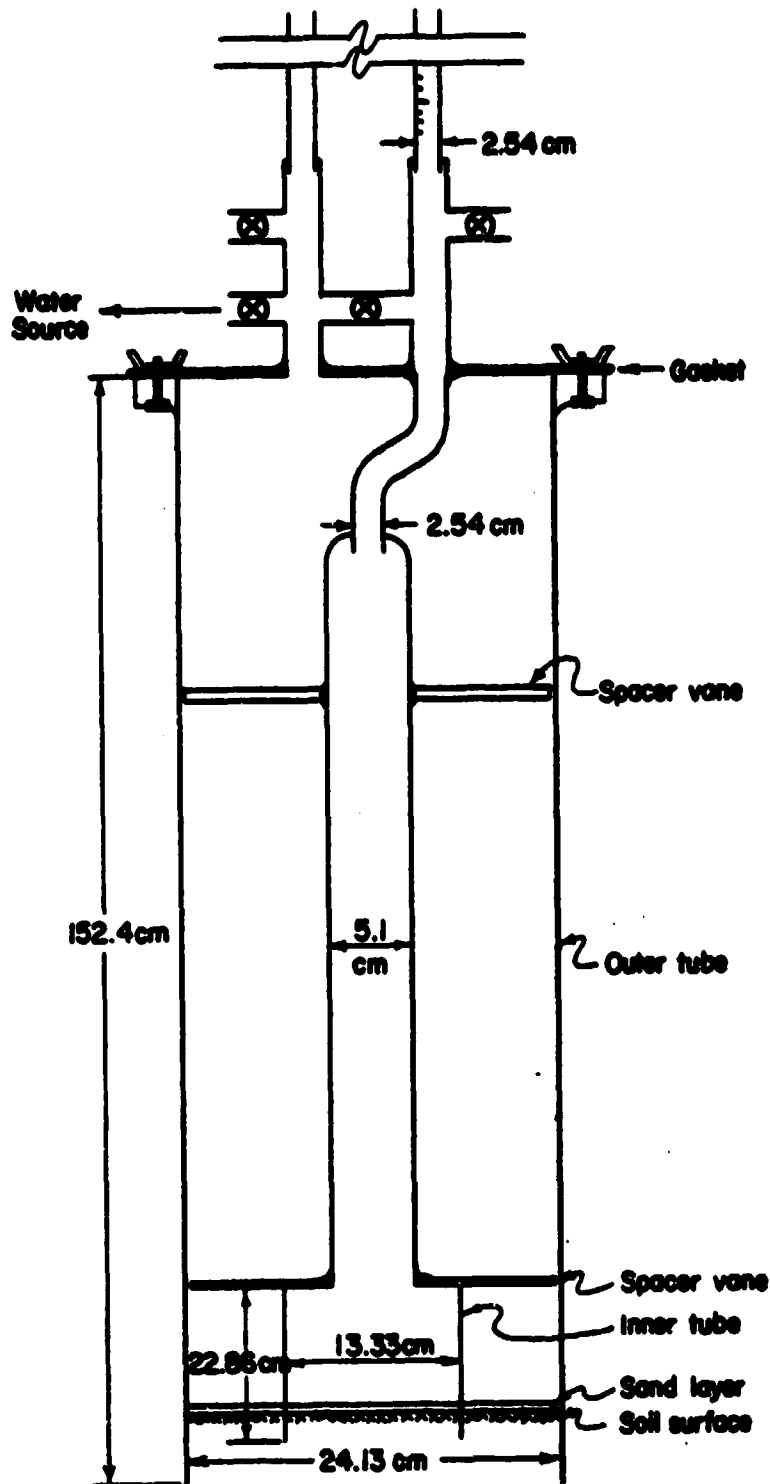


Fig. 1. Detail of double-tube apparatus showing dimensions, inner tube, outer tube and standpipes.

at time t (L), Q_H is the flow rate leaving or entering the inner due to a difference in head between the tubes (L^3/T) and R_v is the radius of the inner tube standpipe (L).

Bouwer (1961) shows the development of the flow factor which is dependent on soil hydraulic conductivity, system geometry and difference in head between the tubes, i.e.:

$$F = \frac{Q_H}{\pi K_s \Delta H B R_c} \quad (11)$$

where F is the flow factor (dimensionless), R_c is the radius of the inner tube (L), K_s is the saturated hydraulic conductivity (L/T), and the other variables are as defined in Eq. 10. A graphical solution of F as a function of D/R_c , d/R_c and D_p/R_c was developed by Bouwer (1961), and is reproduced in Fig. 2 (p. 14) from Bouwer and Jackson (1974). In Fig. 2, D is the depth of the slowly permeable material beneath the auger hole (L), D_p is the depth of the highly permeable material below the auger hole (L), and d is the depth of penetration of the inner tube into the bottom of the auger hole (L). For values of $D > 3R_c$ and $D_p > 3R_c$, the curves in Fig. 2 are similar. Thus, for a relatively uniform soil with a large depth either graph could be used. If Eq. 11 is substituted into Eq. 10, a solution for saturated hydraulic conductivity K_s is:

$$K_s = \frac{HB_s R_v^2}{FR_c \int_0^{\Delta H} HB_1 dt} \quad (12)$$

ORIGINAL PAGE IS
OF POOR QUALITY

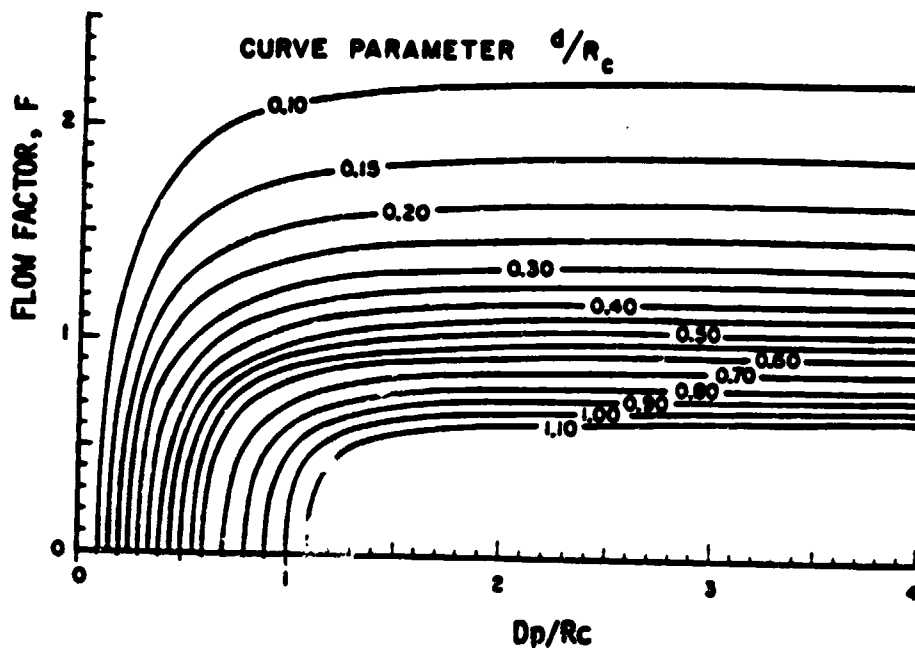
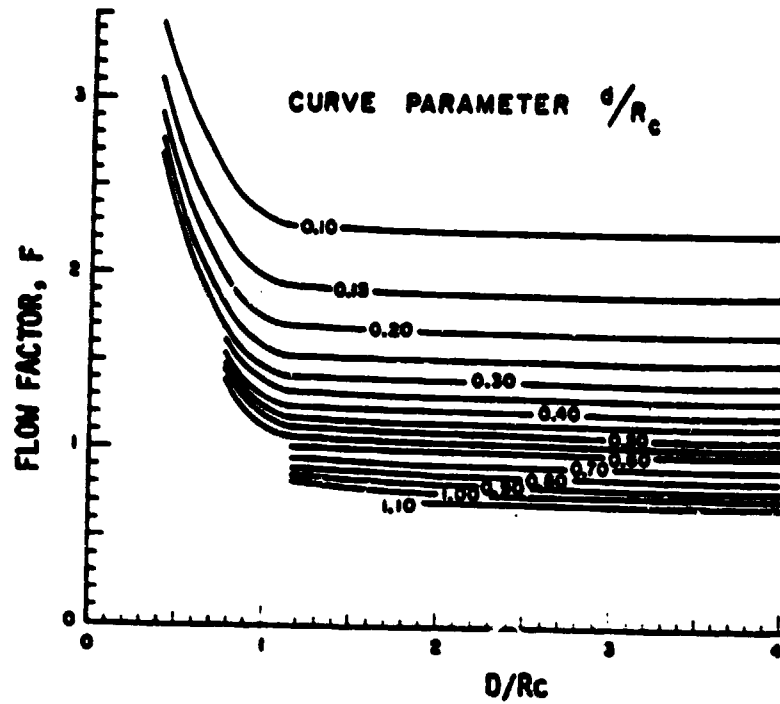


Fig. 2. Values of Flow Factor, F (Bouwer and Jackson, 1974).

where $\int_0^t HB_1 dt$ is the area under the head-time curve when the water level in the outer tube is kept constant (LT) and other variables are as defined in Eqs. 10 and 11.

The capability of accurately predicting water movement within the soil profile has been the object of extensive research. Measurements of these properties in situ yield representative results but are time consuming and expensive. Numerous methods for determining soil hydraulic properties have been developed to facilitate the process, yet maintain the desired accuracy. A few of these methods were described in the above discussion. Although these techniques have been tested on specific soils, the diversity of elements in field situations which affect soil hydraulic properties are cause for additional experimentation.

PRECEDING PAGE BLANK NOT FILMED

CHAPTER III

EXPERIMENTAL PROCEDURE

Measurement of Soil Hydraulic Properties in the Laboratory

Pressure Chamber Method

The water retention properties of the soil were obtained in the laboratory using the pressure chamber method (Richards, 1947). The equipment for this test consisted of six pressure chambers (Soil Moisture Extractor, Cat. No 1 700-2, Soilmoisture Equipment Corp.) attached to pressure regulators which maintain a constant predetermined pressure within each chamber. Porous, ceramic plates, designed to fit within each chamber were used to hold the soil samples and allow water to move out of the samples, through the plate, and into a rubber membrane underneath the bottom side of the ceramic plate. To maintain atmospheric pressure on the bottom side of the ceramic plate, a rubber hose ran from the inside of this membrane to outside the extractor.

Loose soil samples were obtained with a soil auger in the field from soil depths of 15-55 cm and 55-90 cm. A volumetric sampler was utilized to acquire soil cores from the 0-15 cm depth. The loose soil was poured into

The use of trade names in this study does not imply endorsement by Texas A&M University.

plastic rings (5 cm diameter, 2 cm length) on each ceramic plate; the soil cores were left in the original volumetric rings (5.7 cm diameter, 6 cm length) and placed on the ceramic plates. They were left standing in water until the soil was saturated. The ceramic plates were then placed inside the pressure chambers and pressures ranging up to 1500 kPa were applied. Specifically, the pressures applied were 10 kPa (.1 bar), 33 kPa (.33 bar), 67 kPa (.67 bar), 100 kPa (1 bar), 200 kPa (2 bar), 500 kPa (5 bar), 1000 kPa (10 bar) and 1500 kPa (15 bar). Allowing four days for the soil water content to reach equilibrium with the applied pressure, the soil samples were removed and soil water contents were determined gravimetrically. Bulk densities, which were previously determined in the field with a volumetric sampler, were used to calculate the volumetric water content from the gravimetric water contents. The pressures applied to the pressure chambers were then plotted versus the resulting volumetric water contents to yield the pressure potential versus volumetric water content function for each soil depth increment.

Centrifuge Method

The unsaturated hydraulic conductivity was determined from diffusivity values obtained using a centrifugation technique described by Alemi, et al., (1976). Fifteen soil cores were obtained from the field using a volumetric sampler with brass cylinders 5.7 cm in

diameter and 6 cm in length. Immediately after taking the soil samples, both ends were sealed with parafin film, a rubber gasket, and plastic end caps to prevent any water loss. Simultaneous soil samples were taken from each location to determine the gravimetric water contents.

Each soil core was centrifuged (International Centrifuge, Size 1, Type SB) for periods of at least 60 minutes at speeds ranging from 600 to 800 rpm. A plexiglass bridge, with one end on an analytical balance and the other on an adjustable stand, was devised for measuring the redistribution of water within the soil core as shown in Fig. 3 (p. 19). Upon cessation of the centrifuge operation the soil core was placed on the bridge with the dry end towards the balance, and the rate of weight change was measured with the analytical balance. The resulting weight was plotted versus the corresponding time. The equation:

$$R_1(t) = R_1(\infty) - \frac{96 R_1(\infty) - R_1(0)}{\pi^4} \sum_{j=1}^{\infty} \frac{1}{(2j-1)^4} \exp\left[-\frac{(2j-1)^2 \pi^2 D_w t}{L^2}\right] \quad (13)$$

was graphed as $R(t)$ versus t for various values of D_w where $R_1(t)$ is the reaction measured on the balance at a specific time (M), $R_1(\infty)$ is the balance reaction at $t=\infty$ (M) and is obtained from the data plot, $R_1(0)$ is the balance reaction at $t=0$ (M) and is obtained from the data plot, L is the length of the soil core (L), t is time (T), and D_w is the soil water diffusivity (L^2/T). Diffusivity is determined by laying the plot of weight versus time over the plots of $R_1(t)$ versus t and D_w until a

ORIGINAL PAGE IS
OF POOR QUALITY

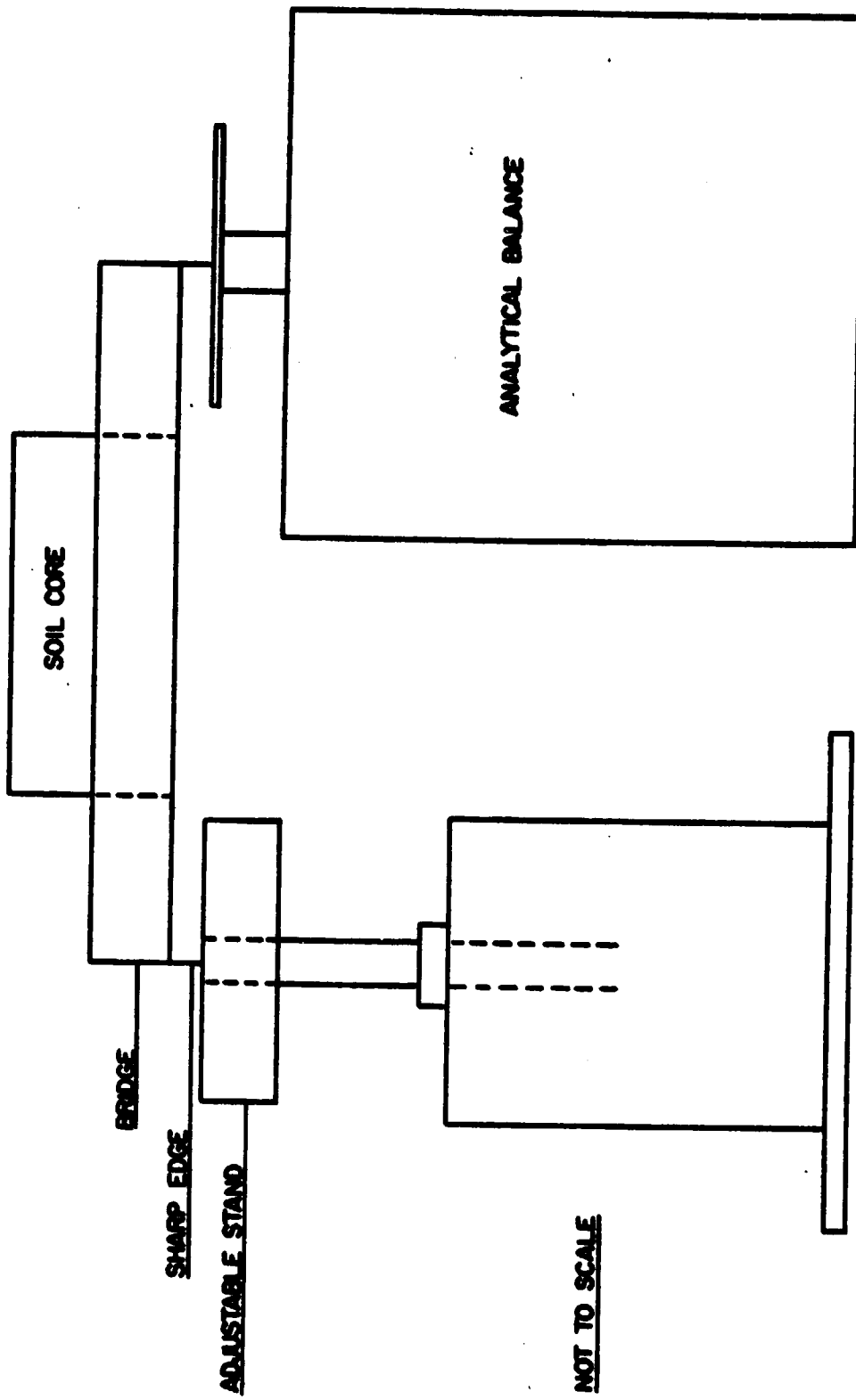


Fig. 2. Soil core weighing apparatus for centrifuge method.

match is achieved. When the two curves match, D_w is equal to the resulting value on the match curve. After a diffusivity was determined unsaturated conductivity (K) was calculated from Eq. 3, $D_w = K \frac{dh}{d\theta}$, and $\frac{dh}{d\theta} = \frac{48gL_m R_1(\infty) - R_1(0)}{\rho R \omega^2 L^2 V (4 + LR^{-1})}$ where g is the gravitational acceleration (L/T^2), L_m is the length of the bridge (L), ρ is the density of water (M/L^3), ω is the constant angular velocity of the centrifuge ($1/T$), L is the length of the soil core (L), V is the bulk volume of the soil core (L^3), R is the radial distance from the center of the centrifuge to the inside edge of the soil core sample, and $R_1(\infty)$, $R_1(0)$ are as previously defined.

Measurement of Soil Hydraulic Properties in the Field

Double-Tube Method

The method selected for measuring saturated hydraulic conductivity was the double-tube method (Bouwer, 1961). The equipment required for this procedure was a double-tube apparatus, water tank and hole cleaner. The outer tube on the double-tube apparatus was made of aluminum tubing (24.23 cm I.D., 152.40 cm length) with a 1.27 cm bottom edge beveled inward. The inner tube was made of iron pipe (13.34 cm I.D.) connected by couplings and reducers to the inner tube standpipe (see Fig. 1., p. 12). The standpipes were made of 2.54 cm plexiglass tubing with a meter stick attached to each.

The hole cleaner was made of a 24 cm diameter wooden plate, with grooves 1.2 cm apart, attached to a metal plate of equal diameter. Metal strips were hammered into the grooves and left protruding 2 cm. When pushed into the soil surface, soil would become entrapped between the blades and be sheared away from the soil surface.

The double-tube method allows the saturated hydraulic conductivity to be measured at various depths. Saturated hydraulic conductivity was determined at depths of 10, 40 and 70 cm. The bottom of each hole was leveled and the hole cleaner was used to clear the disturbed portion of the soil surface. A sand layer, about 2 cm deep, was placed in the bottom of the hole to avoid disturbing the soil surface. The outer tube was put in the hole and forced down about 5 cm below the bottom of the hole. The water was then added, avoiding any soil surface disturbance. The inner tube was placed inside the outer tube when enough time had elapsed to assure saturation and was forced down at least 3 cm below the bottom of the hole. The inner tube was attached to the standpipe and the top plate was secured to make a watertight seal. The valve connecting the standpipes was turned off following simultaneous filling of the standpipes.

Two sets of measurements were necessary for determining the hydraulic conductivity at each depth. The first was the rate of water level change in the inner tube while the water level in the outer tube

was kept at a constant head. The second was a measurement of the change in water head within the inner tube while the head in the outer tube was manipulated to move simultaneously with the head in the inner tube. Saturated hydraulic conductivity was determined from Eq. 12,

$$K_s = \frac{HB_t Rv^2}{F R_c \int_0^{HB_1} dt}$$

Instantaneous Profile Method

The purpose of measuring the soil hydraulic properties in situ is to eliminate errors associated with disturbing the soil by sampling and to maintain natural conditions. The procedure used for these measurements was described by Hillel, et al., (1972). The tilled field plot was a bordered 2x2 m section surrounded by a 1.5 m buffer area as shown in Fig. 4 (p. 23). The borders were made of 4x30 cm lumber buried halfway into the soil.

The instrumentation consisted of two neutron access tubes and twenty tensiometers with mercury manometers. The tensiometers were situated at 10 cm depth increments with maximum depth at two meters. The tensiometers were at least 30 cm from each other and 50 cm from the neutron access tubes, as suggested by Hillel, et al., (1972), (Fig. 5, p. 24).

The neutron access tubes were made from 3.81 cm I.D. thin walled aluminum tubing with neoprene stoppers at both ends to protect the

ORIGINAL PAGE IS
OF POOR QUALITY

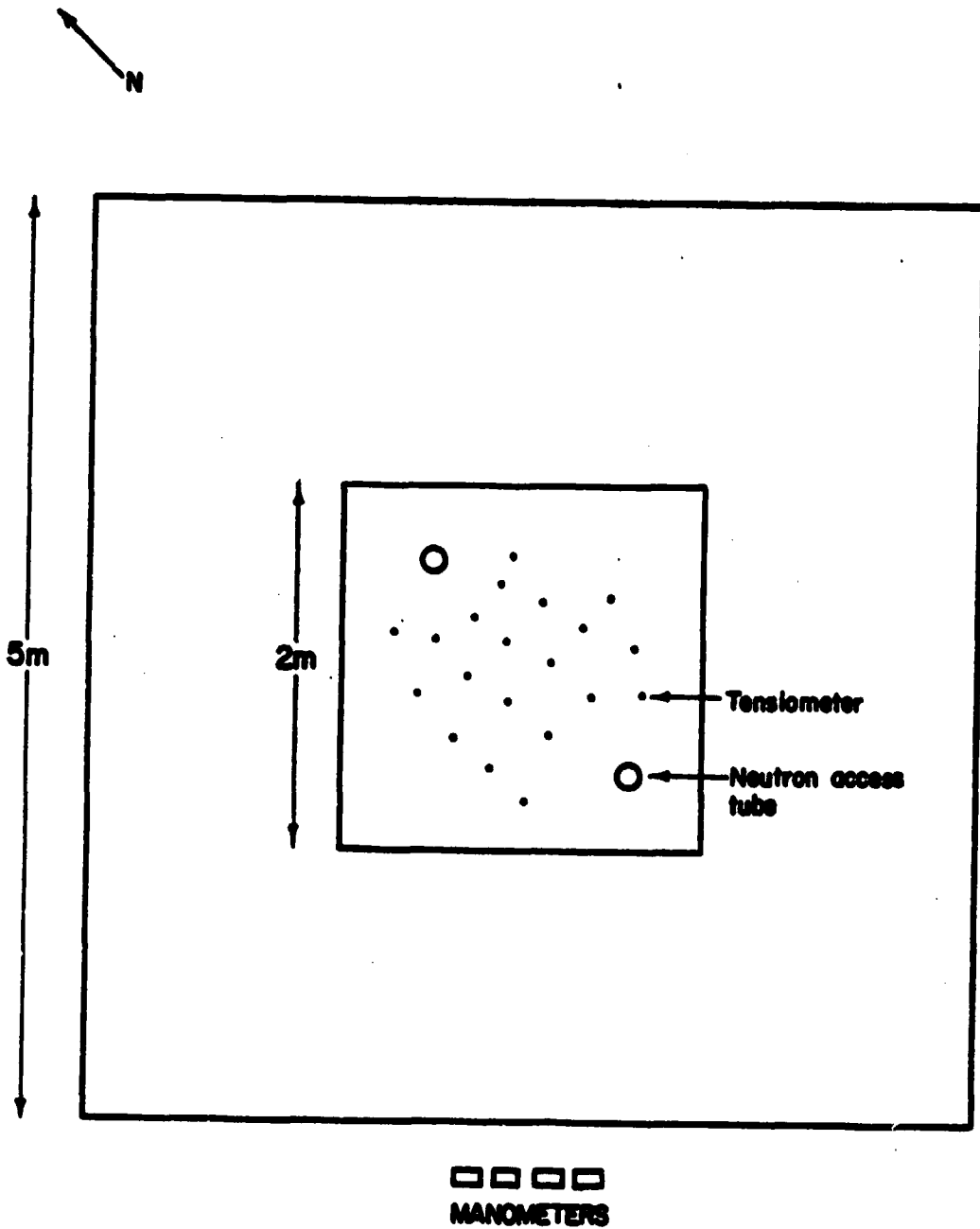


Fig. 4. Schematic diagram of plot layout showing dimensions, instrumented section and manometer location.

ORIGINAL PAGE IS
OF POOR QUALITY

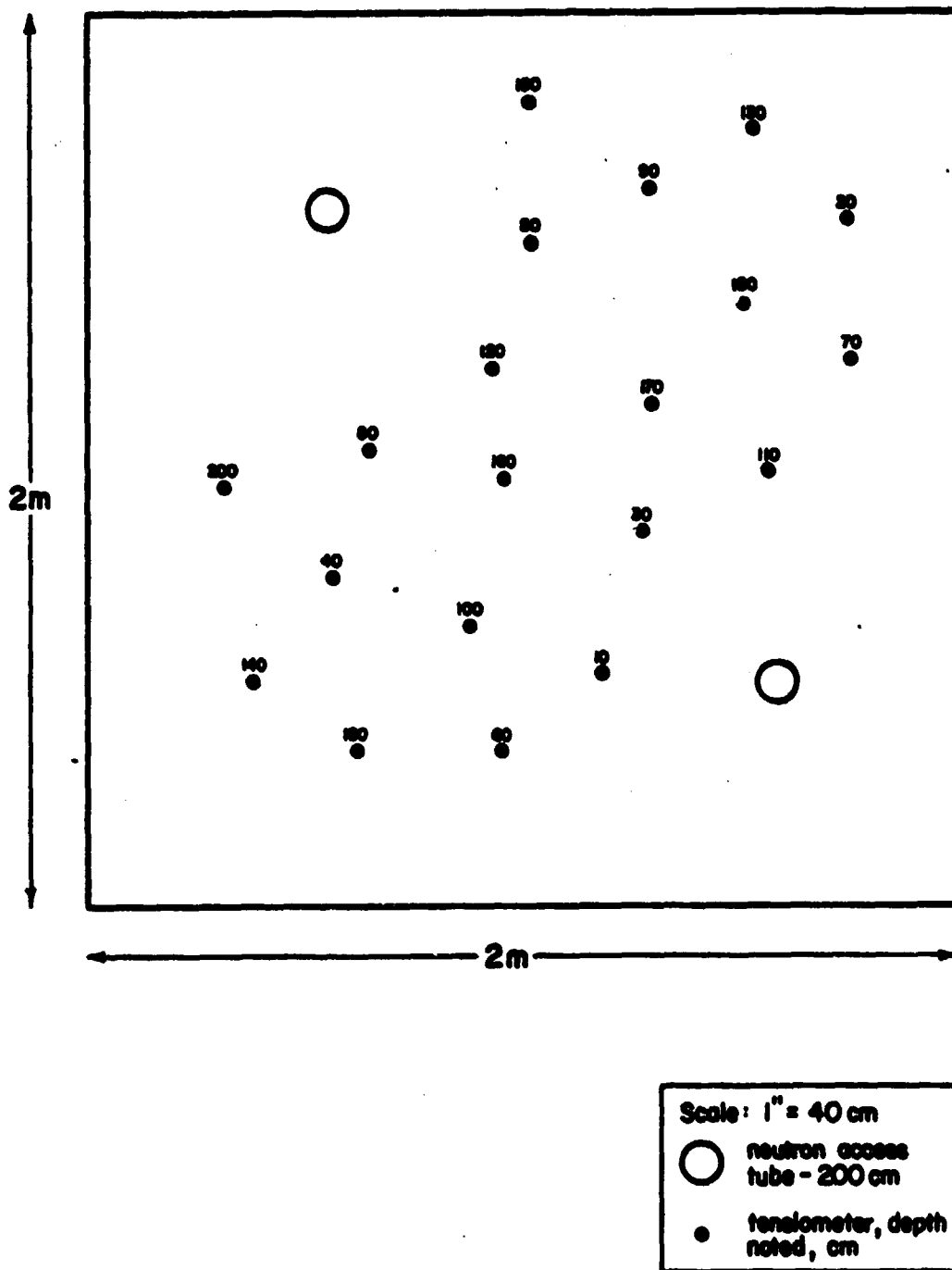


Fig. 5. Schematic diagram of instrument layout showing relative positions of neutron access tubes, tensiometers and tensiometer depths.

inside. Moisture measurements were taken with a neutron soil moisture meter (Model 105A Depth Moisture Probe, Model 600 Scaler, Troxler Electronics Laboratories). Three one-minute standard counts were obtained prior to and following each set of soil moisture readings while the neutron probe was inside the shield and wooden box on the soil surface. The standard counts for each set of data were averaged and divided into the soil moisture counts to obtain a count ratio. Several neutron access tubes were inserted outside the field plot for calibration purposes. Following neutron measurements at known depths, soil samples were taken at equivalent depths with a volumetric sampler to obtain bulk density and gravimetric water content for determining volumetric water content. A correlation was computed for the count ratio and the calculated volumetric water contents. To obtain a wider range of water contents than was available in the field, areas surrounding selected access tubes were irrigated. Bulk density readings in the plot were obtained with a depth density gauge (Model 1352 SN108, Troxler Electronics Laboratories).

The tensiometers were constructed from 1.27 cm I.D. PVC pipe. Porous ceramic cups (Soilmoisture Equipment Co., Cat. No. 2105-1) 0.6 cm O.D. and 2 cm in length were glued to one end of the pipe with epoxy and a small hole was drilled near the other end to allow passage

of a small nylon tube which ran from inside the tensiometer to a reservoir of mercury to become the manometer. Epoxy secured the nylon tubing to the pipe. To install the tensiometer, holes were augered in the soil to the desired depth, the tensiometer was pushed into the soil, and the manometers were installed (Soilmoisture Equipment Corp., Single Manometer Kit, Model 2300). Each tensiometer was maintained with distilled water and checked for air bubbles daily. One tensiometer at the 160 cm depth was faulty after installation in the field.

The plot was initially saturated and the resulting drainage period was monitored. To assure an even distribution of water and minimal soil disturbance during the saturation phase, a 6 mil polyethylene sheet with holes punched in a 10 cm grid pattern was used to cover the plot prior to saturation. A total of 102 cm of water was applied over a one-week period. Evaporation was minimal due to the climactic conditions.

Following the final application of water, the plot was covered with a black polyethylene sheet to prevent plant growth and evaporation. A third transparent sheet was also added. In addition, a polyethylene covered wooden shelter was constructed to cover the 2.2 m plot. The shelter protected the tensiometers, insured that rainfall would not reach the ground and aided in thermal insulation. The top was hinged for easy access to the tensiometers and neutron access tubes.

Neutron readings were started when the final water application

was estimated to have infiltrated. These readings were taken at 10 cm depth increments every two to four hours the first two days, twice per day the following four days, and daily for the following 40 days. Tensiometer readings were taken simultaneously with the soil moisture measurements.

CHAPTER IV

RESULTS AND DISCUSSION

The field site was located in the center of field 29 on the Texas A&M University farm. The soil was of the Norwood Series, Typic Udifluent. Using the pipette method of Day (1965) and a sieve analysis, a particle size distribution was obtained for each soil depth and then used to define the soil textural profile. The soil was predominately a silt loam, but silty clay loam dominated the top 20 cm of the soil profile and a thin layer of silty clay loam also occurred at a depth of 160 cm. Despite the general classification, a high clay content (above 24%) existed in the top 30 cm and again at the 120 cm depth as shown in Table 1 (p. 29).

The bulk density of the soil profile, obtained with a gamma density probe and a volumetric soil sampler, varied with depth as shown in Fig. 6 (p. 30). The values of bulk density decreased from 1.59 g/cm³ at the soil surface to 1.45 g/cm³ at a depth of 70 cm; and then increased to 1.65 g/cm³ at the 120 cm depth.

Results from the neutron probe calibration procedure, described earlier, are presented in Fig. 7 (p. 31) as count ratio versus volumetric water content. Two curves were obtained; one curve for the 10 cm soil depth and another for all depths greater than 10 cm. The 10 cm depth calibration curve accounted for the loss of fast neutrons at

TABLE 1

Texture Profile of Field Site

Depth	% Sand	% Silt	% Clay	Textural Class
0-15	6.40	61.84	31.76	Silty clay loam
15-25	4.00	69.86	26.14	Silt loam
25-35	9.32	74.54	16.14	Silt loam
35-55	10.55	76.84	12.58	Silt loam
55-85	32.20	55.66	12.14	Silt loam
85-95	14.80	73.81	11.39	Silt loam
95-105	23.60	66.16	10.24	Silt loam
105-115	6.95	75.79	17.26	Silt loam
115-145	4.20	71.21	24.59	Silt loam
145-155	10.00	70.00	20.00	Silt loam
155-165	1.75	58.23	40.02	Silty clay
165-185	30.00	56.00	14.00	Silt loam

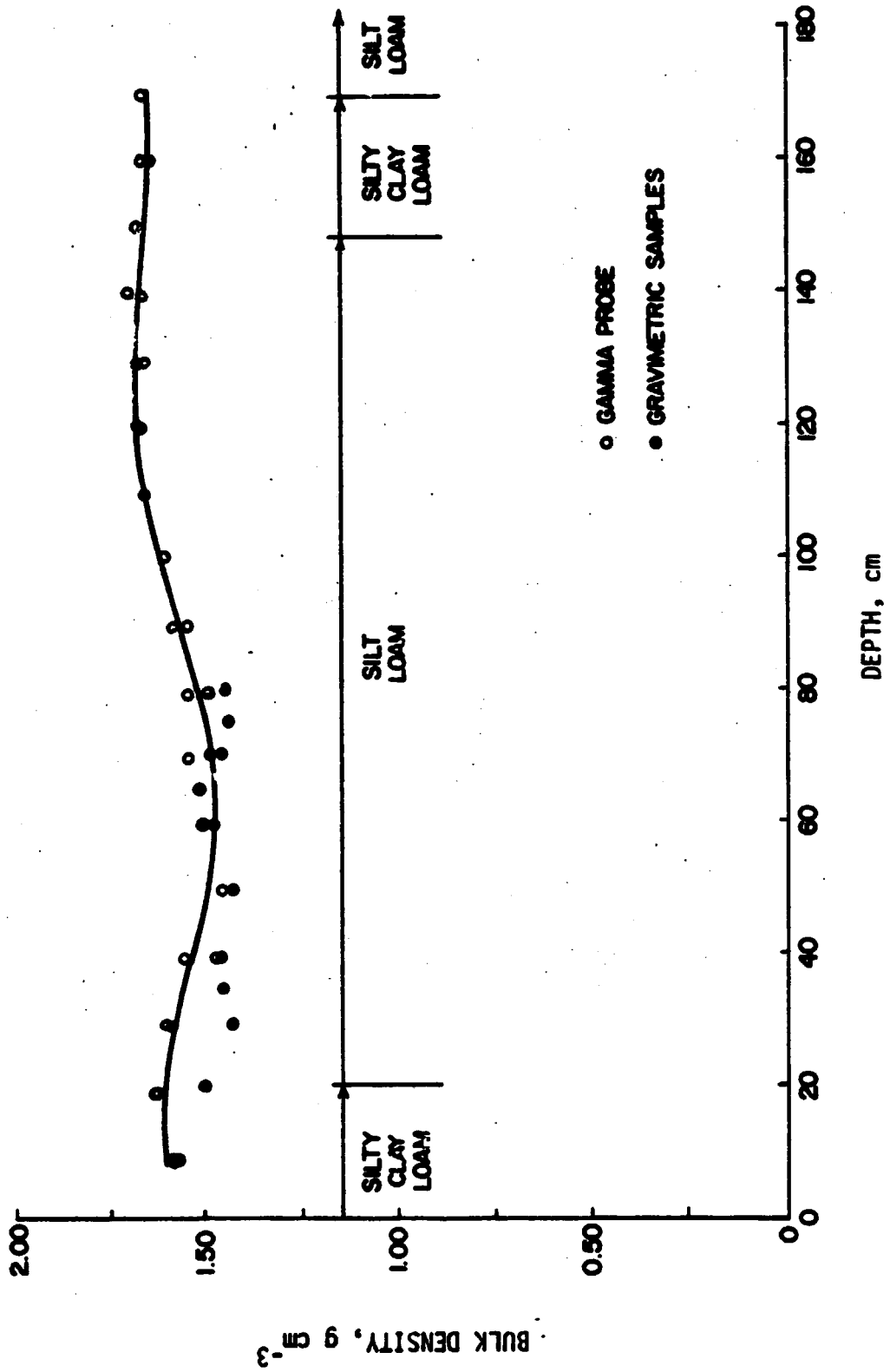
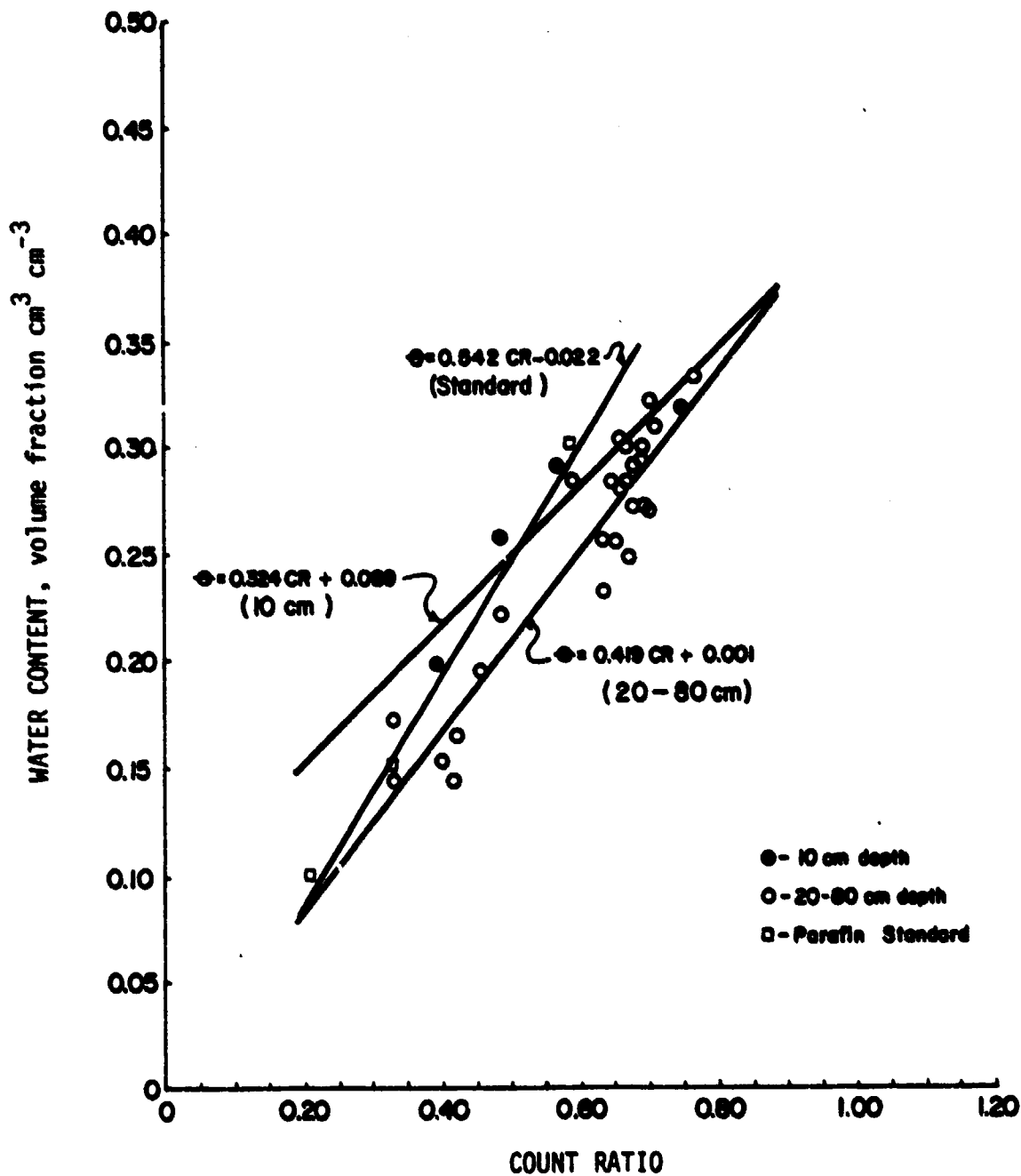


Fig. 6. Bulk density profile showing gamma probe data, gravimetric results and texture profile.

ORIGINAL PAGE IS
OF POOR QUALITY



Calibration curve for neutron soil moisture probe.

the soil surface. A lower neutron count reading was obtained for an equivalent water content in the 0 to 15 cm layer as compared to all depths greater than 15 cm. This is demonstrated by the higher intercept value for the 0 to 15 cm curve. Also, the radius of influence increases as the water content decreases causing a greater loss of fast neutrons which results in a lower slope for the 0 to 15 cm layer.

Accuracy of soil water content measurements obtained with the neutron probe is limited by the accuracy of the gravimetric soil water contents used to develop the calibration curves.

Soil Profile Hydrology

During the first few days of data collection, fluctuations in the tensiometer manometer readings were observed. These fluctuations were caused in part by temperature variations, since the readings were not taken at the same time each day. After the first few days, all readings were taken at 8 a.m. The tensiometer readings were referenced to the soil surface, yielding hydraulic head measurements. Pressure head was calculated by subtracting the depth of the respective tensiometer from the referenced values. The pressure potential for each tensiometer depth is shown in Fig. 8 (p. 33) and the hydraulic head profile for various times is plotted in Fig. 9 (p. 34).

A discontinuity in the average hydraulic head occurred in the 90 to 100 cm depth range. Slopes in hydraulic head averaged

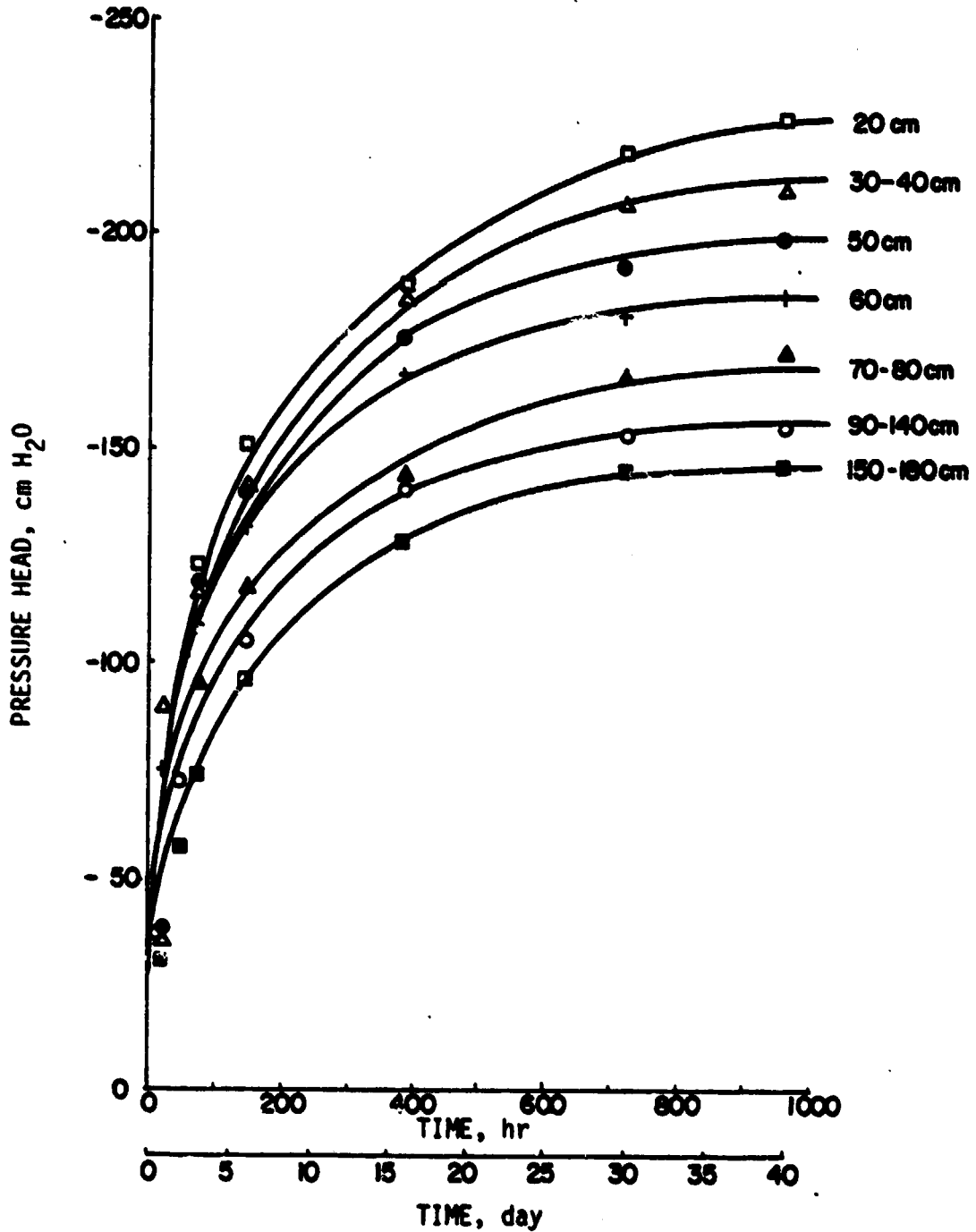
ORIGINAL PAGE IS
OF POOR QUALITY

Fig. 8. Tensiometry showing pressure head versus drainage period for each depth. (smoothed data)

ORIGINAL PAGE IS
OF POOR QUALITY

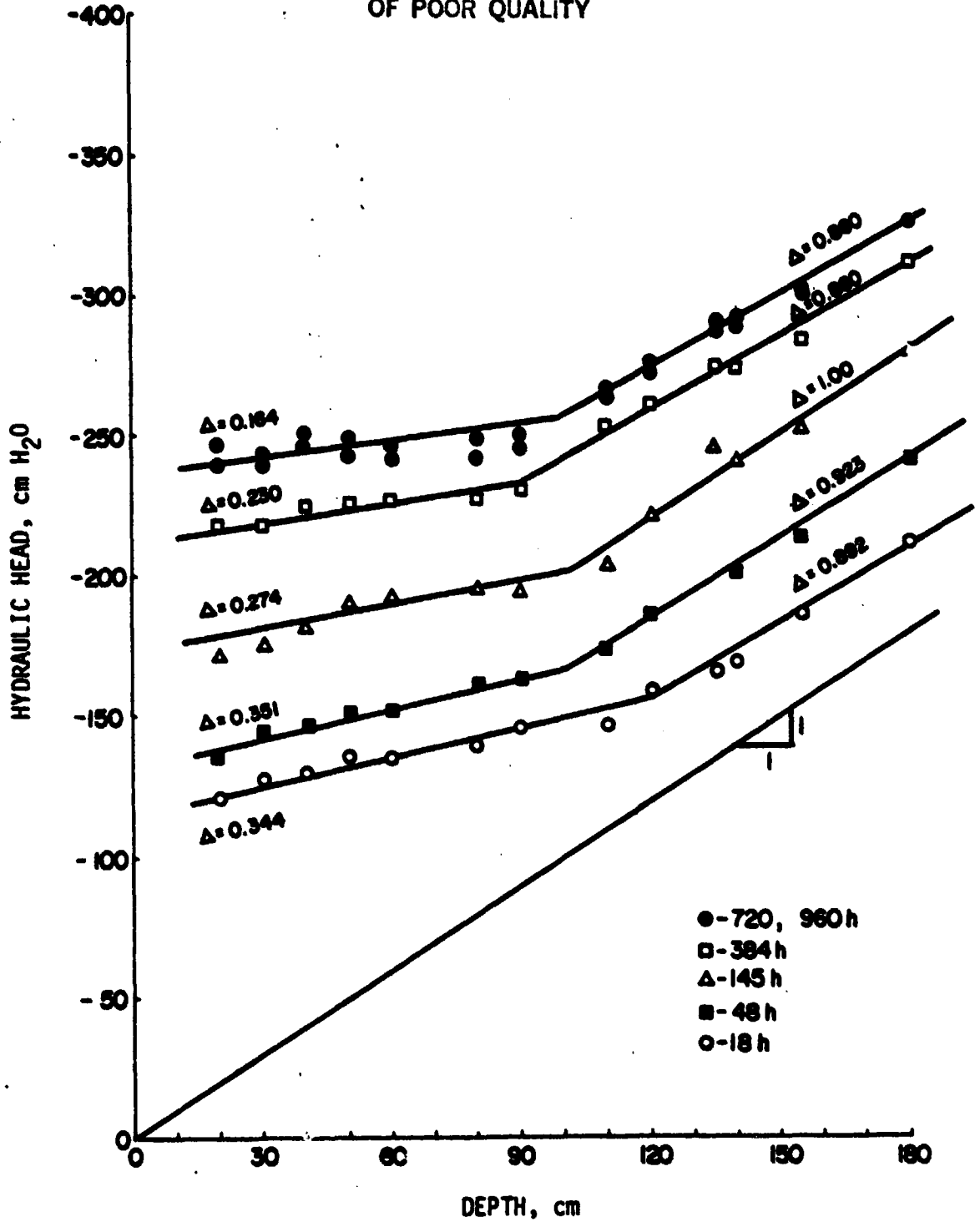


Fig. 9. Hydraulic head profiles for different times. (smoothed data)

less than 0.4 from 0 to 90 cm, but increased sharply to values near unity for depths greater than 90 cm.

The soil water content data are shown in Fig. 10 (p. 36) as volumetric water content versus depth for various times since saturation. The 6-hour data show the maximum water contents; thus, it was used as the initial soil water content curve. The change in water content with time at depths below 90 cm was minimal when compared to the change in soil water content which occurred above this depth. This fact plus the fact that values of dH/dz were near unity for depths greater than 90 cm (refer to Fig. 9, p. 34) indicated that approximate steady-state flow conditions prevailed in the lower soil layers.

To demonstrate the drainage process, the soil moisture content in each soil layer is plotted versus time in Fig. 11 (p. 37). The rate of change in water content as a function of time was determined from this figure. The volume flux or the total water content change per unit time, through each soil layer, is shown in Fig. 12 (p. 38). Volume flux through each depth increment was obtained by integrating the soil moisture versus time curve (Fig. 11) with respect to depth.

The volume fluxes for the lower soil depths varied only slightly from each other. However, the volume flux in the upper soil layer (30 cm) was less than the volume flux obtained at the other soil

ORIGINAL PAGE IS
OF POOR QUALITY

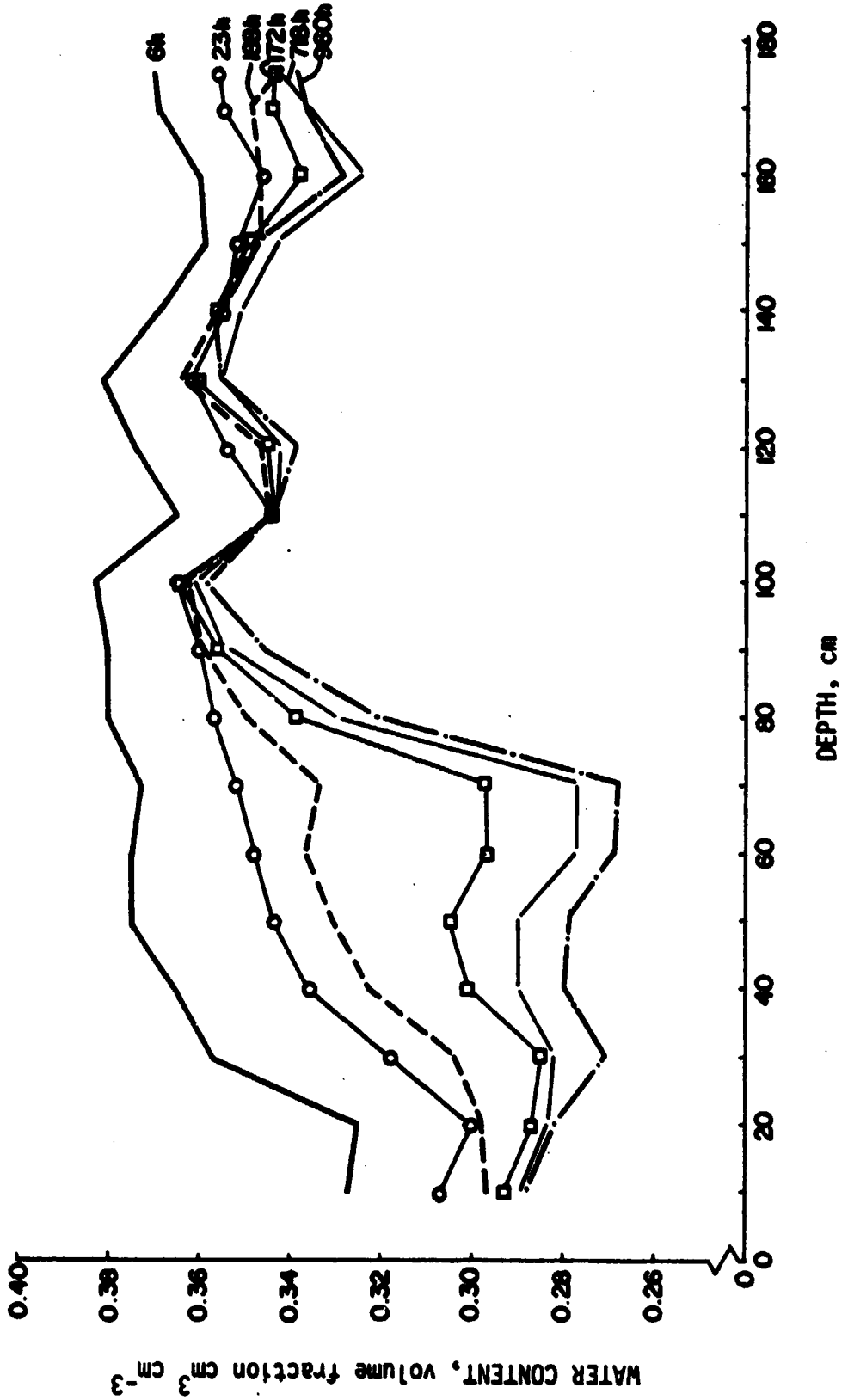


Fig. 10. Soil moisture profiles for different times.

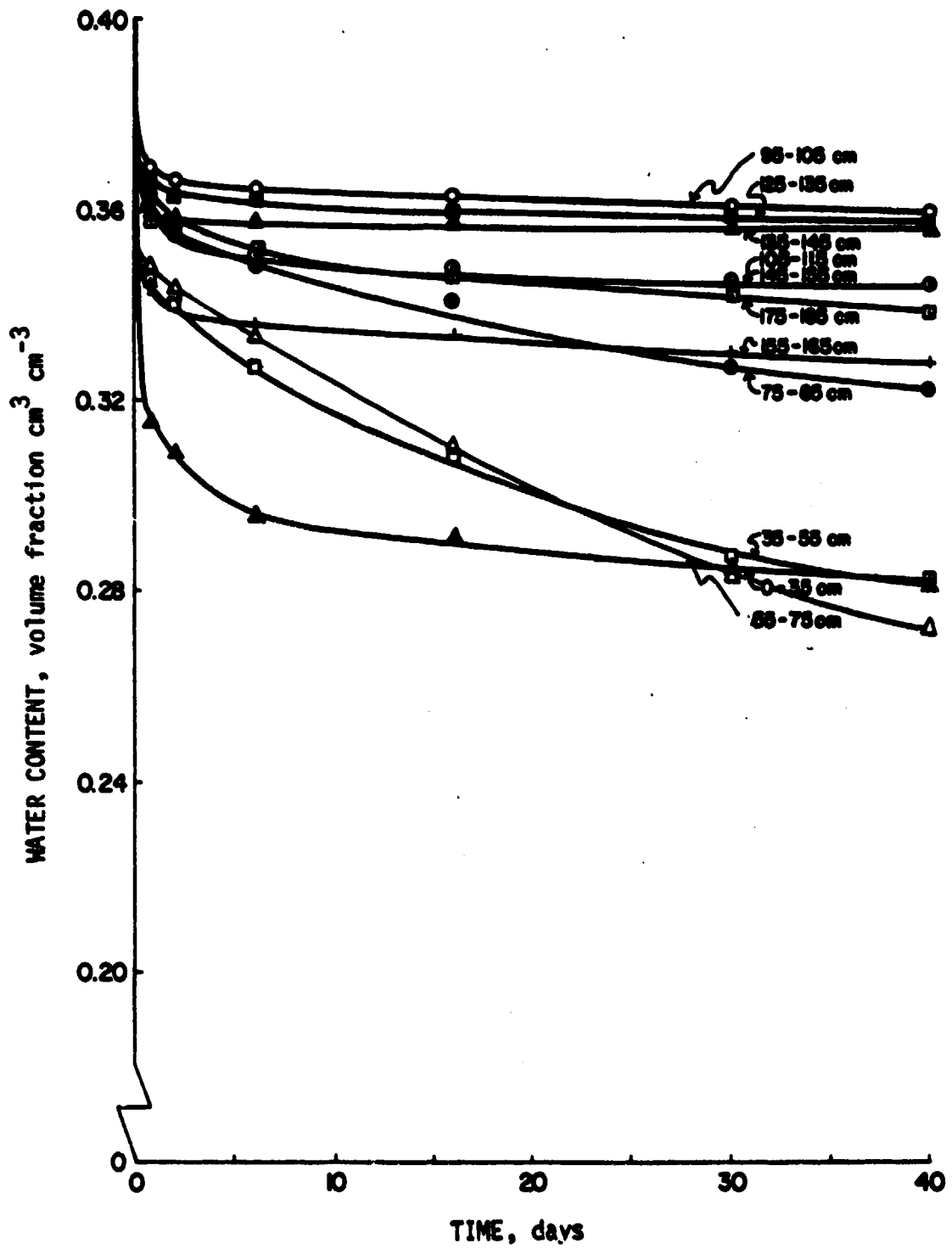


Fig. 11. Soil moisture for different depths.

ORIGINAL PAGE IS
OF POOR QUALITY

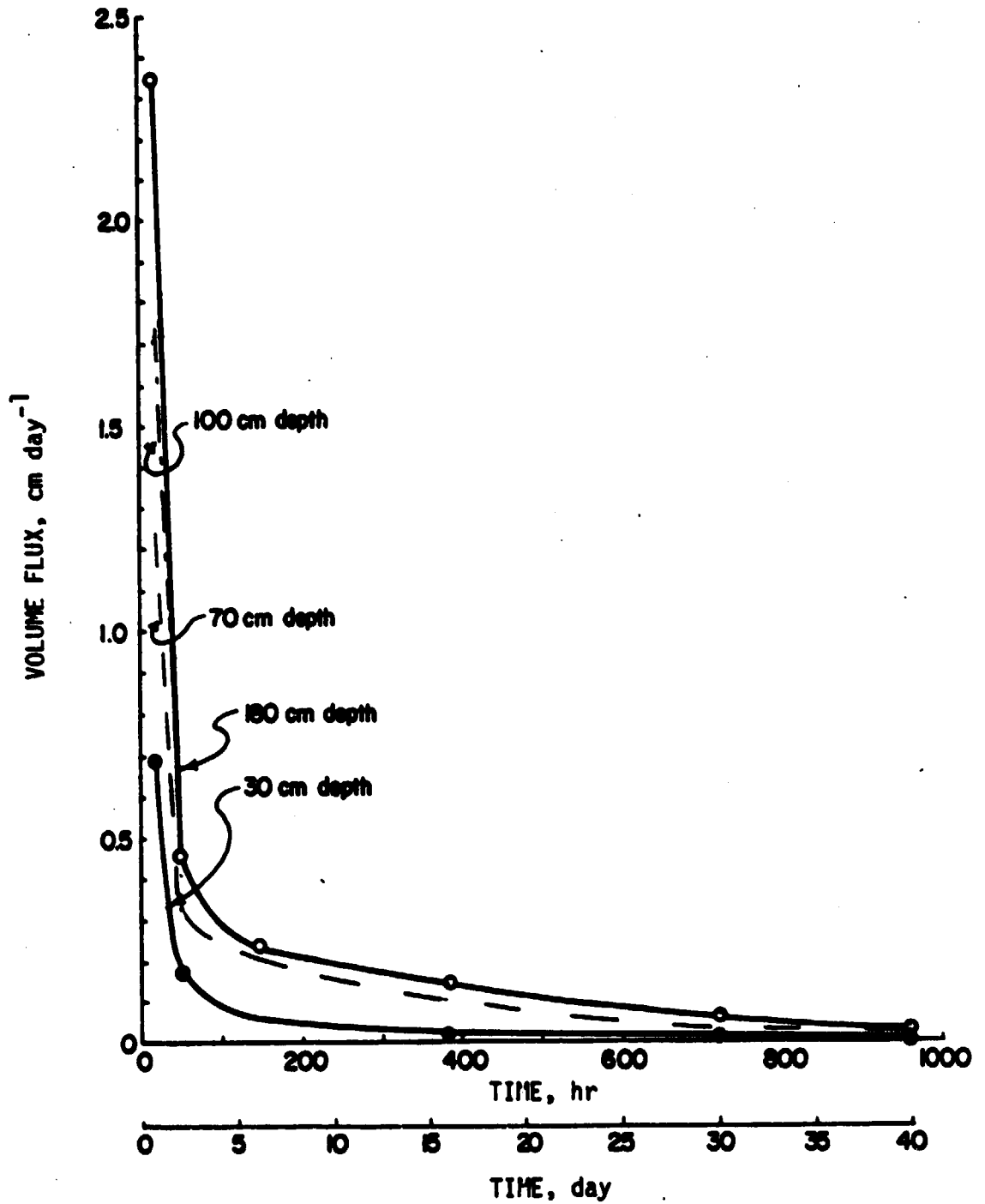


Fig. 12. Volume flux versus time for various depths.

depths. The drainage process for the deeper soil layers continued over a much longer period of time than for the shallow soil depths.

Hydraulic conductivity was calculated at known times and water contents by dividing the volume flux, q , by the change in hydraulic head, dH/dz (see Fig. 9, p. 34). It was evident that the relationship between hydraulic conductivity and water content varied with soil depth. Curves for each soil depth are shown in Figs. 13-17 (pp. 40, 41, 42, 43, 44, respectively) and calculations are demonstrated in Appendix A (pp. 75-80). The large slopes (dH/dz) for depths below 80 cm would cause considerable error in estimating fluxes with measured gradients for even a small change in water content.

Double-tube method.

Saturated hydraulic conductivity was determined for three depths: 10, 40 and 70 cm. Several runs with the double-tube apparatus were necessary before a successful run was executed. Difficulties stemmed from inserting the inner tube into the soil too shallow and poor cleaning of the hole surface. These factors are not recognized until both tubes are in the ground and preliminary data are collected.

The final runs at the three soil depths worked well, however. The data used to calculate the saturated conductivities are presented in Table A-7 and Figs. A-1, A-2 and A-3 of Appendix A. Table 2 (p. 45) shows the outcome of the test and Fig. 18 (p. 46) shows the saturated conductivities versus depth.

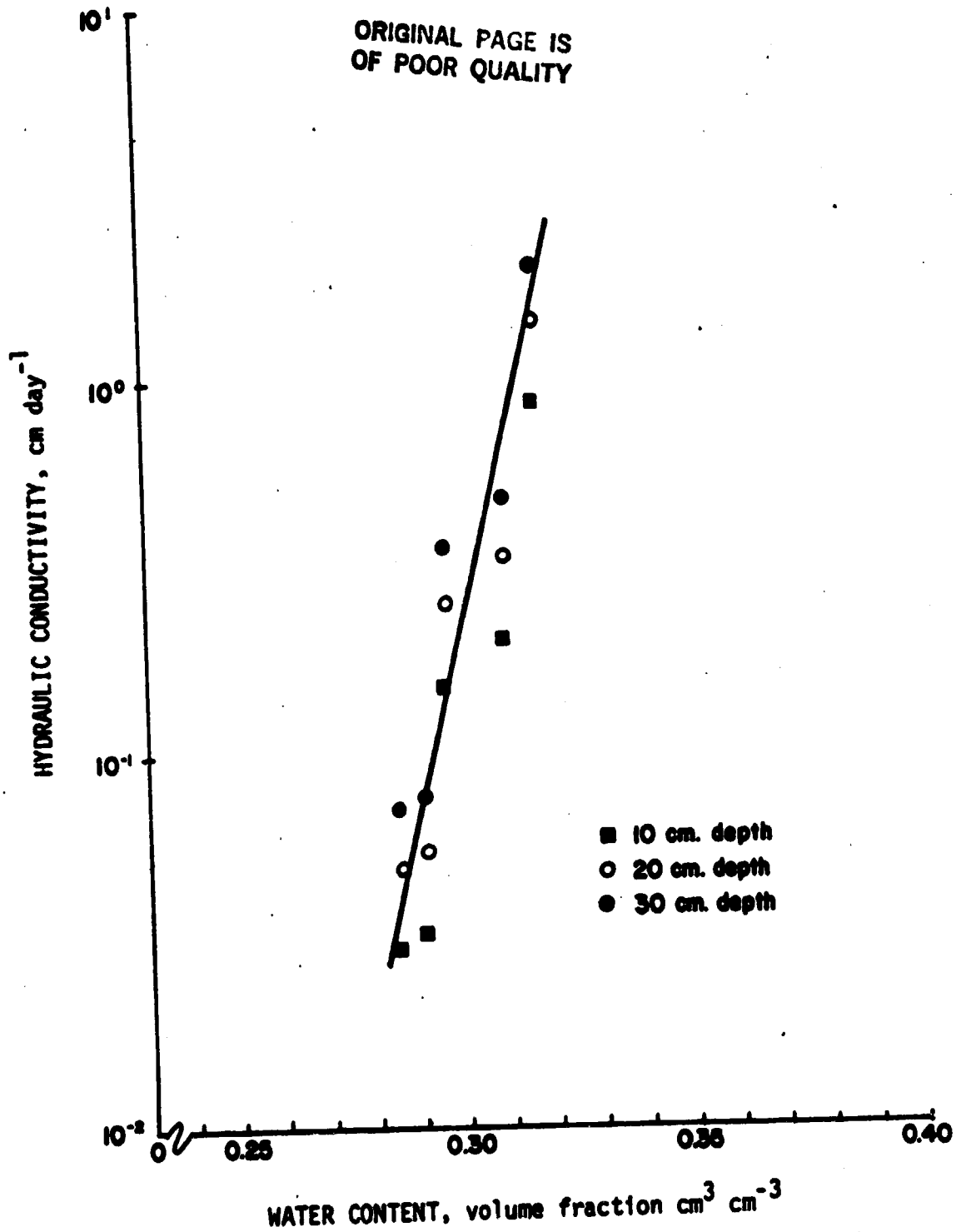


Fig. 13. Relationship between hydraulic conductivity and water content determined from field measurements for 10-30 cm soil depth.

ORIGINAL PAGE IS
OF POOR QUALITY

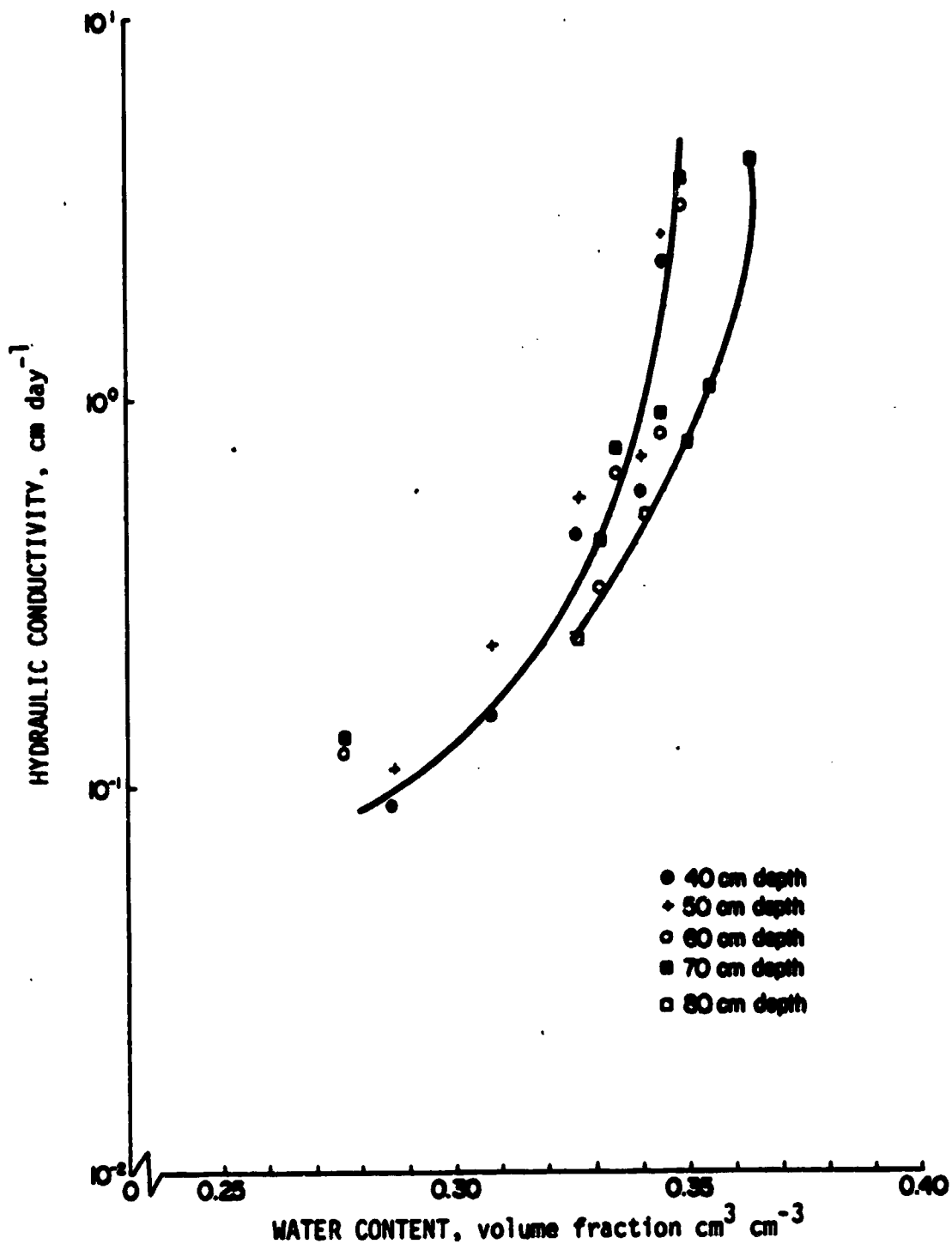


Fig. 14. Relationship between hydraulic conductivity and water content determined from field measurements for 40-80 cm soil depth.

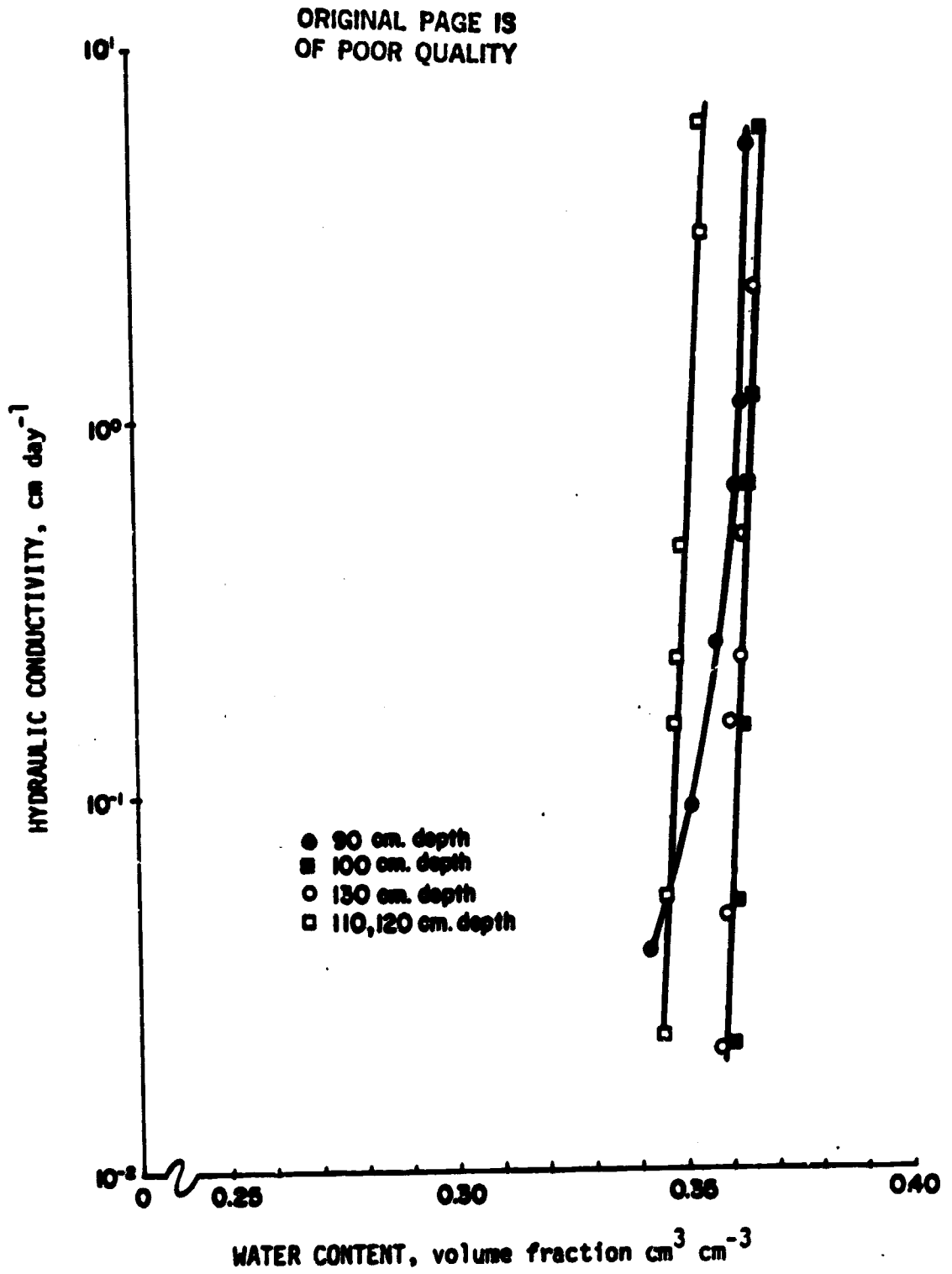


Fig. 15. Relationship between hydraulic conductivity and water content determined from field measurements for 90-120 cm soil depth.

ORIGINAL PAGE IS
OF POOR QUALITY

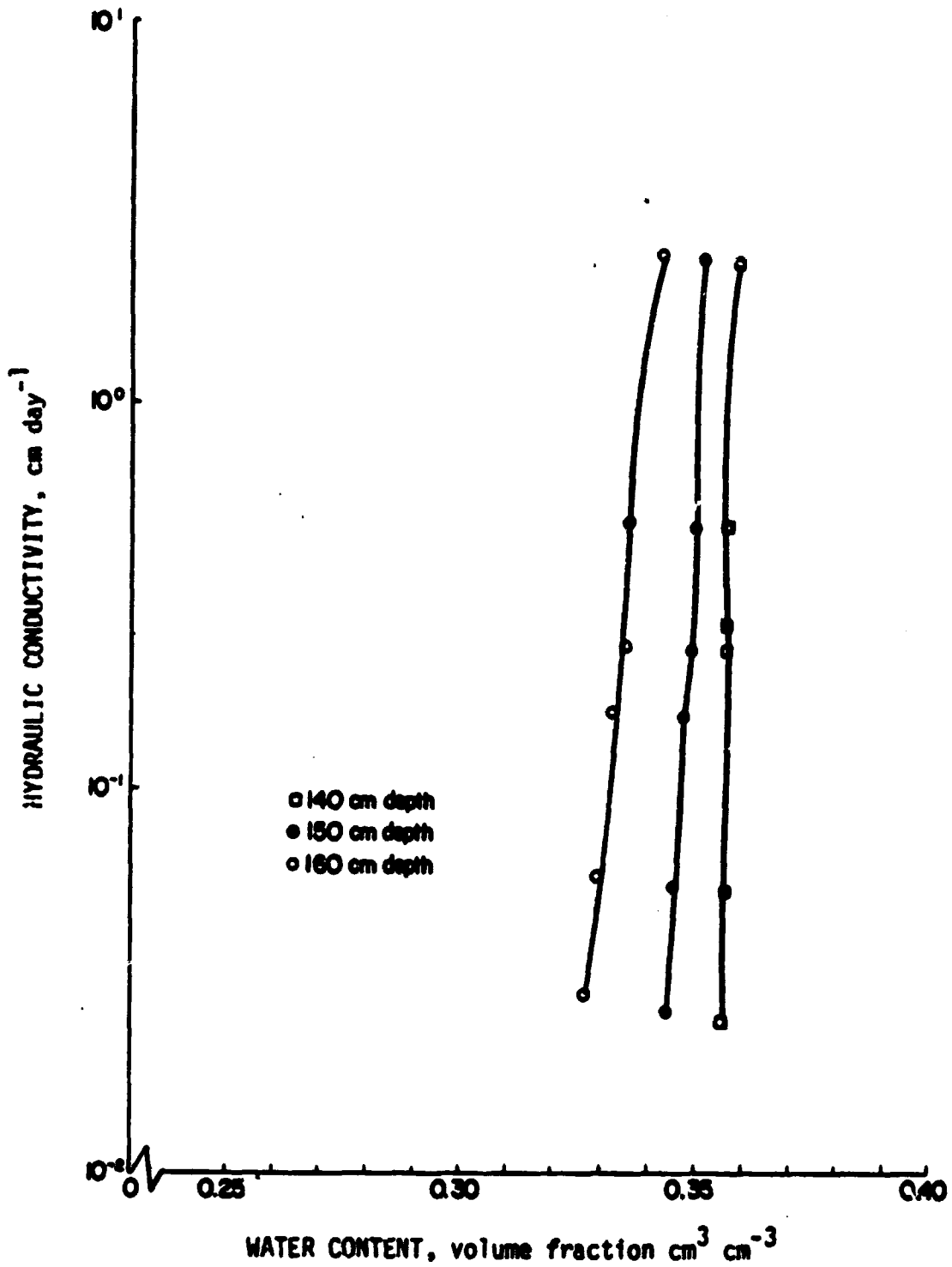


Fig. 16. Relationship between hydraulic conductivity and water content determined from field measurements for 140-160 cm soil depth.

ORIGINAL PAGE IS
OF POOR QUALITY

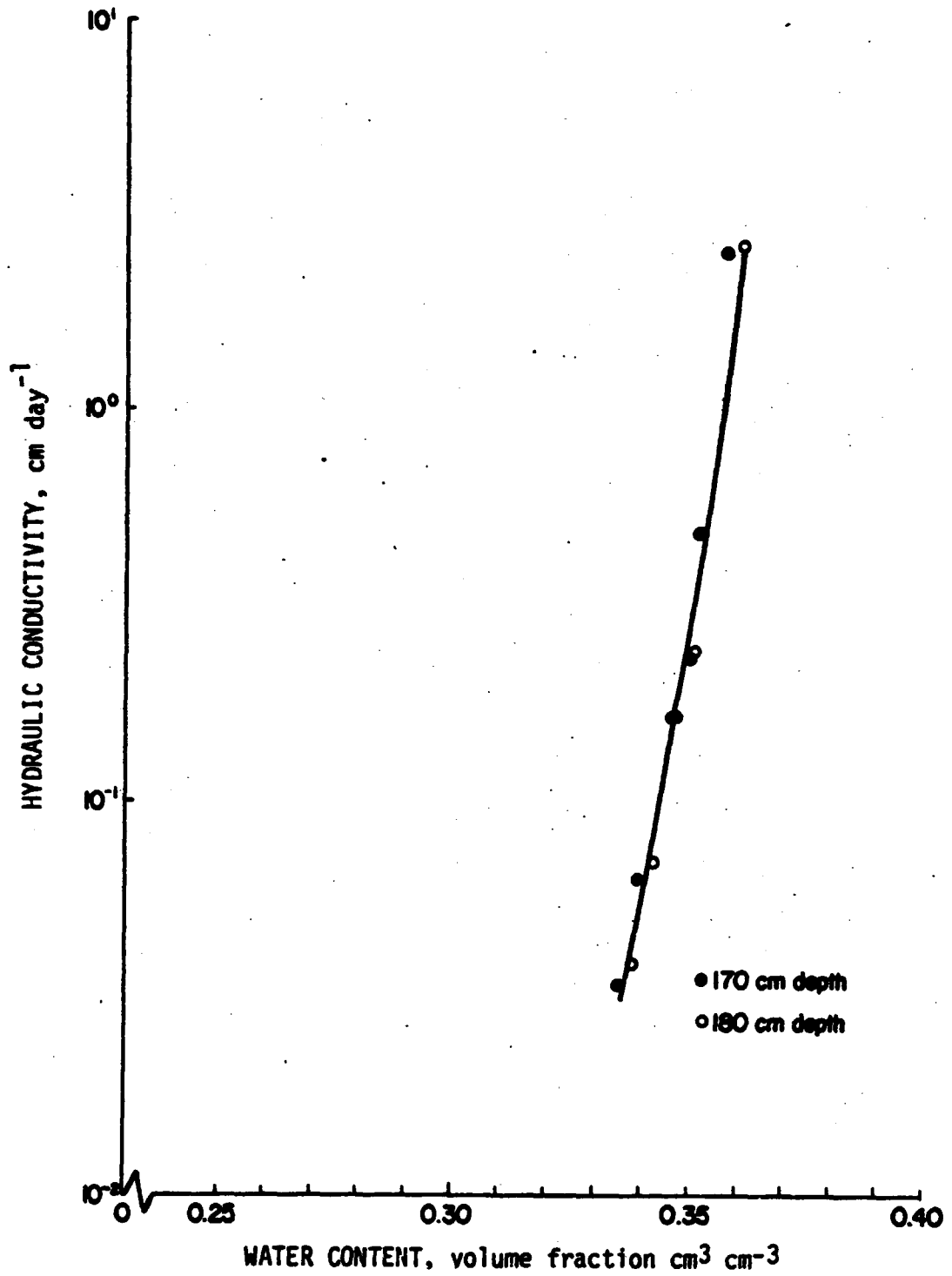


Fig. 17. Relationship between hydraulic conductivity and water content determined from field measurements for 170-180 cm soil depth.

TABLE 2

Saturated Conductivities Measured with Double-Tube Apparatus

<u>Depth, cm</u>	<u>Ks, cm/day</u>	<u>Ks, m/s</u>
10	4.25	4.9×10^{-7}
40	40.90	4.7×10^{-6}
70	53.44	6.2×10^{-6}

SATURATED CONDUCTIVITY
(measured with double-tube apparatus)

Depth (cm)	Ks (cm/day)	Ks (m/s)
10	4.2	4.91×10^{-7}
30	20.9	2.42×10^{-6}
40	48.2	5.58×10^{-6}
50	60.9	7.05×10^{-6}
70	64.8	7.50×10^{-6}

ORIGINAL PAGE IS
OF POOR QUALITY

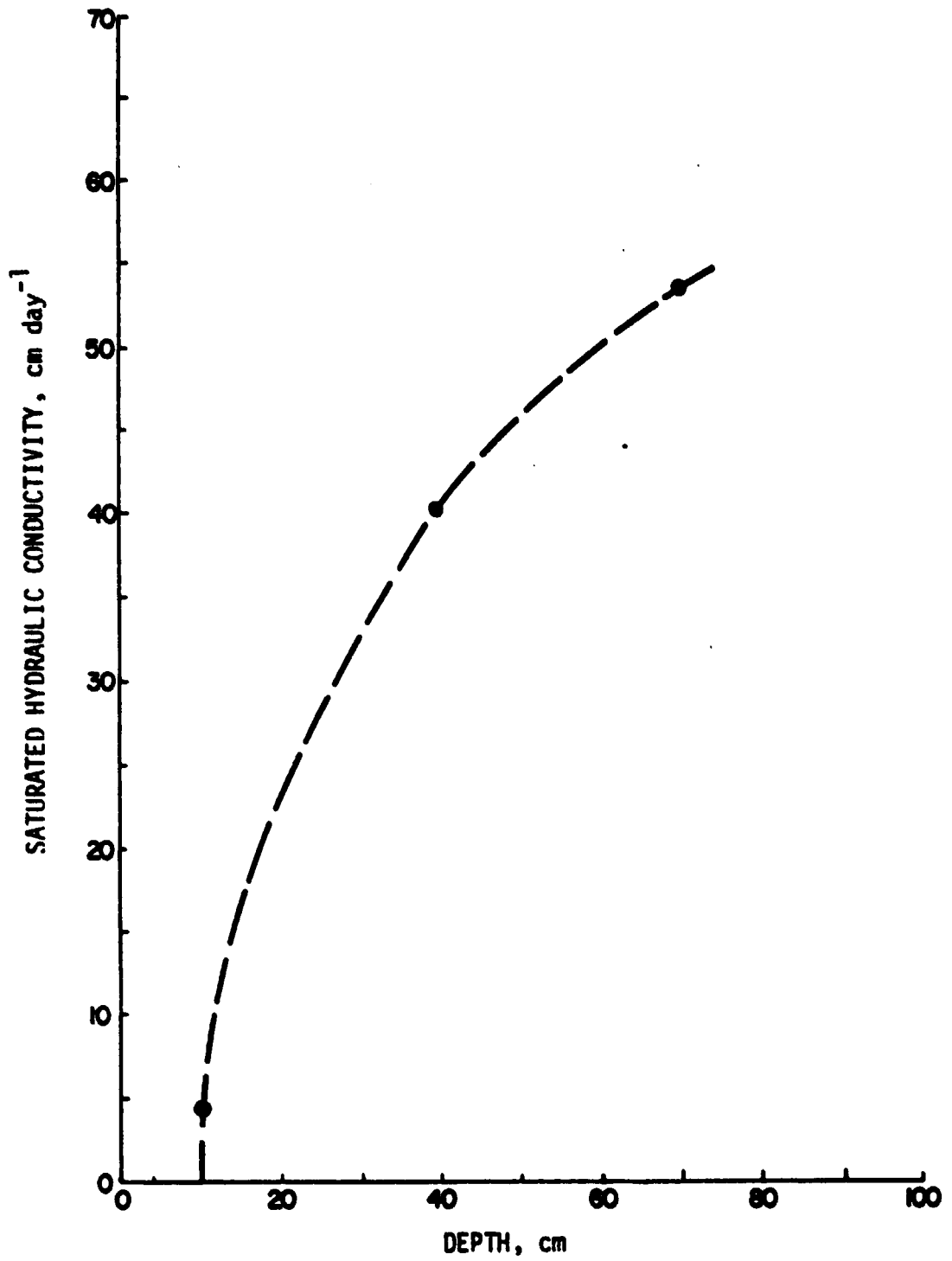
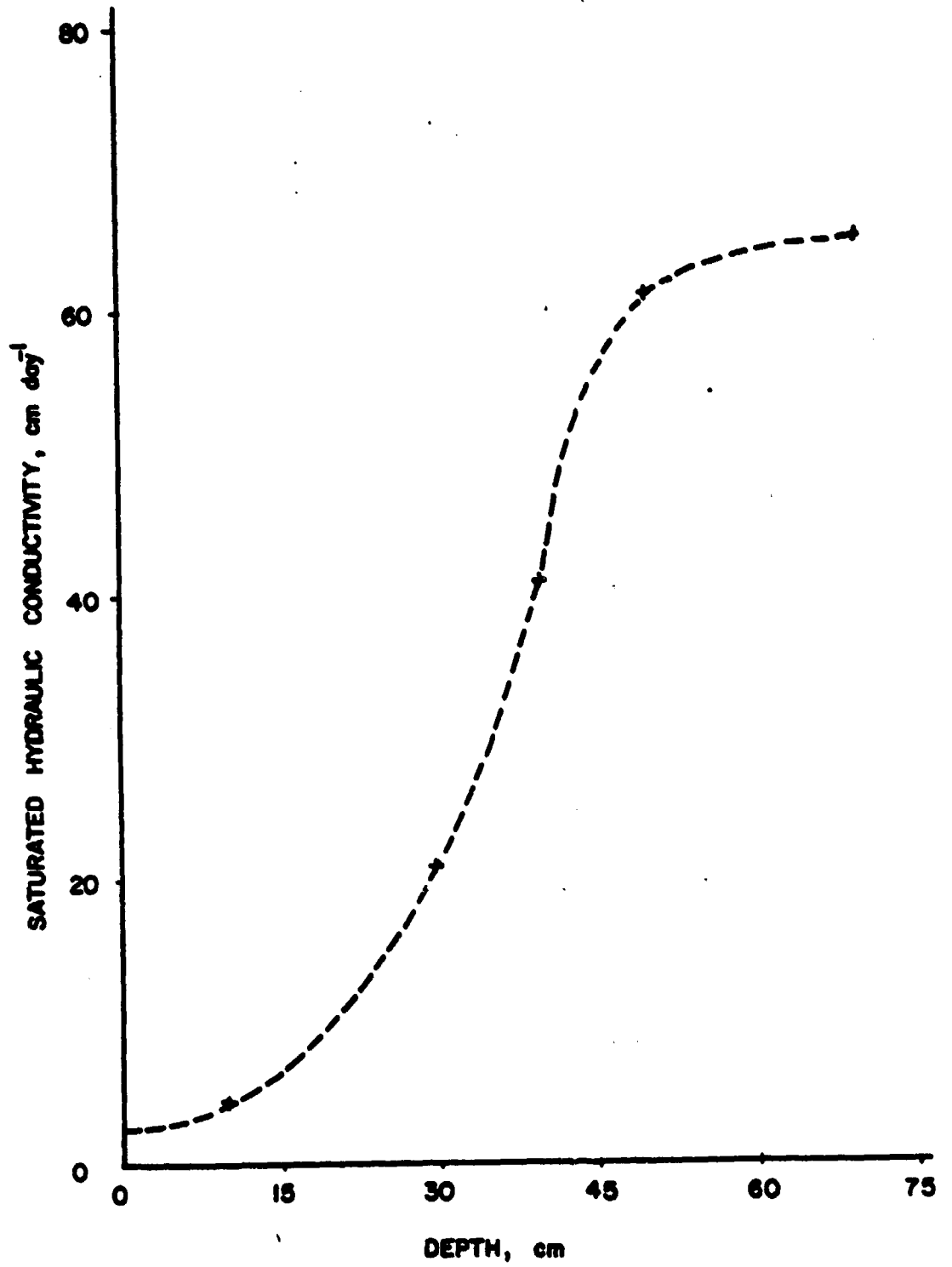


Fig. 18. Saturated hydraulic conductivity versus depth.

ORIGINAL PAGE IS
OF POOR QUALITY



Saturated hydraulic conductivity from double-tube method.



Laboratory Measurements

Water retentivity curves were determined using the pressure-plate extractor data. Soil samples from 0-15, 15-55 and 55-90 cm depth increments were used. However, results for the latter two soil depths were very similar, as can be seen in Figs. 19-21 (pp. 48, 49, and 50, respectively). The values of saturated water contents shown in these figures were theoretically calculated from:

$$S = \frac{100 (p - D_b)}{p} \quad (14)$$

where S is the total porosity (%), p is the particle density (M/L^3), and D_b is the bulk density (M/L^3). A value of 2.65 g/cm^3 was used for p .

Calculations of hydraulic conductivity were made using the relationship in Jackson's procedure. The solid lines in Fig. 22 (p. 51) are the calculated values for the soil depth from 0 to 25 cm using the retentivity curve in Fig. 19 and various saturated hydraulic conductivity (K_s) values. $K_s = 4.25 \text{ cm/day}$ was the measured saturated hydraulic conductivity in the field at the 10 cm soil depth. The other two, $K_s = 20 \text{ cm/day}$ and $K_s = 30 \text{ cm/day}$ were roughly estimated from the curve of saturated conductivity versus depth (Fig. 18, p. 46) for the 20 to 25 cm soil depth. The solid dots are the measured values of hydraulic conductivity from the instantaneous profile method for the 0 to 25 cm soil depth. The correlation of calculated (Jackson) to

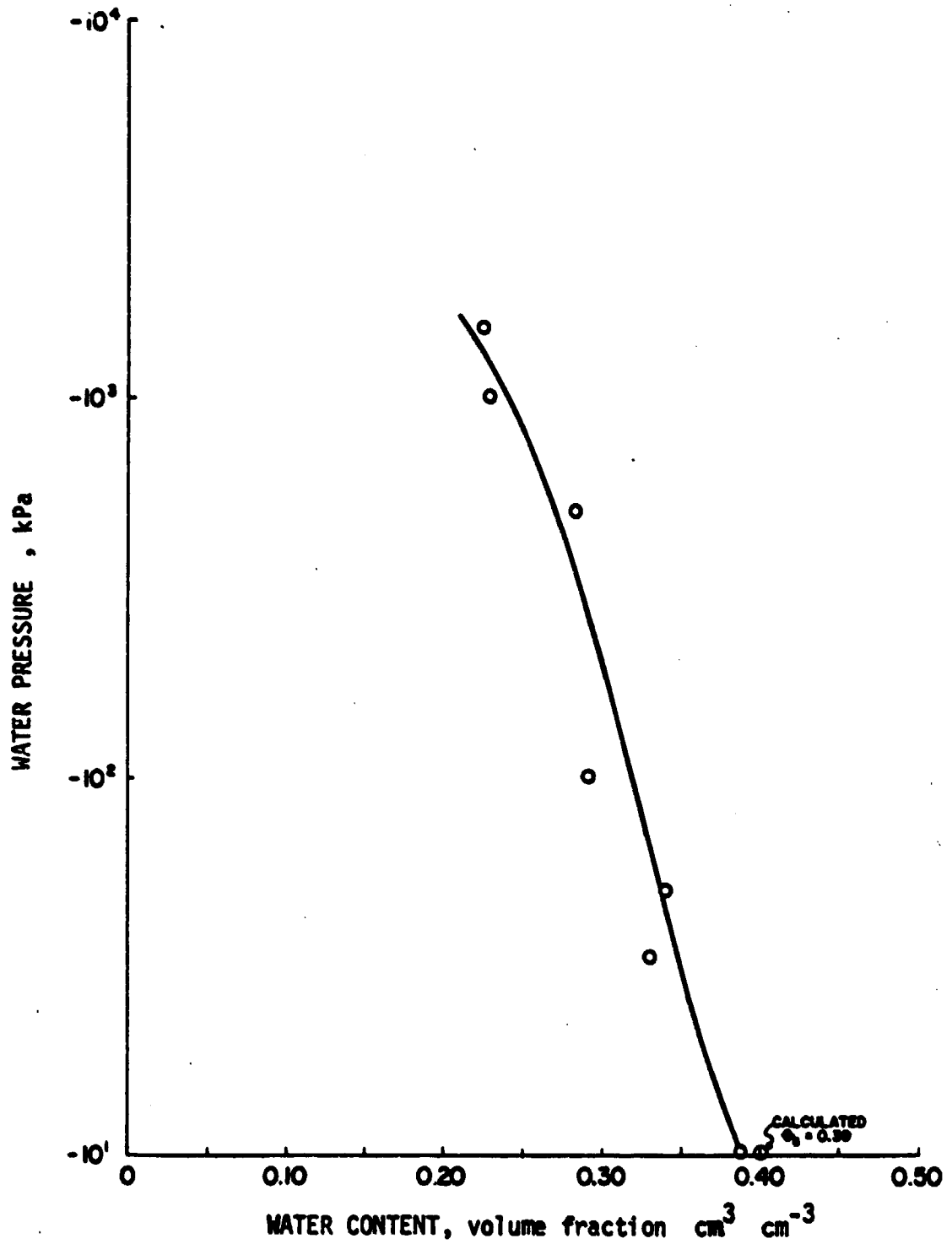


Fig. 19. Water retentivity determined in the laboratory,
0-15 cm soil depth.

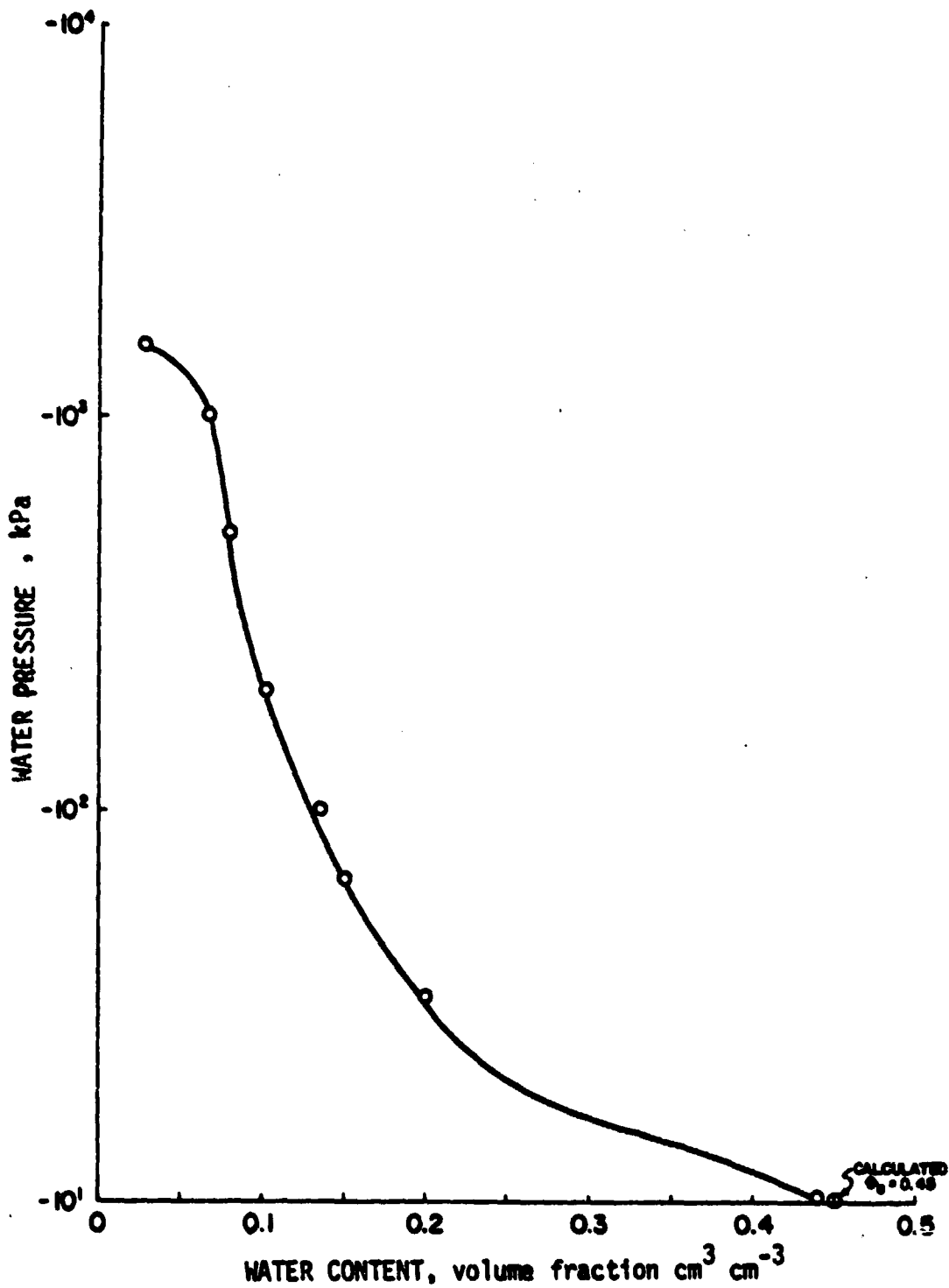
ORIGINAL PAGE IS
OF POOR QUALITY

Fig. 20. Water retentivity determined in the laboratory, 15-55 cm soil depth.

ORIGINAL PAGE IS
OF POOR QUALITY

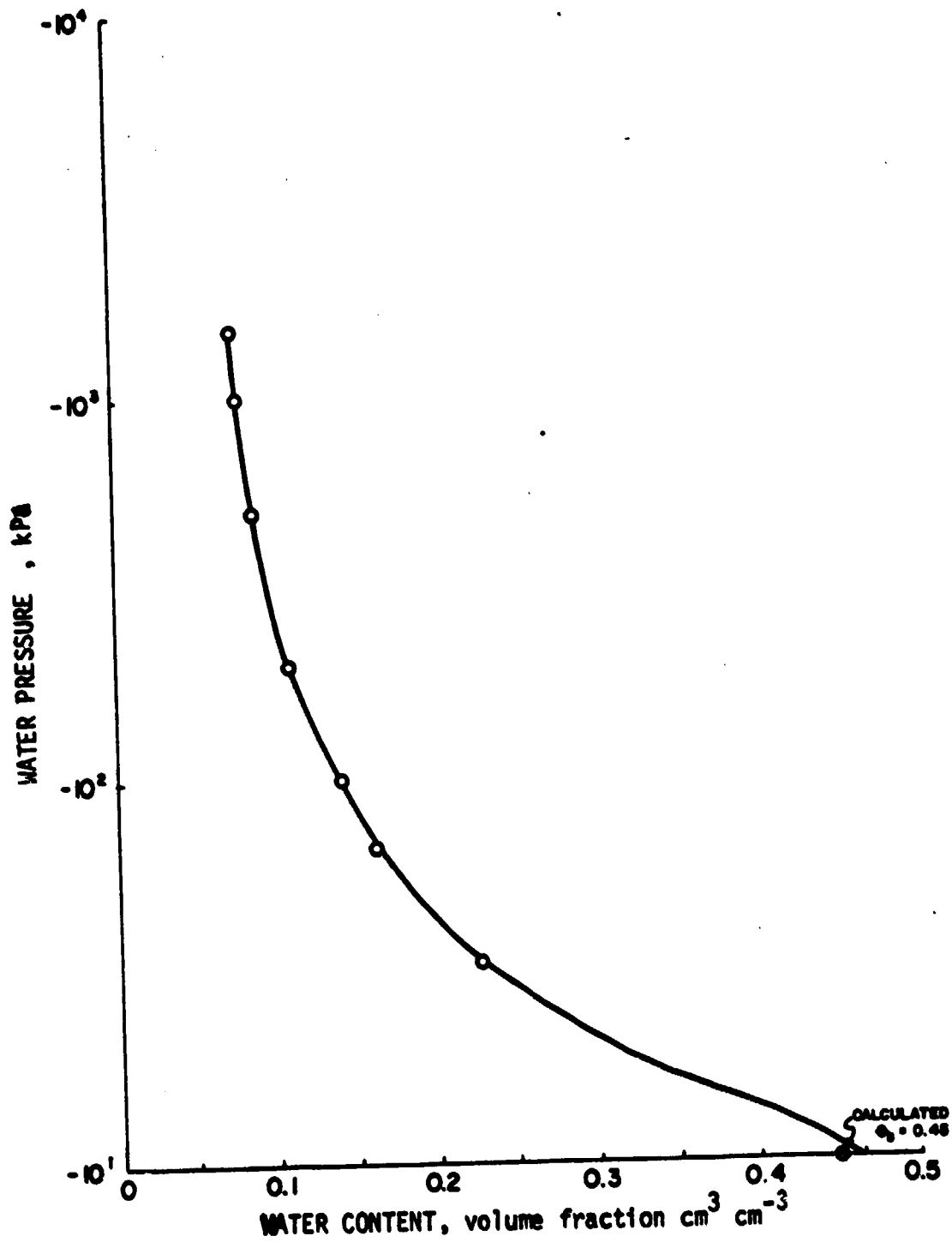


Fig. 21. Water retentivity determined in the laboratory,
55-90 cm soil depth.

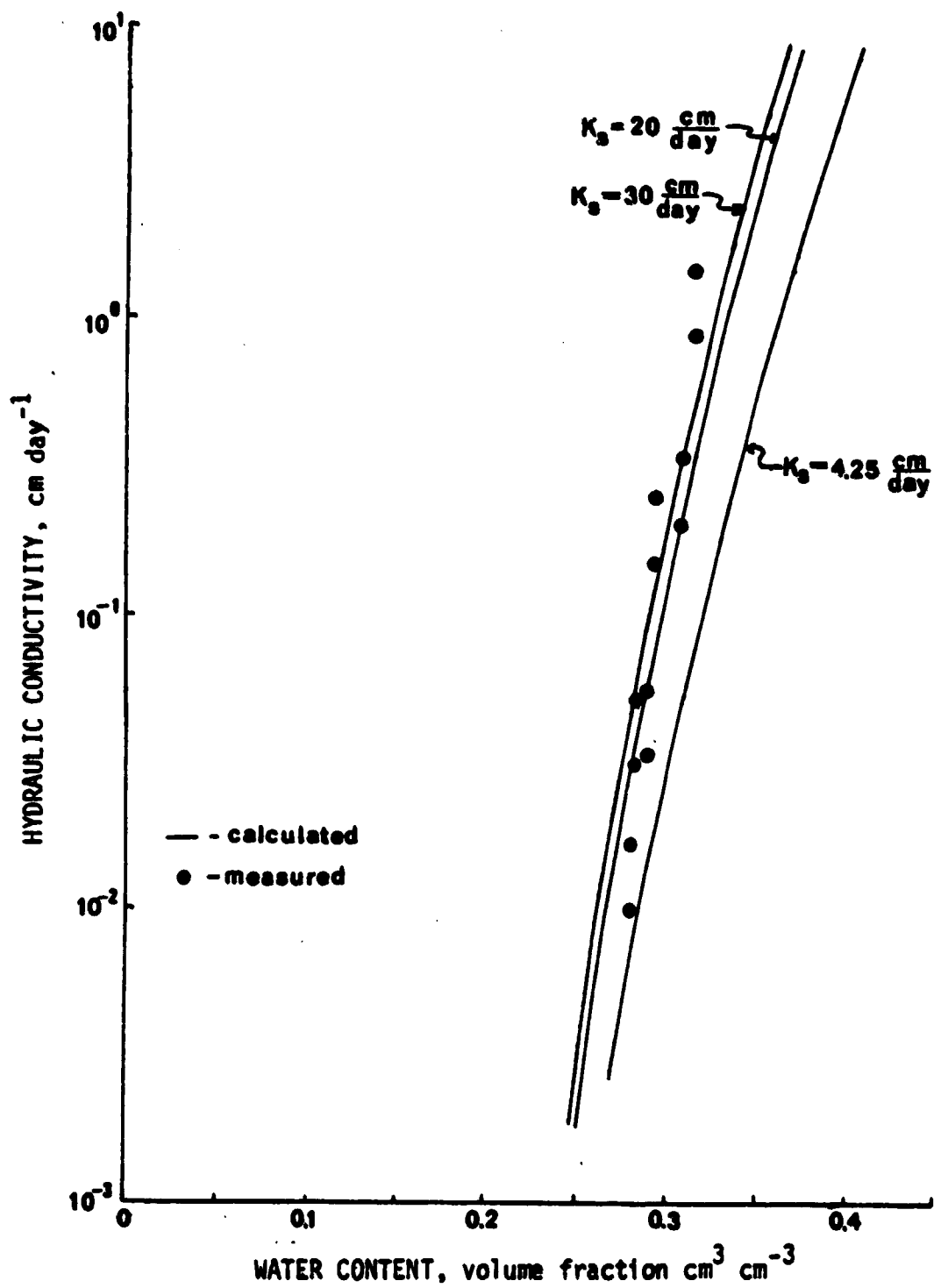


Fig. 22. Comparison of calculated to measured hydraulic conductivity, 0-25 cm soil depth.

to measured (instantaneous profile) is quite good for the 0 to 25 cm depth, particularly for the higher saturated hydraulic conductivity values.

Fig. 23 (p. 53) shows the same comparison, Jackson's procedure for calculation (solid line) and in situ measured values (solid dots) of hydraulic conductivity, for 15 to 55 cm and 55 to 90 cm soil depths. The values of hydraulic conductivity for the 15 to 55 cm depth were calculated from the respective water retention curve (Fig. 20, p. 49) and using $K_s = 40.9$ cm/day (measured at 40 cm soil depth). The hydraulic conductivity for the second soil depth, 55 to 90 cm, was calculated from the respective water retention curve (Fig. 21, p.50) and with $K_s = 53.4$ cm/day (measured at 70 cm soil depth). The solid dots are measured hydraulic conductivity for the 30 to 80 cm soil depth. The correlation observed in this comparison was not very good.

Another approach for evaluating the theoretical method for calculating hydraulic conductivity was to use field pressure potential in conjunction with the laboratory retention curves. Because of the limited water content range occurring during the field experiment the field data fell within the higher pressure region so that the laboratory data was used to extrapolate the curves into the lower pressure range as shown in Figs. 24 and 25 (pp. 54 and 55). When these combined retention curves were used with Jackson's procedure, little difference

ORIGINAL PAGE IS
OF POOR QUALITY

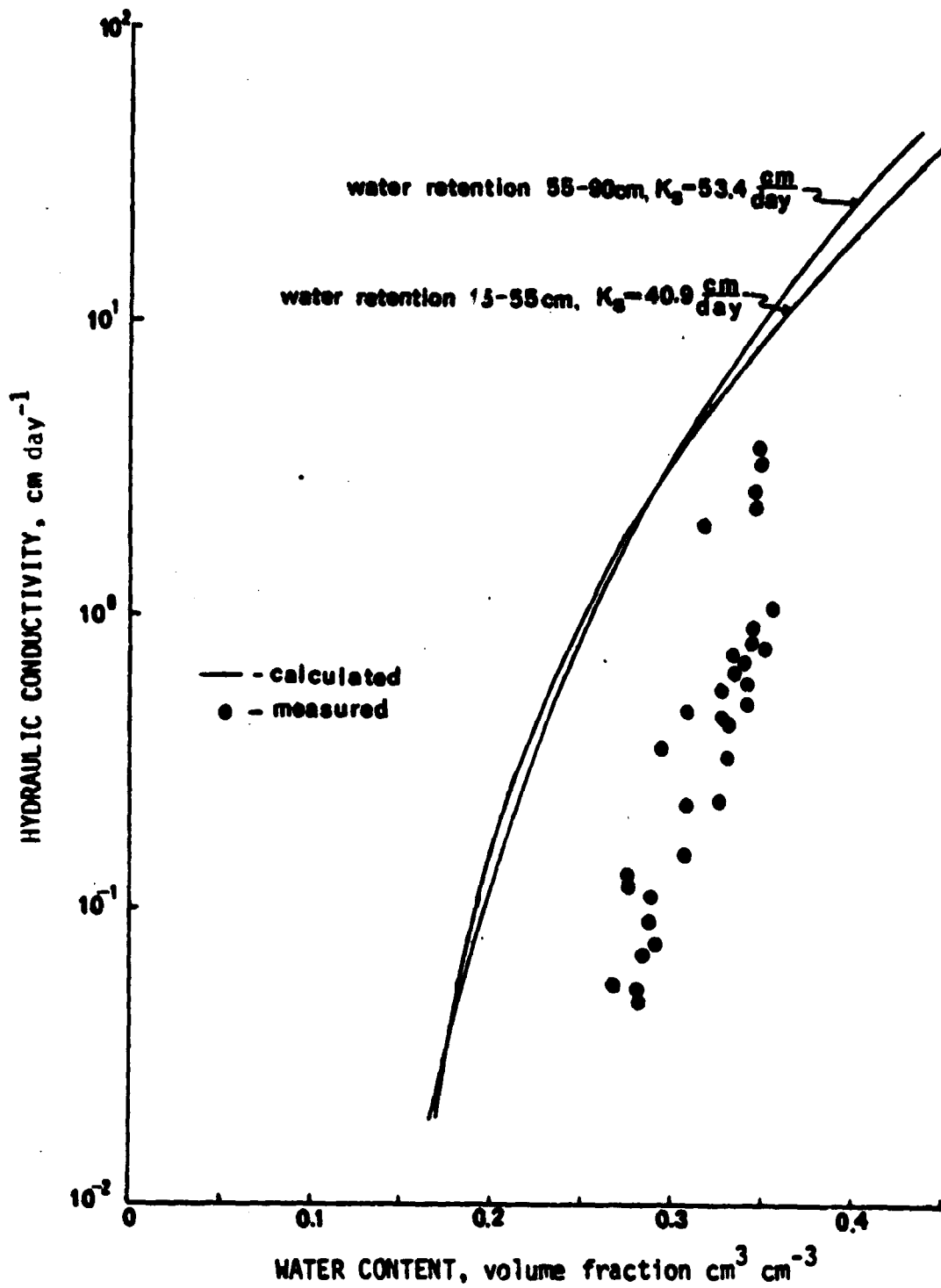


Fig. 23. Comparison of calculated to measured hydraulic conductivity, 30-80 cm soil depth.

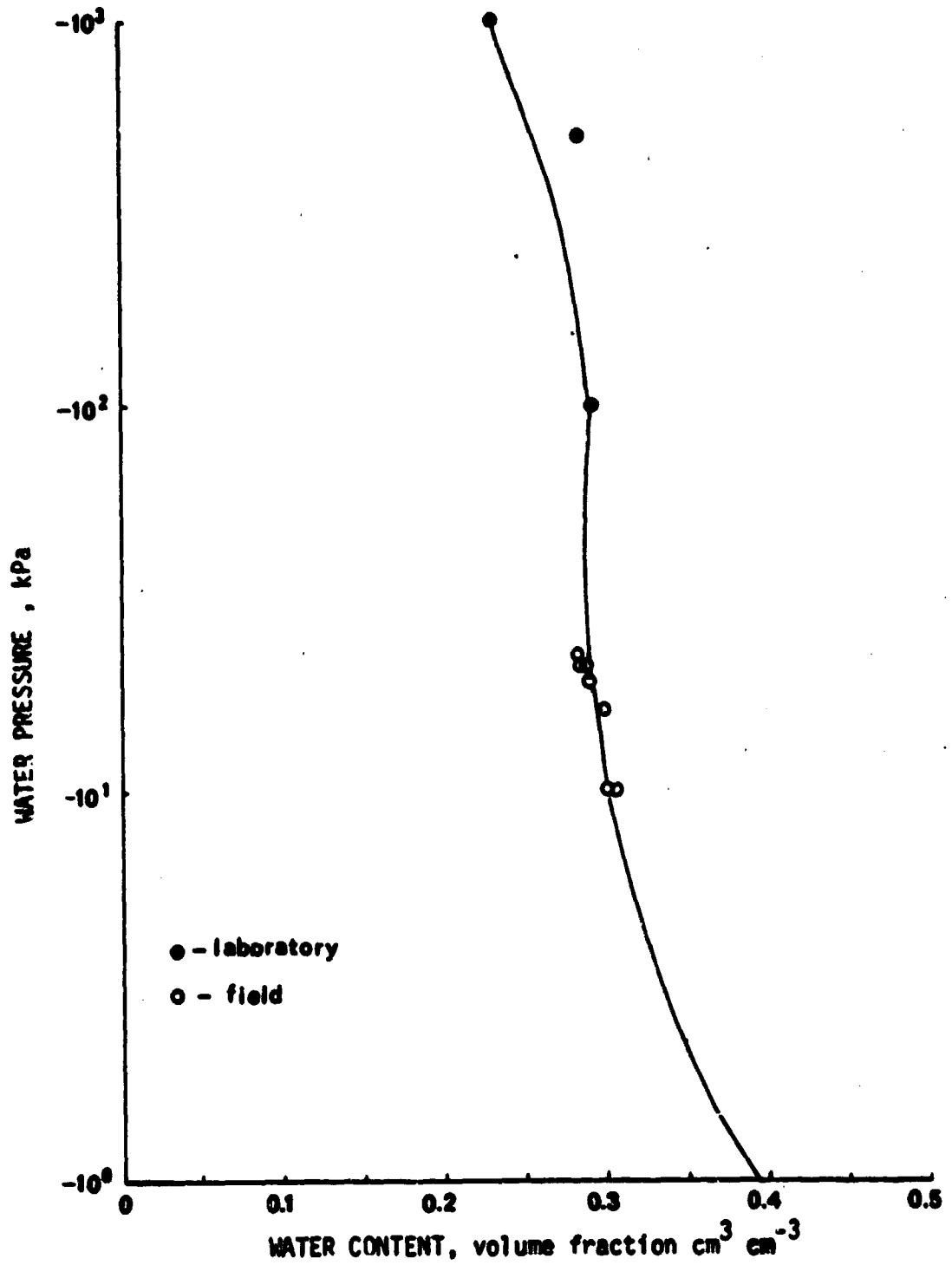


Fig. 24. Water retentivity from field data combined with laboratory data, 0-25 cm soil depth.

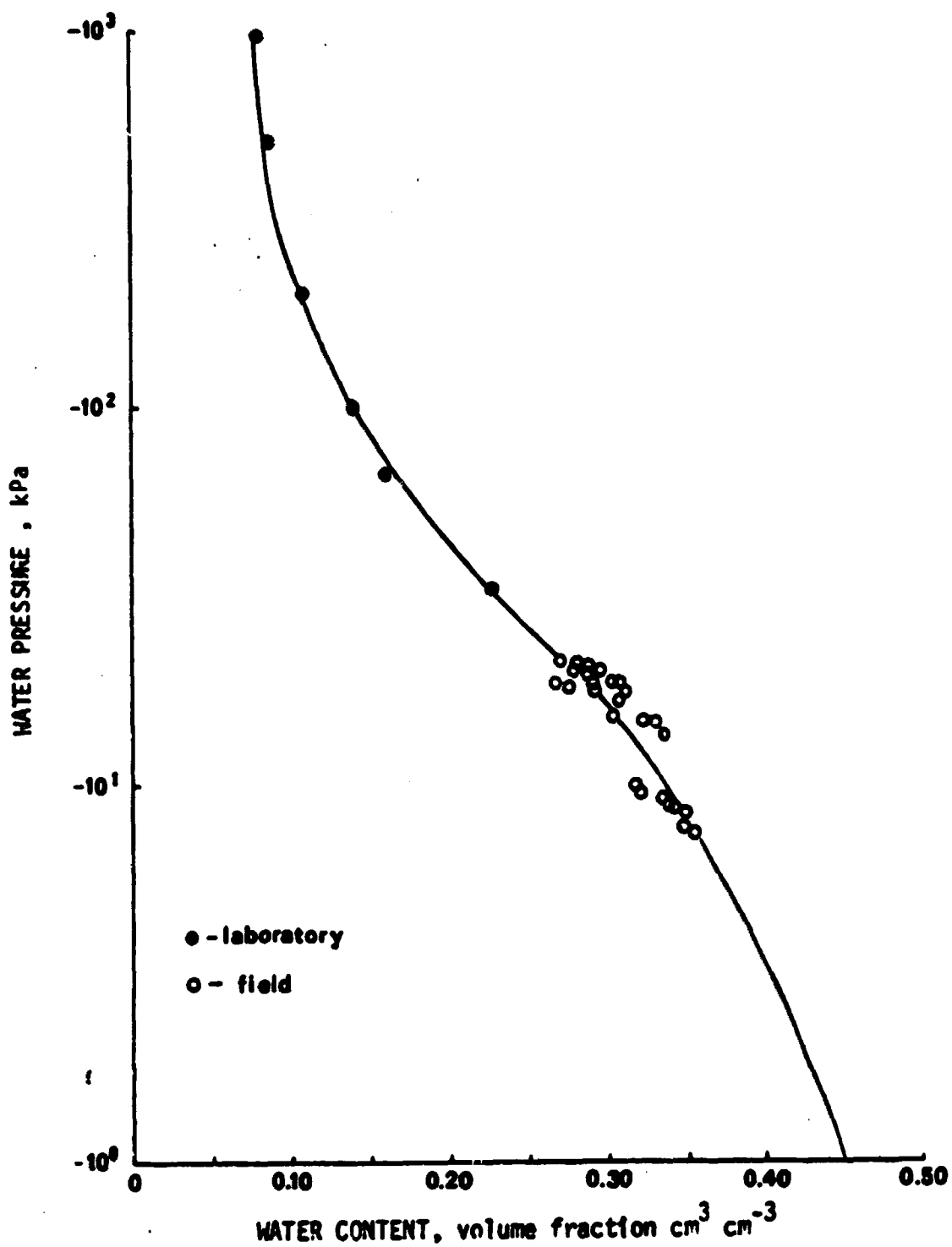
ORIGINAL PAGE IS
OF POOR QUALITY

Fig. 25. Water retentivity from field data combined with laboratory data, 15-55 cm soil depth.

was observed for the 0 to 25 cm soil depth (Fig. 26, p. 57) but a better correlation was obtained between the field and calculated values of hydraulic conductivity for the 30 to 80 cm soil depth range (Fig. 27, p. 58).

The method used to obtain soil samples for measuring water retention in the laboratory was the major cause for these discrepancies between measured and calculated values of hydraulic conductivity. The difference between using the laboratory only and the combined laboratory and field retentivity curves was small at the 0 to 15 cm soil depth yet the difference between the two approaches was much greater at the deeper soil depths. The 0 to 15 cm soil depth was sampled with a volumetric soil sampler, and the entire soil core was used in the test; whereas, the deeper soil depths were sampled using a soil auger and the soil used in the test was loose. It was concluded that Jackson's method of calculating soil hydraulic conductivity versus water content is relatively accurate provided the input data from the water retentivity curves are representative.

Centrifuge Method

The technique was set up to utilize readily available laboratory equipment. Difficulties were encountered with the weighing method. The soil cores weighed approximately 400 g and an analytical balance to accurately weigh above 200 g in milligrams was not available.

ORIGINAL PAGE IS
OF POOR QUALITY

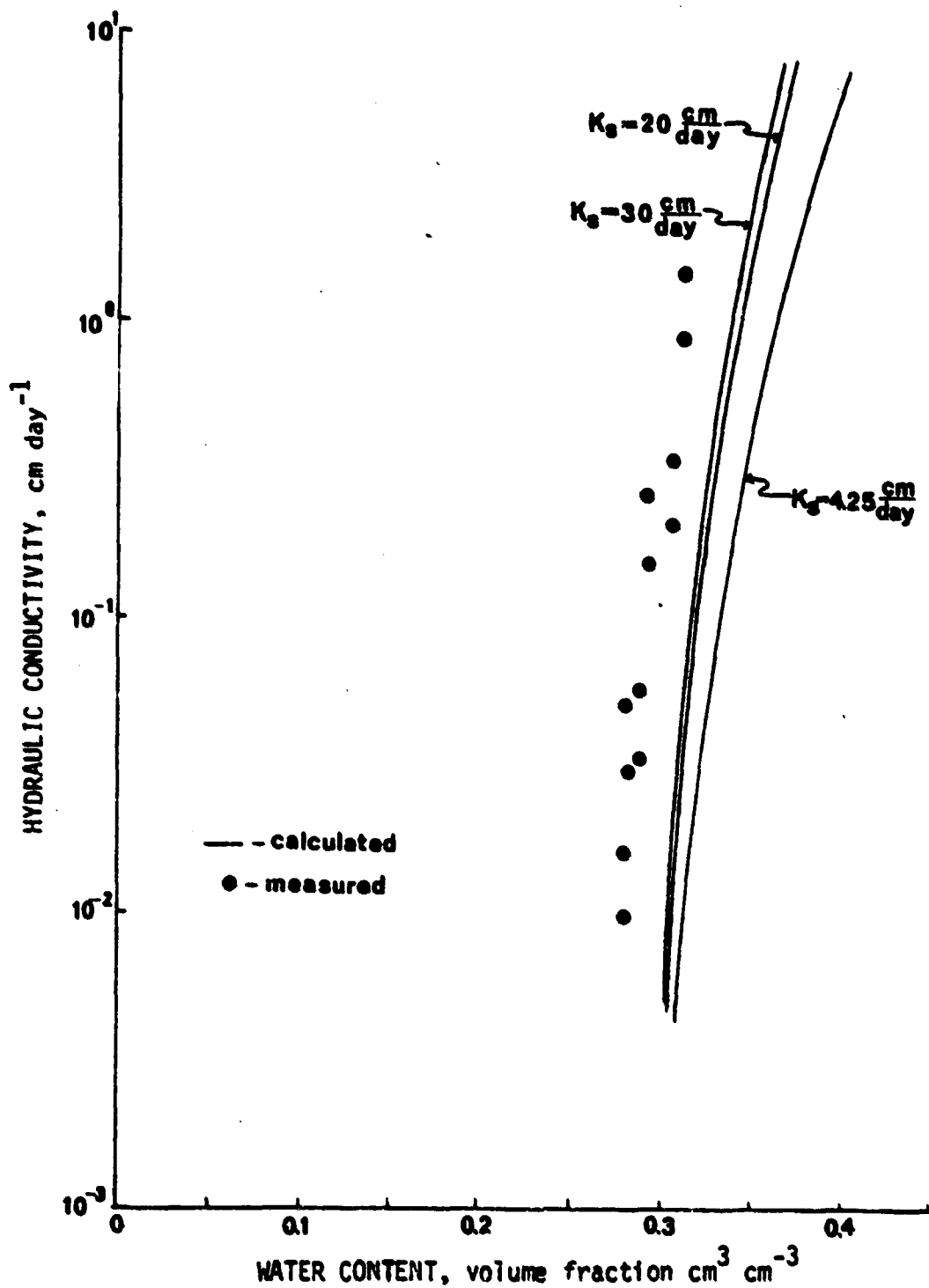


Fig. 26. Comparison of calculated to measured hydraulic conductivity, 0-25 cm soil depth.

ORIGINAL PAGE IS
OF POOR QUALITY

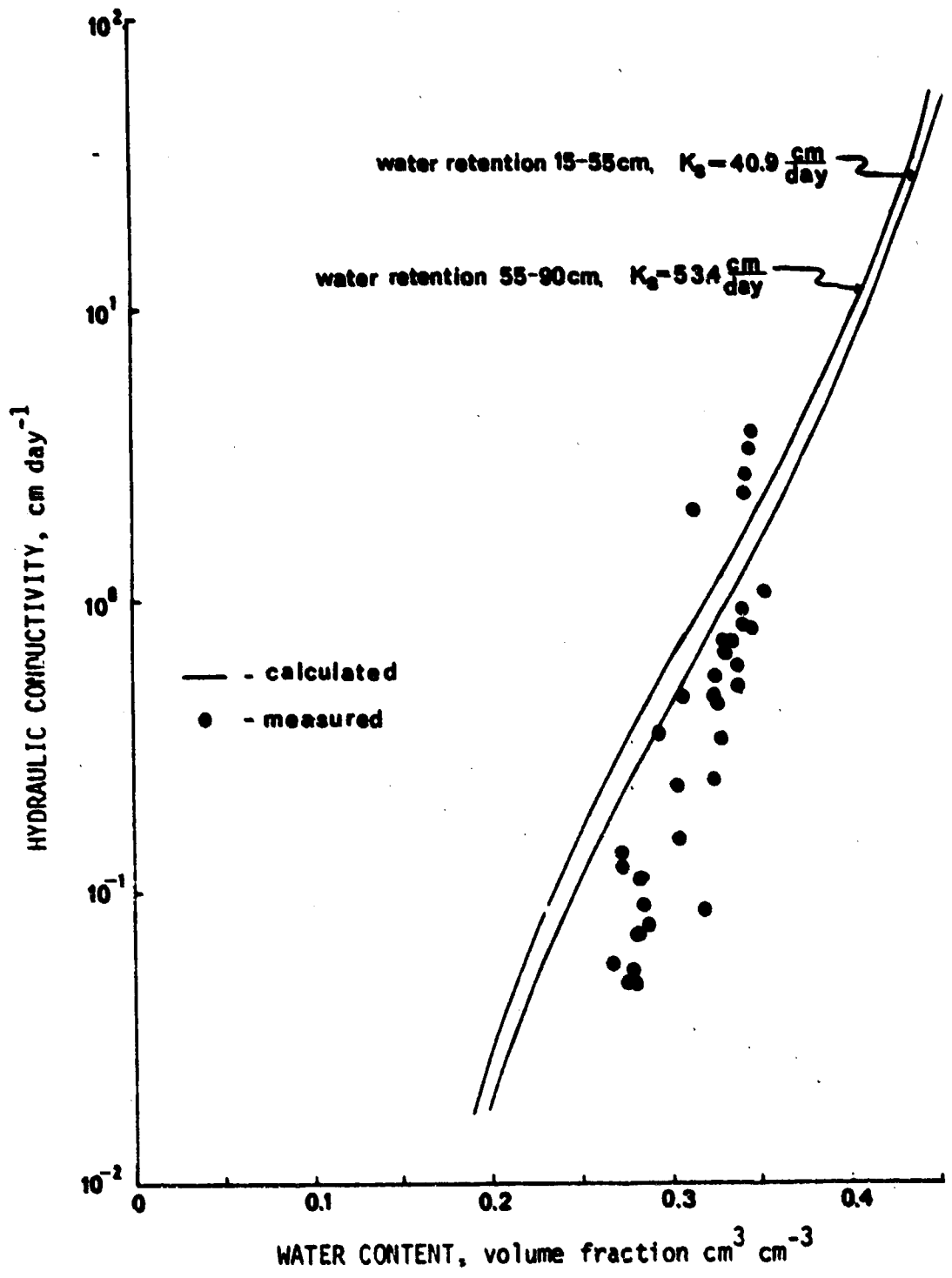


Fig. 27. Comparison of calculated to measured hydraulic conductivity, 30-80 cm soil depth.

Therefore, a balance with an accuracy in centigrams was used and estimation of milligrams was made.

Most of the measurements obtained with the centrifuge method were clearly erroneous. When measurements were plotted to match the theoretical curve for diffusivity, there was no possible correlation. Certain runs, however, yielded data consistent with the theoretical equation. The discrepancies were attributed in part to drafts and air movement within the room which interfered with readings on the analytical balance and reduced the desired accuracy. As a matter of interest, values of hydraulic conductivity obtained from these data are presented in Figs. 28, 29 and 30 (pp. 60, 61 and 62). Definite conclusions could not be made as to the applicability of the centrifuge method in this study.

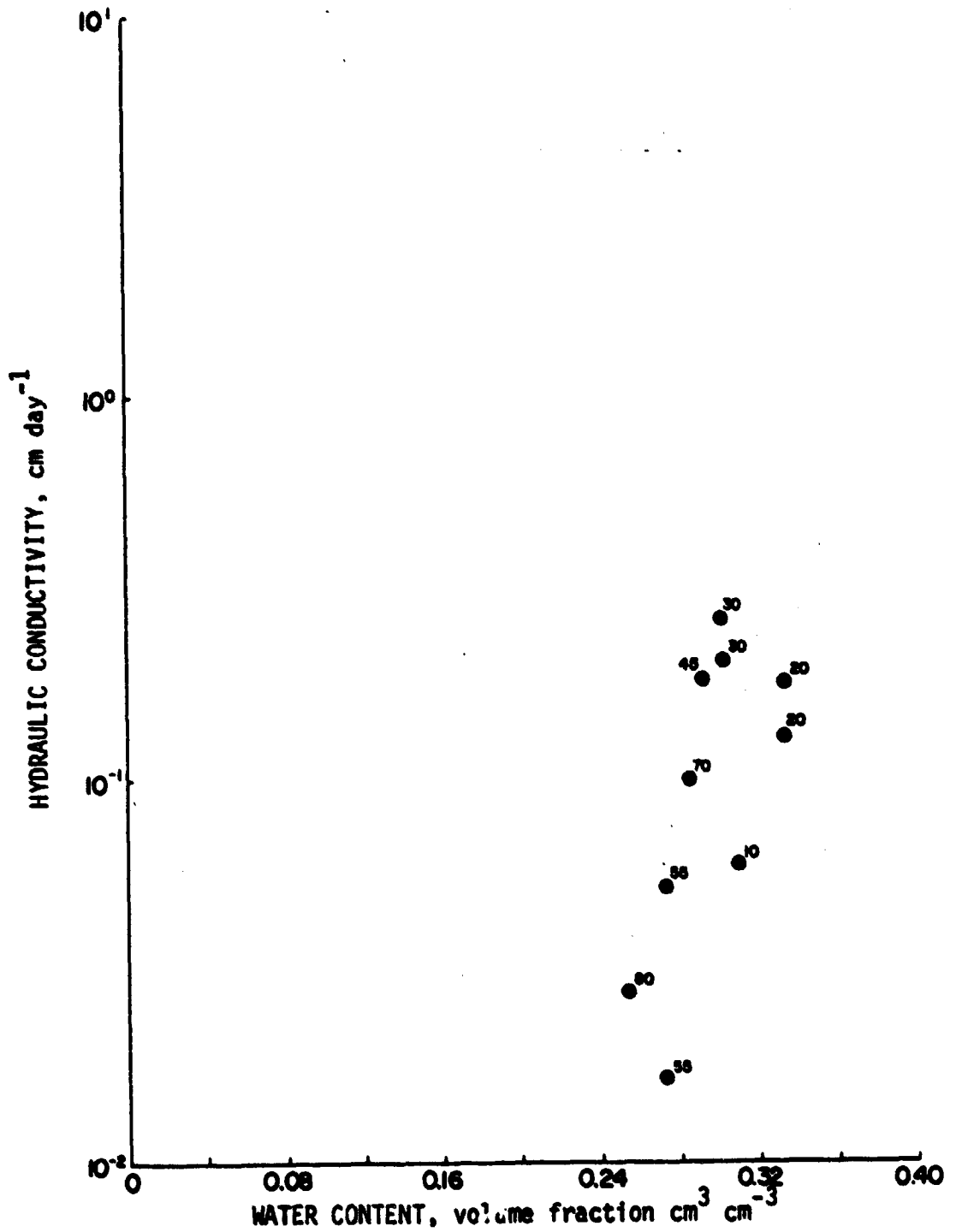


Fig. 28. Hydraulic conductivity versus water content determined from centrifuge data for noted soil depths.

ORIGINAL PAGE IS
OF POOR QUALITY

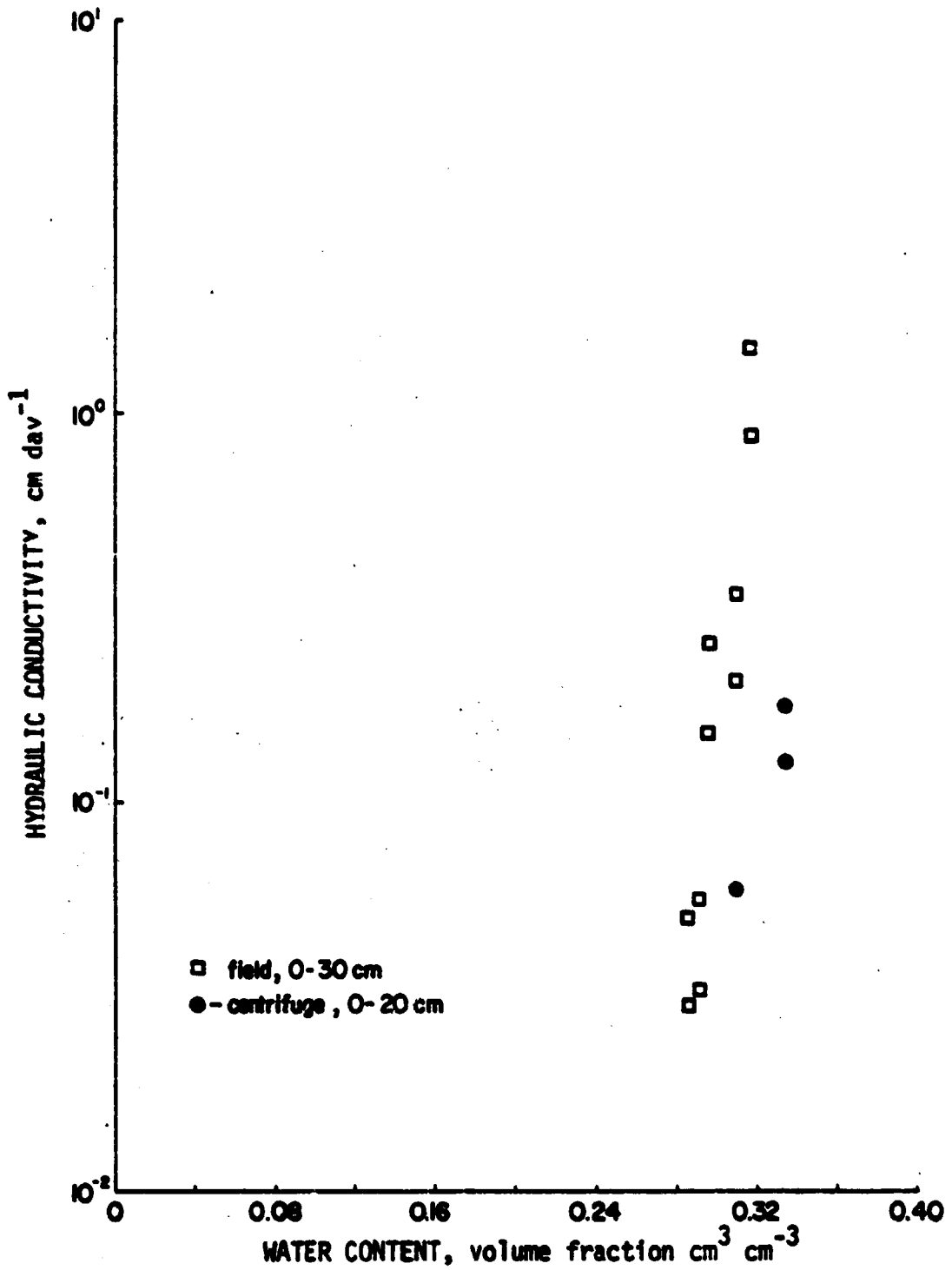


Fig. 29. Comparison of laboratory to field hydraulic conductivity, 0-30 cm soil depth.

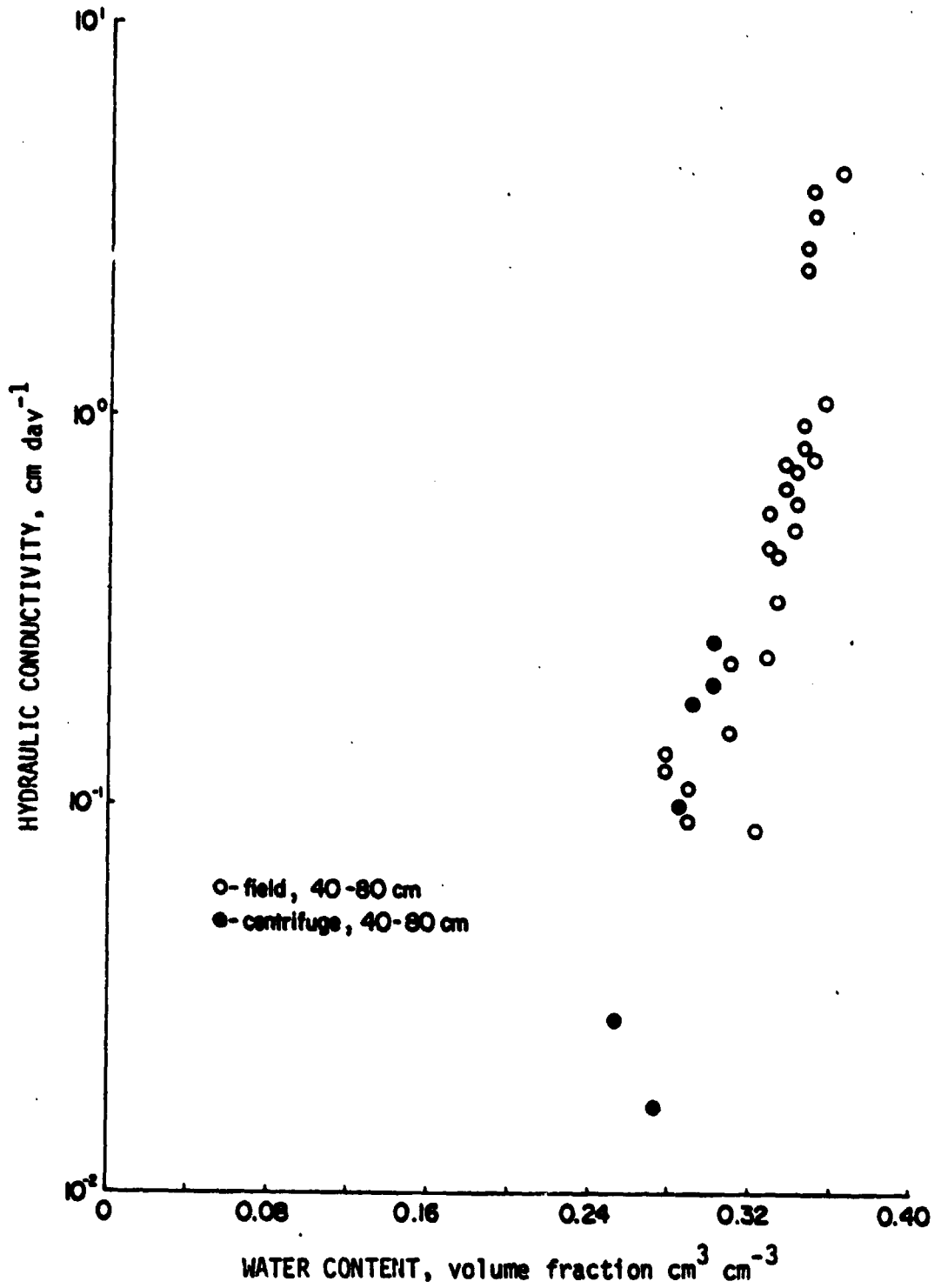


Fig. 30. Comparison of laboratory to field hydraulic conductivity, 40-80 cm soil depth.

CHAPTER V

SUMMARY AND CONCLUSIONS

Laboratory or mathematical techniques for determining soil hydraulic properties are more practical than field experiments provided they yield accurate results. The purpose of this study was to evaluate a theoretical technique and a laboratory method of determining hydraulic conductivity by comparison with results measured in situ.

The soil was of the Norwood Series, Typic Udifluent. A field plot was monitored for water content and pressure head during drainage from saturation with evaporation prevented. Measurements were obtained with a neutron moisture probe and tensiometers. The resulting data from the soil profile provided the necessary information for calculation of hydraulic conductivity.

The soil profile was characterized by several relations of hydraulic conductivity, varying with depth. The reason for this was attributed to the heterogeneous nature of the profile due to variance in clay content. Because of the narrow range of water content over the period of measurement, particularly below a soil depth of 100 cm, the range of hydraulic conductivity values was also limited.

The laboratory method for measuring hydraulic conductivity was centrifugation (Alemi, et al., 1972). Because of difficulties with the

weighing procedure, results were extremely inconsistent and few runs were successful. Conclusive recommendations cannot be made as to the applicability of this method from this study because of limited results.

The theoretical method for predicting hydraulic conductivity utilized water retention curves and saturated hydraulic conductivity values. The pressure-water content curve was obtained with pressure plate extractors using disturbed soil samples. Saturated conductivities were determined for 10, 40 and 70 cm soil depths using Bower's (1961) double-tube method.

The theoretical method underpredicted hydraulic conductivities at the soil surface (0 to 15 cm soil depths) and grossly overpredicted hydraulic conductivities in the 30 to 80 cm range of soil depths. When the water retention curves were modified by including data obtained in the field with the laboratory data, the resulting calculations of hydraulic conductivity reasonably predicted field values. This model was sensitive to the pressure versus water content relationship and accuracy in measuring this relationship is necessary.

Recommendations for Future Study

It is suggested that for additional studies using the methods described (1) evaluation of the centrifuge method will require a measuring device to accurately detect the movement of water within the

soil core and (2) extensive measurements of water retentivity relations in the laboratory and field are necessary for further comparison and evaluation. Spatial variation of soil properties in the field should be determined and possibly described by statistical methods to aid in determining in situ sample size for further studies of this type.

PRECEDING PAGE BLANK NOT FILMED

REFERENCES

- 1 Alemi, M. H., D. R. Nielsen and J. W. Biggar. 1976. Determining the hydraulic conductivity of soil cores by centrifugation. *Soil Science Society of America Proceedings* 40:212-218.
- 2 Bower, Herman. 1961. A double tube method for measuring hydraulic conductivity of soil in situ above a water table. *Soil Science Society of America Proceedings* 25:334-449.
- 3 Bower, H. and R. D. Jackson. 1974. Determining soil properties. p. 611-666. In: Jan van Schilfgearde (ed.). *Drainage for Agriculture. Agronomy Nomograph 17, American Society of Agronomy, Madison, WI.*
- 4 Bruce, R. R. and A. Klute. 1956. The measurement of soil moisture diffusivity. *Soil Science of America Proceedings* 20:458-462.
- 5 Childs, E. C. and N. Collis-George. 1950. The permeability of porous materials. *Proceedings Royal Society* 201A:392-405.
- 6 Day, D. R. 1965. Particle fractionation and particle-size analysis. p. 545-566. In: C. A. Black (ed.). *Methods of soil analysis. Agronomy Nomograph 9, American Society of Agronomy, Madison, WI.*
- 7 Doering, E. J. 1964. Soil water diffusivity by the one step method. *Soil Science* 99:322-326.
- 8 Gardner, W. R. 1956. Calculation of capillary conductivity from pressure plate outflow data. *Soil Science Society of America Proceedings* 20:317-320.
- 9 Green, R. E. and J. C. Corey. 1971. Calculation of hydraulic conductivity: a further evaluation of some predictive methods. *Soil Science Society of America Proceedings* 35:3-8.
- 10 Hillel, D., V. D. Krentos and Y. Syllianou. 1972. Procedures and test of an internal drainage method for methods for measuring soil hydraulic characteristics in situ. *Soil Science* 114:395:400.
- 11 Jackson, R. D. 1972. On the calculation of hydraulic conductivity. *Soil Science of America Proceedings* 36:380-382.

- 12 Jackson, R. D., R. J. Reginato, and C. H. M. van Bavel. 1965. Comparison of measured and calculated hydraulic conductivities of unsaturated soils. *Water Resources Research* 1:375-380.
- 13 Klute, A. 1965a. Laboratory measurement of hydraulic conductivity of unsaturated soil. p. 253-261. In: C. A. Black (ed.). *Methods of soil analysis. Agronomy Nomograph 9*, American Society of Agronomy, Madison, WI.
- 14 Klute, A. 1965b. Soil water diffusivity, p. 262-272. In: C. A. Black (ed.). *Methods of soil analysis. Agronomy Nomograph 9*, American Society of Agronomy, Madison, WI.
- 15 Kunze, R. J., G. Uzhara, and K. Graham. 1968. Factors important in the calculation of hydraulic conductivity. *Soil Science Society of America Proceedings* 32:760-765.
- 16 Marshall, T. J. 1958. A relation between permeability and size distribution of pores. *Journal of Soil Science* 9:1-8.
- 17 Millington, R. J., and Quirk, J. P. 1959. Permeability of porous media. *Nature* 183:387-388.
- 18 Millington, R. J., and Quirk, J. P. 1960. Transport in porous media. *International Congress of Soil Science Transactions 7th*, Madison, WI 1:97-107.
- 19 Richards, L. A. 1931. Capillary conduction of liquids through porous systems. *Journal of Applied Physics* 1:318-333.
- 20 Richards, L. A. 1947. Pressure-membrane apparatus, construction and use. *Agricultural Engineering* 28:451-454, 460.
- 21 Richards, S. J. 1965. Soil suction measurements with tensiometers. p. 153-163. In: C. A. Black (ed.). *Methods of soil analysis. Agronomy Nomograph 9*, American Society of Agronomy, Madison, WI.
- 22 van Bavel, C. H. M., P. R. Nixon and V. L. Hauser. 1963. Soil moisture measurement with the neutron method. ARS-41-70. 39 pp.

- 23 van Bavel, C. H. M., G. B. Stirk and K. J. Brust. 1968. Hydraulic properties of a clay loam soil and the field measurement of water uptake by roots, I, Interpretation of water content and pressure profiles. Soil Science of America Proceedings 32:310-317.
- 24 Watson, K. K. 1966. An instantaneous profile method for determining the hydraulic conductivity of unsaturated porous media. Water Resources Research 2:709-715.

APPENDIX A
Supplementary Data

TABLE A-1

Field Measurement of Bulk Density

<u>Depth</u> (cm)	<u>Gamma Probe</u> (g/cm ³)	<u>Avg. Gravimetric</u> (g/cm ³)
10	1.570	1.590
	1.562	
20	1.643	1.497
	1.631	
	1.592	
30	1.610	1.439
35		1.458
40	1.470	1.465
	1.560	
50	1.465	1.426
	1.467	
60	1.486	1.505
	1.491	
65		1.520
70	1.550	1.430
	1.491	
75		1.436
80	1.550	
	1.495	
90	1.591	
	1.551	
100	1.610	
	1.605	
110	1.660	
	1.664	
120	1.669	
	1.686	
130	1.674	
	1.653	
140	1.690	
	1.660	
150	1.681	
	1.672	
160	1.665	
	1.643	
170	1.663	

TABLE A-2

Neutron Probe Calibration Data

Surface, 0-15 cm

Line of Best Fit, $\theta = 0.324CR + 0.089$ $r^2 = 0.889$ Count Ratio, CR
(Actual/Standard)Water Content, θ
(cm^3/cm^3)

.485

.257

.391

.198

.568

.291

.748

.319

Subsurface, 15-85 cm

Line of Best Fit, $\theta = 0.419CR + 0.001$ $r^2 = 0.872$ Count Ratio, CR
(Actual/Standard)Water Content, θ
(cm^3/cm^3)

.664

.282

.670

.284

.703

.321

.636

.232

.647

.284

.670

.300

.691

.293

.693

.300

.489

.221

.455

.195

.422

.165

.402

.153

.659

.304

.661

.281

.674

.248

.696

.272

.702

.270

.634

.256

.669

.301

.621

.291

.679

.272

TABLE A-2 (Continued)

<u>Count Ratio, CR</u> <u>(Actual/Standard)</u>	<u>Water Content, θ</u> <u>(cm^3/cm^3)</u>
.592	.284
.419	.144
.331	.144
.330	.172
.767	.333
.711	.309
.654	.250

TABLE A-3

**Soil Moisture Measured at Different Depths for
Various Times During Drainage**

Field Measurements of Soil Moisture (Neutron Probe)

Depth (cm)	6h	9h	23h	168h	360h	408h	492h	575h	718h	910h
10	.327	.320	.307	.297	.295	.293	.293	.287	.289	.288
20	.325	.316	.300	.298	.292	.287	.287	.287	.283	.282
30	.357	.328	.318	.304	.292	.292	.285	.286	.282	.271
40	.365	.345	.336	.323	.312	.305	.301	.296	.290	.280
50	.375	.362	.344	.331	.314	.311	.305	.303	.290	.279
60	.375	.365	.348	.337	.314	.302	.297	.292	.277	.269
70	.373	.364	.352	.334	.311	.302	.297	.291	.277	.268
80	.380	.368	.357	.350	.348	.341	.339	.337	.330	.321
90	.380	.368	.360	.360	.361	.355	.356	.355	.354	.346
100	.383	.370	.365	.363	.362	.363	.364	.365	.361	.359
110	.365	.352	.344	.345	.352	.348	.344	.346	.343	.344
120	.374	.352	.354	.347	.348	.346	.345	.350	.342	.339
130	.381	.370	.362	.364	.362	.362	.362	.363	.355	.356
140	.369	.360	.355	.356	.359	.364	.357	.355	.356	.357
150	.359	.424	.352	.347	.348	.350	.349	.351	.343	.348
160	.360	.390	.346	.347	.341	.337	.338	.337	.324	.329
170	.369	.403	.355	.349	.348	.345	.344	.342	.336	.337
175	.370	.381	.356	.344	.348	.346	.344	.344	.342	.339

ORIGINAL PAGE IS
OF POOR QUALITY

TABLE A-4
Soil-water Pressure Head (cmH₂O) Measured at Different Depths for
Various Times During Drainage

Field Measurements of Pressure Head		18h	48h	72h	145h	195h	384h	596h	720h	864h	960h
Depth (cm)											
20		100	115	123	151	181	195	213	220	227	229
30		97	114	122	145	161	186	198	207	211	213
40		90	106	116	141	155	185	200	207	210	210
50		85	101	119	140	154	176	188	192	197	199
60		75	91	109	132	144	167	177	181	184	185
75			84	95	117	130	153	163	167	170	172
80		59	80	90	115	126	147	156	161	165	168
90		35	72	92	104	124	140	143	154	157	160
110		36	63	68	93	105	143	152	153	155	155
120		38	65	88	99	121	141	145	151	153	154
135		30	72	80	115	120	139	148	151	152	153
140		28	60	76	100	111	133	141	147	149	150
155		30	57	74	96	108	130	141	145	147	148
180		30	60	70	99	111	132	141	145	145	145

TABLE A-5
Calculation of Hydraulic Conductivity from Field Data

Average Time - 18h	Depth increment (cm)	$d\theta/dt$ (1/day)	$q = \int z d\theta/dt$ (cm/day)	dH/dZ (cm/cm)	$K = q/dH/dZ$ (cm/day)	θ (cm ³ /cm ³)	Depth (cm)
	0-15	1.967×10^{-2}	0.295	0.344	0.858	0.3161	10
	15-25	1.967×10^{-2}	0.492		1.430	0.3161	20
	25-35	1.967×10^{-2}	0.688		2.001	0.3161	30
	35-45	1.102×10^{-2}	0.799		2.322	0.3449	40
	45-55	1.102×10^{-2}	0.909		2.642	0.3449	50
	55-65	1.836×10^{-2}	1.092		3.176	0.3485	60
	65-75	1.836×10^{-2}	1.276		3.709	0.3485	70
	75-85	1.574×10^{-2}	1.433		4.166	0.3639	80
	85-95	1.77×10^{-2}	1.610		4.680	0.3655	90
	95-105	1.495×10^{-2}	1.760		5.116	0.3689	100
	105-125	7.869×10^{-3}	1.838		5.343	0.3549	110, 120
	125-135	1.062×10^{-2}	1.945		2.180	0.3666	130
	135-145	9.840×10^{-3}	2.043		2.290	0.3592	140
	145-155	5.902×10^{-3}	2.102		2.356	0.3521	150
	155-165	3.93×10^{-3}	2.142		2.401	0.3441	160
	165-175	7.869×10^{-3}	2.220		2.489	0.3584	170
	175-185	1.259×10^{-2}	2.346		2.463	0.3613	180

TABLE A-5 (Continued)

Average Time - 48h	Depth Increment (cm)	$d\theta/dt$ (1/day)	$q = \int z d\theta/dt$ (cm/day)	dH/dZ (cm/cm)	$K = q/dH/dZ$ (cm/day)	θ (cm ³ /cm ³)	Depth (cm)
	0-15	4.721×10^{-3}	0.0708	0.351	0.202	0.3090	10
	15-25	4.721×10^{-3}	0.1180	↓	0.336	0.2090	20
	25-35	4.721×10^{-3}	0.1652		0.471	0.3090	30
	35-45	4.000×10^{-3}	0.2052		0.585	0.3400	40
	45-55	4.000×10^{-3}	0.2452		0.699	0.3400	50
	55-65	3.93×10^{-3}	0.2845		0.810	0.3439	60
	65-75	3.93×10^{-3}	0.3238		0.922	0.3439	70
	75-85	4.721×10^{-3}	0.3710		1.060	0.3554	80
	85-95	1.784×10^{-3}	0.3888		1.108	0.3634	90
	95-105	1.888×10^{-3}	0.4077		1.162	0.3665	100
	105-125	4.197×10^{-4}	0.4119		0.923	0.3495	110,120
	125-135	3.147×10^{-3}	0.4434	↓	0.4804	0.3633	130
	135-145	2.317×10^{-5}	0.4436		0.4806	0.3347	140
	145-155	1.639×10^{-4}	0.4453		0.4806	0.3369	150
	155-165	2.373×10^{-4}	0.4476		0.4832	0.3369	160
	165-175	4.434×10^{-4}	0.4521		0.4876	0.3525	170
	175-185	3.35×10^{-4}	0.4559		0.4921	0.3528	180

TABLE A-5 (Continued)

Average Time - 145 h												
Depth Increment (cm)	$d\theta/dt$ (1/day)	$q = \int z d\theta/dt$ (cm/day)	dH/dZ (cm/cm)	$K=q/dH/dZ$ (cm/day)	θ (cm^3/cm^3)	Depth (cm)						
0-15	2.754×10^{-3}	0.0412	0.274	0.150	0.2957	10						
15-25	2.754×10^{-3}	0.0687	↓	0.251	0.2957	20						
25-35	2.754×10^{-3}	0.0962		0.351	0.2957	30						
35-45	2.72×10^{-3}	0.1234		0.450	0.3271	40						
45-55	2.72×10^{-3}	0.1506		0.550	0.3271	50						
55-65	2.52×10^{-3}	0.1758		0.642	0.3344	60						
65-75	2.52×10^{-3}	0.2016		0.736	0.3344	70						
75-85	8.544×10^{-4}	0.2095		0.765	0.3502	80						
85-95	1.500×10^{-3}	0.2245		0.819	0.3620	90						
95-105	1.299×10^{-4}	0.2258		0.824	0.3646	100						
105-125	1.23×10^{-4}	0.2270		1.000	0.2270	0.3485	110,120					
125-135	1.23×10^{-4}	0.2283	↓	0.2283	0.3626	130						
135-145	2.317×10^{-5}	0.2285		0.2285	0.3570	140						
145-155	1.639×10^{-4}	0.2302		0.2302	0.3498	150						
155-165	2.373×10^{-4}	0.2325		0.2325	0.3359	160						
165-175	4.43×10^{-4}	0.2370		0.2370	0.3508	170						
175-185	3.85×10^{-4}	0.2408		0.2408	0.3513	180						

TABLE A-5 (Continued)

Average Time - 384h	Depth Increment (cm)	de/dt (l/day)	$q = \sum z de/dt$ (cm/day)	dH/dZ (cm/cm)	$K=q/dH/dZ$ (cm/day)	θ (cm ³ /cm ³)	Depth (cm)
	0-15	5.04×10^{-4}	0.00756	0.230	0.0329	0.2908	10
	15-25	5.04×10^{-4}	0.0126	↓	0.0548	0.2908	20
	25-35	5.04×10^{-4}	0.0176		0.0756	0.2908	30
	35-45	1.73×10^{-3}	0.0349	↓	0.1520	0.3082	40
	45-55	1.73×10^{-3}	0.0522		0.2270	0.3082	50
	55-65	2.361×10^{-3}	0.0758	↓	0.3300	0.3310	60
	65-75	2.361×10^{-3}	0.0994		0.4320	0.3310	70
	75-85	1.574×10^{-3}	0.1151	↓	0.5000	0.3410	80
	85-95	1.259×10^{-4}	0.1277		0.555	0.3574	90
	95-105	1.299×10^{-4}	0.1290	0.860	0.1500	0.3633	100
	105-125	1.230×10^{-4}	0.1302	↓	0.1513	0.3479	110,120
	125-135	1.230×10^{-4}	0.1315		0.1529	0.3601	130
	135-145	2.317×10^{-5}	0.1317	↓	0.2657	0.3482	140
	145-155	1.639×10^{-4}	0.1333		0.155	0.3482	150
	155-165	2.373×10^{-4}	0.1357	↓	0.1578	0.3336	160
	165-175	4.434×10^{-4}	0.1402		0.1630	0.3465	170
	175-185	3.850×10^{-4}	0.1440		0.1674	0.3474	180

TABLE A-5 (Continued)

Average Time - 720h	Depth Increment (cm)	$d\theta/dt$ (1/day)	$q = \int z d\theta/dt$ (cm/day)	dH/dZ (cm/cm)	$K = q/dH/dZ$ (cm/day)	θ (cm^3/cm^3)	Depth (cm)
	0-15	3.279×10^{-4}	4.918×10^{-3}	0.164	0.0300	0.2850	10
	15-25	3.279×10^{-4}	8.198×10^{-3}	↓	0.0500	0.2850	20
	25-35	3.279×10^{-4}	1.148×10^{-2}		0.0700	0.2850	30
	35-45	3.200×10^{-4}	1.468×10^{-2}	↓	0.0895	0.2872	40
	45-55	3.200×10^{-4}	1.788×10^{-2}		0.1090	0.2872	50
	55-65	1.967×10^{-4}	1.984×10^{-2}	↓	0.1210	0.2758	60
	65-75	1.967×10^{-4}	2.181×10^{-2}		0.1330	0.2758	70
	75-85	1.729×10^{-3}	3.910×10^{-2}	↓	0.2380	0.3269	80
	85-95	5.200×10^{-4}	4.430×10^{-2}		0.0515	0.3510	90
	95-105	1.300×10^{-4}	4.560×10^{-2}	0.860	0.0535	0.3615	100
	105-125	1.200×10^{-4}	4.680×10^{-2}	↓	0.0544	0.3456	110, 120
	125-135	0.000×10^{-4}	4.680×10^{-2}		0.0468	0.3590	0.3590
	135-145	2.317×10^{-5}	4.700×10^{-2}	↓	0.05465	0.3566	140
	145-155	1.639×10^{-4}	4.870×10^{-2}		0.0566	0.3459	0.3459
	155-165	2.373×10^{-4}	5.100×10^{-2}	↓	0.0593	0.3303	160
	165-175	4.434×10^{-4}	5.550×10^{-2}		0.0645	0.3404	0.3404
	175-185	3.850×10^{-4}	5.930×10^{-2}	0.0689	0.3420	0.3420	180

TABLE A-5 (Continued)

Average Time - 910h											
Depth Increment (cm)	$d\theta/dt$ (1/day)	$q = \int z d\theta/dt$ (cm/day)	dH/dZ (cm/cm)	$k = q/dH/dZ$ (cm/day)	θ (cm^3/cm^3)	Depth (cm)					
0-15	1.049×10^{-4}	1.573×10^{-3}	0.164	0.00959	0.2826	10					
15-25	1.049×10^{-4}	2.622×10^{-3}	↓ 0.860 ↓	0.01599	0.2826	20					
25-35	1.049×10^{-4}	3.671×10^{-3}		0.04091	0.2826	30					
35-45	4.720×10^{-4}	8.393×10^{-3}		0.0512	0.2820	40					
45-55	4.720×10^{-4}	8.864×10^{-3}		0.05405	0.2820	50					
55-65	1.570×10^{-4}	9.022×10^{-3}		0.05501	0.2687	60					
65-75	1.570×10^{-4}	9.180×10^{-3}		0.05598	0.2687	70					
75-85	4.720×10^{-4}	1.390×10^{-2}		0.08476	0.3226	80					
85-95	3.279×10^{-4}	1.720×10^{-2}		0.10488	0.3419	90					
95-105	1.299×10^{-4}	.0185		0.0215	0.3602	100					
105-125	1.230×10^{-4}	1.970×10^{-2}		0.0229	0.3443	110, 120					
125-135	1.230×10^{-4}	2.090×10^{-2}	0.0209	0.3574	130						
135-145	2.317×10^{-4}	2.113×10^{-2}	0.02457	0.3563	140						
145-155	1.639×10^{-4}	2.278×10^{-2}	0.0265	0.3442	150						
155-165	2.373×10^{-4}	2.514×10^{-2}	0.0292	0.3279	160						
165-175	4.434×10^{-4}	2.957×10^{-2}	0.0344	0.3360	170						
175-185	3.850×10^{-4}	3.342×10^{-2}	0.0389	0.3382	180						

TABLE A-6

**Water Retentivity Values of Pressure Potential and
Water Content Used in the Calculation
of Hydraulic Conductivity**

Laboratory Data

Surface, 0-15 cm $\theta_s = 0.39 \text{ cm}^3/\text{cm}^3$

h_1 (kPa)	θ_1 (cm^3/cm^3)	$K_g=4.25\text{cm/day}$	$K_s=20\text{cm/day}$	$K_s=30\text{cm/day}$
		K_1 (cm/day)	K_1 (cm/day)	K_1 (cm/day)
10.7	0.39	4.25×10^0	2.000×10^1	3.000×10^1
13.0	0.38	2.60×10^0	1.223×10^1	1.835×10^1
16.2	0.37	1.60×10^0	7.529×10^0	1.129×10^1
20.0	0.36	-9.33×10^{-1}	4.390×10^0	6.586×10^0
25.5	0.35	5.46×10^{-1}	2.569×10^0	3.854×10^0
32.0	0.34	-3.15×10^{-1}	1.482×10^0	2.223×10^0
41.0	0.33	-1.78×10^{-1}	8.376×10^{-1}	1.256×10^0
52.0	0.32	9.80×10^{-2}	4.612×10^{-1}	6.918×10^{-1}
66.0	0.31	5.20×10^{-2}	2.447×10^{-1}	3.671×10^{-1}
88.0	0.30	2.68×10^{-2}	1.261×10^{-1}	1.892×10^{-1}
115.0	0.29	1.33×10^{-2}	6.259×10^{-2}	9.388×10^{-2}
155.0	0.28	6.20×10^{-3}	2.918×10^{-2}	4.365×10^{-2}
215.0	0.27	2.70×10^{-3}	1.270×10^{-2}	1.906×10^{-2}
300.0	0.26	1.10×10^{-3}	5.176×10^{-3}	7.765×10^{-3}
450.0	0.25	3.76×10^{-4}	1.769×10^{-3}	2.65×10^{-3}
660.0	0.24	8.86×10^{-7}	4.169×10^{-6}	6.254×10^{-6}

Laboratory data

Subsurface, 15-55 cm $\theta_s = 0.45 \text{ cm}^3/\text{cm}^3$

$K_s=40.9\text{cm/day}$

h_1 (kPa)	θ_1 (cm^3/cm^3)	K_1 (cm^3/cm^3)
11.2	0.45	4.09×10^1
14.2	0.43	3.08×10^1
15.1	0.41	2.28×10^1
17.0	0.39	1.69×10^1
18.8	0.37	1.22×10^1
20.7	0.35	8.69×10^0
22.3	0.33	5.98×10^0

TABLE A-6 (Continued)

h_1 (kPa)	$K_s=40.9\text{cm/day}$	
	θ_1 (cm^3/cm^3)	K_1 (cm/day)
24.2	0.31	4.04×10^0
26.4	0.29	2.59×10^0
29.5	0.27	1.62×10^0
33.1	0.25	-9.54×10^{-1}
35.5	0.23	-5.11×10^{-1}
44.0	0.21	-2.55×10^{-1}
54.0	0.19	-1.13×10^{-1}
70.0	0.17	2.00×10^{-2}
99.0	0.15	1.44×10^{-2}
152.0	0.13	3.74×10^{-3}
270.0	0.11	6.10×10^{-4}
830.0	0.09	3.97×10^{-5}

Laboratory Data

Subsurface, 55-90 cm $\theta_s = 0.45 \text{ cm}^3/\text{cm}^3$

h_1 (kPa)	$K_s=53.4\text{cm/day}$	
	θ_1 (cm^3/cm^3)	K_1 (cm/day)
11.0	0.43	4.01×10^1
12.0	0.41	2.96×10^1
13.0	0.39	2.14×10^1
14.0	0.37	6.52×10^1
15.0	0.35	1.04×10^1
16.2	0.33	6.98×10^0
17.8	0.31	4.50×10^0
19.6	0.29	2.78×10^0
21.8	0.27	1.63×10^0
25.6	0.25	8.97×10^{-1}
28.2	0.23	-4.47×10^{-1}
33.0	0.21	1.99×10^{-1}
40.0	0.19	7.70×10^{-2}
54.0	0.17	2.60×10^{-2}
78.0	0.15	7.34×10^{-3}
122.0	0.13	1.70×10^{-3}
220.0	0.11	3.38×10^{-4}

TABLE A-6 (Continued)

h_1 (kPa)	θ_1 (cm ³ /cm ³)	$K_s=53.4$ cm/day
		K_1 (cm/day)
440.0	0.09	6.60×10^{-5}
1100.0	0.07	1.10×10^{-5}
1350.0	0.05	

Combined Laboratory and Field Data
Surface, 0-20 cm $\theta_s = 0.39$ cm³/cm³

h_1 (kPa)	θ_1 (cm ³ /cm ³)	$K_s=4.25$ cm/day	$K_s=20$ cm/day	$K_s=30$ cm/day
		K_1 (cm/day)	K_1 (cm/day)	K_1 (cm/day)
1.10	0.39	4.25		
1.28	0.38	2.58		
1.55	0.37	1.50	7.06×10^0	1.01×10^1
1.85	0.36	8.24×10^{-1}	3.88×10^0	5.82×10^0
2.35	0.35	4.24×10^{-1}		
2.90	0.34	2.00×10^{-1}	1.99×10^0	2.99×10^0
3.90	0.33	8.27×10^{-2}	9.41×10^{-1}	1.41×10^0
5.60	0.32	2.90×10^{-2}	3.89×10^{-1}	5.83×10^{-1}
8.00	0.31	7.50×10^{-3}	1.36×10^{-1}	2.04×10^{-1}
18.00	0.30	9.59×10^{-4}	3.53×10^{-2}	5.29×10^{-2}
180.00	0.29	4.00×10^{-5}	4.52×10^{-3}	6.78×10^{-3}
290.0	0.28			
420.0	0.27			
580.0	0.26			
760.0	0.25			
920.0	0.24			

Combined Laboratory and Field Data
Subsurface, 15-55 cm $\theta_s = 0.45$ cm³/cm³

h_1 (kPa)	θ_1 (cm ³ /cm ³)	$K_s=40.9$ cm/day
		K_1 (cm/day)
1.30	0.45	4.09×10^1
2.20	0.43	1.81×10^1

TABLE A-6 (Continued)

h_i (kPa)	θ_i (cm^3/cm^3)	$K_s=40.9\text{cm/day}$
		K_i (cm/day)
3.30	0.41	8.77×10^0
4.90	0.39	4.60×10^0
7.00	0.37	2.54×10^0
9.80	0.35	1.49×10^0
13.50	0.33	9.01×10^{-1}
17.00	0.31	5.53×10^{-1}
21.00	0.29	3.31×10^{-1}
25.00	0.27	1.96×10^{-1}
29.50	0.25	1.11×10^{-1}
35.50	0.23	5.80×10^{-2}
44.00	0.21	2.90×10^{-2}
54.00	0.19	1.29×10^{-2}
70.00	0.17	5.13×10^{-3}
99.00	0.15	1.66×10^{-3}
152.00	0.13	4.17×10^{-4}
270.00	0.11	6.90×10^{-5}
830.00	0.09	4.50×10^{-6}

Combined Laboratory and Field Data

Subsurface, 55-90 cm $\theta_s = 0.45 \text{ cm}^3/\text{cm}^3$

h_i (kPa)	θ_i (cm^3/cm^3)	$K_s=53.40\text{cm/day}$
		K_i (cm/day)
1.30	0.45	5.34×10^1
2.20	0.43	2.36×10^1
3.30	0.41	1.15×10^1
4.90	0.39	6.05×10^0
7.00	0.37	3.36×10^0
9.80	0.35	1.98×10^0
13.50	0.33	1.20×10^0
17.00	0.31	7.45×10^{-1}
21.00	0.29	4.50×10^{-1}
25.00	0.27	2.69×10^{-1}
29.00	0.25	1.53×10^{-1}
35.50	0.23	8.10×10^{-2}

C-5

TABLE A-6 (Continued)

h_1 (kPa)	θ_1 (cm^3/cm^3)	$K_s=53.40\text{cm/day}$ K_1 (cm/day)
44.00	0.21	4.00×10^{-2}
54.00	0.19	1.80×10^{-2}
69.00	0.17	7.60×10^{-3}
92.20	0.15	2.60×10^{-3}
148.00	0.13	7.20×10^{-4}
250.00	0.11	1.53×10^{-4}

TABLE A-7

Double-Tube Data Used for Calculation
of K_s

	Outer-Tube Constant		Equal Levels	
	<u>H₁ (cm)</u>	<u>t (min)</u>	<u>H₁ (cm)</u>	<u>t (min)</u>
5 cm depth	0.00	0	0.0	0
Rv = 2.54 cm	0.20	15	0.1	10
Rc = 6.67 cm	0.35	25	0.3	18
d = 5 cm	0.55	39	0.5	31
F = 0.75	0.80	56	0.8	52
	1.10	74	1.1	69
			1.3	85
40 cm depth	4	0.9	5	1.3
Rv = 2.54 cm	11	3.1	8	2.1
Rc = 6.67 cm	15	4.5	12	3.5
d = 3 cm	20	6.0	15	4.0
F = 1.10	25	8.0	20	5.4
	30	9.6	25	6.8
			30	8.25
			35	9.70
70 cm depth	5	1.4	5	1.3
Rv = 2.54 cm	8	2.3	8	2.0
Rc = 6.67 cm	12	3.5	13	3.0
d = 3 cm	15	4.5	15	4.0
F = 1.10	20	6.2	20	5.5
	25	8.0	25	6.8
	30	9.9	30	8.25
	35	12.1	35	9.70

ORIGINAL PAGE IS
OF POOR QUALITY

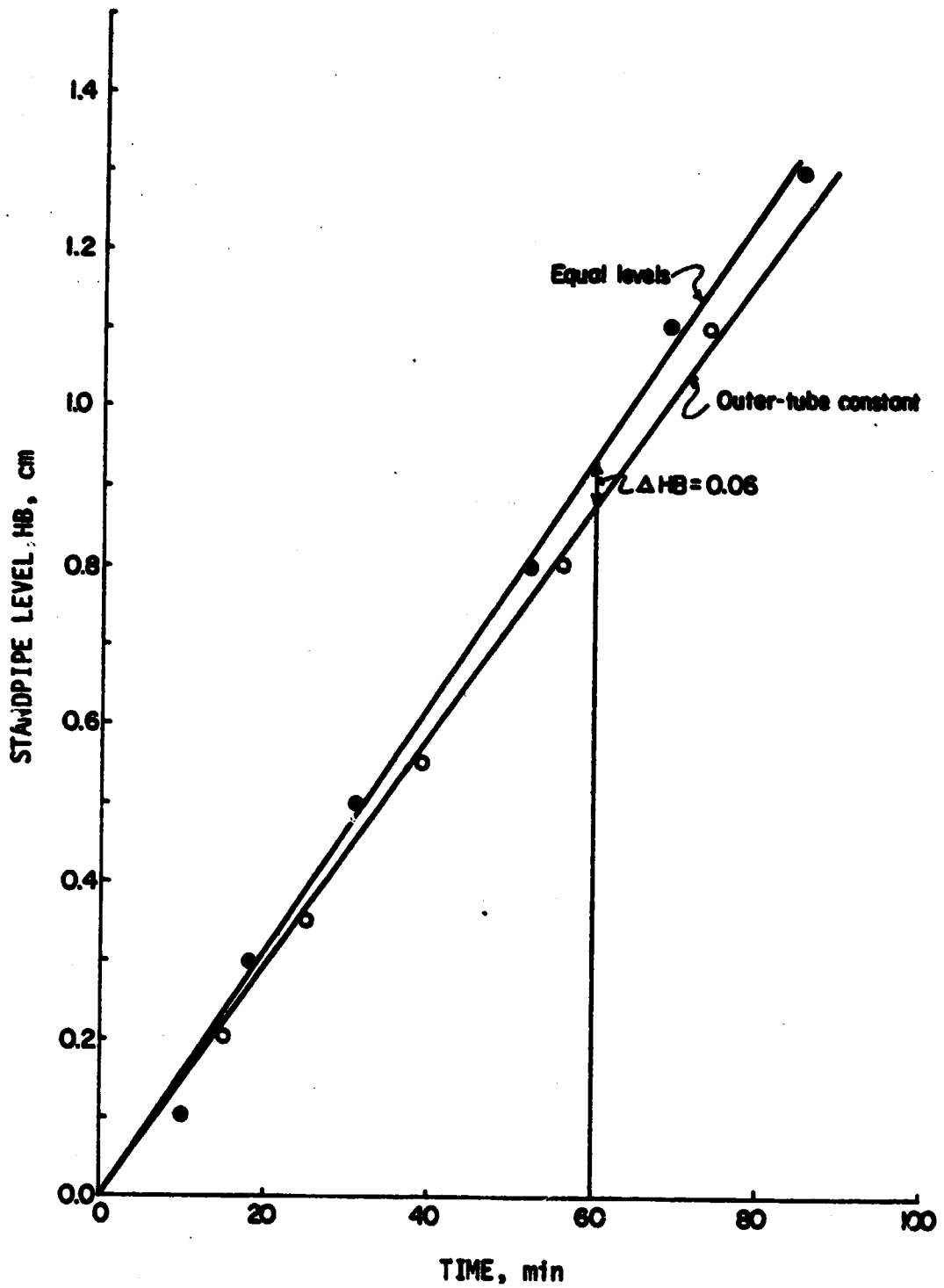


Fig. A-1. Double-tube data for 5 cm depth.

ORIGINAL PAGE IS
OF POOR QUALITY

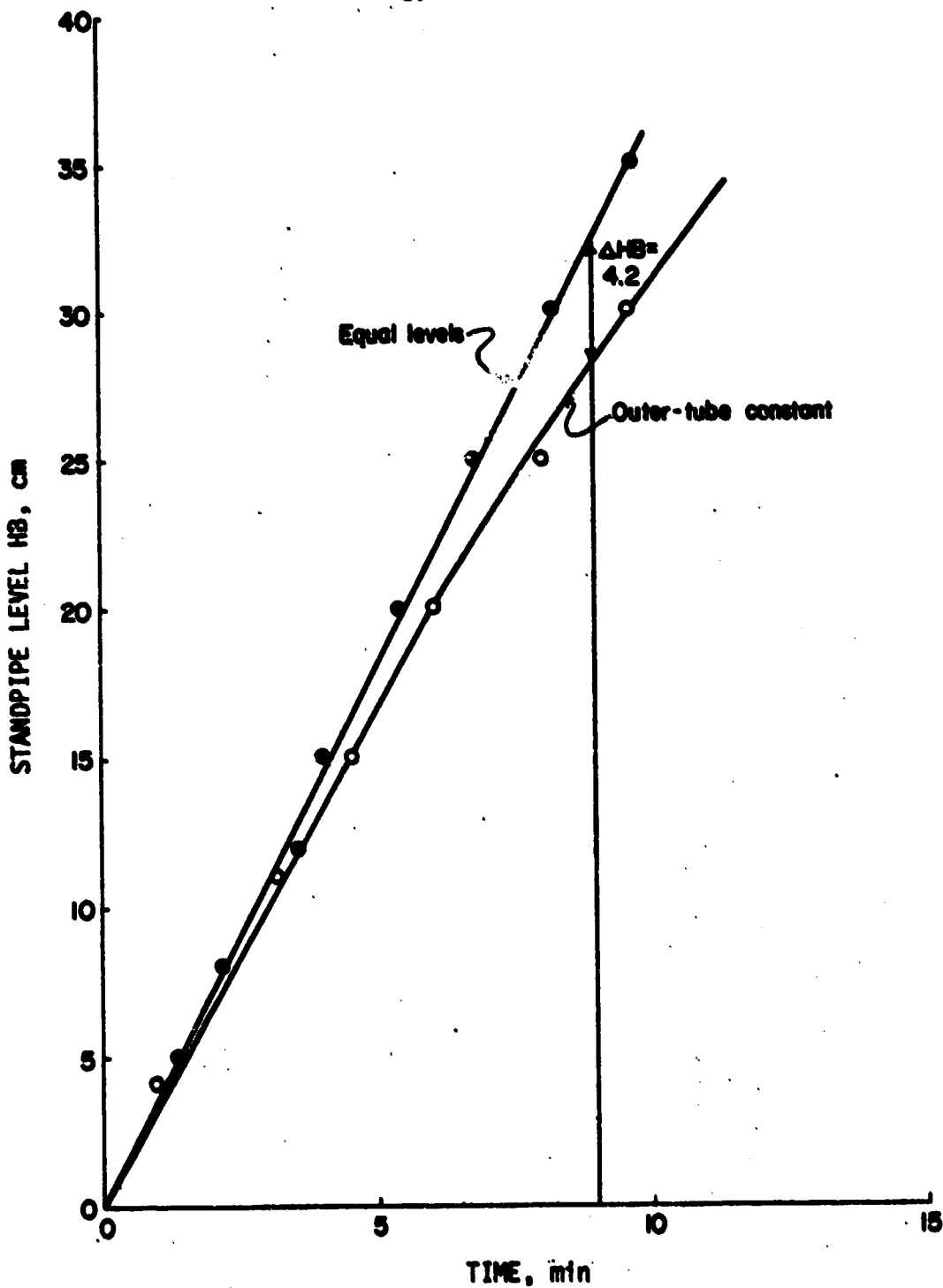


Fig. A-2. Double-tube data for 40 cm depth.

ORIGINAL PAGE IS
OF POOR QUALITY

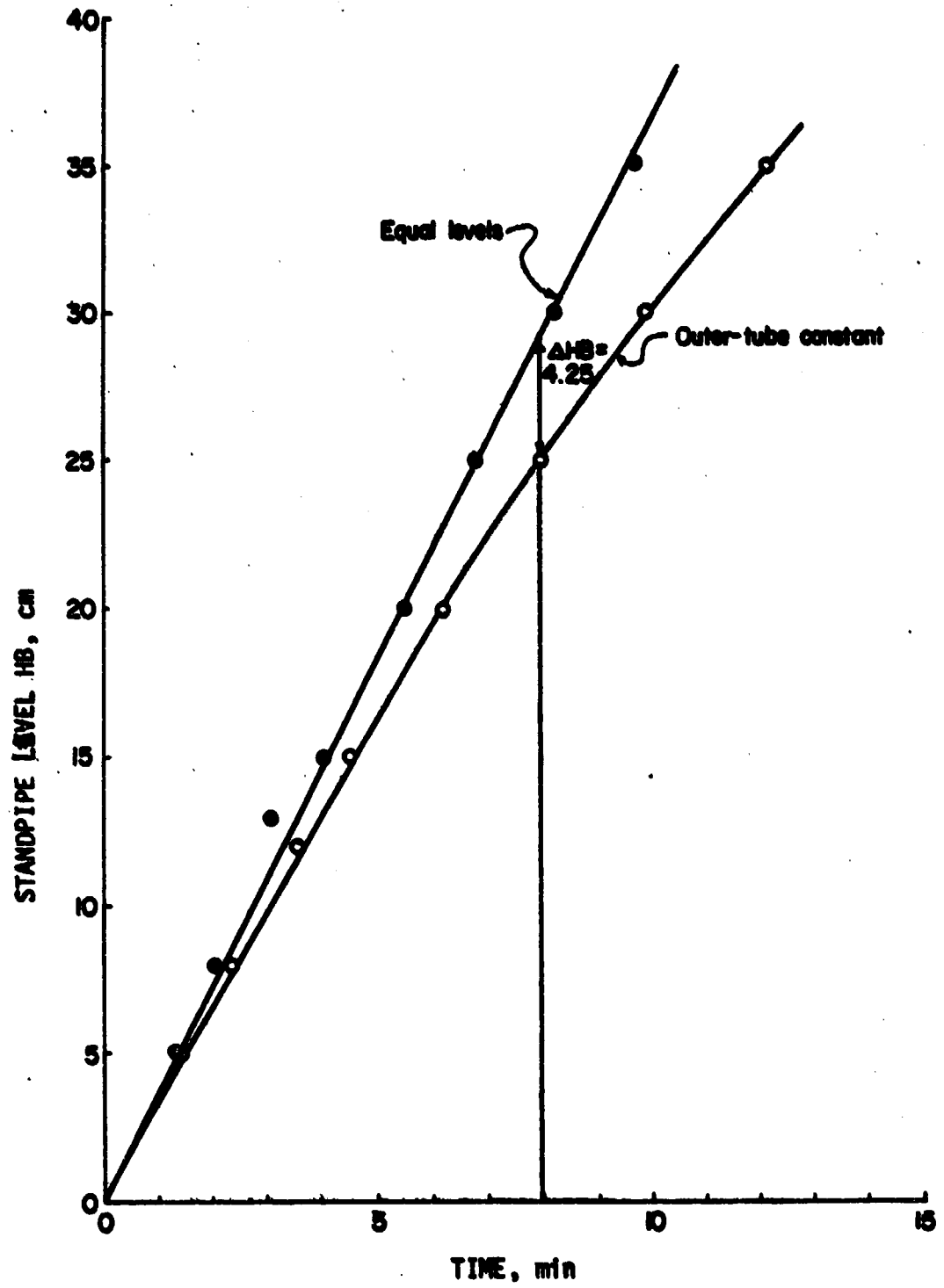


Fig. A-3. Double-tube data for 70 cm depth.

TABLE A-8

Centrifuge Data

Core #	Depth (cm)	2m+L (cm)	L (cm)	ω (1/sec)	$R_1(\omega) - R_1(0)$ (g)	D (cm ² /min)	K (cm/day)	ϕ (cm ³ /cm ³)
1	30	30.9	6	62.832	0.155	0.900	0.200	0.301
2	42-52	30.9	6	62.832	0.190	0.700	0.181	0.291
3	30	30.9	6	83.771	0.330	0.350	0.258	0.301
3a	50-60	28.5	6	73.304	0.040	0.425	0.099	0.272
3b	50-60	28.5	6	83.771	0.30	0.220	0.129	0.272
4	65-75	28.5	6	78.540	0.275	0.425	0.099	0.284
6	30	31.7	6	78.540	0.042	0.700	0.0277	0.253
7	35-55	30.9	6	86.394	0.330	0.500	0.129	0.144
9	65-85	30.9	6	83.771	0.390	0.35	0.1068	0.172
11	15-25	31.6	6	83.771	0.70	0.172	0.177	0.333
12	25-45	31.6	6	83.776	0.12	0.60	0.0594	0.301